Geohazards in Subduction Zone Environments and their Implications for Science and Society

Preface

Guest Editors

YUJIRO OGAWA[1], YILDIRIM DILEK[2] and SHINJI TAKARADA[3]

[1]University of Tsukuba, Japan. *E-mail: fyogawa45@yahoo.co.jp*
[2]Miami University, USA. *E-mail: dileky@miamioh.edu*
[3]Geological Survey of Japan, AIST, Japan. *E-mail: s-takarada@aist.go.jp*

A joint meeting of the 2nd G-EVER (Asia-Pacific Region Global Earthquake and Volcanic Eruption Risk Management) International Symposium and the 1st IUGS (International Union of Geological Sciences) & SCJ (Science Council of Japan) International Workshop on Natural Hazards was held on October 19-20, 2013, in Sendai, Japan. The workshop also included a field trip on October 21 (please refer to the article by E. Tsukuda in this issue for details). The aim of the joint meeting and workshop was to examine the most recent observations and data from seismically active subduction zone environments and to discuss the most effective methods in order to reduce the risks from natural disasters such as earthquakes, tsunamis, landslides, and volcanic eruptions, particularly in and around active subduction zones. The workshop was well attended, with 94 participants representing 12 countries, and thirty national and international institutes contributed to and produced the content of the "Sendai Agreement". The agreement was unanimously endorsed by all participants (please refer to the article by E. Tsukuda for details).

There were 55 papers presented during the workshop, followed by intensive and thematic discussions on the scientific and societal implications of the exchanged data, observations, and results. The organizers and the participants also considered the relevant outstanding questions and problems regarding various natural hazards, the level of preparedness of different societies and nations for such hazards and potential future workshops to better understand the mode of natural hazards and the related societal and governmental issues. This special issue of *Episodes* is one of the manifestations of this workshop in Sendai and contains thirteen of the papers presented at the workshop.

The Sendai joint meeting and workshop were planned after the devastating earthquake and tsunami of the March 2011 Tohoku-oki Earthquake (Mw = 9.0) in this region. The large magnitude earthquake was a result of slip on a subduction-type low-angle thrust fault along the Japan Trench. The Japanese word "oki" means offshore, while "Tohoku" refers to the regional name of Northeast Honshu, Japan, where the city of Sendai is located. The major property damage and the fatalities associated with the Tohoku-oki disaster were caused almost entirely by the tsunami, which occurred immediately after the earthquake. Rapid tsunami flooding (inundation) along the shorelines of northeastern Japan and deep into the land along some of the river systems resulted in more than 18,000 fatalities, including numerous missing people. The aftershock of this double disaster was enormous for the usually very resilient Japanese nation, and showed to the world that even one of the most physically and emotionally well prepared society for such disasters needed more sophisticated, long-term planning for effective forecasting, rapid evacuation, efficient mitigation, and government response than before.

The Fukushima Daiichi ("Daiichi" means No. 1) nuclear power plant in the towns of Okuma and Futaba in the Fukushima Prefecture was also damaged extensively by the tsunami flood and the loss of electric power after the events took place. Subsequent radioactive leakage from the storage units caused some level of contamination of the soil and water nearby, creating further concerns and problems for the local people and government. Such large-scale, subduction-type earthquakes (≥ Mw 9.0) occurred previously in Chile (1960), Alaska (1964), and Sumatra (2004). However, an earthquake of such magnitude was not anticipated near the Japan Trench, although some observations and discussions on its potential were made by geophysicists, geologists, and geomorphologists in the past. Just after the earthquake and the ensuing tsunamic event, numerous scientific papers were edited, published, and presented at scientific meetings in a short period of time. However, the societal aspects and the ramifications of these kinds of natural geohazards for the welfare of nations and societies received less attention in the publication media and were thus significantly underscored.

Subduction zones, where one lithospheric plate dives under another one, are also known for other types of natural hazards associated with volcanism, earthquake-induced landslides, and coastal flooding–erosion. The nature of these geohazards is relatively well

understood in recent years as a result of technologically driven fundamental and frontier research, linking such events to dynamic processes on Earth. Less accomplished over the years, in comparison, is the efficiency of transferring all this scientific knowledge to policy-making and societal understanding of the real causes of such disasters and to the development of early warning systems and risk assessment and reduction plans and strategies. This goal requires collective and collaborative efforts, and skills of earth scientists, engineers, socio-economists, health organizations and governmental policy-makers at regional and global scales. Increasingly, responding to the consequences of geohazard events has become the responsibility of international scientific unions and intergovernmental organizations. Therefore, we also need to better learn and practice how to disseminate and transfer the learned knowledge, science and data in a trans-disciplinary fashion, while avoiding the technical jargon in communicating with the governmental bodies, policy-makers, and people.

This special issue of *Episodes* is intended to serve this purpose. The papers herein focus on the nature of crustal movements, seismic events, paleo-tsunamological and tsunami-modeling studies, and landslides particularly in Asia and the Pacific Rim, along the trench systems of Japan (from the Japan Trench to the Ryukyu Trench, through the Sagami and Nankai Troughs), the Russian and Chinese continental margins. The subduction zone and continental margin geohazards studies include potential risk assessment and management plans. Some effective strategic and ethical issues are also presented in this issue.

World leaders (and policy-makers) often have an impression that geohazards and natural disasters as very serious but rather rare events. We hope that the new generation of leaders shall express more concern on the enormous potential risks to their people brought about by the occurrence of geohazards and related disasters in the future.

We gratefully acknowledge all the people who participated in the preparation of the Sendai joint meeting and workshop, particularly the G-EVER Consortium Promotion Team, AIST international management division, Tohoku University researchers, International Research Institute of Disaster Science (IRIDeS) of the Tohoku University, IUGS, SCJ, and the IUGS Branch of Earth and Planetary Science Board of SCJ, for their financial and spiritual support. We also express our sincere thanks to the authors for their valuable contributions to this special issue and to the reviewers for their constructive and timely comments on the manuscripts. Finally, we would like to thank the IUGS Executive Committee for helping us materialize this special issue, and Dr. Brian Marker and Dr. Fareed Fareeduddin, in charge of the publication of *Episodes*, for their help, encouragement and editorial processing of the papers for publication in the special issue.

by Ian Lambert[1] and Roland Oberhaensli[2]

Towards more effective risk reduction: Catastrophic tsunami

[1] Former Secretary General IUGS & Senior Advisor Australian Geoscience Council. *E-mail: ian.lambert@homemail.com.au*
[2] President IUGS & Department of Earth and Environmental Science, University of Potsdam. *E-mail: Roland.Oberhaensli@geo.uni-potsdam.de*

The International Union of Geological Sciences (IUGS) is evaluating whether there are additional geoscientific activities that would be beneficial in helping mitigate the impacts of tsunami. Public concerns about poor decisions and inaction, and advances in computing power and data mining call for new scientific approaches. Three fundamental requirements for mitigating impacts of natural hazards are defined. These are: (1) improvement of process-oriented understanding, (2) adequate monitoring and optimal use of data, and (3) generation of advice based on scientific, technical and socio-economic expertise. International leadership/ coordination is also important.

To increase the capacity to predict and mitigate the impacts of tsunami and other natural hazards a broad consensus is needed. The main needs include the integration of systematic geological inputs - identifying and studying paleo-tsunami deposits for all subduction zones; optimising coverage and coordination of geodetic and seismic monitoring networks; underpinning decision making at national and international scales by developing appropriate mechanisms for gathering, managing and communicating authoritative scientific and technical advice information; international leadership for coordination and authoritative statements of best approaches. All these suggestions are reflected in the Sendai Agreement, the collective views of the experts at the International Workshop on Natural Hazards, presented later in this volume.

Introduction

In line with its role in promoting international, broad-based, and inter-disciplinary scientific studies relevant to the entire System Earth, the International Union of Geological Sciences (IUGS) is evaluating whether there are additional geoscientific activities that would be beneficial in helping mitigate the impacts of tsunami that have been of great international concern since the devastating Boxing Day tsunami of 2004 in Indonesia.

There is currently considerable tsunami-related research being undertaken, and huge investments have been made in tsunami warning systems, which many people have interpreted as a quick technological fix. Unfortunately, the research and one of the best warning systems in the world did not save the many Japanese who died in the major Tohoku tsunami of March 2011.

It appears that currently available information in the light of data sharing and data networking is not adequate to rule out any subduction zone hosting a magnitude 9 or greater earthquake, and therefore generating a catastrophic tsunami.It is thus important to assess what could be done to increase our capability to predict and mitigate the impacts of tsunami globally. A broad consensus on the priorities for filling knowledge gaps and how to achieve more effective communication of advice to guide decisions and policies is vital both for reducing risks and attracting the funding and expertise necessary for the additional activities.

Different stake-holders need to be involved. Academic and applied research is vital for understanding processes. Government agencies have important roles in monitoring, conducting systematic field observations, and providing advice in support of policy development and decision-making. Further, international Unions/Councils are well placed to provide leadership and to facilitate international collaboration.

IUGS sponsored the 1st International Workshop on Natural Hazards in October 2013, held in conjunction with the 2nd International G-EVER meeting in Sendai, Japan. The objective was to bring together leading tsunami researchers, representatives of government and international agencies, to discuss and agree on priorities for mitigating the risks of natural hazards – the "Sendai Agreement". This paper summarises the introductory presentation, which set the scene for this workshop.

Consideration of priorities

There are four fundamental requirements for mitigating impacts of natural hazards:

1. Good understanding of the processes involved
2. Adequate monitoring and optimal use of data
3. Production of advice and options for mitigation based on scientific, technical and socio-economic expertise. This must include effective means of getting advice used in policies/ decisions
4. International leadership/coordination.

Uncertainties remain in relation to the regions with the highest imminent risks and options for minimising impacts on people and critical infrastructure. We now discuss each of the four fundamental

requirements in turn, identifying issues that we suggest need more attention.

Good understanding of processes

Over the last decade there has been a considerable increase in research, involving geologists, seismologists, and oceanographers, into the processes and complexity of the oceanic lithosphere and other issues related to catastrophic tsunamigenic events. A summary of the main research activities is provided in Appendix 1.

There has been research in some regions aimed at recognising paleo-tsunami deposits, which can provide a good guide to the magnitude, extent and dates of previous events. This should be conducted systematically in Recent coastal sequences of all subduction zones where currently there is not sufficient information to assess tsunami risk.

Recognising tsunami deposits is not always straightforward. Tsunami deposits are deposited over sediments in low-lying areas landward of the coastline, such as lagoons and deltaic plains. Both tsunami deposits and storm deposits may have strongly erosive bases and mainly consist of sand, but major tsunamis inundate areas farther inland than storms. Furthermore, the presence of material eroded from the shelf is considered more likely to suggest a tsunami rather than a storm event due to the much greater energy and erosive power associated with individual waves in the tsunami, and the movement of very large boulders also implies a tsunami origin.

A long history of tsunami has been documented in Japan, with many significant events and several very large and destructive examples. Investigated tsunamigenic deposits provide evidence of the regional extents of their impact on coastal environments– for the major 869 AD Sanriku earthquake (Ref1) (*http://en.wikipedia.org/wiki/869_Sanriku_earthquake_and_tsunami)*, tsunami deposits have been found over 4.5 km inland in the Sendai Plain. Two earlier deposits with similar character were also identified and dated in this area. This led to the conclusion of a recurrence interval for large tsunamigenic earthquakes along the Sendai coast of approximately one thousand years, suggesting that a repeat of this event was overdue and that large-scale inundation was very likely. Clearly, it was not a surprise to scientists when the Tohoku tsunami struck.

In this context, we suggest that systematic peer-reviewed mapping and dating tsunami deposits should be undertaken to provide updated risk maps in areas where information is inadequate. Peer-reviewed risk assessments for all subduction zones would be beneficial in raising awareness of the potential risks and potential return periods of major events. This activity should include evaluation of the significance of subducting seamounts as a major factor in collision processes in subduction zones, followed by catastrophic release of stress. Also, there is a need for systems analysis to understand other concatenated events better, e.g., mega-earthquake recurrence - tsunami – flooding.

Monitoring and applications of data

In acknowledging the considerable monitoring of events and trends using seismic and geodetic networks, ocean buoys, and so on, it is suggested that there would be benefit in detailed evaluation of the types and coverage of data being gathered, and priorities for addressing any shortcomings in these, taking account of the capabilities of emerging technologies and how these could be rolled out.

There is also a need to optimise the use of monitoring and mining data, making use of cloud and computing power to produce valuable applications. This is illustrated by the TsuDAT web application (Ref2) (http://boundlessgeo.com/case-study/tsudat-geonode-disaster-modeling/), which is summarised in Box 1.

Box 1. TsuDAT: Web application indicating likely impacts of tsunami

TsuDAT is underpinned by, and provides access to, pre-computed database of 70,000 tsunami events from all subduction zone sources in Pacific/Indian oceans. It draws on a pre-computed database of offshore waveforms, and only the inundation component needs to be modelled. A web-server and tsunami simulations are hosted in the Cloud, giving scalable computing resources. Spatial data is managed through a GeoNode that facilitates data uploading, editing and sharing via the web. All data is Open Geospatial Consortium compliant and all software is open-source. Given basic training, the inundation modelling can be done rapidly by non-experts, who have an option to include any available detailed local bathymetric data, to indicate the likely impacts of a tsunami.

It is suggested that there is a case to consider what other similarly innovative and practical web applications, using available data, can be developed and/or refined.

Scientific and technical advice to decision makers

It is one thing for scientists to understand risks. But it is another to have decision-makers fully informed of these risks and the options for addressing them. This is illustrated well by the situation in Japan, where no concrete actions were taken in response to the warnings of scientists that a tsunami striking the north-eastern coast of Honshu was highly likely in the foreseeable future, (Ref3) (*http://en.wikipedia.org/wiki/2011_T%c5%8dhoku_earthquake_and_*tsunami). The owner of the nuclear power plants in the coastal areas at risk, TEPCO,revised its estimates of likely tsunami heights at theFukushima Daiichi Nuclear Power Plantto greater than 9 m, but took no immediate action. The 2011 Tohoku earthquake resulted in a wave height at Fukushima of about 15 m, well above the 5.7 m for which the plant's defences had been designed, and the impact was exacerbated by land subsidence. The inundation distance and lateral extent of the tsunami were similar to the earlier major events mapped in the region.

In general, a number of factors can distort decision-making processes, including political paralysis stemming from the overwhelming magnitude of an issue, dominating personalities, ideologies, ineptitude, and incentives for inaction. However, in this communications age, poor decisions are becoming more obvious and communities around the word are demanding better and effective actions. This creates opportunities for building mechanisms, at both national and international scales, for communicating the significance of research and observations to decision makers and working with them on options. This has not yet been achieved in many cases.

There is not a universal approach that can be applied to getting scientific advice factored into major decisions. The approach pursued

in Australia, which is summarised in Appendix 2, should provide useful guides to what is important and what can be achieved - this approach is working well and is adequately funded by Government. It is summarised below, followed by the partly different German approach.

Australian approach: Given geoscientists are commonly viewed narrowly and negatively in terms of mining and environmental disruption, there was a need at the outset to establish the geosciences' crucial applications in addressing many challenges and their complementarity with the environmental and social sciences, in part through demonstration projects. The key elements of Australia's approach to provision of scientific and technical advice into government decision makers are:

- Flexible, interactive approaches which present scientific advice along with an economic and social basis for considering/ acceptance of various options
- A comprehensive information base for decision-making, with no crucial knowledge gaps that are limiting effectiveness of advice
- Multidisciplinary systems-science approaches
- Taking advantage of on-going advances in computing power, data management and access
- Dedicated advisory groups of broadly-based scientists working in/with government, which focus on practical applications of scientific data and research, can see "the big picture" and are aware of government expectations and constraints. They interact regularly with a wide range of researchers and bring together all relevant research findings, facilitate/lead research aimed at filling gaps, promote cross-disciplinary approaches, and foster linkages to social scientists and economists.

Advisory groups are understood and trusted by decision makers, with whom they have regular communication. Their main activities are approved and funded by Government (and other key clients). Their careers are not dependent on external funding and peer-reviewed publications, or subject to other potential distractions and conflicts of interest. They provide regular briefings and prepare authoritative scientific/technical papers, national approaches, guidelines, standards and options for addressing current and potential issues. Their publicly available outputs are open to peer review.

German approach: This involves less direct government involvement. Geoscientific inputs are coordinated in two principal ways. First, the senate commission of the German Science Foundation (DFG) works on future tasks and challenges that the geosciences are confronted with (Senatskommissionfür Zukunftsaufgaben in den Geowissenschaften; ZAG: *http://www.sk-zag.de*). This is a purely scientific and non-governmental think-thank of experts representing different fields in the geosciences. Second, the German government has set up task forces for tsunami and hazard research in its research organisations of the Helmholtz Gemeinschaft (http://www.helmholtz.de).Joint efforts among these organisations and universities have come to fruition in closer cooperation between the geosciences and political and administrative sciences (*http://earth-in-progress.de)*, efforts in improving knowledge transfer and the introduction of governance issues in geoscience education *(http://www.geogovernance.de*).

International leadership and coordination

There would be clear benefits in enhanced international coordination and support for multidisciplinary systems-science and monitoring programs related to major global issues. There is a need to set priorities, to facilitate international collaboration, to ensure that the information for decision-making is comprehensive, and to develop/facilitate authoritative statements/guidelines for major issues.

The International Council for Science (ICSU) is well placed to provide leadership and coordination for agreed priority activities. In the case of tsunami, this should be done through ICSU's Integrated Research on Disaster Risk (IRDR) program, which is currently being revitalised. ICSU's member states and Unions support this leadership and coordination role.

Summary

A broad consensus is needed on proposals for increasing capacity to predict and mitigate the impacts of tsunami and other natural hazards. Feedback is sought on the scope for better links between various activities already in place, for conducting some activities more systematically, and for innovative applications of data to help further mitigate risks of catastrophic tsunami.

The time for action is now, given increasing public concerns about poor decisions and inaction, plus advances in computing power, data management and access make it possible to use and integrate data in ways that were not previously possible.

It is suggested that the main needs are:

- Integrated systematic geological inputs, particularly identifying and studying paleo-tsunami deposits in the recent geological records to establish the occurrence, magnitude and frequency of tsunami – peer-reviewed risk assessments are needed for all modern subduction zones.
- Optimising coverage and coordination of geodetic and seismic monitoring networks and introduction of new technologies, including remote sensing applications. Also, development of useful applications of monitoring data.
- Developing appropriate mechanisms for gathering, managing and communicating authoritative scientific and technical advice information, to underpin decision making at national and international scales.
- International leadership, coordination and authoritative statements of best approaches.

These suggestions are reflected in the Sendai Agreement, the collective views of the experts at the International Workshop on Natural Hazards, presented later in this volume.

References

Lambert and McFadden, 2013,Episodes, v. 36 No.1, pp.2-7.

Ref1:http://en.wikipedia.org/wiki/869_Sanriku_earthquake_and_tsunami

Ref2: http://boundlessgeo.com/case-study/tsudat-geonode-disaster-modeling/

Ref3: http://en.wikipedia.org/wiki/2011_T%c5%8dhoku_earthquake_and_tsunami

Appendix 1

Major current and recent activities directed at mega-earthquakes and tsunami

(drawn from a report by Lambert & McFadden, 2013)

- There is on-going compilation and analyses of historical records of earthquakes and tsunamis. Japan has by far the best historical records in the world, but this wasn't enough to predict a magnitude 9 event. A basic problem is that historical records are very short in geological timescales.
- An Intergovernmental Oceanographic Commission (IOC, UNESCO) committee is tasked with identifying the subduction zones around the world that can produce giant earthquakes and tsunamis, as well as tsunami earthquakes (events that are dangerous because their slow ruptures can be misread by warning systems and coastal populations). Understandably, the IOC is very much dominated by oceanographers and meteorologists and yet the bulk of the evidence for past events is geologic in nature.
- The Global Earthquake Model (GEM) is developing global databases and global scientific consensus on the state of knowledge. This work is being done through a series of Global Components studies that will be underpinned by a computational modelling framework and tools: *http://www.globalquakemodel.org/global-components*. In particular, it is intended that the Global Active Faults and Seismic Source Database will represent the authoritative source for information on active earthquake sources, including the world's subduction zones. However, GEM is not directly addressing tsunamis and is certainly not doing paleo- seismic or paleo-tsunami studies to increase the knowledge base. GEM's work will, however, provide an excellent baseline from which to identify knowledge gaps and to expose the risks associated with them. GEM is trying to develop a global scientific consensus on Mmax for earthquake hazard calculations. This will at least help establish the state of play from a hazard/risk assessment perspective.
- The Extreme Natural Hazards and Societal Implications Project (ENHANS; *http://www.iugg.org/programmes/enhans.php)* of the International Union of Geodesy and Geophysics (IUGG) launched in 2010 is supported by several ICSU bodies including the ICSU Regional Office for Asia and the Pacific. It aims (i) to improve understanding of critical phenomena associated with extreme natural events and to analyse impacts of the natural hazards on sustainable development of society; (ii) to promote studies on prediction of extreme events reducing predictive uncertainty and on natural hazards mitigation; to bring the issues into the political and economic policies; (iii) to disseminate knowledge and data on natural hazards for the advancement of research and education in general and especially in developing countries.
- Paleo-tsunami research (including trenching etc.) is one of the essential tools in tsunami research and is covered under the umbrella of ICSU, which established a new 10-year program dedicated to disaster risk research, Integrated Research on Disaster Risk (IRDR, http://www.irdrinternational.org/). IRDR tries to bridge natural and social sciences, engineers and policy makers etc. to mitigate, if not fully prevent, disasters.
- In 2011, the Geological Survey of Japan (GSJ) initiated a project related to Asia-Pacific region global earthquake and volcanic eruption risk management (G-EVER, http://g-ever.org/index.html). The first workshop was held in Tsukuba in Feb. 2012 (*http://g-ever.org/en/gever1/index.html)* and co-sponsored by IUGG and two IUGG associations dealing with seismology (IASPEI) and volcanology (IAVCEI). One of the major topics was earthquake- and volcano-generated tsunamis.
- The first bilateral symposium on geohazards and disaster risk under the US–Russian Presidential Commission on Science and Technology was held in Moscow in July 2012. One of the important topics was joint paleo-tsunami studies.

Appendix 2

Geoscience underpinning policies and decisions addressing major challenges in Australia

The Australian Academy of Science's National Committee for Earth Sciences produced a *National Strategy for Earth Sciences* in 2003 (http://www.science.org.au/natcoms/nc-es/documents/nc-es-strategic.pdf), which emphasized the key-underpinning role of the geosciences in approaches to a wide range of major issues. In many cases decision-making processes require: (i) information on surface features, including through remote sensing; (ii) information on subsurface materials and processes, including through collation of information from direct sampling and integration of geological and geophysical data; (iii) systematic monitoring as required to track important trends and events; and (iv) strategic analyses involving integrated consideration and modelling of all relevant data and information. It also identified the need for integration of the efforts of academic researchers and government agencies and collaborative approaches to sharing expertise and infrastructure needed for major research programs. This national strategy was influential in achieving wider appreciation of, and increased funding for, the vital underpinning roles of the Earth Sciences, as well as in developing important new roles for the national geological and geospatial agency, Geoscience Australia (GA: *http://www.ga.gov.au/)*.

GA is currently a vibrant government agency with a strong public profile. It is a primary source of scientific and technical advice in support of policy development and major decisions on a wide range of issues requiring geoscientific and geospatial inputs. But this was not always the case. Two decades ago its predecessor organization, the Bureau of Mineral Resources (BMR) was underfunded and struggling to be seen as relevant to the government that was funding it. This motivated the agency to transform in an effort to reverse this

perception, involving it contributing to and implementing the national strategy.

In changing its attitude and culture, GA transformed from an introverted agency with poor communication channels into the main body of government to a vibrant agency with a culture that said its job is "to apply geoscience to Australia's most important challenges" and with effective communication channels to ensure that its work is recognised, relevant, and used.

The success of the transformation from the beleaguered BMR to the present-day GA is evidenced by a 2010 review by the Department of Finance and the Department of Resources and Energy (http://www.finance.gov.au/publications/strategic- reviews/docs/strategic_review_ga.pdf). That review recognized the importance of the agency's work to many major issues facing the nation and recommended that its funding be increased to (i) strengthen capabilities for collection of regional-scale data and for monitoring, (ii) invest in custodianship of Australia's exponentially increasing geoscientific and geospatial data, and (iii) enable continuation of fundamental capabilities in areas such as groundwater, natural hazards, mineral resources and clean energy. This was a unique outcome for a review involving the Department of Finance, particularly at a time when the focus is on reducing government expenditure.

- Australia is a major supplier of a wide range of mineral and energy commodities to world markets. The strength of its economy is linked to its considerable mineral endowment. In 2010, recognising the falling success rate of mineral exploration in Australia, the Australian Academy of Science ran a Think Tank for young scientists to try to develop fresh approaches to exploration under cover. The Academy then drew together a representative group, now known as the UNCOVER group, from across the spectrum of academia, government agencies, and industry to develop from this Think Tank an appropriate research and data- acquisition vision and to improve collaboration and coordination across the sector. In 2012, UNCOVER released the document *Searching the Deep Earth: A Vision for Exploration Geoscience in Australia* (http://www.science.org.au/policy/uncover.html/). This vision, which includes enhanced information on the subsurface through comprehensive integration and modelling of geological information and a range of geophysical datasets, has now informed strategic planning for the state geological surveys and for Geoscience Australia. It is noteworthy that enhanced understanding of sub-surface materials and processes has wider applications in relation to issues such as understanding groundwater systems, building cities and infrastructure, mitigating hazards and risks, and managing wastes.

Amongst the numerous other important geoscience contributions to high profile government policies and decisions are

- Improved water management through better knowledge of groundwater systems and their links with surface waters.
- Addressing community concerns about the rapidly growing coal seam gas sector, particularly centred on potential impacts on ground and surface waters.
- National guidelines to facilitate decisions on proposed uranium mines.
- Enhanced monitoring of environmental health and vegetation cover through developing improved remote sensing approaches.
- Establishing links between geology and bioregions.

Reinforcing Australia's leadership role in mitigating the impacts of geohazards in its region by building fit-for-purpose tsunami warning systems, an online bushfire status system used by fire-fighting authorities and the wider public, and TsuDAT - a web application for non-experts to conduct inundation modelling to assess their own tsunami risk.

by Yasutaka Ikeda

Strain buildup in the Northeast Japan orogen with implications for gigantic subduction earthquakes

Department of Earth and Planetary Science, the University of Tokyo, Hongo, Bunkyo-ku, Tokyo 113-0033, Japan.
E-mail: ikeda@eps.s.u-tokyo.ac.jp

Although recent GPS observations have made it possible to detect crustal strain precisely and extensively, we have not yet observed a whole cycle of strain buildup and release in orogenic zones by any geodetic methods. From the viewpoint of earthquake forecasting, we need to extract elastic strain from GPS-derived strain data. However, we do not have any (practical) geophysical method by which to discriminate between elastic and inelastic strains from GPS data. Based on the lesson from the 2011 Tohoku earthquake of Mw 9.0, we propose here that geological methods (and ways of thinking as well) should be used to estimate inelastic strain buildup quantitatively, thereby to evaluate present-day elastic strain buildup, which may eventually cause gigantic earthquakes. We review here a case history of the 2011 Tohoku earthquake, and present a global comparison with other gigantic (Mw ≥ 9.0) subduction earthquakes in the world.

Introduction

Strain buildup: elastic or inelastic?

Crustal strain is built up in and around a subduction zone in association with interseismic coupling on the plate interface (Fig. 1). The elastic portion of the crustal strain is released during episodic decoupling events on the plate boundary; the remainder is accommodated as permanent (= inelastic) deformation mainly within the subduction-related orogenic zone, which is thermally weakened by magmatic heating (Fig. 1). Inelastic deformation within the subduction-related orogen includes brittle deformation associated with active intra-arc faulting in the upper crust especially near the volcanic front and on the backarc side (Fig. 1). Coseismic deformation is basically elastic, although damped by asthenospheric viscosity and thereby followed by postseismic deformation decaying exponentially with time.

Recent GPS observations have made it possible to detect crustal strain precisely in time and extensively in space. However, the duration of such advanced observations is too limited to cover a whole cycle of strain buildup and release in subduction-related orogens. Furthermore, we do not have any (practical) geophysical methods by which to discriminate between elastic and inelastic strains from GPS-derived strain data. Any attempts to discriminate between elastic and inelastic strains using only geodetic data fall into a typical inversion problem. That is to say, solutions are not unique at all. In order to get a solution, transcendental knowledge (i.e., "model") is necessary, but it becomes more and more difficult to test the validity of the solution with increasing complexity of the model. Then, what can we do to avoid this deadlock?

For effective earthquake forecasting, we need to know how much elastic strain has been built up in a subduction zone. We propose here that geological methods should be used to evaluate inelastic strain buildup quantitatively, thereby to evaluate present-day elastic strain buildup, which may eventually result in gigantic earthquakes. In this paper, we review the process of strain buildup and release in the Northeast Japan (NEJ) arc on a geologic time scale, and discuss its implications for the occurrence of gigantic subduction earthquakes. A global comparison is also made with other gigantic (Mw ≥ 9.0) subduction earthquakes in the world.

Full strain release or partial strain release?

In order to evaluate the seismic hazards of a subduction zone, we first need to know the maximum size of earthquakes that are produced from the plate interface (e.g., Ruff and Kanamori, 1980; Goldfinger et al., 2013). Obviously, instrumentally recorded earthquake data are

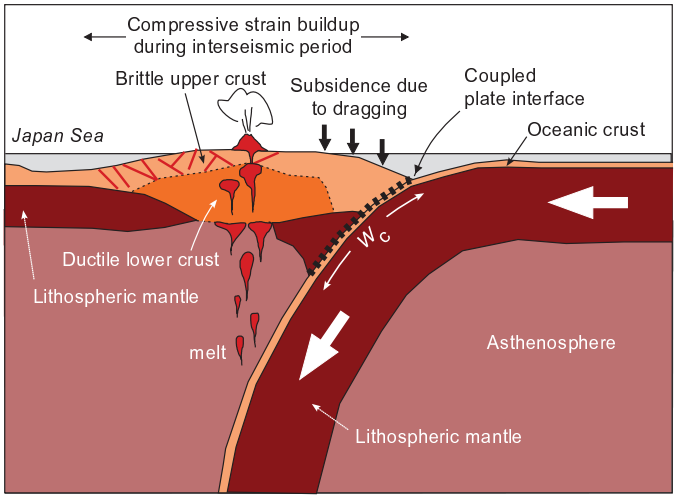

Figure 1. Schematic cross section of the Northeast Japan orogen. Rheological properties are simplified from Shimamoto (1989). W_C denotes along-dip width of plate interface that is coupled in interseismic periods. Note that the Japan Sea is floored mostly by extended continental crust; the back-arc side of the NEJ arc was also extended in conjunction with the Japan Sea opening in early to middle Miocene time.

not enough in terms of duration to evaluate the maximum size. Further problematic is the fact that some gigantic earthquakes ruptured a wide area of plate interface that encompasses a number of rupture areas of previous earthquakes as big as Mw 7~8, indicating that elastic strain has only been partially released in association with Mw 7~8 events. Examples include the 2004 Sumatra-Andaman earthquake of Mw 9.2 (e.g., Bilham et al., 2005) and the 2011 Tohoku earthquake of Mw 9.0 (discussed later in this paper).

Before going into details about the NEJ's case, let us define two terms: (a) *full strain-release event* and (b) *partial strain-release event*. In order to completely release the elastic strain that has been built up in and around a subduction-related orogen, it is necessary to rupture the whole down-dip width (W_c) of the coupled plate interface (Fig. 1). Matsu'ura and Sato (1997) also suggested that the amount of slip (D) on a plate interface increases with the length (L) along strike of the rupture area, and becomes saturated as L reaches 2~3 times as long as W_c. In this paper hereafter, we refer to such a slip-saturated event as a *full strain-release event*. If the strength of plate interface is constant, then the amount of slip (D_{max}) at saturation is proportional to W_c. The maximum moment release from a subduction zone, therefore, is expressed as

$$\max M_0 = \mu D_{max} W_c L \propto W_c^2 L ,$$

where μ is the rigidity. This indicates that the maximum amount of seismic moment release is proportional only linearly to the length, but squarely to the width, of coupled plate interface. Thus, the most important parameter in evaluating the maximum size of subduction earthquakes is the down-dip width of plate coupling (Ikeda et al., 2012).

We can estimate the maximum size of earthquakes from a subduction zone by the above equation and an empirical law by Fujii and Matsu'ura (2000). If W_c ~100 km as is approximately the case of the Nankai trough, D_{max} is ~5 m according to an empirical law by Fujii and Matsu'ura (2000). In this case, the maximum size is about Mw 8.7 even when the rupture propagates over the full length (~700 km) of the Nankai trough. In contrast, if W_c is 200 km wide, then the amount of slip does not saturate until L ~500 km, producing a gigantic earthquake of Mw ~9.0 at L ~500 km as was the case for the 2011 Tohoku earthquake.

The most characteristic to a *full strain-release earthquake* is that the rupture propagates to the free surface (= sea bottom), forming an "open end". Consequently, the distribution of slip in the full strain-release earthquake has its maximum at the free surface (Wu et al., 1991; Rudnicki and Wu, 1995), and the maximum amount of slip is about twice as large as that of an earthquake whose rupture surface is similar in size and geometry but does not reach to the free surface (e.g., Rudnicki and Wu, 1995). Therefore, the full strain release earthquake could produce larger surface deformation on the sea bottom and thereby result in a larger tsunami than the "constrained-end" earthquake does (Geist and Dmowska, 1999). It should be emphasized that the physical essence of the Tohoku gigantic earthquake of 2011 is rather simple and can be understood in terms of full strain release.

Geological setting of the Northeast Japan arc

Rheological structure of the Japan arc based on explosion seismology, heat-flow measurements, and laboratory experiments indicates that the back-arc region (west of the volcanic front) of NEJ arc, including continental slopes on the Japan Sea side, is mechanically very weak (e.g., Shimamoto, 1989; Fig. 1); only the upper ~15 kilometers of crustal rocks behave elastic, and ductile lower crust is underlain directly by asthenospheric mantle (e.g., Iwasaki et al., 2001). As described below, this zone of weakness was rifted and stretched during the Miocene back-arc spreading event, and coincides broadly with the distribution of active faults since the Pliocene.

The geologic structure of the Japan arc is a product of multiple phases of tectonic activity since the Mesozoic. The proto-Japan arc had been situated at the Eurasian continental margin until the late Oligocene, forming an Andean-type volcanic arc associated with subduction of the Pacific plate beneath Eurasia. Major geologic structures of the present-day Japan arc were formed during the period from the late Oligocene to the middle Miocene, when the proto-Japan arc separated from Eurasia in association with back-arc spreading (Fig. 2). The back-arc opening started in the north of the Japan Basin with the focus of spreading migrating southward (e.g., Kaneoka et al., 1992; Tamaki et al., 1992; Yoshida et al., 1995; Sato et al., 2004). Crustal extension within the NEJ arc occurred mainly in the later stage (16-13 Ma) of the Japan Sea opening (Sato, 1994), when the

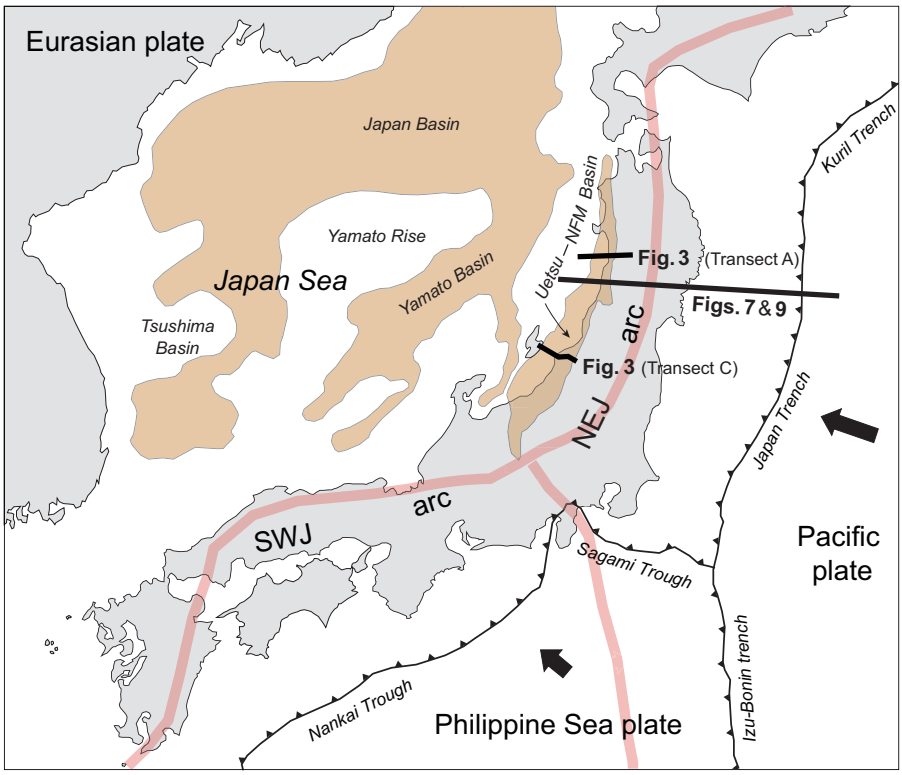

Figure 2. Regional setting of the Northeast Japan (NEJ) arc. Volcanic fronts are shown in pink solid lines. Light-brown colored areas indicate Early-Middle Miocene basins in the Japan Sea and the back-arc side of the NEJ arc.

Southwest Japan (SWJ) arc rotated clockwise by as much as ~50° (Otofuji et al., 1985); the extension was particularly strong in the eastern margin of the Japan Sea, where the Uetsuand the Northern Fossa Magna (NFM) Basins developed (Fig. 2).

The style of the Miocene extension in the back-arc region of NEJ is highly asymmetric with a zone of concentrated extension along the Uetsu–NFM Basin (Figs 2 and 3). This extension zone is characterized by a break-away fault on the west, a rollover basement anticline on the east, and unusually deep (~10 km) basins and strongly rotated fault blocks in between (Fig. 3; Okada and Ikeda, 2012), suggesting the existence of a large-scale detachment fault at a mid-crustal level beneath the extended zone. Such a style of deformation is best explained by Weissel and Karner's (1989) model, in which the brittle upper crust is capable of being deformed independently from the ductile lower crust and uppermost mantle (Fig. 4b). This model requires a detachment fault that mechanically decouples the upper crust from the lower crust and uppermost mantle; a beak-away fault soles into the detachment fault, forming a large-scale listric normal fault (Fig. 4b; Okada and Ikeda, 2012). The total amount of crustal extension across the NFM-Uetsu Basin is estimated by area-balancing restoration using seismic reflection, gravity, and surface-geologic data, and is found to be as large as 31-56 km (Fig. 3; Okada and Ikeda, 2012).

After ~10 Myr of tectonic quiescence following the opening of the Japan Sea, the NEJ arc has been subjected to crustal shortening perpendicular to the arc since 3.5 Ma (Sato and Amano, 1991; Sato, 1994) or 5 Ma (Moriya et al., 2008). The Pliocene and Quaternary contractional deformation is concentrated again within the Uetsu–NFM Basin (Figs 2 and 3), where Miocene and younger rift-fill sediments have been folded and faulted to form a fold-and-thrust belt (Matsuda et al., 1967; Sato, 1989). The total amount of crustal shortening across the NFM–Uetsu Basin during the past 3.5~5 Myr is estimated at 8~14 km (Fig. 3; Okada and Ikeda, 2012). As the asymmetric crustal extension model (Fig. 4b) proposed for the Miocene NEJ implies, under compressive stress field since the early Pliocene tectonic inversion, deformation could occur in the opposite

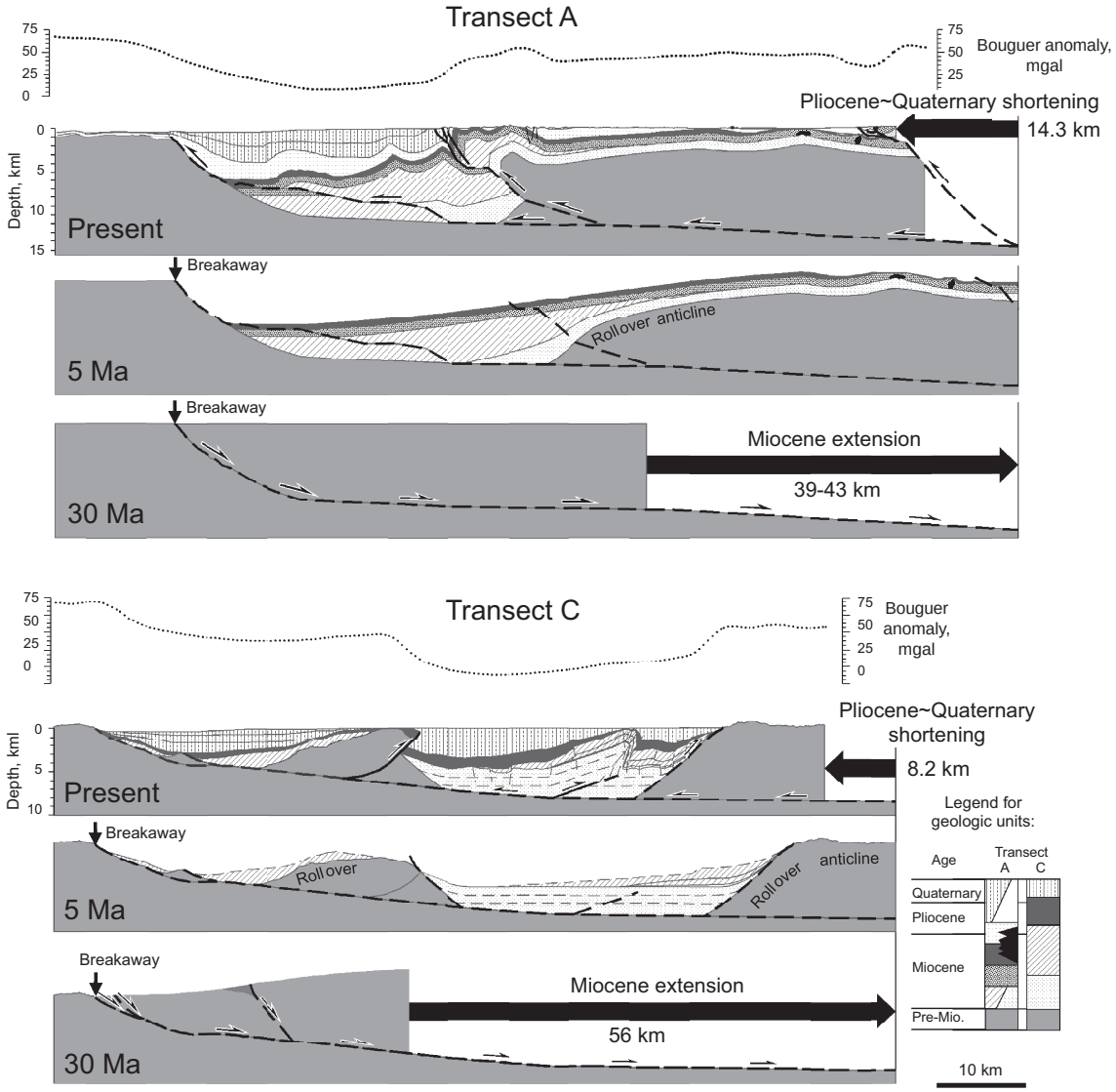

Figure 3. Present-day and restored geologic cross-sections along two transects across the Uetsu–Northern Fossa Magna Basin on the back-arc side of Northeast Japan (simplified from Okada and Ikeda, 2012). See Figure 2 for location. Each set of four figures shows, from the top to the bottom, Bouguer gravity anomaly, present-day geologic section, restored geologic section before the Pliocene positive tectonic inversion, and restored geologic section before Miocene extension.

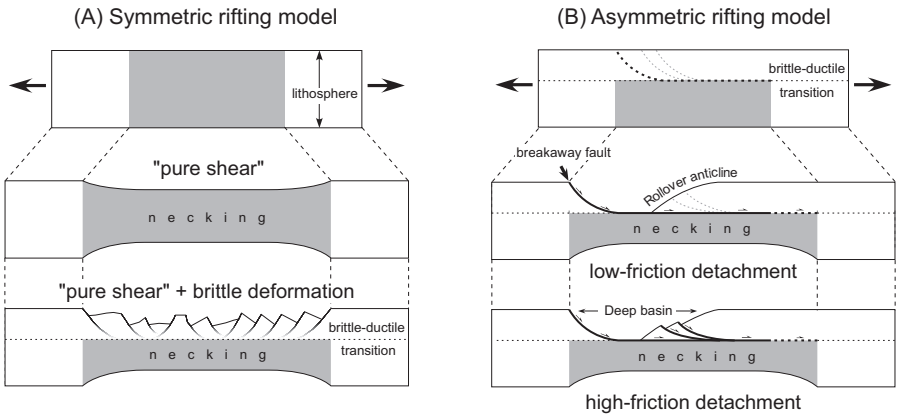

Figure 4. Symmetric and asymmetric rifting models (Okada and Ikeda, 2012). (A) Symmetric "pure shear" rifting model proposed by McKenzie (1978), and modified by Le Pichon and Sibuet (1981) with brittle deformation in the upper crust. (B) Asymmetric rifting model proposed by Weissel and Karner (1989), with modification into "high friction detachment" and "low friction detachment" cases by Okada and Ikeda (2012). Note that symmetric "pure shear" extension occurs below the brittle-ductile transition depth, whereas the upper crustal deformation is highly asymmetric. The asymmetric rift zone typically consists of a breakaway fault scarp on one side, a rollover basement anticline on the other side, and an abnormally deep basin in between. The asymmetric rifting becomes identical to the symmetric rifting with increasing friction on the detachment fault at the brittle-ductile transition. Note also that, under compressive stress field after positive tectonic inversion, deformation could occur in the opposite sense.

sense both in the upper and lower crustal layers. It follows from this inference that lower-crustal strain could be distributed across a zone much wider than the Uetsu–NFM inverted basin (Fig. 4b), as has been observed by GPS (Fig. 5).

Long-term versus short-term strain observations

There has been much debate about discrepancies between long-term crustal deformation that have been observed by geological methods, and short-term crustal deformation that have been observed for ~100 years by geodetic methods, over the Japan arc (e.g., Ikeda, 1996). Recent technological development in both geological and geodetic methods (e.g., space geodesy, geological dating techniques, etc.) has not reduced, but instead has enhanced, the discrepancies, as described below.

Horizontal shortening

Recent continuous GPS observations have indicated that the rate of horizontal shortening across the NEJ arc is in a direction almost parallel to the direction of convergence between the Pacific plate and Eurasia, and is as high as 30-50 mm/yr (Fig. 5), which is about a half of the plate convergence rate (80-90 mm/yr) at the Japan trench. The GPS-derived horizontal strain rate is on an order of 10^{-7} strain/yr, which is broadly concordant with the horizontal shear strain rate derived from triangulation and trilateration survey data for the past ~100 years (e.g., Nakane, 1973). Thus, it is likely that the NEJ arc has been contracted at a very high rate for at least the last ~100 years.

On the other hand, geologically derived, long-term-averaged values of horizontal strain/shortening are one order of magnitude smaller than geodetically derived values. As already described, Pliocene-Quaternary horizontal shortening in the upper crust of the NEJ's back-arc is inelastic (permanent), and amounts to 8-14 km (Fig. 3). The amount of shortening outside the transects is estimated to be not more than a few kilometers (Okada and Ikeda, 2012). Because the present-day contractional tectonic regime started at 3.5~5 Ma (Sato and Amano, 1991; Sato, 1994; Moriya et al., 2008), the average rate of inelastic shortening is 3~5 mm/yr, whose value is one order of magnitude slower than the GPS-derived shortening rate (30-50 mm/yr). Therefore, we conclude that most of the horizontal strain that has been accumulating at abnormally-high rates in the past ~100 years is elastic; only a fraction (~10%) of the geodetically observed strain is inelastic, and is accommodated in the NEJ arc as permanent deformation (Ikeda, 1996, 2005, 2006; Ikeda et al., 2012).

Vertical movements

Discrepancy between long-term (geologic) and short-term (geodetic) observations exists also in vertical movements. Figure 6 (right) shows vertical crustal movements revealed by tide-gauge observations during the period 1955-1981 (Kato and Tsumura, 1979; Kato, 1983). Particularly striking in this figure is the fact that the Pacific coast of NEJ and Hokkaido has been subsiding at very high rates. Subsidence rate increases toward the trench, and reaches the maximum value as high as ~10 mm/yr (Fig. 6, right). Time series data at tide gauge stations along the Pacific coast indicates that the rapid subsidence has continued for at least 60-80 years (Fig. 8; Kato and Tsumura, 1979; Kato, 1983; Geographical Information Authority of Japan, 2010).

However, there is no evidence for long-term subsidence along the Pacific coast. Instead, late Quaternary marine terrace data indicate slow uplift (e.g. Koike and Machida, 2001; Ota and Saito, 2001). Figure 6 (left) shows height distribution of Last Interglacial (~125 ka) shorelines. Since the eustatic sea level at the Last Interglacial maximum (LIM; ~125 ka) is believed to be nearly the same as the present-day eustatic sea level, the height of a LIM shoreline relative to the present-day sea level approximately equals the amount of uplift during the past 125 kyr. Rates of uplift thus estimated are 0.1~0.5 mm/yr along the Pacific coast of NEJ and Hokkaido. Such long-term uplift at moderate rates is not local but extensive over the NEJ (Fig.ure 6, left), and is attributed to isostatic uplift due to crustal thickening, which in turn is caused mainly by (inelastic) crustal shortening possibly enhanced by magmatic underplating (Tajikara, 2004; Ikeda et al., 2012).

Scenario of strain buildup and release

Interseismic coupling

Observational data that we have reviewed so far indicate that most of the strain (both vertical and horizontal) that has accumulated in the NEJ arc during the last ~100 years at abnormally high rates is elastic. The cause of the elastic strain buildup is coupling on the plate

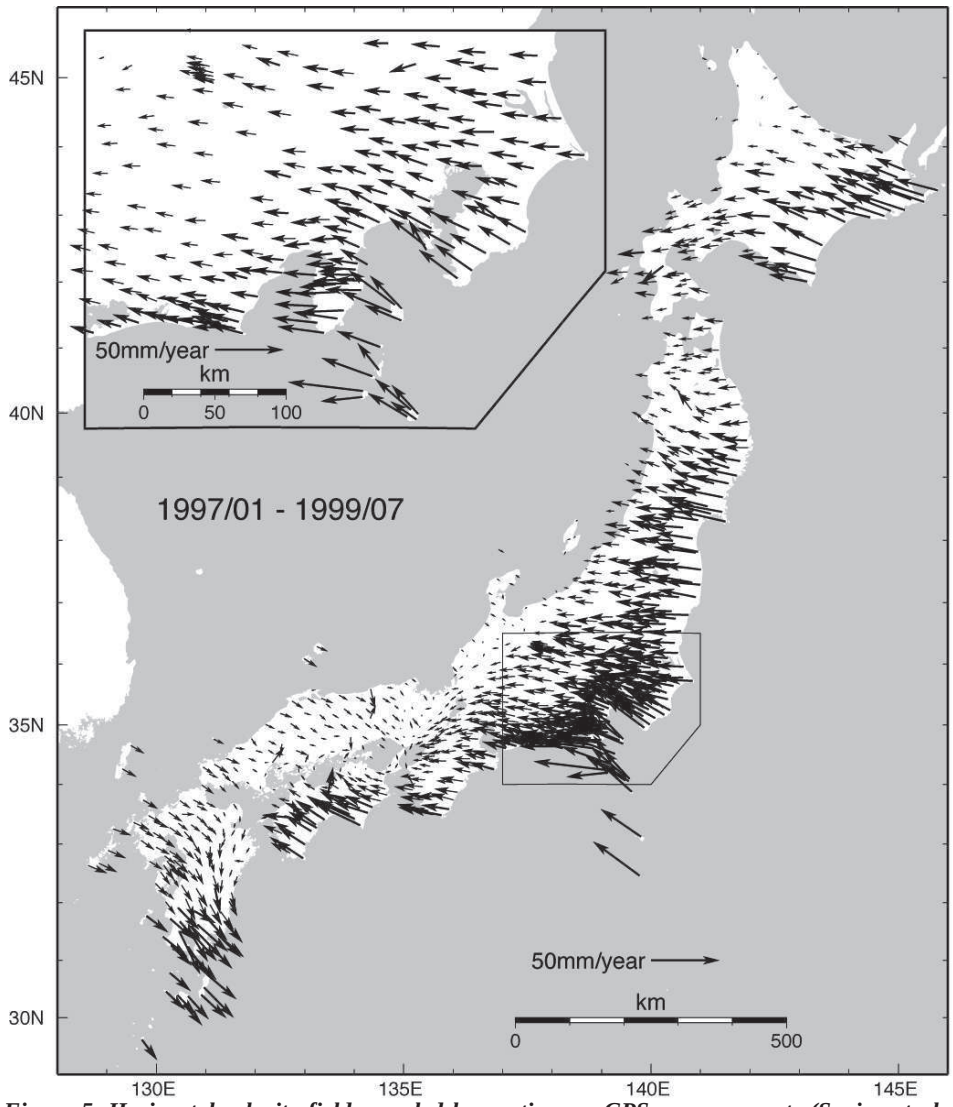

Figure 5. Horizontal velocity field revealed by continuous GPS measurements (Sagiya et al., 2000). Vectors are relative to the stable part of Eurasia. Inset magnifies Kanto area. Note high rates (30-50 mm/yr) of horizontal shortening across Northeast Japan.

interface; the overriding plate is shortened and dragged down by the subducting Pacific plate when the plate interface is mechanically coupled (e.g., Shimazaki, 1974). Fig. 7 shows calculated pattern of interseismic deformation along a transect crossing the Northeast Japan and the Japan Trench. The calculation was performed by the simple back-slip model (Savage, 1983) in an elastic half space. Since a calculated pattern of displacements is sensitive to the geometry of plate interface, we determined the geometry by using a simple elastic plate-bending model (e.g., Watts, 2001) fitted with hypocenter distribution (Hasegawa et al., 1994).

In the NEJ-Kuril subduction zone, the depth to the down-dip limit of subduction-type earthquakes (i.e., shallow-angle, thrust-type earthquakes that occur on the plate interface) is about 50 km, which is similar to (or slightly deeper than) those in other subduction zones in the world (i.e., Oleskevich et al., 1999). Many researchers have believed that subduction interface deeper than the ~50 km down-dip limit is not coupled. However, the observed interseismic subsidence along the Pacific coast (Fig. 6, right) cannot be explained by such shallow coupling (Fig. 7). Our forward model calculations indicate that deep coupling (to a depth ~100 km) and a back-slip rate of 50 mm/yr is needed to subside the Pacific coast at a maximum rate ~10 mm/yr (Ikeda et al., 2012; Fig. 7).

Recent studies of GPS data inversion have yielded significantly different patterns of slip deficit on the Kuril-Japan trench plate interface. Suwa et al. (2006) indicated that the crustal deformation over the NEJ arc is well reproduced by deep coupling to a depth of ~100 km, whereas Nishimura et al. (2004) and Hashimoto et al. (2009) estimated shallower coupling at seismogenic depths (0~50 km). Suwa et al. (2006) assumed dislocation sources only on the plate interface, and attributed all the observed crustal deformation to slip on the plate interface. In this sense, the model of Suwa and others (2006) is identical to our model (Figs 7 and 9). On the other hand, Nishimura et al. (2004) assumed dislocation sources not only on the Pacific side but also on an "incipient collision zone", which was supposed to exist along the Japan Sea coast "absorbing" crustal deformation on the backarc side (west of the volcanic front) of the NEJ are. This is the reason why Nishimura et al. (2004) failed to detect deep coupling on the Kuril-Japan subduction interface. It is not clear why the results of Hashimoto and others (2009) differ from those of Suwa and others (2006) and our results. It should be pointed out, however, that their slip-deficit distribution does not account for the observed rapid subsidence along the Pacific coast, but instead produces rapid uplift along the coast (Supplementary Fig. 2 of Hashimoto et al., 2009) as is predicted by the shallow coupling model of this study (Fig. 7).

Episodic decoupling

Both horizontal contraction and coastal subsidence in the NEJ arc in interseismic periods result from a common cause; i.e., the dragging force produced by the subducting slab (Fig. 1). The elastic strain that had progressively been built up in and around the NEJ subduction zone until March 11, 2011, was to be eventually released in association with episodic slip on the plate interface that had been coupled so far. However, many seismologists believed, before the Tohoku gigantic earthquake of 2011, that elastic strain due to interseismic coupling should have been released by many subduction-type Mw 7~8 earthquakes that have occurred during the past ~100 years (Fig. 8, left). Their belief was based on the asperity hypothesis, which assumes decoupled (or very weakly coupled) plate interface outside asperity patches (e.g., Yagi, 2011; Iio and Matsuzawa, 2012). Their belief was based also on an implicit assumption that the strain buildup during the past ~100 years at high rates should have been mostly inelastic without any sound theoretical or observational justification.

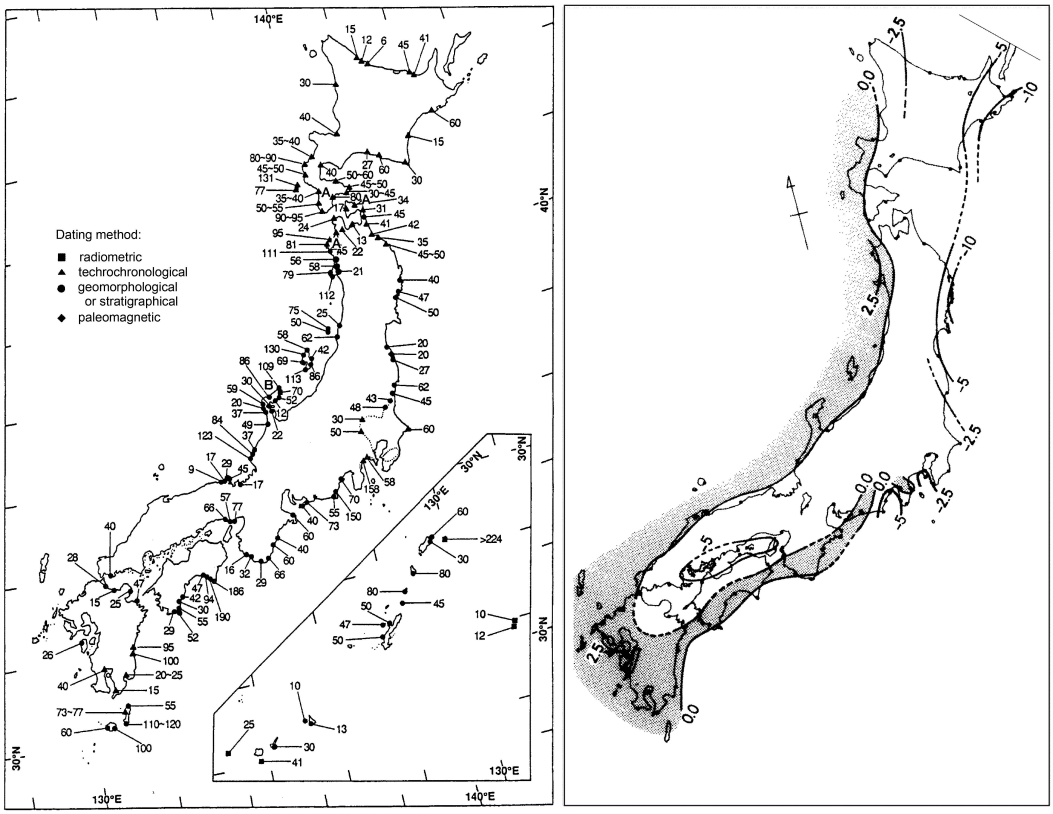

Figure 6. Rates of vertical deformation over the Japan arc on different time scales. [Left] Height distribution (in meters) of Last Interglacial (~125 ka) shorelines (Ota and Saito, 2001). [Right] Recent vertical crustal movements revealed by tide-gauge observations during the period 1955-1981 (Kato, 1983). Contours indicate rates of uplift (in mm/yr). Shadow indicates uplift. Note that the Pacific coast of NEJ and Hokkaido has been subsiding at extremely high rates (as large as 10 mm/yr), whereas marine terrace data (left figure) indicate moderate rates (0.1-0.5 mm/yr) of uplift.

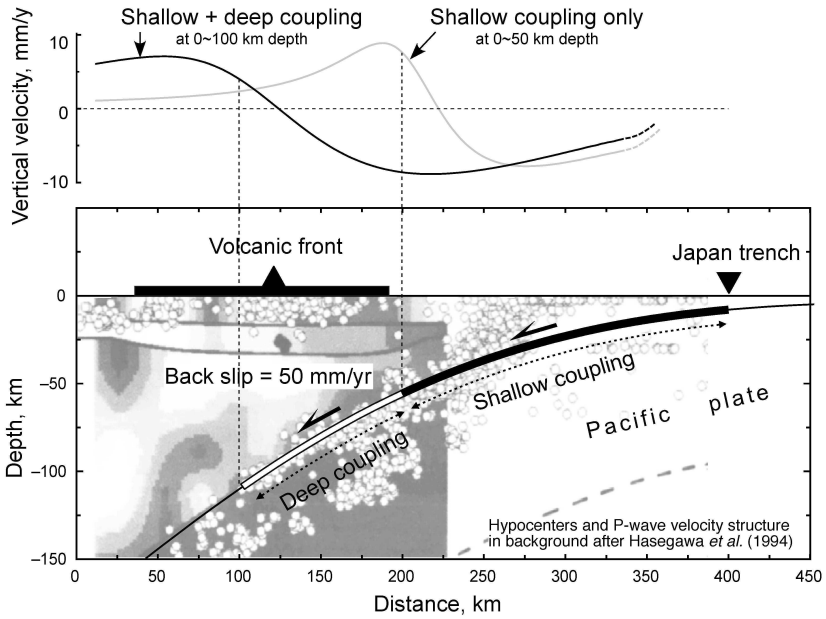

Figure 7. [Top] Calculated patterns of interseismic deformation along a transect crossing the NEJ arc and the Japan Trench (Ikeda et al., 2012). Calculations were performed by using a dislocation fault model in an elastic half space. Gray line curve shows interseismic deformation caused by shallow coupling (thick black line in the bottom figure) on the plate interface at 0~50 km depths. Black line curve shows interseismic deformation caused by deep coupling (thick black line plus thick white line in the bottom figure) at 0~100 km depths. A uniform back-slip rate of ~50 mm/yr over the deeply coupled plate interface is needed to subside the Pacific coast at a maximum rate ~10 mm/yr. [Bottom] Geometry of plate interface along the same transect as of the top figure. Earthquake hypocenters and P-wave velocity structure in the background are after Hasegawa et al. (1994) using tomography data by Zhao et al. (1992).

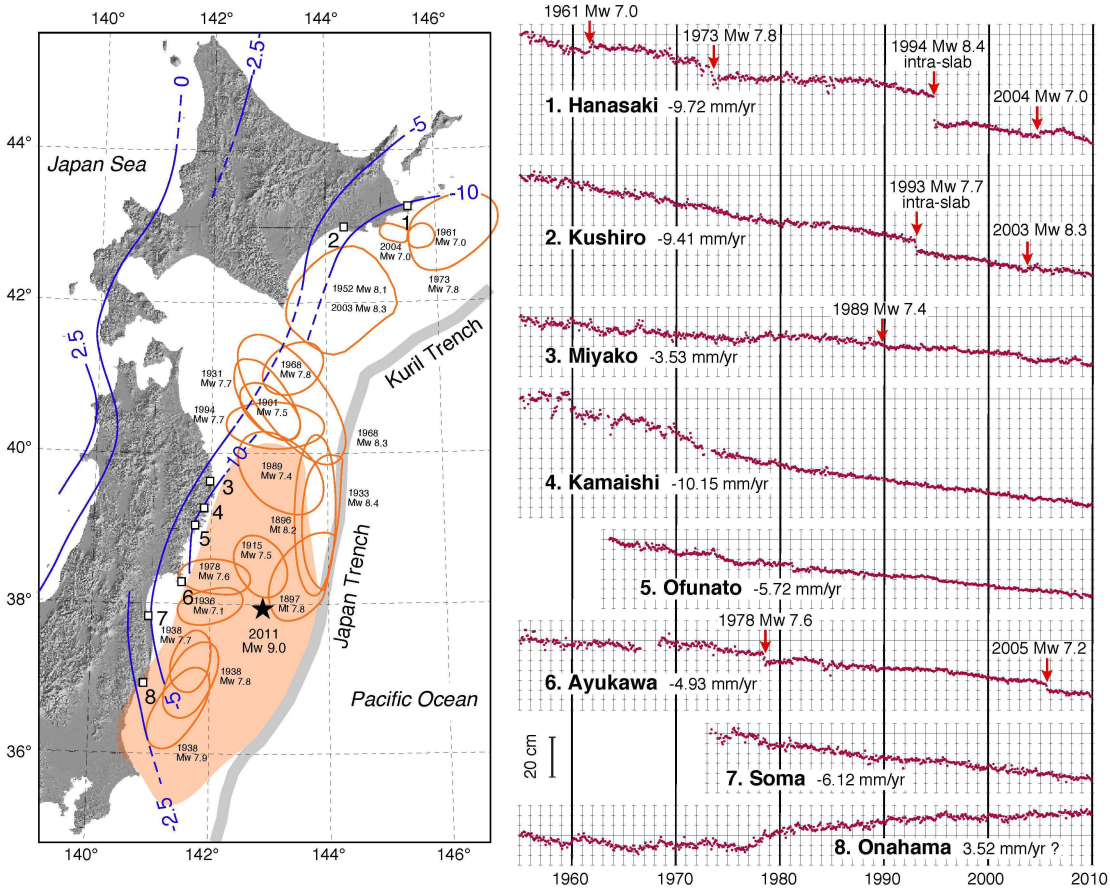

Figure 8. [Left] Map showing recent vertical crustal movements and source areas of large subduction earthquakes (Ikeda et al., 2012). Contour lines (in blue) indicate rates of uplift (in mm/yr) revealed by tide gauge observations during the period 1955-1981 (Kato, 1983). Open ovals indicate source areas of subduction earthquakes of Mw ≥ 7.0 since 1896. The epicenter and source area of the 2011 Tohoku earthquake of Mw 9.0 are indicated by an asterisk and a shaded oval (in orange), respectively. Open squares indicate tide-gauge stations; station numbers correspond to those in the right figure. [Right] Selected tide-gauge records along the Pacific coast (Geographical Information Authority of Japan, 2010). See the left figure for the location of each station. Arrows indicate large earthquakes (Mw ≥ 7.0) that occurred near each station. Note progressive subsidence of the Pacific coast at rates as high as 5-10 mm/yr, except for the Onahama station, which has likely been affected by coal mining.

However, tide-gauge records along the Pacific coast have indicated progressive subsidence due to strong drag of the subducting Pacific plate during the past 60-80 years (Fig. 8). It is clearly demonstrated in this figure that subduction earthquakes of Mw 7~8 during this period had nothing to do with strain release, i.e., uplifting the Pacific coast. Instead, some of these Mw 7~8 earthquakes further enhanced coastal subsidence (Fig. 8, right).

As shown in Figure 8 (left), the source areas of these Mw 7-8 earthquakes are just small patches isolated within the coupled plate interface as wide as ~300 km. (compare Figs 7 and 8.). Slip on such small patches is far from sufficient to cause full strain release, and therefore crustal strain was not effectively released in association with these Mw 7~8 earthquakes. As discussed earlier in this paper, a full strain-release event should have a rupture surface that extends along-dip over the whole width (W_c) of the coupled plate interface and extends along strike for more than 2~3 times as long as W_c. For instance, the 2003 Tokachi-oki earthquake of Mw 8.3 (for location, see Fig. 3 left) was produced by slip on a rupture surface ~150 km wide and ~150 km long; the rupture did not reach the free surface and hence was “closed-ended”. For these reasons, it released elastic strain just partially.

The 2011 Tohoku earthquake of Mw 9.0

Coseismic deformation

It seemed likely that the 2011 earthquake of Mw 9.0 is a *full strain-release event*, because its rupture surface (~500 km long along strike and ~200 km wide) encompassed those of previously occurred Mw 7~8 subduction earthquakes (Fig. 8, left). However, the Pacific coast was not uplifted but further subsided by 120 cm at the maximum (Geographical Information Authority of Japan, 2011). This is because the down-dip limit of the coseismic rupture was ~50 km deep, and the deeper coupled interface (50~100 km depths) remains still unbroken (Fig. 9). Note again that the down-dip limit of the 2011 coseismic rupture coincides approximately with the maximum depth of previously occurred subduction-type earthquakes in the NEJ-Kuril subduction zone. Then, what will happen on the deeper coupled interface?

Postseismic deformation

Paleoseismological observations give some insights into the

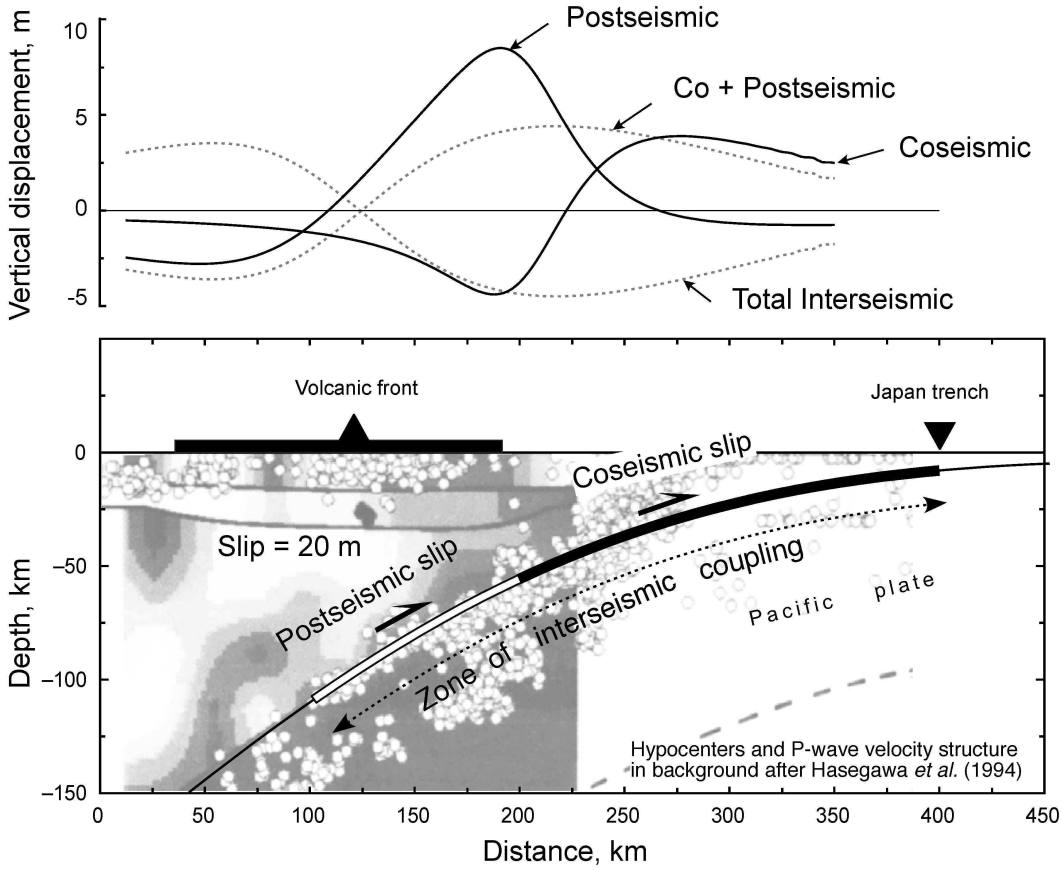

Figure 9. Coseismic, postseismic and interseismic deformation during a whole cycle of strain buildup and release over the Northeast Japan arc–trench system (Ikea et al., 2012). The line of profile and the geometry of plate interface are the same as those in Figure 7. Total amount (= 20 m) of back slip is given over the coupled plate interface at 0-100 km depths; slip is assumed to be uniform (20 meters) over the coupled portions of the plate interface down to ~100 km depth. Coseismic slip on the shallow plate interface at 0-50 km depths results in coseismic subsidence along the Pacific coast, whereas subsequent aseismic slip at 50-100 km depths causes uplift, thereby cancelling both the interseismic and the coseismic subsidence along the Pacific cast. The 2011 Tohoku event is unique in that the decoupling occurs seismically on the shallower interface (0~50 km depths) and probably aseismically on the deeper interface (50~100 km depths).

decoupling process below seismogenic depths in the NEJ-Kuril subduction zone. Paleo-tsunami and coastal-uplift evidence has indicated the occurrence of a gigantic earthquake off the Pacific coast of Hokkaido in the 17th century (Hirakawa, 2000; Atwater et al., 2004; Nanayama et al., 2003). Atwater et al. (2004) and Sawai et al. (2004) investigated coastal uplift associated with this 17th-century event on the basis of environmental-change analysis using diatom microfossils in tidal-flat sediments, and found that, following the deposition of tsunami sand, the tidal flat was gradually uplifted for tens of years to become emerged.

The above observations suggest that, in the NEJ-Kuril subduction zone, the deep decoupling at 50~100 km depths occurs aseismically following a sudden (i.e., seismic) decoupling event at shallower depths (0~50 km). Simple dislocation calculation (Fig. 9) predicts that aseismic after-slip on the deeper coupled interface would cause uplift along the Pacific coast of the NEJ and eventually would cancel the subsidence that has been accumulated before and during the 2011 Tohoku earthquake (Ikeda et al., 2012).

Uplift along the Pacific coast has been detected by GPS observations at rates of 5~8 cm/month during one month after the 2011 earthquake (Geographical Information Authority of Japan, 2011), and is continuing at reduced but quite constant rates (~1 cm/month) as of May 2014. Ozawa et al. (2011) analyzed geodetic data in just a short period (10 days) following the 2011 earthquake. Their analysis indicated that, during this short period, after-slip occurred dominantly on the shallower plate interface (0~50 km deep), but significantly on the deeper interface to a depth of 90-100 km beneath the volcanic front (Fig.s 2b and 3 of Ozawa et al., 2011). GPS time-series data in the past 2-3 years clearly indicate constant uplift at a rate of ~1 cm/month as of May 2014 (Geographical Information Authority of Japan, 2014a, 2014b); the area of the recent uplift extends far inland to the volcanic front, resembling the predicted pattern of vertical movements due to deep after-slip at 50-100 km depths (Fig. 9). Visco-elastic effects, if existed, would decay exponentially with time, but were not significantly detected from recent GPS data.

Although visco-elastic relaxation in the upper mantle may have caused part of the post-2011 vertical deformation in the NEJ arc, it cannot account for the cancellation of the large amount of coastal subsidence that had been built up until and during the 2011 earthquake. Viscosity of the upper mantle causes only a subtle amount of deformation (< 10%) in total compared with near-field (i.e., near the dislocation source) coseismic deformation, because it just damps the elastic response of the overlying lithosphere due to dislocation within the lithosphere (e.g., Matsu'ura and Tanimoto, 1981). Tide-gauge

records suggest that the total seismic and interseismic subsidence along the Pacific coast of Tohoku is as large as 5-10 meters on an assumption of 500-1000 year recurrence of Mw 9 events. Such a large amount of deformation can never be cancelled through visco-elastic relaxation. Thus, the only plausible mechanism for causing large postseismic recovery would be after-slip on the deeper part of the subduction interface (Fig. 9).

Gigantic decoupling cycles

Recurrence interval of gigantic decoupling events from the NEJ-Kuril subduction zone not only is a key to quantitatively understanding the strain buildup-and-release process, but also is crucial to assess earthquake hazards. Studies of tsunami deposits in Sendai-Ishinomaki area first revealed that a tsunami with large inundation depths and distances occurred in association with the AD 869 Jogan earthquake (Minoura and Nakaya, 1991; Minoura et al., 2001; Sawai et al., 2008). The magnitude of the tsunami is similar to that associated with the 2011 earthquake. Therefore, the AD 869 Jogan earthquake could be a predecessor of the 2011 earthquake of Mw 9.0. Hirakawa (2000) examined tsunami deposits at many sites at different altitudes along the Hokkaido coast, and revealed that tsunamis with exceptionally large inundation heights have repeatedly occurred at an average recurrence interval about 500 years. Thus, available data suggest that the recurrence interval of gigantic decoupling events is 500-1100 years. It should be noted, however, that tsunami evidence is not sensitive to discriminating between full and partial strain-release events. More direct evidence is coastal uplift and subsidence, as discussed in the next section.

A global comparison

A global survey was made of subduction zones that have produced gigantic (Mw ≥ 9.0) earthquakes. It was found that these subduction zones are classified, in terms of coupling–decoupling behavior, into two types: (1) the Northeast Japan type and (2) the Chilean type (Fig. 10; Ikeda et al., 2012).

The Chilean type strain buildup/release process is simple and straightforward in the sense that seismogenic zone (down to a 40-50 km depth) plays everything (Fig. 10a). The source areas of the 1960 Chile, 1964 Alaska, and 1700 Cascadia earthquakes lack evidence for interseismic deep coupling. Paleoseismological evidence indicates interseismic uplift around the down-dip edge of coseismic rupture, where coseismic subsidence is observed (e.g., Atwater, 1987; Atwater et al., 1992; Cisternas et al., 2005; Shennan and Hamilton, 2006). This implies that the deeper plate interface is basically decoupled in interseismic periods, although subtle postseismic slip could exist on a transition zone down-dip of the coseismic rupture (e.g., Wang et al., 2003; Freymueller et al., 2000; Suito and Freymueller, 2009). In the Chilean-type subduction zones, both transitional after slip and visco-elastic relaxation in the upper mantle would cause postseismic coastal uplift. However, such postseismic deformation would be much less in total amount than, and difficult to distinguish from, interseismic coastal uplift due to restored coupling on the plate interface.

On the other hand, the Northeast Japan type strain buildup/release process seems to be exceptional (Fig. 10b). In the Northeast Japan subduction zone, interseismic coupling occurs to a depth as deep as ~100 km. Its decoupling process is two-fold: seismic decoupling occurs only on the shallower plate interface (0~50 km depths) while

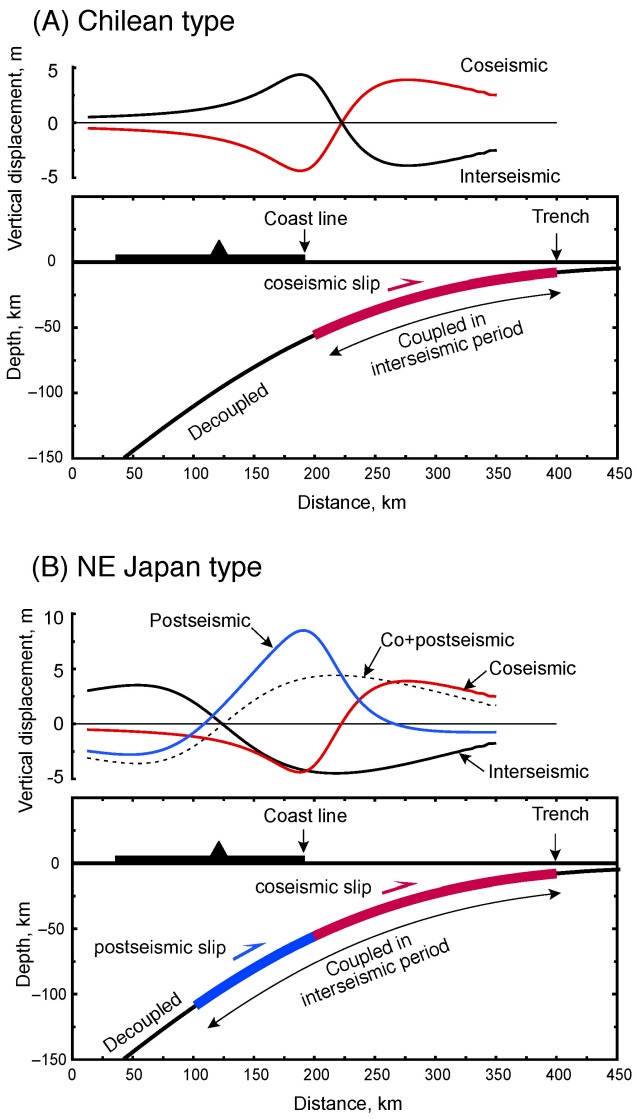

Figure 10. Two types of strain buildup and release at subduction zones that produce gigantic (Mw ≥ 9.0) subduction earthquakes (Ikeda et al., 2012). The geometry of plate interface and amounts of surface deformation could be arbitrary but are represented in this figure by those of the 2011 Tohoku earthquake (Figures 7 and 9). (A) Chilean type strain buildup/release process. Interseismic deformation is basically opposite to coseismic deformation. (B) Northeast Japan type strain buildup/release process, characterized by deep interseismic coupling to a depth ~100 km. Seismic decoupling occurs only on the shallower plate interface (0~50 km depths), while the deeper interface (50~100 km depths) decouples aseismically following the earthquake. Note that coseismic and postseismic deformation in total is just opposite to total interseismic deformation.

the deeper interface (50~100 km depths) decouples aseismically following the earthquake. Although we do not know the mechanism controlling the complex behavior of the NEJ-Kuril subduction zone, a possible cause for such deep coupling would be thermal. The oceanic lithosphere of the western Pacific is very old and therefore cold, and it has been subducted beneath the NEJ-Kuril arc. The cold slab may affect rheological properties of the plate interface at depth.

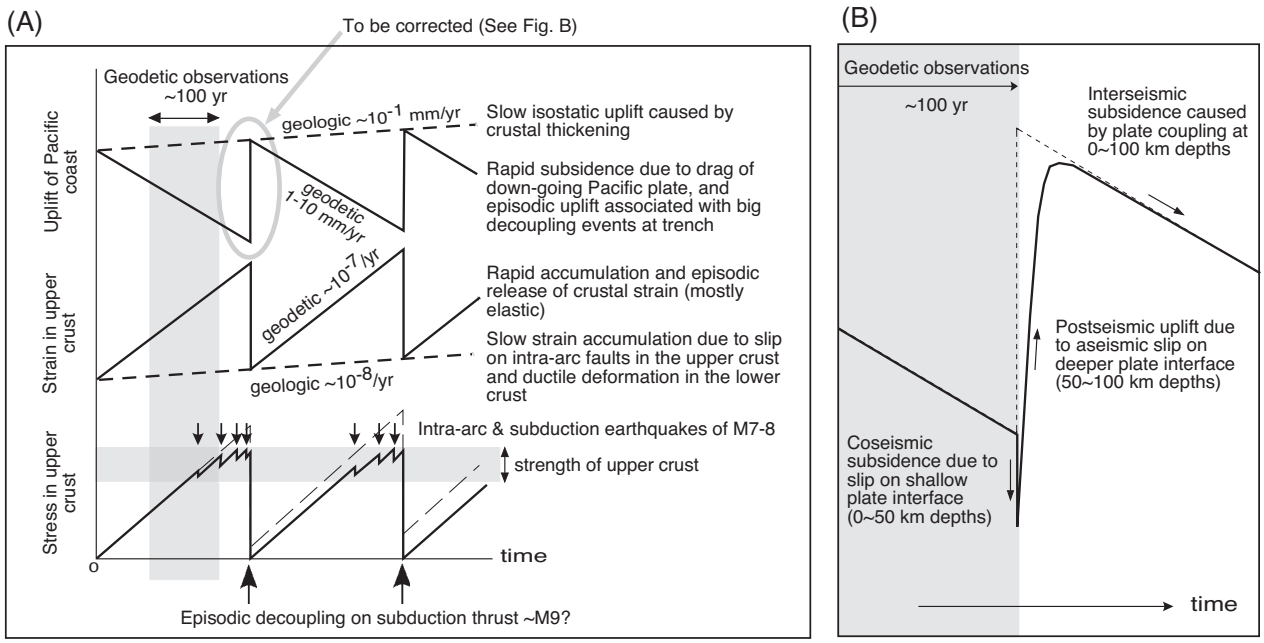

Figure 11. Summary of strain buildup and release in the NEJ arc (Ikeda et al., 2012). (A) The process of strain buildup and release in the NEJ arc proposed by Ikeda (2003, 2005, 2006). A modification is needed for detailed coseismic response. (B) Coseismic response associated with two-fold decoupling. Observations of the 2011 Tohoku earthquake (Mw 9.0) indicated that coseismic slip occurs only on the shallower part (0~50 km depths) of the locked plate interface, resulting in additional coastal subsidence. Following the main shock, aseismic slip occurs on the deeper plate interface (50-100 km depths), thereby resulting in postseismic coastal uplift.

Conclusions

There has been a discrepancy between long-term (geologic) and short-term (geodetic) strain observations in both horizontal and vertical directions over the NEJ arc. Geodetic observations in the past ~100 years have revealed strain accumulation over the NEJ arc at a rate as high as 10^{-7} strain/yr, whereas geologically observed strain rates are one order of magnitude slower (Figs 3, 5 and 11a). A similar discrepancy exists also in vertical movements; tide gauge records along the Pacific coast have indicated subsidence at a rate as high as ~10 mm/yr during the last ~80 years, despite the fact that Late Quaternary marine terraces along the Pacific coast indicate long-term uplift at 0.1-0.5 mm/yr (Figs 6, 8 and 11a). Thus, most of the strain accumulated in the last 100 years at unusually high rates is elastic, and is to be released by slip on the coupled plate interface. Only a fraction (~10%) of geodetically-observed crustal shortening is accommodated within the NEJ arc as long-term (inelastic) deformation (Fig. 11a).

In order to release the elastic strain that has been accumulating at high rates, a large slip event is needed. Although a number of large (Mw 7~8) subduction earthquakes have occurred in the past ~100 years, they had nothing to do with strain release or coastal uplift (Fig. 8); this is because their rupture areas were only small isolated patches in the ~300 km wide zone of coupled plate interface (Figs. 7 and 8 left). The 2011 earthquake of Mw 9.0, whose rupture surface encompassed those of previously occurred Mw 7-8 earthquakes, is likely to be such a decoupling event that effectively releases elastic strain due to plate coupling. However, at 50~100 km depths down-dip of the 2011 rupture, there still exists a coupled part of plate interface, on which a large amount of aseismic after-slip may occur in the coming decades (Fig. 11b).

We conclude that a full elastic-strain-release event on the NEJ-Kuril subduction zone is two-fold: seismic slip on the shallower plate interface (0~50 km deep), and aseismic slip on the deeper interface (50~100 km deep) following the seismic slip (Figs 9, 10b, 11b). The two-fold decoupling behavior of the NEJ-Kuril subduction zone could be unique. A global survey was made of other subduction zones that produced gigantic (Mw ≥ 9.0) earthquakes, but no such deep coupling was found (Fig. 10a).

Acknowledgements

I would like to thank Yujiro Ogawa and Yildirim Dilek for their editorial comments and suggestions on the manuscript, and Kiichiro Kawamura and Teruyuki Kato for reviewing the manuscript. This paper benefited greatly from many in-depth comments by Teruyuki Kato.

References

Atwater, B.F., 1987, Evidence for great Holocene earthquakes along the outer coast of Washington State: Science, v. 236, pp. 942-944.

Atwater, B.F., Jiménez, N.H. and Vita-Finzi, C., 1992, Net late Holocene emergence despite earthquake-induced submergence, south-central Chile: Quaternary International, v. 15/16, pp. 77—85.

Atwater, B.F., Furukawa R., Hemphill-Haley, E., Ikeda Y., Kashima K., Kawase K., Kelsey, H.M., Moore, A.L., Nanayama F., Nishimura Y., Odagiri S., Ota Y., Park S.C., Satake K., Sawai Y., and Shimokawa K., 2004, Seventeenth-century uplift in eastern Hokkaido, Japan: Holocene, v. 14, pp. 487-501.

Bilham, R., Engdahl, E.R., Feldl, N., and Satyabala, S.P., 2005, Partial and complete rupture of the Indo-Andaman plate boundary 1847-2004: Seismological Research Letters, v. 76, pp. 299-311, doi: 10.1785/gssrl.76.3.299.

Cisternas, M., Atwater, B.F., Torrejon, F., Sawai, Y., Machuca, G., Lagos, M., Eipert, A., Youlton, C., Salgado1, I., Kamataki, T., Shishikura, M., Rajendran, C.P., Malik, J.K., Rizal, Y. and Husni, M., 2005, Predecessors of the giant 1960 Chile earthquake: Nature, v. 437, pp. 404-407.

Freymueller, J.T., Cohen, S.C., Fletcher, H.J., 2000, Spatial variations in present-day deformation, Kenai Peninsula, Alaska, and their implications: Journal of Geophysical Research, v. 105, pp. 8079-8101.

Fujii, Y., and Matu'ura, M., 2000, Regional difference in scaling laws for large earthquakes and its tectonic implication: Pure and Applied Geophysics, v. 157, pp. 2283-2302.

Geist, E. and Dmowska, R., 1999, Local tsunamis and distributed slip at the source: Pure and Applied Geophysics, v. 154, pp. 485-512.

Geographical Information Authority of Japan, 2010, Crustal deformation of entire Japan: Report of the Coordinating Committee for Earthquake Prediction, v. 84, pp. 8-31 (in Japanese).

Geographical Information Authority of Japan, 2011, Crustal movements in the Tohoku district: Report of the Coordinating Committee for Earthquake Prediction, v. 86, pp. 184-272 (in Japanese).

Geographical Information Authority of Japan, 2014a, Crustal movements in the Tohoku district: Report of the Coordinating Committee for Earthquake Prediction, v. 91, pp. 77-104 (in Japanese).

Geographical Survey Institute, 2014b, Crustal movements in the Tohoku district: Report distributed at the 203rd Coordinate Committee on the Earthquake Prediction, May 19, 2014.

Goldfinger, C., Ikeda, Y., Yeats, R.S., and Ren, J., 2013, Superquakes and supercycles: Seismological Research Letters, v. 84, n. 1, pp. 24-32, doi: 10.1785/0220110135.

Hasegawa, A., Horiuchi, S., and Umino, N., 1994, Seismic structure of the northeastern Japan convergent margin: A synthesis: Journal of Geophysical Research, v. 99, pp. 22,295-22,311.

Hashimoto, C., Noda, A., Sagiya, T., and Matsu'ura, M., 2009, Interplateseismogenic zones along the Kuril–Japan trench inferred from GPS data inversion, Nature Geoscience, v. 2, 141-144.

Hirakawa, K., Nakamura, Y. and Haraguchi, T., 2000, Gigantic tsunamis along the Pacific coast of Hokkaido and their recurrence intervals: The Earth Monthly, Spec. Issue, v. 28, pp. 154-161 (in Japanese).

Iio, Y., and Matsuzawa, T., 2012, The generation process of the Tohoku earthquake: Why did the magnitude 9 event occur?: Journal of the Geological Society of Japan, v. 118, 248-277, doi: 10.5575/geosoc.2012.0023 (in Japanese with English Abstract).

Ikeda, Y., 1996, Implications of active fault study for the present-day tectonics of the Japan arc: Active Fault Research, v. 15, pp. 93-99 (in Japanese with English Abstract).

Ikeda Y., 2005, Long-term and short-term rates of horizontal shortening over the Northeast Japan arc: Hokudan International Symposium on Active Faulting, Hokudan City, Japan, January 17-24, 2005, Program and Abstracts, pp. 48-49.

Ikeda Y., 2006, Long-term and short-term rates of crustal deformation over the northeast Japan arc, and their implications for gigantic earthquakes at the Japan Trench: International Workshop on Tectonics of Plate Convergence Zones, University of Tokyo, Sep. 28-29, 2006, Program and Abstracts, pp. 64-68.

Ikeda, Y., Okada, S., and Tajikara, M., 2012, Long-term strain buildup in the Northeast Japan arc-trench system and its implications for gigantic strain-release events: Journal of the Geological Society of Japan, v. 118, pp. 294-312, doi: 10.5575/geosoc.2012.0018 (in Japanese with English Abstract).

Iwasaki, T., Kato, W., Moriya, T., Hasemi, A., Umino, N., Okada, T., Miyashita, K., Mizogami, T., Takeda, T., Sekine, S., Matsushima, T., Tashiro, K., and Miyamachi, H., 2001, Extensional structure in northern Honshu arc as inferred from seismic refraction/wide-angle reflection profiling: Geophysical Research Letters, v. 28, pp. 2329-2332.

Kaneoka, I., Takigami, Y., Takaoka, N., Yamashita, S., and Tamaki, K., 1992, 40Ar-39Ar analysis of volcanic rocks recovered from the Japan Sea floor: constraints on the age of formation of the Japan Sea: Proceedings of the Ocean Drilling Program, Scientific Results, v. 127/128, Pt. 2, pp. 819-836.

Kato, T. and Tsumura, K. (1979). "Vertical land movement in Japan as deduced from tidal record (1951-1978)," Bull. Earthquake Res. Inst., v. 54, pp. 559-628 (in Japanese with English Abstract).

Kato, T., 1983, Secular and earthquake-related vertical crustal movements in Japan as deduced from tidal records (1951–1981): Tectonophysics, v. 97, pp. 183-200.

Koike, K., and Machida, H., eds, 2001, Atlas of Quaternary Marine Terraces in the Japanese Islands: University of Tokyo Press (in Japanese).

Le Pichon, X., and Sibuet, J.C., 1981: Passive margins – a model of formation: Journal of Geophysical Research, v. 86, pp. 3708-3720.

Matsuda, T., Nakamura, K., and Sugimura, A., 1967, Late Cenozoic orogeny in Japan: Tectonophysics, v. 4, pp. 349-366.

Matsu'ura, M., and Sato, T., 1997, Loading mechanism and scaling relations of large interpolate earthquakes: Tectonophysics, v. 227, pp. 189–198.

Matsu'ura, M. and Tanimoto, T., 1981, Quasi-static displacements due to faulting in a layered half-space with an intervenient visco-elastic layer: Journal of Physics of the Earth, v. 29, 23-54.

McKenzie, D., 1978, Some remarks on development of sedimentary basins: Earth and Planetary Science Letters, v. 40, pp. 25-32.

Minoura, K., Imamura, F., Sugawara, D., Kono, Y., and Iwashita, T., 2001, The 869 Jogan tsunami deposit and recurrence interval of large scale tsunami on the Pacific coast of northeastern Japan: Journal of Natural Disaster Science, v. 23, pp. 83–88.

Minoura, K., and Nakaya, S., 1991, Traces of tsunami preserved in intertidal lacustrine and marsh deposits: Some examples from northeast Japan: Journal of Geology, v. 99, pp. 265-287.

Moriya, S., Chinzei, K., Nakajima, T., and Danhara, T., 2008, Uplift of the Dewa Hills recorded in the Pliocene paleogeographic change of the western Shinjobasin, Yamagata Prefecture: Journal of the Geological Society of Japan, v. 114, pp. 389-304 (in Japanese with English abstract).

Nakane, K., 1973, Horizontal tectonic strain in Japan (I) and (II): Journal of the Geodetic Society of Japan, v. 19, pp. 190-199 and 200-208 (in Japanese with English abstract).

Nanayama, F., Satake, K., Furukawa, R., Shimokawa, K., Atwater, B.F., Shigeno, K., and Yamaki, S., 2003, Unusually large earthquakes inferred from tsunami deposits along the Kuril trench: Nature, v. 424, pp. 660-663.

Nishimura, T., Hirasawa, T., Miyazaki, S., Sagiya, T., Tada, T., Miura, S., and Tanaka, K., 2004, Temporal change of interplate coupling in northeastern Japan during 1995-2002 estimated from continuous GPS observations: Geophysical Journal International, v. 157, 901-916.

Okada, S., and Ikeda, Y., 2012, Quantifying crustal extension and shortening in the back-arc region of Northeast Japan: Journal of Geophysical Research, v.117, B01404, doi: 10.1029/2011JB008355.

Oleskevich, D.A., Hyndman, R.D., and Wang, K., 1999, Theupdip and downdip limits to great subduction earthquakes: Thermal and structural models of Cascadia, south Alaska, SW Japan, and Chile: Journal of Geophysical Research, v. 104, pp. 14,965–14,991, doi: 10.1029/1999JB900060.

Ota, Y., and Saito, K., 2001, Terrace topography, in Yonekura, N., Kaizuka, S., Nogami, M., and Chinzei, K., eds, Regional Geomorphology of the Japanese Islands, Volume 1: University of Tokyo Press, Tokyo, Japan, pp. 222-237 (in Japanese).

Otofuji, Y., Matsuda, T., and Nohda, S., 1985, Opening mode of the Japan Sea inferred from the palaeomagnetism of the Japan arc: Nature, v. 317, pp. 603-604.

Ozawa, S., Nishimura, T., Suito, H., Kobayashi, T., Tobita, M., and Imakiire, T., 2011, Coseismic and postseismic slip of the 2011 magnitude-9 Tohoku-Oki earthquake: Nature, v. 745, 373-377, doi:10.1038/nature10227.

Rudnicki, W., and Wu, M., 1995, Mechanics of dip-slip faulting in an elastic half-space: Journal of Geophysical Research, v. 100, pp. 22,173-22,186.

Ruff, L., and Kanamori, H., 1980, Seismicity and the subduction process:Physics of the Earth and Planetary Interiors, v. 23, pp. 240–252.

Sagiya T., Miyazaki, S., and Tada, T., 2000, Continuous GPS array and present-day crustal deformation of Japan: Pure and Applied Geophysics, v. 157, pp. 2303-2322.

Sato, H., 1989, Degree of deformation of late Cenozoic strata in the northeast Honshu arc: Memoirs of the Geological Society of Japan, v. 32, pp. 257-268 (in Japanese with English abstract).

Sato, H., 1994, The relationship between Late Cenozoic tectonic events and stress-field and basin development in northeast Japan: Journal of Geophysical Research, v. 99, pp. 22261-22274.

Sato, H., and Amano, K., 1991, Relationship between tectonics, volcanism, sedimentation and basin development, Late Cenozoic, central part of northern Honshu, Japan: Sedimentary Geology, v. 74, pp. 323-343.

Sato, H., Yoshida, T., Iwasaki, T., Sato, T., Ikeda, Y., and Umino, N., 2004, Late Cenozoic tectonic development of the back arc region of central northern Honshu, Japan, revealed by recent deep seismic profiling: Journal of the Japanese Association of Petroleum Technology, v. 69, pp. 145-154 (in Japanese with English abstract).

Savage, J. C., 1983, A dislocation model of strain accumulation and release at a subduction zone: Journal of Geophysical Research, v. 88, pp. 4984-4996.

Sawai, Y., Satake, K., Kamataki, T., Nasu, H., Shishikura, M., Atwater, B.F., Horton, B.P., Kelsey, H.M., Nagumo, T., and Yamaguchi, M., 2004, Transient uplift after a 17th-century earthquake along the Kuril subduction zone: Science, v. 306, pp. 1918-1920, doi: 10.1126/science.1104895.

Sawai, Y., Shishikura, M., and Komatsubara, J., 2008, A study on paleotsunami using hand corer in Sendai plain (Sendai City, Natori City, Iwanuma City, Watari Town, Yamamoto Town), Miyagi, Japan: Annual Report on Active Fault and Paleoearthquake Researches, Geological Survey of Japan, AIST, n. 8, pp. 17-70 (in Japanese with English abstract).

Shennan, I., and Hamilton, S., 2006, Coseismic and pre-seismic subsidence associated with great earthquakes in Alaska: Quaternary Science Reviews, v. 25, pp. 1–8.

Shimamoto, T., 1989, Rheology of rocks and plate tectonics: From rigid plates to deforming plates: Kagaku, v. 59, pp. 170-180 (in Japanese).

Shimazaki, K., 1974, Pre-seismic crustal deformation caused by an underthrusting oceanic plate, in eastern Hokkaido, Japan: Physics of the Earth and Planetary Interiors, v. 8, pp. 148-157.

Suito, H., and Freymueller, J.T., 2009, A viscoelastic and afterslippostseismic deformation model for the 1964 Alaska earthquake: Journal of Geophysical Research, v. 114, B11404, doi: 10.1029/2008JB005954.

Suwa, Y., Miura, S., Hasegawa, A., Sato, T., and Tachibana, K., 2006, Interplate coupling beneath NE Japan inferred from three-dimensional displacement field: Journal of Geophysical Research, v. 111, B04402.

Tajikara M., 2004, Vertical Crustal Movements of the Northeast Japan Arc in Late Quaternary Time: Dr. Thesis, University of Tokyo, 159 pp.

Tamaki, K., Suyehiro, K., Allan, Ingle, J.C. Jr., and Pisciotto, K.A., 1992, Tectonic synthesis and implications of the Japan Sea ODP drilling: Proceedings of the Ocean Drilling Program, Scientific Results, v. 127/128, pt. 2, pp. 1333-1348.

Wang, K., Wells, R., Mazzotti, S., Hyndman, R.D., and Sagiya, T., 2003, A revised dislocation model of interseismic deformation of the Cascadia subduction zone: Journal of Geophysical Research, v. 108, 2026, doi: 10.1029/2001JB001227.

Watts, A.B., 2001, Isostasy and Flexure of the Lithosphere: Cambridge University Press, 458 pp.

Weissel, J.K., and Karner, G.D., 1989, Flexural uplift of rift flanks due to mechanical unloading of the lithosphere during extension: Journal of Geophysical Research, v. 94, pp. 13919-13950.

Wu, M., Rudnicki, J.W., Kuo, C.H., and Keer, L.M., 1991, Surface deformation and energy release rates for constant stress drops lip zones in an elastic half-space: Journal of Geophysical Research, v. 96, pp. 16,509-16,524.

Yagi, Y., 2011, Enhance ocean-floor observation: Nature, v. 473, pp. 147-148.

Yoshida, T., Ohguchi, T., and Abe, T., 1995, Structure and evolution of source area of the Cenozoic volcanic rocks in northeast Honshu arc, Japan: Memoirs of the Geological Society of Japan, v. 44, pp. 263-308 (in Japanese with English abstract).

Zhao, D., Hasegawa, A., and Horiuchi, S., 1992, Tomographic imaging of P and S wave velocity structure beneath northeastern Japan: Journal of Geophysical Research, v. 97, pp. 19,909-19,928.

by Masanobu Shishikura

History of the paleo-earthquakes along the Sagami Trough, central Japan: Review of coastal paleo-seismological studies in the Kanto region

Development of recent research of crustal movement of Japan, Geological Survey of Japan, National Institute of Advanced Science and Technology (AIST), Tsukuba 305-8567, Japan. *E-mail: m.shishikura@aist.go.jp*

Two subduction zone interplate earthquakes have been recorded along the Sagami Trough, the first in AD 1703 (Genroku Earthquake) and the second in AD 1923 (Taisho Earthquake). While the source areas of these two events overlapped within and around the Sagami Bay, the 1703 Genroku Earthquake had a larger rupture area, which propagated to off the Boso Peninsula. Currently, our understanding of prehistorical earthquakes has been facilitated by Holocene marine terraces and tsunami deposits, through which we have come to the understanding that past Kanto earthquakes can be divided into two types – the Taisho-type and the Genroku-type. Taisho-type earthquakes are thought to be more common, occurring approximately every 400 years on average, but after several occurrences (at 2,000-2,700 year intervals) a Genroku-type earthquake would take place and propagate to off the Boso Peninsula. These less frequent coseismic Genroku-type ruptures are not consistent with global navigation satellite system (GNSS) geodetic data, which show strong plate interface coupling in this area due to a high slip-deficit rate. To resolve this discrepancy, it is necessary to consider hypotheses such as changes to the long-term slip-deficit rate, the occurrence of aseismic fault slips, or even the existence of another earthquake type. Furthermore, recent marine terrace survey reports in the Boso Peninsula have shown that the emergent ages between the eastern coast and western coast do not necessarily correlate, which lends credence to the possibility that another earthquake type occasionally occurs in the region off the Boso Peninsula.

Introduction

Located off the Kanto region of central Japan (which includes the Tokyo metropolitan area), the Sagami Trough is a convergent plate boundary extending from Sagami Bay to the area off the Boso Peninsula where the Philippine Sea Plate subducts beneath the North American Plate (Fig. 1). While historical records show that two great earthquakes, the 1703 Genroku Kanto Earthquake (*M* 8.2) and the 1923 Taisho Kanto Earthquake (*M* 7.9) (hereafter, the 1703 Genroku Earthquake and the 1923 Taisho Earthquake, respectively), occurred along this trough (Usami et al., 2013), records of earthquakes occurring before the 1703 Genroku Earthquake are ambiguous.

However, instead of concentrating on the few remaining historical records of past eras, tectonic geomorphological studies have aimed at recovering information on past earthquakes from marine terraces. Such studies have been conducted since the coseismic uplift associated with the 1923 Taisho Earthquake was discovered along the coasts facing the Sagami Trough (Imamura, 1925; Watanabe, 1929). Although the progress of paleoseismological records of the past 40 years in this area has helped elucidate the history and cycle of interplate earthquakes along the Sagami Trough (e.g. Shishikura, 2003), the observed results do not fully agree with more recently obtained geodetical observation data. The resulting contradictions are very important, not only in terms of scientific understanding, but also because of their relevance when formulating disaster prevention plans for metropolitan areas. In fact, Japanese government offices tasked with disaster prevention measures have recently announced seismic hazard breakdowns for Japan's metropolitan areas (Cabinet Office, 2013; Earthquake Research Committee, 2014), but those efforts did not consider this problem in detail.

Therefore, in this paper, I will provide an overview of current research into paleoearthquakes and associated tsunami events in this region, discuss the distribution of the region's seismically active faults, and then examine their possible slip recurrence, terrace uplift magnitudes, and tsunami deposit records.

Historical earthquakes and tsunamis along the Sagami Trough

1923 Taisho Kanto Earthquake

The 1923 Taisho Kanto Earthquake, which killed more than 105,000 people, was one of the worst natural disasters in recorded Japanese history (Moroi and Takemura, 2004). Significant crustal movements and tsunamis accompanied this earthquake.

According to tide gauge data and the re-leveling of benchmarks and triangular points undertaken by the Land Survey Department (1926), the Boso Peninsula, Miura Peninsula, and Oiso coastal area

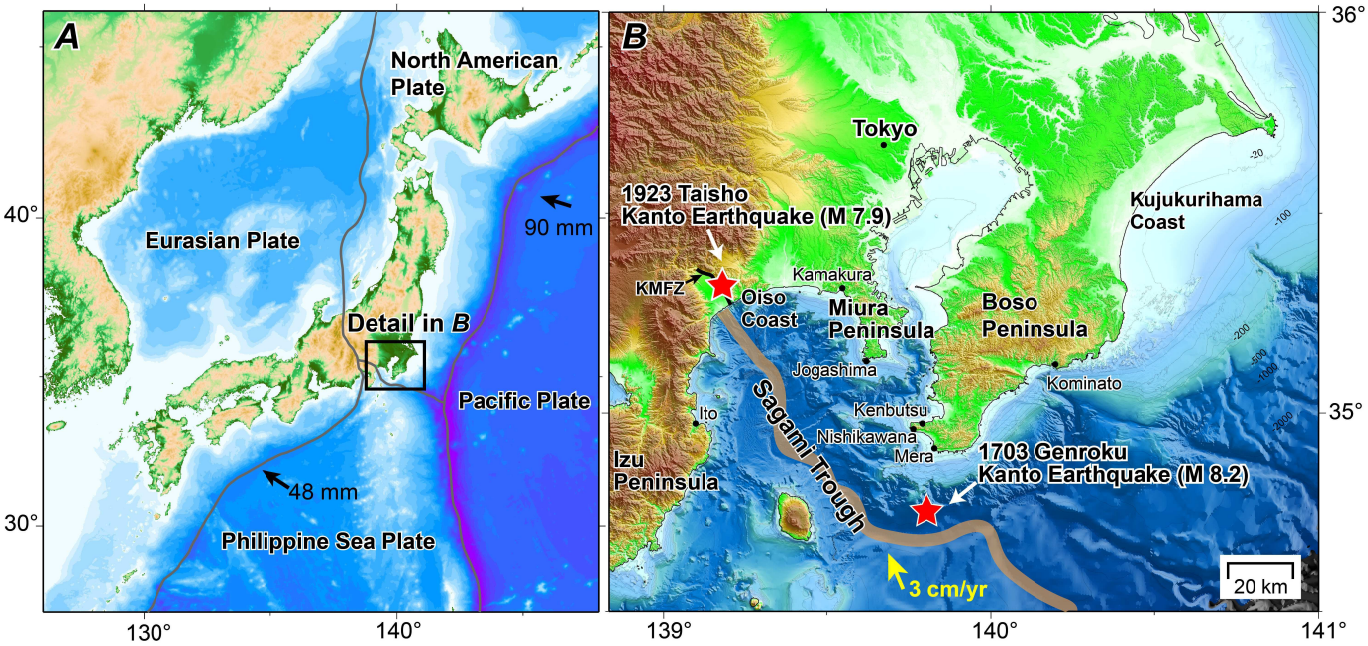

Figure 1. Tectonic setting of Japan Islands (A) and study areas in Kanto region (B). KMFZ: Kozu-Matsuda Fault Zone. Red stars in B are epicenter of main shock during historical earthquakes. Plate motion is after Bird (2003) and Uchida et al. (2009).

were uplifted by as much as 2 m and moved horizontally 2-3 m during the 1923 earthquake (Fig. 2) (Miyabe, 1931). This uplift produced a coastal emergence that has been recorded as marine terraces or as emerged littoral bio-constructions (Fig. 3, 4) (Yamasaki, 1926; Tanakadate, 1926). Tsunami heights of up to 12 m were observed in the coastal area surrounding Sagami Bay, but were somewhat smaller on the Pacific coast of the Boso Peninsula (Fig. 5) (Hatori et al., 1973).

Based on such observational data, a number of fault models have been created for the 1923 Taisho Earthquake along the northern edge of the Philippine Sea Plate (Fig. 6). For example, Ando (1974) inferred a model involving reverse and right-lateral faulting on a low-angle fault plane that strikes along the trough, and Matsu'ura and Iwasaki (1983) proposed an improved model using the then newly-developed inversion analysis method. In 1995, Wald and Somerville discussed a heterogeneous slip-distribution model based on teleseismic data that was later reevaluated by Kobayashi and Koketsu (2005) and Nyst et al. (2006) in the light of new data, even though their conclusions were not significantly different from those of previous models.

1703 Genroku Kanto Earthquake

While, for obvious reasons, there are no instrumental observation data for the 1703 Genroku Earthquake, historical records and tectonic geomorphology provide useful clues that can be used to recreate data on crustal movements and their resultant tsunami (Fig. 2-5, 7-9).

Matsuda et al. (1974) measured the height of the 1703 shoreline and compared it with the accumulated vertical crustal movements that occurred since the earthquake in order to calculate the pattern of coseismic movements occurring during the 1703 event. However, the results obtained were not fully consistent with what could be deduced from interpretations of historical records. Therefore, Shishikura (2000) and Shishikura and Echigo (2001) reevaluated the distribution of the 1703 shoreline while taking into consideration

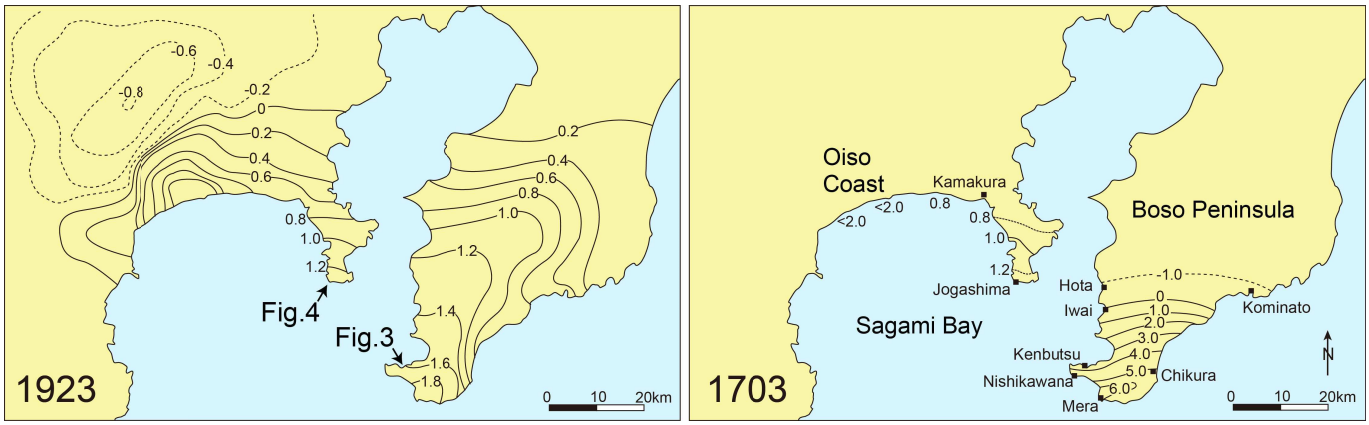

Figure 2. Coseismic vertical crustal movements during the 1703 Genroku and 1923 Taisho Kanto Earthquakes. In the case of the 1703 Genroku Earthquake, data was restored from emerged shoreline features (Shishikura, 2000; Shishikura and Echigo, 2001) and historical records (Usami* et al., *1977; Sasou; 2003). In the case of the 1923 Taisho Earthquake, it was based on Miyabe (1930).

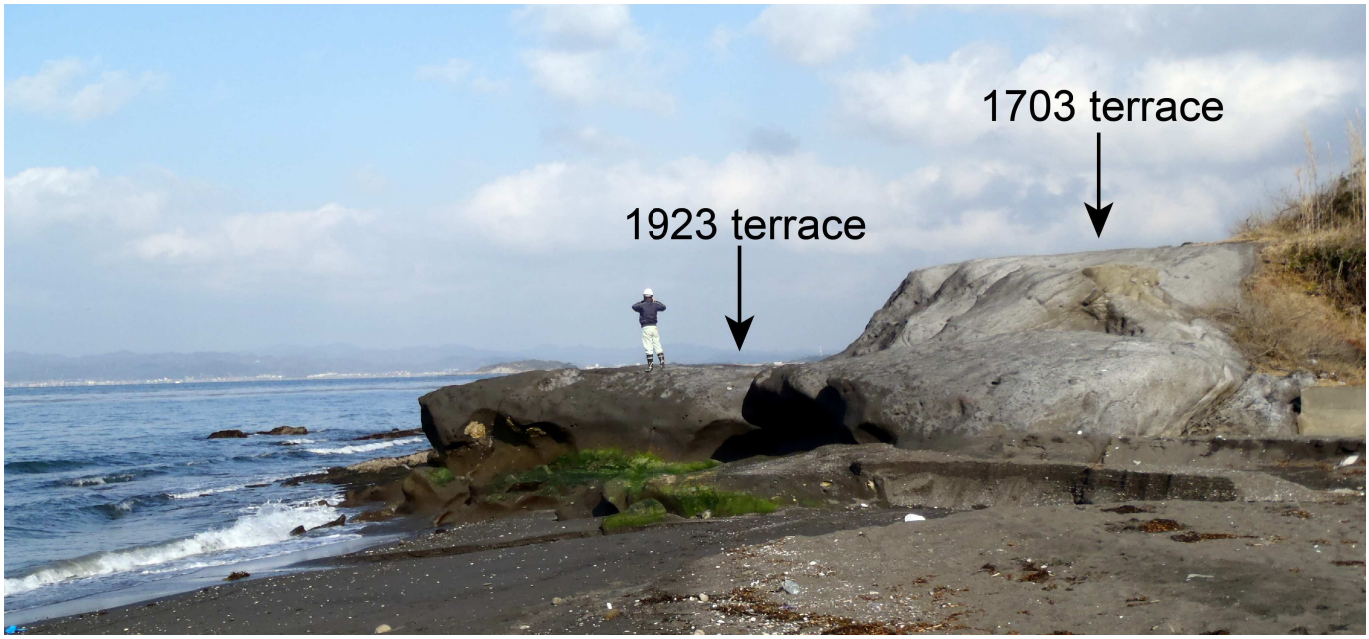

Figure 3. Marine terraces associated with uplifts during the 1703 Genroku and 1923 Taisho Kanto Earthquakes in Kenbustu beach, the southernmost part of the Boso Peninsula. The location is shown in Fig. 2.

historical evidence (Usami et al., 1977), and proposed a renewed coseismic vertical crustal movement model for the 1703 Genroku event. This allowed them to infer that the Miura Peninsula and the Oiso coastal area were uplifted for 1-2 m, as in the 1923 Taisho Kanto Earthquake. In contrast, the Boso Peninsula experienced steep tilting accompanied by an uplift of more than 6 m in the southernmost part of the cape, and subsidence of at least 1 m in its central areas (Fig. 2).

Hatori (1975a, 1976) calculated tsunami heights associated with the 1703 earthquake by identifying inundation limits from historical records such as documents and monuments. When compared with the 1923-tsunami limits, it shows that magnitudes were similar around Sagami Bay, but significantly larger along the Pacific coast of the Boso Peninsula (Fig. 5). One of the most divergent points was the inundation distances of up to 2-4 km deep inland from the 1703 shoreline in the strand plain of the Kujukurihama Coast, which were determined based on the locations of memorials erected in remembrance of tsunami victims (Fig. 9) (Koyama, 1987; Namegaya et al., 2011).

Fault models for the 1703 Genroku Earthquake have been proposed from parameters based on the above-mentioned historical and tectonic data (Fig. 10). For example, the model created by Matsuda et al. (1978) using the vertical crustal movement data of Matsuda et al. (1974) involved a series of three thrust faults extending off the Boso Peninsula. Additionally, Aida (1993) proposed a model involving two fault planes that was based on tsunami inversion and the findings of Kasahara (1973), while Murakami and Tsuji (1999) also suggested a three fault plane model extending southeastward. Later, Satake et al. (2008) examined the effect of the fault plane on the eastern side using these models.

More recently, Namegaya et al. (2011) attempted to verify fault models for the 1703 Genroku and 1923 Taisho Earthquakes by establishing fault distributions based on the consolidation of recently accumulated data involving the surface topology of the Philippine Sea Plate (Fig. 11) (e.g. Sato et al., 2005; Tsumura et al., 2009). It is believed that, in the case of the 1923 Taisho Earthquake, the tectonic

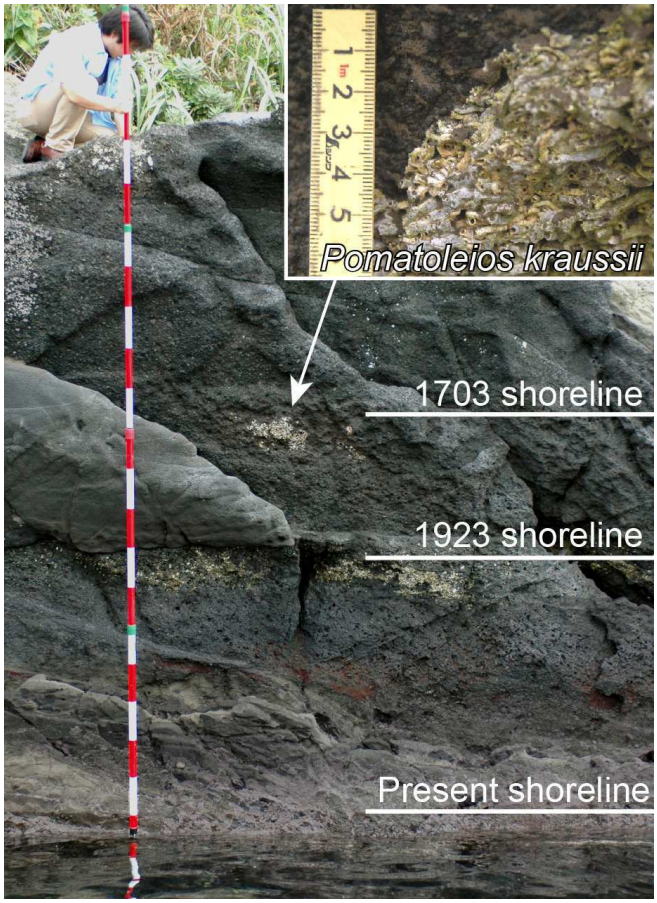

Figure 4. Two levels of emerged sessile assemblages composed primarily of Pomatoleios kraussii, associated with uplifts during the 1703 Genroku and 1923 Taisho Kanto Earthquakes in Jogashima, the southernmost part of the Miura Peninsula. The location is shown in Figure. 2. Revised from Shishikura et al. (2007).

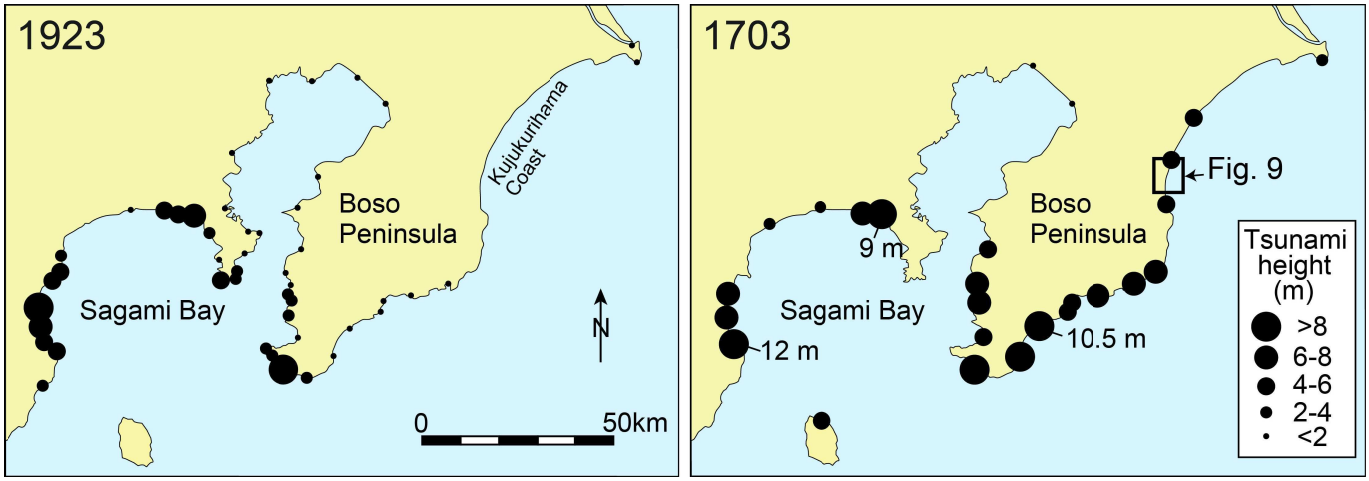

Figure 5. Tsunami heights associated with the 1703 Genroku and 1923 Taisho Kanto Earthquakes in Kanto region. Compiled from Hatori et al. (1973), Hatori (1975a) and Hatori (1976)

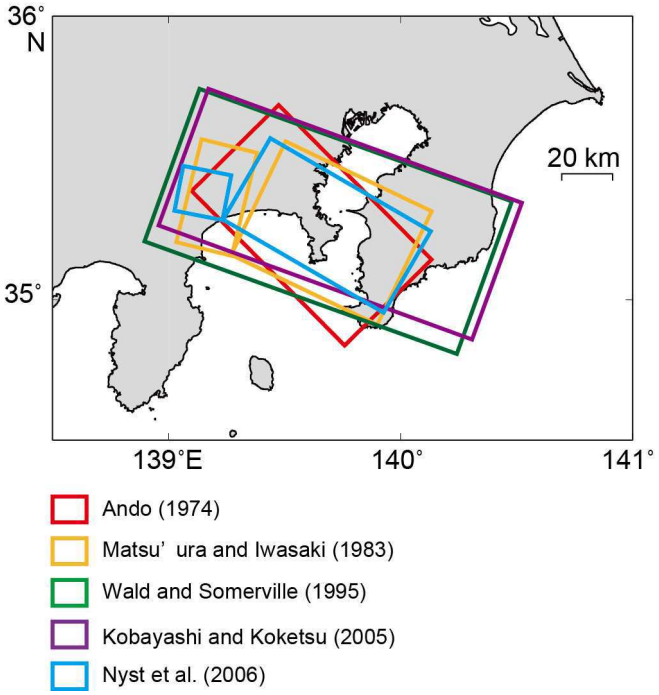

Figure 6. Location of the fault models for the 1923 Taisho Kanto Earthquake

movement primarily entailed a fault rupture near Sagami Bay (Fig. 11A). In the case of the 1703 Genroku Earthquake, this rupture was accompanied by a large fault slip near the southernmost part of the Boso Peninsula (Fig. 11B) of up to approximately 10 m. Tsunami simulations revealed that, in the case of the 1703 Genroku Earthquake, the tsunami-induced inundation starting at the Kujukurihama Coast could not be reproduced without positing a fault off the coast of the Boso Peninsula (Fig. 11C), thereby demonstrating the necessity of an additional offshore fault. However, further research will be needed to determine its position, topography, and slip magnitude of this fault.

Historical earthquakes prior to the 1703 Genroku Kanto Earthquake

Given the 220-year separation between the 1703 Genroku and 1923 Taisho Earthquakes, and considering the plate convergence rate of 3-4 cm/year (e.g. Seno, 1993), it is estimated that the recurrence interval of earthquakes in the Kanto-region is 200-300 years (e.g. Ishibashi, 1977). However, even though there are no reliable historical earthquake records prior to the 1703 Genroku Earthquake, some candidates have been proposed based on previous studies. For example, the Einin Kanto Earthquake that struck Kamakura in 1293 was associated with massive damage resulting from the strong temblor and tsunami inundation (Ishibashi, 1991), and probable geomorphological/geological evidence of this earthquake has been recorded in the marine terrace of the Boso Peninsula (Shishikura, 1999), as well as tsunami deposits in the Miura Peninsula (Shimazaki et al., 2011).

Recently Kaneko (2012) proposed new interpretations of historical documents related to the existence of the 1495 Meio Kanto Earthquake, which could be considered a predecessor of the 1703 and 1923 earthquakes. This earthquake was previously referred to as the 1498 Meio Tokai Earthquake whose source was inferred to be along the eastern part of the Nankai Trough because historical documents from that period show that some parts of the Kanto region, such as Kamakura and Kominato, had been damaged by a large tsunami during AD 1498 (Hatori, 1975b). However, while some references to a tsunami occurring during the 1495 to 1498 timeframe exist in historical documents, no geomorphological/geological evidence has been found in the Miura and Boso Peninsulas to support them – with the exception of a probable tsunami deposit in Ito City on the Izu Peninsula (Fujiwara et al., 2007). If the plausibility of the 1495 earthquake is accepted, it would indicate a recurrence interval for the historical Kanto earthquake series of approximately 200 years. However, decisive data has not yet been obtained.

Prehistorical earthquakes and tsunamis along the Sagami Trough

While there were little reliable historical records prior to the 1703 Genroku Earthquake, the region's seismic history has been reconstructed primarily based on analysis of the distribution and the age of Holocene marine terraces and tsunami deposits.

Research focusing on the marine terrace in this area started after the 1923 Taisho Earthquake (Imamura, 1925; Watanabe, 1929). Later,

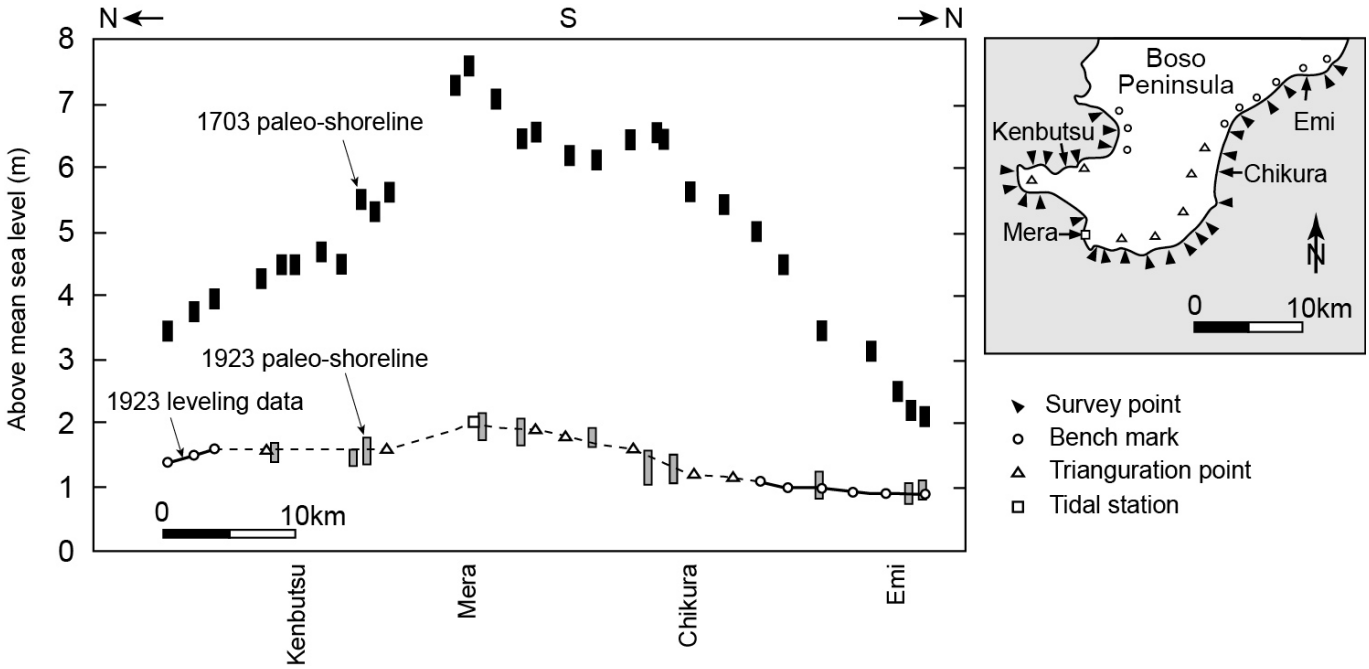

Figure 7. Height distribution of paleoshorelines emerged during the 1703 Genroku and 1923 Taisho Kanto Earthquakes projected along coast of the southern part of the Boso Peninsula. Leveling data related to the 1923 Taisho Earthquake is from re-leveling between (Land Survey Department, 1926).

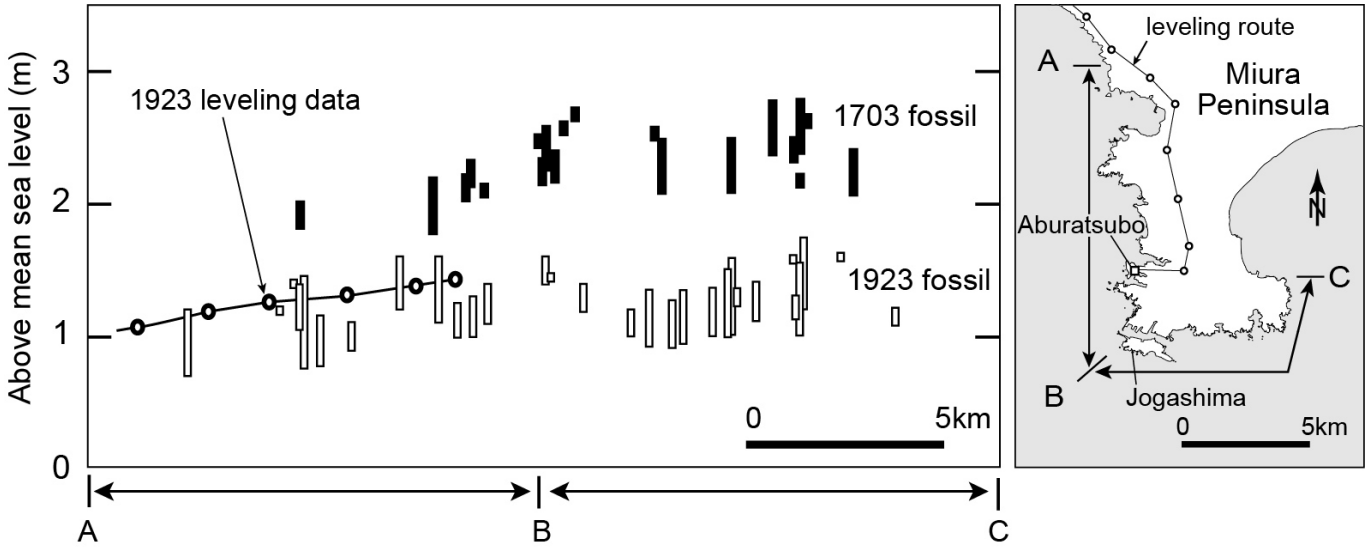

Figure 8. Height distribution of fossil sessile assemblages emerged during the 1703 Genroku and 1923 Taisho Kanto Earthquakes projected along the coast of southern part of the Miura Peninsula. Revised from Shishikura* et al. *(2007). Leveling data related to the 1923 Taisho Earthquake is from comparison of re-leveling results before and after the earthquake (Land Survey Department, 1926).

Sugimura and Naruse (1954) discovered that the height of the Holocene highest marine terrace was constrained by the accumulation of repeated characteristic uplifts associated with the 1923 earthquake. The terraces, which had raised cumulatively up to 30 m in altitude in the southernmost part of the Boso Peninsula, can be divided into four separate levels (Fig. 12, 13A) (Matsuda et al., 1974; Yonekura, 1975; Yokota, 1978; Nakata et al., 1980). Nakata et al. (1980) named and radiocarbon-dated them in a stratigraphic descending order as Numa I, which was dated at 7,200 calibrated years before the present (cal yBP), Numa II (5,000 cal yBP), Numa III (3,000 cal yBP) and Numa IV (the Genroku terrace that emerged during AD 1703), respectively. Kayanne and Yoshikawa (1986) clarified that these four wide platforms, including the 1703 terrace, could be sub-divided into several narrow steps around each boundary (Fig. 13(B)). Because the shape of each narrow step is similar to that of the 1923 terrace that was caused by an uplift of 1 to 2 m, it can be conjectured that four great earthquakes, with magnitudes similar to that of the 1703 Genroku Earthquake (Genroku-type), and several earthquakes with magnitudes similar to that of the 1923 Taisho Earthquake (Taisho-type), have occurred since 7,200 cal yBP between the Genroku-type megaquakes. Analyzing the emerged beach ridges in the southwestern coast of the Boso Peninsula, at least 11 distinct, Taisho-type earthquake

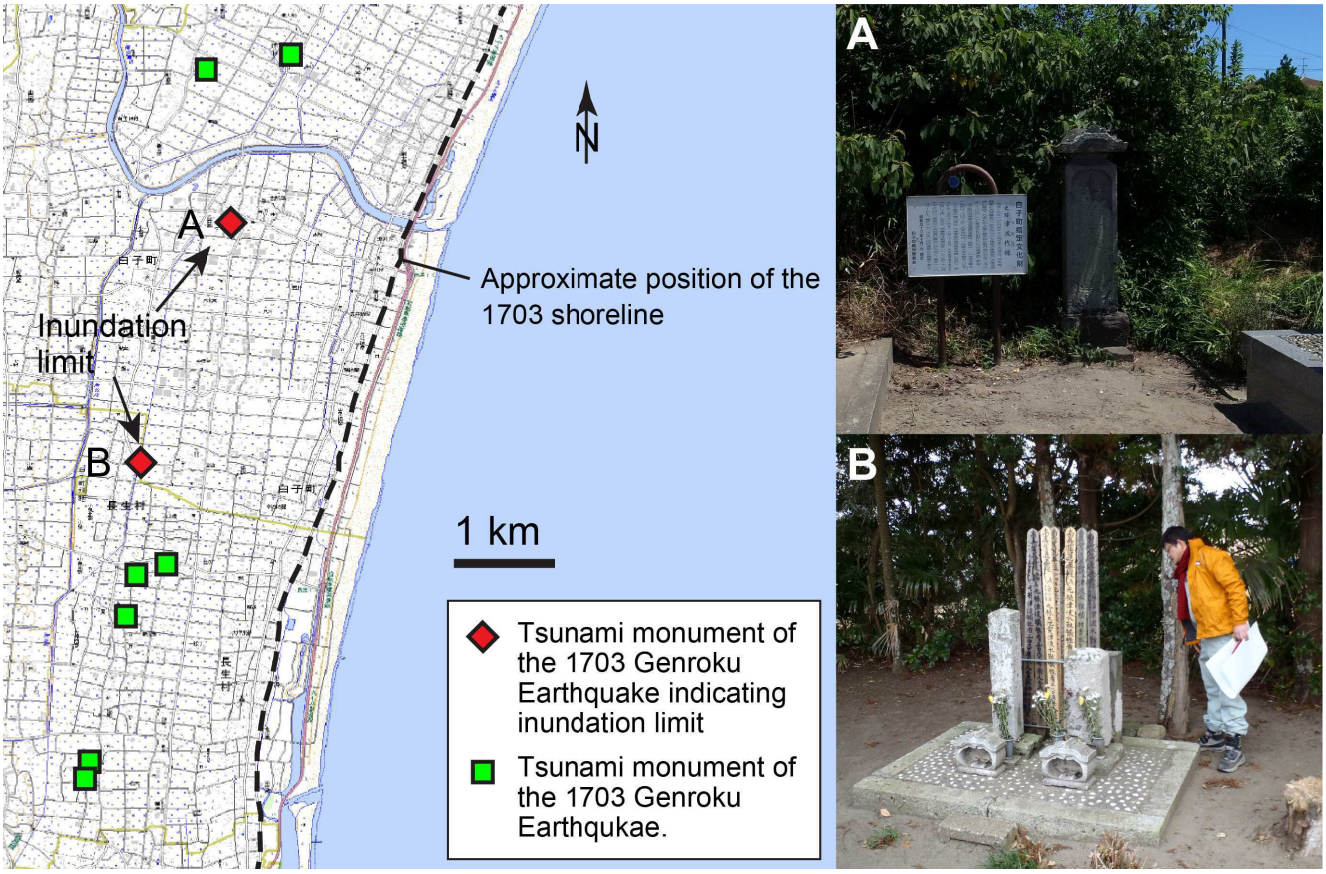

Figure 9. Location and photos of tsunami monuments related to the 1703 Genroku Kanto Earthquake in the Kujukurihama Coast. A: Tsunashiro-sama, B: Muenzuka-tsunami-seirei-sama. Base map is 1/25,000 topographic map of "Mobara", "Kazusaichinomiya", "Shitengi" and "Torami" published by Geospatial Information Authority of Japan. Location is shown in Figure 5. Revised from Namegaya et al. (2011).

were identified, and their timings were dated from radiocarbon ages as 6,800-6,650 cal yBP, 6,000-5,900 cal yBP, 5,400-5,300 cal yBP, 3,800-3,600 cal yBP, 3,300-3,100 cal yBP, 2,800-2,700 cal yBP, 2,500-2,400 cal yBP, 1,300-1,200 cal yBP and 1,050-650 cal yBP. The latter is believed to be the 1293 Einin Earthquake, and, when taken together with the others on the list, indicates a mean recurrence interval of almost 400 years (Shishikura et al., 2001, 2005).

In the Miura Peninsula, at least three Holocene marine terrace steps of up to 20 m in altitude have been identified. These were dated to approximately 7,000 cal yBP, 5,200, cal yBP, and 3,400 cal yBP in

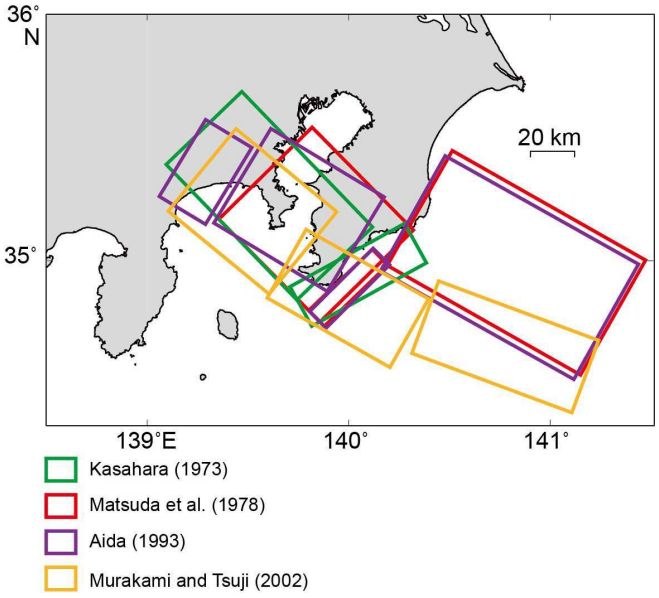

Figure 10. Location of the fault models for the 1703 Genroku Kanto Earthquake

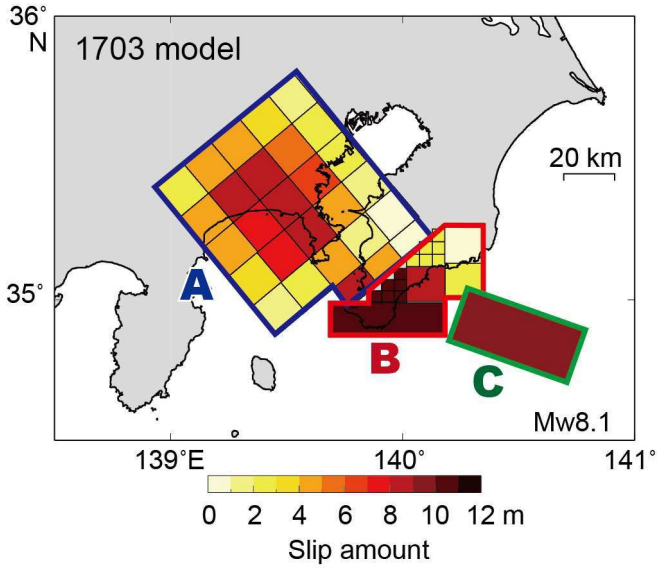

Figure 11. Fault model for the 1703 Genroku Kanto Earthquake taking into consideration the upper plane geometry of the Philippine Sea plate. Revised from Namegaya et al. (2011).

Figure 12. Holocene marine terraces in Nishikawana, the southernmost part of the Boso Peninsula.

descending order (Kumaki, 1985). Sub-divided terraces also were partly identified, but have not yet been dated.

Holocene marine terraces that are partly divided into three or four levels can be identified in the Oiso coast (Kumaki, 1985). Although the height of the highest paleoshoreline reaches 30 m in altitude or more in some places, the emergence of these terraces may not be related to interplate earthquakes alone. Instead, they may also indicate an active inland fault, such as the Kozu-Matsuda Fault Zone that lies in the western end of the Oiso Coast. This fault zone extends from the Sagami Trough and is inferred to branch from the plate boundary as an imbricate thrust (Sato et al., 2005). However, it does not appear that this fault ruptured during the 1923 earthquake. The results of a trench excavation survey (Kanagawa Prefecture, 2003) reveal that the most recent event occurred between the 12th and early 14th centuries, and probably correlated with the 1293 Einin Earthquake. Note that vertical fault displacement is estimated to be 3.0 to 6.5 m per event.

The tsunami deposit record in the Miura Peninsula also indicates prehistorical Kanto earthquakes whose timings have been dated to 5,400-5,250 cal yBP, 4,250-3,950 cal yBP, and 2,750-2,600 cal yBP. These dates are consistent with the age of marine terraces (Fujiwara et al., 1999). Older events, before being recorded into marine terraces,

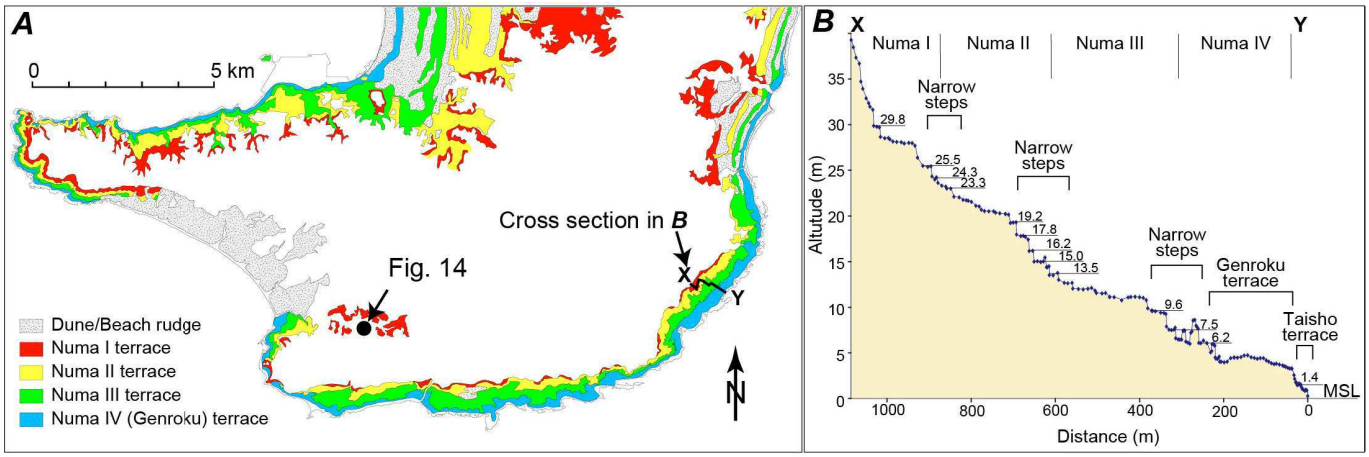

Figure 13. Terrace classification map (A) and measured topographic profile (B) in the southern part of the Boso Peninsula. Revised from Kawakami and Shishikura (2006).

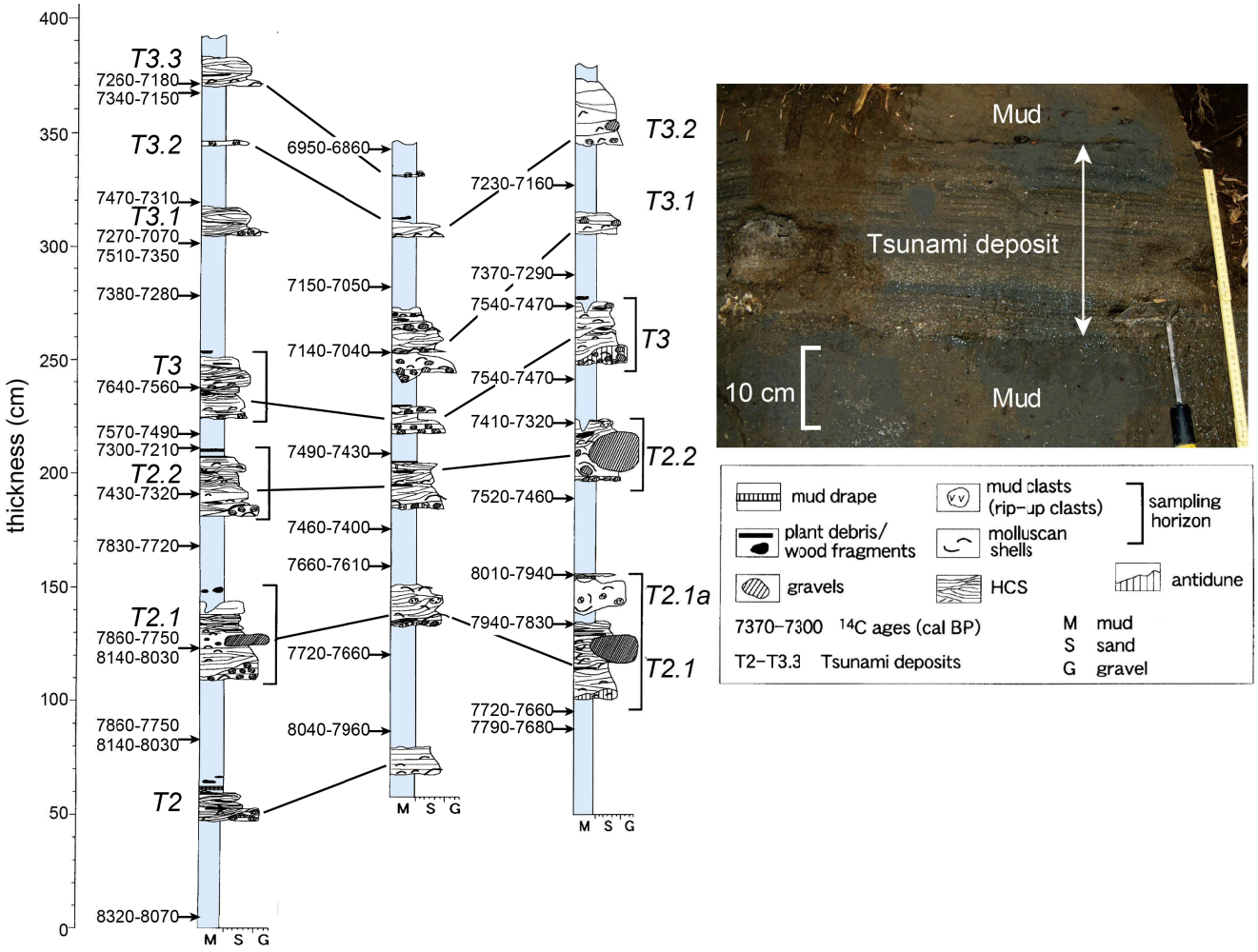

Figure 14. Geological columnar sections and photo in outcrop of the Tomoe River near Mera, southernmost part of the Boso Peninsula. Revised from Fujiwara et al. (2003).

can also be detected from an uplifted postglacial buried valley deposit in the southernmost part of the Boso Peninsula, where at least seven event deposits composed of sand and gravel have been intercalated with inner-bay mud deposited during the period from 8,100 to 7,000 cal yBP, thus suggesting that tsunami events have occurred at intervals of 100 to 300 years (Fig. 14) (Fujiwara and Kamataki, 2007).

Compiling all the age data mentioned above, a rupture history along the Sagami Trough is presented in Fig. 15. Interpretation of the results from a tectonic standpoint has led to the conclusion that the fault in the vicinity of the Sagami Bay (Segment A in Figs. 11 and 15), ruptures approximately every 400 years on average, and that the fault near the southernmost part of the Boso Peninsula (Segment B-C in Figs. 11 and 15) undergoes massive slippage every 2,000 to 2,700 years during the Genroku-type earthquake (Shishikura, 2003).

Inconsistencies between geomorphic/ geologic and geodetic data

According to recent geodetic analysis, the slip-deficit rate of the plate along the Sagami Trough is approximately 20 mm/year in the vicinity of the Sagami Bay and 30 mm/year near the southernmost part of the Boso Peninsula (Fig. 16) (Sagiya, 2004; Nishimura, 2012). As described in the previous section, based on tectonic

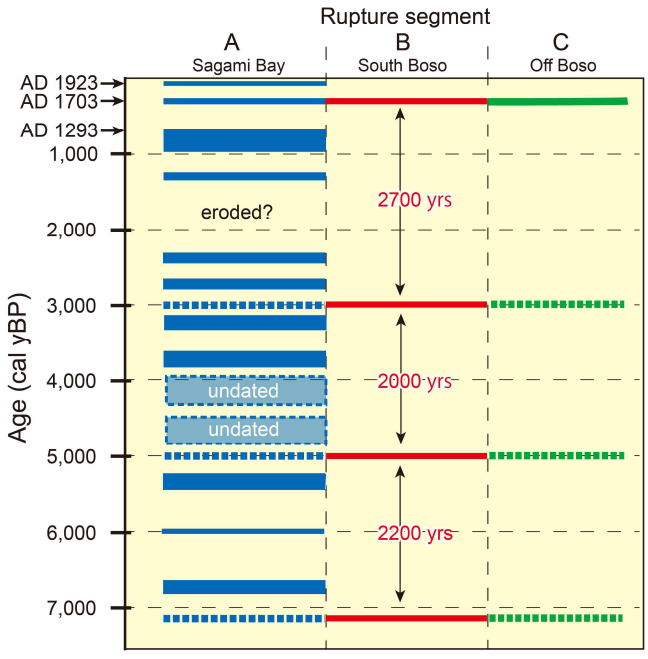

Figure 15. Rupture history of the earthquakes along the Sagami Trough, deduced from the age and distribution of Holocene marine terraces. Compiled from Shishikura et al. (2001, 2005).

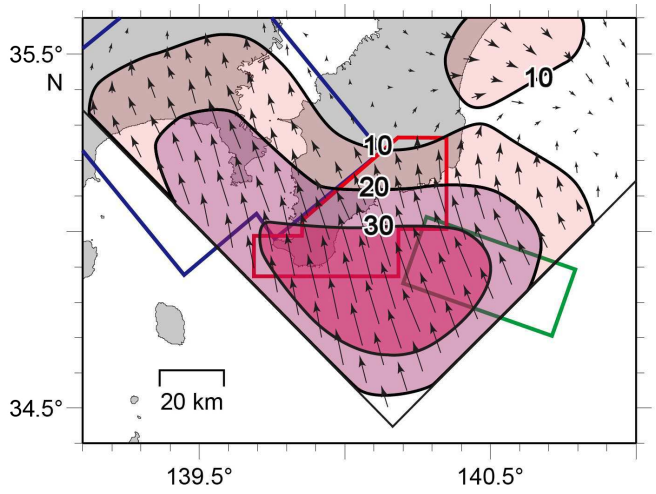

Figure 16. Slip deficit rate in South Kanto deduced from onshore GNSS data between April 1996 and March 2000, and a simplified fault model for the 1703 Genroku Kanto Earthquake. Contours are in millimeters. Slip deficit rate is based on Sagiya (2004). Fault model is from Namegaya et al. (2011).

geomorphological analysis, it is estimated that earthquakes causing rupture of the Segment A (Figs. 11 and 15) in the vicinity of the Sagami Bay occur on an average of approximately every 400 years. If the resulting slip per event is assumed to be in the order of 5 to 10 m, from a geodetic standpoint, it is estimated are 250 to 500 years are required for the accumulation of stress to become sufficient to cause a rupture, resulting in a recurrence interval estimate that is consistent with that of tectonic analysis. Meanwhile, if we assume that the Segment B-C (Figs. 11 and 15) area near the southernmost part of the Boso Peninsula only shifts during the Genroku-type Earthquakes, it should continue to accumulate stress over a longer period of time – roughly between 2,000 to 2,700 years. A simple calculation based on the slip-deficit rate yields an estimated accumulated slip amount of 60 to 80 m. However, as explained earlier, the slip amount of the Segment B (Figs. 11 and 15) during the 1703 Genroku Earthquake is believed to have been up to approximately 10 m, which indicates that there is a substantial discrepancy between the geomorphologic and geodetic estimates.

To resolve this problem, at least three hypotheses can be considered. First, because global navigation satellite system (GNSS) observation is very recent technique and its data accumulation covers too short of a period to evaluate a large earthquake cycle, the past slip-deficit rate might actually be variable and could have been slower than present phenomena. Second, if the plate interface sometimes slips more slowly, it can reduce crustal stress. However, the strong coupling area shows both coseismic and aseismic behaviors, which is somewhat physically irrational. Third, if the coseismic ruptures of the Segment B (+C) shown in Fig. 11 and 15 have been occurring at the high frequency rate of once every several hundred years (which overturns the conventional interpretation) the inconsistency in slip-deficit estimates is resolved. This hypothesis will be examined in the next section.

Interpretation based on new tectonic evidence

Uno et al. (2007) and Endo and Miyauchi (2008) recently conducted a reexamination of the marine terraces in the southern part of the Boso Peninsula, and concluded that the coastal uplift timing of the western side did not necessarily coincide with that of the eastern side, as had been previously believed. The previous conventional interpretation had been that Genroku-type earthquakes resulting in substantial coastal uplifts of the entire southernmost part of the peninsula recurred at intervals of 2,000 to 2,700 years. However, the varying coastal uplift timing of the western and eastern sides suggests that different earthquakes on each coast caused the uplifts. In terms of the 1703 Genroku Earthquake fault model, it appears that there may be a third type of earthquake that only produces the ruptures of the Segment B, and, in some cases, part of the Segment C. The inconsistency in slip-deficit estimates described in the previous section can be resolved if this type of earthquake is assumed to occur at a frequency of every several hundred years. More specifically, the tsunami deposit record mentioned in previous section indicating that high-frequency tsunami events occur near the southernmost part of the Boso Peninsula may, in fact, constitute a combined record of tsunamis resulting from these different earthquake types.

The two recent studies reviewed in the beginning of this section reported only four to six marine terraces levels in the eastern side, which does not seem to indicate frequent Segment B type ruptures. However, as described in Figure 13(B), the marine terrace geometry actually shows at least 15 levels, with various scale step combinations. Since it is difficult to explain this marine terrace geometry using just three earthquake types, as defined from a simple combination of the three segments shown in figures 11 and 15, the past uplift events should be re-classified based on a reinterpretation of the marine terrace distribution.

Furthermore, Holocene marine terraces are found to exist along the eastern coast of the Boso Peninsula extending up to the Kujukurihama Coast where no historical coseismic uplift, including the 1923 Taisho and 1703 Genroku Earthquakes, has been observed (Fig. 17) (Shishikura, 2001). For example, the Holocene highest foreshore deposit dated around 6,000 years ago is seen raised to 9.6 m in Mobara (Fig. 17A), and some geophysical simulation studies for long-term crustal deformation have proposed that such uplift could also be made by steady plate motion at a subduction zone (e.g., Hashimoto et al., 2004). Although a part of the cumulative uplift component may include such aseismic motion, the existence of several emerged wave-cut-bench levels suggests an intermittent uplift with amounts of at least 1 m per event (Fig. 17B).

Masuda et al. (2001) also reported the repeated occurrence of intermittent coastal uplift events deduced from the height distribution of inter-tidal deposit in the southern part of the Kujukurihama Coast. These observations suggest that it may be necessary to consider the existence of yet more uplift-causing earthquake types in this coastal region. For example, it may be necessary to consider an even deeper plate interface rupture occurring further north than the area covered by the fault model shown in figure 11, or the possibility that an offshore active fault may exist in the North American Plate near the Boso Peninsula.

Future research

The new interpretation presented here is based on limited data, and, as such, remains in the realm of a working hypothesis. In order to verify the existence of the other earthquake types, it will be necessary to conduct a more detailed investigation of marine terraces along the

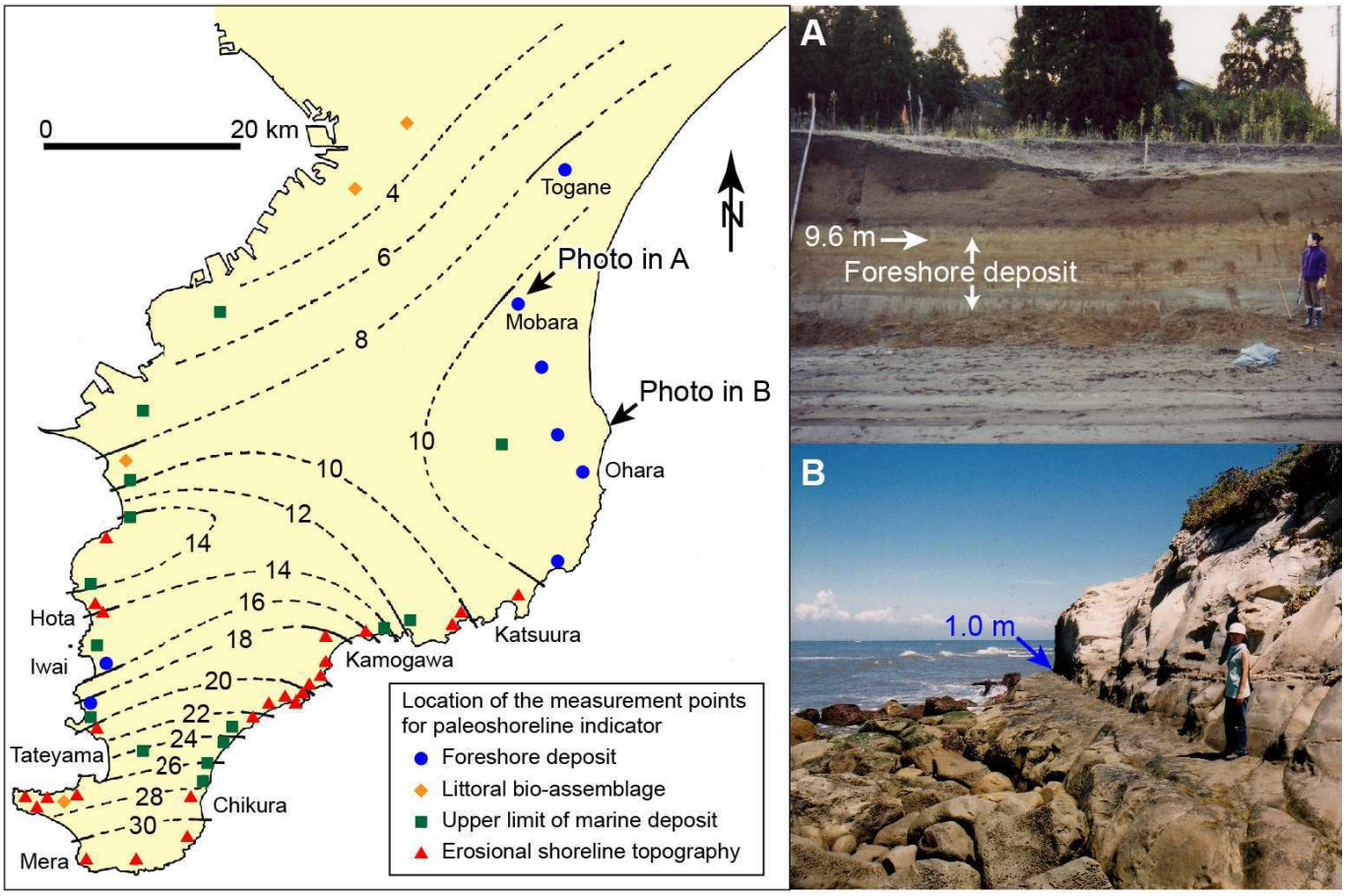

Figure 17. Height distribution of the Holocene highest marine terrace in the Boso peninsula and photos of marine terrace in the eastern part of the Boso Peninsula. Contours are in meters. Revised from Shishikura (2001)

southern and eastern shorelines of the Boso Peninsula. If we are able to identify a specific terrace and trace it over a wide area along the coast, we might be able to reproduce the sequence of uplift events, and would then be able to approximately verify the fault slip distribution.

As we are currently unable to assess the tectonic movement off the coast of the Boso Peninsula (Fig. 15C) based on marine terraces, we must verify the seismic history of the area based on tsunami deposit records and seismic turbidite sequences, such as Kawamura et al. (2014). However, more progress will be necessary in areas other than geomorphological/geological surveys. It will also be necessary to make progress in geophysical simulation studies by incorporating geodetical observations such as those made in Noda et al. (2013) in order to understand the relationship between the plate motions of the Sagami Trough and the variety of large earthquakes.

Acknowledgements

I would like to thank Prof. Yildirim Dilek, Dr. Kiichiro Kawamura, and the anonymous reviewer for their useful comments and suggestions to improve this paper. I also thank Prof. Yujiro Ogawa for his encouragement and for providing me the opportunity to submit this paper.

References

Aida, I., 1993, Historical tsunamis and their numerical models which occurred in the north-western part of Sagami Bay, J. Geogr. (Chigaku zasshi), v. 102, pp. 427-436, (in Japanese with English abstract and figure captions).

Ando, M., 1974, A fault-origin model of the great Kanto earthquake of 1923 as deduced from geodetic data. Bull. Earthq. Res. Inst. Univ. Tokyo, v. 49, pp. 19-32.

Bird, P., 2003, An updated digital model of plate boundaries, Geochemistry Geophysics Geosystems, v. 4 (3), 1027, doi:10.1029/2001GC000252.

Cabinet Office, 2013, Report on seismic source models, seismic intensity distributions and tsunami heights for the M7 class earthquake in the capital and the M8 class earthquake along the Sagami trough, 45p. (in Japanese).

Earthquake Research Committee, 2014, Long term evaluation of seismic activities along the Sagami Trough (second edition), 81p. (in Japanese).

Endo, K. and Miyauchi, T., 2011, Reexamination in ages and altitudes of Holocene emergent coastal geomorphology associated with seismotectonics along the Sagami Trough, Japan, Abstract of Japanese Society for Active Fault Studies 2011 Fall Meeting, P-06 (in Japanese).

Fujiwara, O., Masuda, F., Sakai, T., Irizuki, T. and Fuse, K., 1999, Holocene tsunami deposits detected by drilling in drowned valleys of the Boso and Miura Peninsulas, The Quat. Res. (Daiyonki-Kenkyu), v. 38, pp. 41-58 (in Japanese with English abstract and figure captions).

Fujiwara, O. and Kamataki, T., 2007, dentification of tsunami deposits considering the tsunami waveform: an example of subaqueous tsunami deposits in Holocene shallow bay on southern Boso Peninsula, central Japan, Sedimentary Geology, v. 200, pp. 295-313.

Fujiwara, O., Hirakawa, K., Kaneko, H. and Sugiyama, H., 2007, Tsunami (?) event deposit observed in the Usami site, northern part of Ito City, Shozuoka Prefecture, Research Reports of Tsunami Engineering, v. 24, pp. 77-83 (in Japanese).

Hashimoto, C., Fukui, K. and Matsu'ura, M., 2004, 3-D Modelling of Plate

Interfaces and Numerical Simulation of Long-term Crustal Deformation in and around Japan, PAGEOPH, v. 161, pp. 2053-2068.

Hatori, T., Aida, I. and Kajiura, K., 1973, Tsunamis in the South-Kanto district, in Publications for the 50th Anniversary of the Great Knato Earthquake, pp. 57–66, Earthquake Res. Inst., Tokyo, (in Japanese with English abstract).

Hatori, T., 1975a, Monuments of the tsunami of 1703 and 1923 in the South-Kanto district, Bull. Earthq. Res. Inst. Univ. Tokyo, v. 50, pp. 385-395, (in Japanese with English abstract and figure captions).

Hatori, T., 1975b, Sources of large tsunamis generated in the Boso, Tokai and Nankai regions in 1498 and 1605, Bull. Earthq. Res. Inst. Univ. Tokyo, v. 50, pp. 171-185, (in Japanese with English abstract and figure captions).

Hatori, T., 1976, Monuments of the 1703 Genroku tsunami along the south Boso Peninsula: wave height of the 1703 tsunami and its comparison with the 1923 Kanto tsunami Bull. Earthq. Res. Inst. Univ. Tokyo, v. 51, pp. 63-81, (in Japanese with English abstract and figure captions).

Imamura, A., 1925, Report on the great Kanto earthquake, Rep. Imp. Earthquake Invest. Comm. 100A, pp. 21-65, (in Japanese).

Ishibashi, K., 1977, Source region of the 1703 Genroku Kanto Earthquake and recurrence time of major earthquakes in Sagami Bay, Japan (1), J. Seismol. Soc. Jpn. (Zishin), v. 53, pp. 357-372, (in Japanese with English figure captions).

Ishibashi, K., 1991, The 1293 Einin Kamakura earthquake and the recurrence time of great interplate earthquakes along the Sagami Trough, central Japan, Abstract of 1991 Fall Meeting Seismol. Soc. Jpn., Tokyo, (in Japanese).

Kanagawa Prefecture, 2003, Survey result report of the Kannawa/Kozu-Matsuda Fault Zone, 78p, (in Japanese).

Kaneko, H., 2012, Tsunami deposit detected at the Usami site and reevaluation of the 1495 Meio earthquake and tsunami, Ito shi-shi kenkyu (Research reports of history in Ito city), v. 10, pp. 102-124, (in Japanese).

Kasahara, K., J. Yamada and M. Ando, 1973, Crustal movements in the South Kanto district, and a related working hypothesis: Publications for the 50th anniversary of the great Kanto earthquake, Earthq. Res. Inst. Univ. Tokyo, pp. 103-116, (in Japanese with English abstract and figure captions).

Kawakami, S. and Shishikura, M., 2006, Geological Map 1:50,000. Tateyama, Geological Survey of Japan, (in Japanese with English caption).

Kawamura, K. Nakajima, A., Saito, S., Murayama, M., Shishikura, M., Muraoka, S., Yamamoto, F., Oishi, M. and Kanamatsu, T., 2014, Sedimentation process associated with the Kanto earthquakes along the Philippine Sea plate subduction zone, central Japan: A case study on submarine paleoseismology, Episodes, in this issue.

Kayanne, H. and Yoshikawa, T., 1986, Comparative study between present and emergent erosional landforms on the southeast coast of Boso Peninsula, central Japan. Geogr. Rev. Japan, Ser. A, v. 59, pp. 18-36, (in Japanese with English abstract and figure captions).

Kobayashi, R. and Koketsu, K., 2005. Source process of the 1923 Kanto earthquake inferred from historical geodetic, teleseismic, and strong motion data, Earth Planets and Space, v. 57, pp. 261-270.

Koyama, Y., 1987, Document of the Genroku tsunami in the Kujukuri area, Monthly Earth (Gekkan Chikyu), v. 94, no. 4, pp. 188-194, (in Japanese).

Kumaki, Y., 1985, The deformations of Holocene marine terraces in southern Kanto, central Japan, Geogr. Rev. Jpn. Ser. B, v. 58, pp. 49–60.

Land Survey Department, 1926, The change of elevation of land caused by the great earthquake of September 1st, 1923. Bull. Earthq. Res. Inst.Univ. Tokyo, v. 1, pp. 65-68.

Masuda, F., Fujiwara, O., Sakai, T. and Araya, T., 2001, Relative sea-level changes and co-seismic uplifts over six millennia, preserved in beach deposits of the Kujukuri strand plain, Pacific coast of the Boso Peninsula, Japan, J. Geogr. (Chigaku zasshi), v. 110, pp. 650-664, (in Japanese with English abstract and figure captions).

Matsuda, T., Y. Ota, M. Ando and N. Yonekura, 1974, Geological study for the 1703 Genroku Earthquake. In Kakimi, T. and Y. Suzuki, (edu.), Earthquakes and crustal deformation in the Kanto district, pp. 175-192, Lattice, Tokyo 2, 79p., (in Japanese).

Matsuda, T., Y. Ota, M. Ando and N. Yonekura, 1978, Fault mechanism and recurrence time of major earthquakes in southern Kanto district, Japan, as deduced from coastal terrace data. Geol. Soc. Am. Bull., v. 89, pp. 1610-1618.

Matsu'ura, M. and T. Iwasaki, 1983, Study on coseismic and postseismic crustal movements associated with the 1923 Kanto earthquake. Tectonophysics, v. 97, pp. 201-215.

Miyabe, N., 1931, On the vertical earth movements in Kwanto districts, Bull. Earthquake Res. Inst. Tokyo Univ. • C v. 9•Cpp. 1-21.

Moroi, T. and Takemura, M., 2004, Mortality Estimation by Causes of Death Due to the 1923 Kanto Earthquake, Journal of JAEE, v. 4, no. 4, pp. 21-45, (in Japanese with English abstract).

Murakami, Y. and Tsuji, Y., 2002, Seismic fault model of the Genroku Kanto Earthquake (31, Dec., 1703) considering with tsunami records, Monthly Ocean -extra issue- (Gekkan Kaiyo Gogai), No. 28, pp. 168-175, (in Japanese).

Nakata, T., Koba, M., Imaizumi, T., Jo, W., Matsumoto, H. and Suganuma, T., 1980, Holocene marine terraces and seismic crustal movements in the southern part of Boso Peninsula, Kanto, Japan. Geogr. Rev. Japan, Ser. A, v. 53, pp. 29-44, (in Japanese with English abstract and figure captions).

Namegaya, Y., Satake, K. and Shishikura, M., 2011, Fault models of the 1703 Genroku and 1923 Taisho Kanto earthquakes inferred from coastal movements in the southern Kanto area, Annual Report on Active Fault and Paleoearthquake Researches, v. 11, pp. 107-120, (in Japanese with English abstract and figure captions).

Nishimura, T., 2012, Interseismic deformation and interplate coupling in southern Kanto, Report of CCEP, v.88, pp. 521-525, (in Japanese with English figure captions).

Noda, A., Hashimoto, C., Fukahata, Y. and Matsu'ura, M., 2013, Interseismic GPS strain data inversion to estimate slip-deficit rates at plate interfaces: application to the Kanto region, central Japan, Geophy. Jour. Int., v. 193, pp. 61-77, doi: 10.1093/gji/ggs129.

Nyst, M., Pollitz, F. F., Nishimura, T. and Thatcher, W., 2006, The 1923 Kanto earthquake reevaluated using a newly augmented geodetic data set, Jour. Geoph. Res., 111, B11306, doi:10.1029/2005JB003628.

Sagiya, T., 2004, Interplate coupling in the Kanto District, central Japan, and the Boso Silent earthquake in May 1996, Pure Appl. Geophys., v. 161, pp. 11-12, 2601-2616.

Satake, K., Shishikura, M., Namegaya, Y., Fuji, R. and Takeuchi, H., 2008, Fault models of the Genroku (1703) Kanto Earthquake and Tsunami along the eastern coast of Boso Peninsula, Historical Earthquakes v. 23, pp. 81-90, (in Japanese with English abstract).

Sato, H., H. Hirata, K. Koketsu, D. Okaya, S. Abe, R. Kobayashi, M. Matsubara, T. Iwasaki, T. Ito, T. Ikawa, T. Kawanaka, K. Kasahara and S. Harder (2005), Earthquake source fault beneath Tokyo, Science, v. 309, pp. 462-464.

Seno, T., 1993, A model for the motion of the Philippine Sea Plate consistent with NUVEL-1 and geological data, Jour. Geoph. Res., v. 98, pp. 17,941-17,948.

Shimazaki, K, Kim, H. Y., Chiba, T., and Satake, K., 2011, Geological evidence of recurrent great Kanto earthquakes at the Miura Peninsula, Japan, Jour. Geoph. Res., 116, B12408, doi:10.1029/2011JB008639.

Shishikuira, M., 1999, Holocene marine terraces and seismic crustal movements in Hota lowland in the southern part of the Boso Peninsula, central Japan, The Quat. Res. (Daiyonki-Kenkyu), v. 38, pp. 17-28, (in Japanese with English abstract).

Shishikuira, M., 2000, Coseismic vertical displacement in the Boso Peninsula during the 1703 Genroku Kanto Earthquake, deduced from emerged shoreline topography, Historical Earthquakes (Rekishi Jishin), v. 16, pp. 113-122, (in Japanese with English abstract).

Shishikuira, M., 2001, Crustal movements in the Boso Peninsula, analyzing the height distribution of Holocene highest paleo-shoreline, Annual Report on Active Fault and Paleoearthquake Researches, v. 1, pp. 273-285, (in Japanese with English abstract and figure captions).

Shishikura, M., 2003, Cycle of interplate earthquake along the Sagami Trough, deduced from tectonic geomorphology, Bull. Earthquake Res. Inst. Tokyo Univ. • C v. 78•Cpp. 245-254, (in Japanese with English abstract and figure captions).

Shishikura, M. and Echigo, T., 2001, Coseismic vertical displacement during the 1703 Genroku Kanto earthquake in the southern part of the Miura Peninsula, analyzing height distribution of emerged wave-cut benches and fossilized sessile assemblages, Historical Earthquakes (Rekishi Jishin), v. 17, pp. 32-38, (in Japanese with English abstract).

Shishikura, M., Haraguchi, T. and Miyauchi, T., 2001, Timing and recurrence interval of the Taisho-type Kanto Earthquake, analyzing Holocene emerged shoreline topography in the Iwai Lowland, the southwestern part of the Boso Peninsula, central Japan, J. Seismol. Soc. Jpn. (Zishin), v. 53, pp. 357-372, (in Japanese with English abstract and figure captions).

Shishikura, M., Kamataki, T., Takada, K., Suzuki, K. and Okamura, Y., 2005, Survey report of emerged beach ridges in the southwestern part of Boso Peninsula-Timing of the Taisho-type Kanto earthquake-, Annual Report on Active Fault and Paleoearthquake Researches, v. 5, pp. 51-68, (in Japanese with English abstract and figure captions).

Shishikura, M., Echigo, T.and Kaneda, H., 2007, Marine reservoir correction for the Pacific coast of central Japan using 14C ages of marine mollusks uplifted during historical earthquakes, Quaternary Research, v. 67, pp. 286-291.

Sugimura, A. and Naruse, Y., 1954, Changes in sea level, seismic upheavals, and coastal terraces in the Southern Kanto Region, Japan (I), Jap. Jour. Geol. Geogr., v. 24, pp. 101-113.

Tanakadate, S., 1926, The Kanto earthquake and coastal vertical movements, J. Geogr. (Chigaku zasshi), v. 38, pp. 130-135, 188-201, 324-329, 374-390, (in Japanese).

Tsumura, N., Komada, N., Sano, J., Kikuchi, S., Yamamoto, S., Ito, T., Sato, T., Miyauchi, T., Kawamura, T., Shishikura, M., Abe, S., Sato, H., Kawanaka, T., Suda, S., Higashinaka, M., and Ikawa, T., 2009, A bump on the upper surface of the Philippine Sea plate beneath the Boso peninsula, Japan inferred from seismic reflection surveys: A possible asperity of the 1703 Genroku earthquake, Tectonophysics, v. 472, pp. 39-50.

Uchida, N., Nakajima, J., Hasegawa, A. and Matsuzawa T., 2009, What controls interplatecoupling?: Evidence for abrupt change in coupling across a border between two overlyingplates in the NE Japan subduction zone, Earth Planet. Sci. Lett., v. 283, pp. 111–121.

Uno, T., Miyauchi, T. and Shishikura, M., 2007, Reexamination of earthquakes occurring along the Sagami Trough, analyzed by Holocene marine terraces in the Boso Peninsula, Abstract of Japan Geoscience Union Meeting 2007, S141-007.

Usami, T., M. Uchino and M. Yoshimura, 1977, Historical documents related to the Genroku Earthquake in the southern part of Boso Peninsula, 62p., (in Japanese).

Usami, T., Ishi, H., Imamura, T., Takemura, M. and Matsuura, R., 2013, Materials for comprehensive list of destructive earthquakes in Japan, 599-2012, Univ. Tokyo Press, 694p., (in Japanese).

Wald D. J. and P. G. Somerville, 1995, Variable-slip rupture model of the great 1923 Kanto, Japan, earthquake, Bull. Seism. Soc. Am., v. 85, pp. 159-177.

Watanabe, A., 1929, Marine terraces in the southern part of Boso Peninsula, Geogr. Rev. Japan, v. 5, pp. 119-126, (in Japanese).

Yamasaki, N., 1926, Physiographical studies of the great earthquake of Kwanto district, 1923. Jour. Fac. Sci. Imp. Univ. Tokyo, Sec. v. 2, pp. 77-119, (in Japanese).

Yokota, K., 1978, Holocene coastal terraces on the southern coast of the Boso Peninsula, Geogr. Rev. Japan, Ser. A, v. 51, pp. 349-364, (in Japanese with English abstract and figure captions).

Yonekura, N., 1975, Quaternary tectonic movements in the outer arc of Southwest Japan with special reference to seismic crustal deformation, Bulletin of the Department of Geography, University of Tokyo, v. 7, pp. 19-71.

by Kazuhisa Goto[1], Shigehiro Fujino[2], Daisuke Sugawara[1] and Yuichi Nishimura[3]

The current situation of tsunami geology under new policies for disaster countermeasures in Japan

1 International Research Institute of Disaster Science, Tohoku University, 6-6-11 Aoba, Aramaki, Sendai, 980-8579, Japan.
(E-mail: goto@irides.tohoku.ac.jp)
2 Faculty of Life and Environmental Sciences, University of Tsukuba, Tennodai, Tsukuba, Ibaraki 305-8572, Japan
3 Institute of Seismology and Volcanology, Hokkaido University, Kita 10 Nishi 8, Kita-ku, Sapporo 060-0810, Japan

This paper presents a review of the Japanese policies for tsunami countermeasures before and after the 2011 off the Pacific coast of Tohoku Earthquake and its consequent tsunami. The current status of tsunami geology under the new policies is also discussed. The 2011 event was regarded as an unexpected hazard. Such a large hazard had not been considered for Japanese tsunami countermeasures before, although geological studies have indicated their potential occurrence. Based on lessons learned from the 2011 event, the Japanese government changed policies related to tsunami disaster countermeasures. The salient change is that estimation of the maximum possible earthquake and tsunami along the each coast of Japan is now required. Following this policy change, the maximum possible earthquake and tsunami have been estimated along several coasts of Japan, such as the Nankai Trough region based on seismology, irrespective of past occurrence. Tsunami geology is regarded as an important research field for estimating the maximum possible earthquake and tsunami strength because paleotsunami histories of several thousand years are crucially important for future tsunami risk assessment. However, many issues remain to be resolved to respond to the rapid change of policy. Acceleration of studies, sharing knowledge with governors, and development of schemes for outreach to the public (e.g. a database system) should be considered for improvement of future tsunami countermeasures in Japan.

Introduction

The 2011 off the Pacific coast of Tohoku Earthquake and its consequent tsunami that occurred on 11 March 2011 (Fig. 1a) marked an important turning point for earthquake and tsunami studies in Japan. This was the first known earthquake with a magnitude greater than 9.0 and a recorded maximum tsunami run-up (40.0 m, Mori et al., 2012) in the past 1,300 years of Japanese historical records. The earthquake and tsunami caused 15,885 deaths, with 2,623 missing (as of 10 April 2014; Metropolitan Police Department, 2014), and severe accidents at the Fukushima Daiichi Nuclear Power Plant.

Although no clear differentiation of *hazard* and *disaster* exists in Japanese terminology, the Central Disaster Management Council (CDMC) (2011) defined the terms: "*The 2011 off the Pacific coast of Tohoku Earthquake refers to the earthquake hazard of magnitude 9.0 that occurred on 11 March 2011 and was named by the Japan Meteorological Agency based on a standard naming convention. The Great East Japan Earthquake, named subsequently by the Cabinet, refers to the earthquake and tsunami disaster and the accompanying nuclear accidents*". However, the "2011 Tohoku-Oki (or Tohoku-oki) earthquake and tsunami" is more popularly used among scientists because important scientific journals such as *Nature* and *Science* have adopted the term for this event.

The sizes of both the 2011 earthquake and tsunami were far greater than previously estimated. Therefore, disaster prevention countermeasures against such hazards were insufficient. The event was designated as an unexpected ("*souteigai*" in Japanese) hazard (e.g., Goff et al., in press). However, even before the 2011 event, historical and geological results of studies had suggested the potential occurrence of a low-frequency large earthquake and tsunami along the Pacific coast of Tohoku (e.g., Abe et al., 1990; Minoura, 1990; Watanabe, 2001). In fact, the 869 Jogan earthquake and tsunami, which is now regarded as a possible predecessor of the 2011 event (e.g., Goto et al., 2011; Namegaya and Satake, 2014), has been well studied since the late 1980s. Based on geological studies of the Jogan tsunami, the minimum inundation area was 3–4 km inland from the paleo-shoreline (Sawai et al., 2007). An earthquake of Mw>8.3–8.4 is necessary to explain the distribution of tsunami deposits (Satake et al., 2008a; Namegaya et al., 2010; Sugawara et al., 2011), and the magnitude is now revised as Mw>8.6 based on the lessons learned from the 2011 event (Namegaya and Satake, 2014). The tsunami recurrence interval was estimated based on geological evidence accumulated over 3,000 years: approx. 800 years (Minoura and Nakaya, 1991), 600–1,300 years (Sawai et al., 2007), and now revised to be approx. 500–800 years (Sawai et al., 2012). Therefore, in a geological sense, the occurrence of such a large tsunami at the Pacific coast of Tohoku was almost *on time*. However, geological information

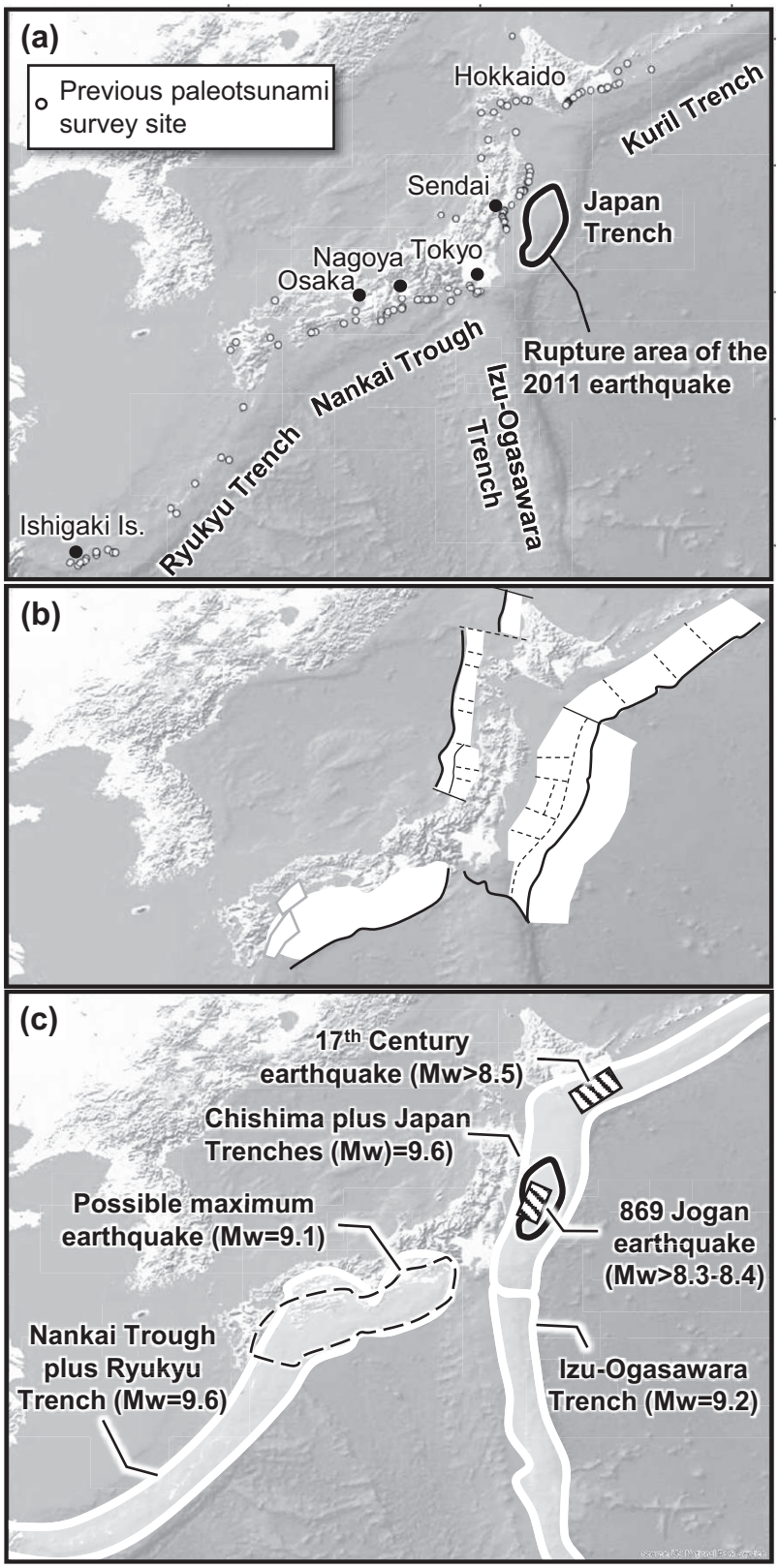

Figure 1. (a) Paleotsunami survey sites (after Goto et al., 2012) and rupture area of the 2011 earthquake (based on Ozawa et al., 2011). (b) Small segments defined by the Headquarters for Earthquake Research Promotion (based on the website of HERP: http://www.jishin.go.jp/main/p_hyoka02_kaiko.htm). (c) Location of paleotsunami source models (Satake et al., 2008b, 2010) as well as possible maximum fault models for the Nankai Trough by CDMC (2012) and other trenches by NRA (2013).

had yet to be included in consideration of local tsunami countermeasures.

Based on lessons learned from the 2011 event, the Japanese government changed its policy for tsunami disaster countermeasures. The major change was that estimation of the maximum possible earthquake and tsunami along each coast of Japan is required, as described below. Paleotsunami histories of several thousand years are extremely valuable. Therefore, tsunami geology is now regarded as a major research field for estimating maximum possible earthquakes and tsunamis for each coast (e.g., CDMC, 2011). However, numerous issues remain, mostly because the geological research of tsunamis takes so much time that it cannot respond quickly to rapid changes in policy. Moreover, it is probably unclear to the governors and to the general public what tsunami geology can or cannot do for them. Therefore, some expectations extend beyond the current knowledge in this research field. Tsunami geologists should perform their duties with clear explanations of what they can accomplish using current knowledge and methods and what geologists should do to bridge the gap to new policy.

The Japanese policy change and recent government estimation of maximum strengths of possible earthquakes and tsunami events are followed closely by the general public in Japan. They receive considerable media attention, although little is reported outside Japan. However, it is probably beneficial for the research community and local governments throughout the world to know the current situation of tsunami countermeasures in Japan after the 2011 event, especially from a standpoint of tsunami geology, because it will be useful to consider future tsunami countermeasures in "at-risk areas" in the geological sense such as the area along the Cascadia subduction zone (e.g., Peterson et al., 2013). We, therefore, summarize the policies of tsunami countermeasures before and after the 2011 event in Japan, and discuss the current status of tsunami geology.

General policies of the tsunami countermeasure before the 2011 event

The CDMC under the Cabinet Office is the main organization responsible for disaster management policymaking in Japan. Separate from CDMC, individual earthquake and tsunami studies are reviewed by the committees under the Headquarters for Earthquake Research Promotion (HERP), which was founded after the Great Hanshin-Awaji Earthquake Disaster on January 17, 1995. The main objective of HERP is "*to promote research into earthquakes with the goal of strengthening disaster prevention measures, particularly for the reduction of damage and casualties from earthquakes*" (HERP, undated). In pursuit of this objective, they evaluate seismic activity of major subduction-zone earthquakes and inland active faults. They sectionalize

the plate boundary into several smaller segments such as faults with Mw>7 (Fig. 1b). Segments may slip simultaneously, generating larger earthquakes (e.g., Furumura et al., 2011; Seno, 2012): so-called multi-segment earthquakes. Before 2011, this was the basic idea for evaluating the probability of future occurrences of large earthquakes along each trench.

For example, estimating the occurrence of large earthquakes along the Nankai Trough is extremely complex (Fig. 2, e.g., Furumura et al., 2011; Seno, 2012). The 1944 Showa Tonankai earthquake (Mw= 7.9) and the 1946 Showa Nankai earthquake (Mw=8.0) occurred individually over a two-year time interval (HERP, 2013). In 1854, the Ansei Nankai earthquake (Mw=8.4) occurred; 30 hours after the Ansei Tokai earthquake (Mw=8.4) occurred (HERP, 2013). In 1707, the Hoei earthquake (Mw=8.6–8.7) occurred and was interpreted as the largest multi-segment earthquake along the Nankai Trough. Before the 2011 event, the Hoei earthquake was regarded as the largest event along the Japanese archipelago in the past 1,300 years (HERP, 2013).

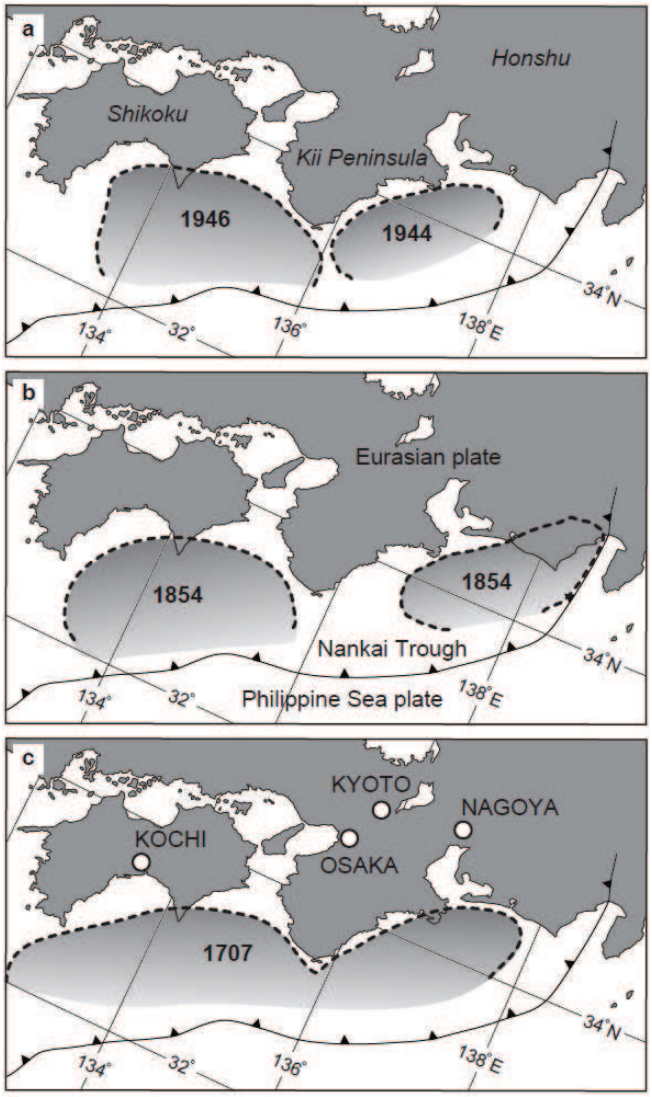

Figure 2. (a) Approximate rupture areas of the 1944 and 1946 earthquakes from Hatori (1974). (b) Approximate rupture areas of the two 1854 earthquakes from Hatori (1976). (c) Approximate rupture area of the 1707 earthquake from Hatori (1974). Western end of the rupture area extends westward for about 70 km based on Furumura et al. (2011).

It is noteworthy that all earthquakes described above were accompanied by large tsunamis (HERP, 2013). Tsunami-affected areas were broader in cases of multi-segment earthquakes, although the maximum run-up heights are almost constant at approx. 10 m (HERP, 2013), which indicates that the geological record of many previous events, whether for multi-segment earthquakes or not, might have been preserved in certain places such as coastal lowlands and lagoons. Nevertheless, it is difficult to ascertain from paleotsunami research whether the generating earthquake was a multi-segment type or not because no time resolution is available to differentiate earthquakes that occurred within several tens of years such as those of the 1944, 1946 or 1854 events.

Along the Japan Trench, large earthquakes, such as the "Miyagiken-oki earthquake", with a magnitude of 7.4 are known to occur on average every 37 years (Miyagi Prefecture, 2011). Since the last event in 1978, HERP predicted the probability of occurrence of a large earthquake as 70% during the subsequent 10 years before 2011 (Miyagi Prefecture, 2011). It was also considered that a multi-segment earthquake with a magnitude of 8.0 might have occurred several times off Sendai Bay after the 17th century, based on the historical record. That probability was included in the consideration of tsunami countermeasures (Fig. 3, Miyagi Prefecture, 2004). However, a larger earthquake such as the 869 Jogan earthquake, with an estimated magnitude of Mw>8.3–8.4 (Satake et al., 2008a; Namegaya et al., 2010; Sugawara et al., 2011), was not considered for disaster countermeasures before the 2011 event.

The Pacific coast of Hokkaido, which faces the Kuril Trench, is one of the rare places in Japan for which geological evidence was incorporated into tsunami countermeasures by the local government before 2011. This is true probably because Hokkaido has a short history in Japan. Fewer historical records pre-date the 17th century (e.g., Takashimizu, 2013), and therefore geological information is more important than for other areas of Japan. According to historical records gathered over the past 100 years, earthquakes with Mw=7 to 8 are well known to occur repeatedly with an interval of a few tens of years in eastern Hokkaido (e.g., Takashimizu, 2013). However, geological records suggest the occurrence of larger events in the past. Nanayama and Shigeno (1998) and Hirakawa et al. (1998) reported tsunami deposits from the 17th century in eastern Hokkaido. Nanayama et al. (2003) further described the maximum inland extent of sand deposits as approx. 3 km and from these results, Nanayama et al. (2003) and Satake et al. (2008b) reported that a multi-segment earthquake with Mw>8.5 must be assumed in order to explain the wide distribution of tsunami deposits in eastern Hokkaido. It is noteworthy that the tsunami recurrence interval in this region is well studied and is estimated to be about 500 years (Nanayama et al., 2003) or 300–500 years (Hirakawa et al., 2005), with aperiodic occurrences during a shorter period of 100–300 years plus a longer period of 600–700 years (Sawai et al., 2009).

The CDMC referred to the large earthquake hazard in eastern Hokkaido as a "500-year interval earthquake" (e.g., CDMC, 2006). This was probably the only case in which geological information had been effectively incorporated into policymaking for disaster prevention countermeasures before the 2011 event.

Policy changes after the 2011 event

After the 2011 event, historical and geological studies of the 869 Jogan event have been highlighted (e.g., Normile, 2011). The CDMC

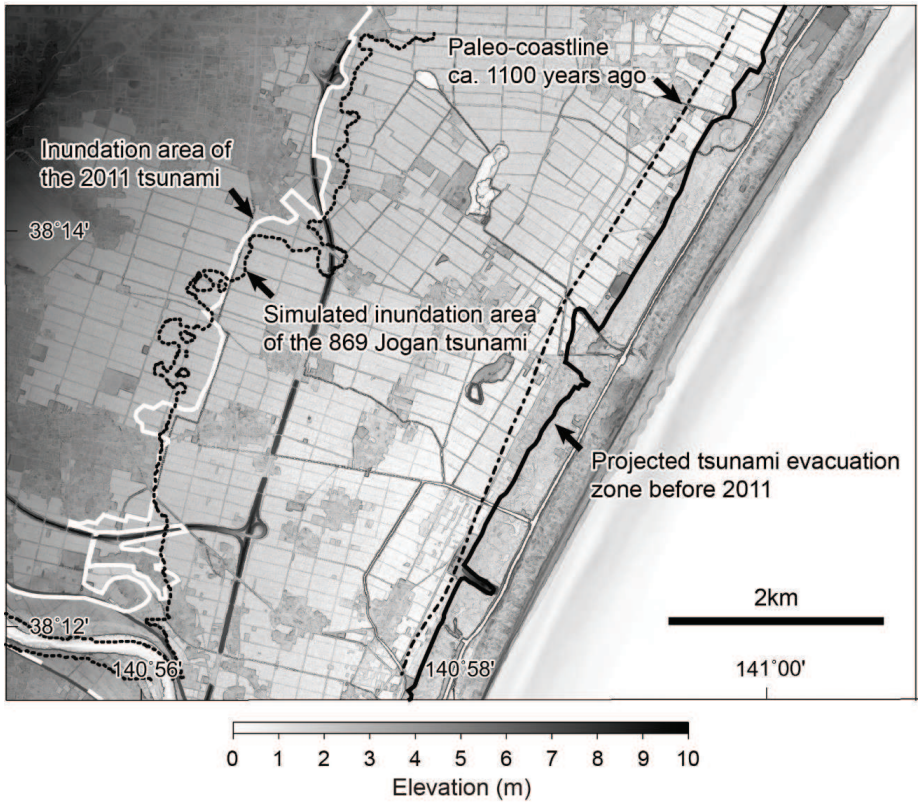

Figure 3. Estimated inundation areas of the 869 Jogan tsunami (after Sugawara et al., 2011) and 2011 tsunami (after Sugawara et al., 2013), and a tsunami hazard map issued before the 2011 event (Miyagi Prefecture, 2004).

established a committee for "*Technical Investigation on Countermeasures for Earthquakes and Tsunamis Based on the Lessons Learned from the "2011 off the Pacific coast of Tohoku Earthquake*" on 27 April 2011. The midterm report of the committee suggested that local governments consider two tsunami levels for future tsunami disaster prevention (Fig. 4):

Level 1 tsunami: One that occurs frequently every few tens of years to a hundred or more years. The estimated tsunami height is the basis for construction of shore protection facilities.

Level 2 tsunami: One that occurs with an extremely low frequency, but generating severe damage once it occurs. Shore protection facilities are probably insufficient to protect against a tsunami of this size. Saving human life is, therefore, the top priority, and hence so an awareness campaign including disaster education is highly recommended.

The final report of the committee was issued on 28 September 2011 (CDMC, 2011). The report concluded that "…*when conducting earthquake and tsunami hazard assumptions in the future, the largest-possible mega earthquakes and tsunamis should be considered from every possible angle*". The report also noted that "…*in order to verify the occurrence of mega tsunamis over a time scale of several thousand years it is vital that further enhancement be made not only to seismological research but also to the comprehensive geological, archaeological and historical research, including research into tsunami deposits on land and the ocean floor, geological research into coastal terraces, and research into biological fossils etc*" (CDMC, 2011). This is a typical change after the 2011 event, inducing the Japanese government to consider every possibility to exclude future unexpected earthquakes and tsunami disasters.

On 27 December 2011, the Ministry of Land, Infrastructure, Transport and Tourism (MLIT) created a new law for urban development against tsunami disasters. Geological research for tsunami risk assessment is strongly recommended before preparing future local disaster prevention plans (MLIT, 2011). Subsequently, many prefectural or city governments, especially those along the coasts of at-risk areas, started to re-evaluate Level 1 tsunami events based mainly on numerical modeling for tsunami inundation by adopting source models that were tuned by historical and geological records as well as seismological data. However, the estimation of Level 2 tsunami events is not easy for local governments.

Following the policy changes described above, CDMC (2012) issued a report on 29 August 2012 concerning the maximum possible earthquake and tsunami strength along the Nankai Trough, where megacities such as Nagoya and Osaka are located. They assumed a magnitude 9.1 earthquake along the Nankai Trough (Fig. 1c) with a possible maximum tsunami run-up height of approx. 30 m. The worst possible human and economic losses are estimated respectively as 320,000 people and 220 trillion yen (e.g., Asahi Newspaper, 2013). As acknowledged by the CDMC (2012), it is important to note that this fault model is not based on historical or geological evidence and that it far surpasses the largest known historical event (i.e., the 1707 Hoei event). The fault model parameters (e.g., slip amount or area) were actually estimated based on seismological lessons learned from

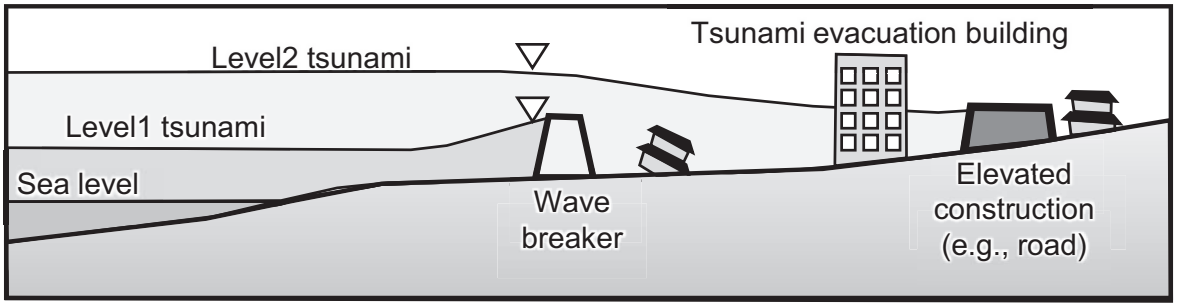

Figure 4. Illustration showing the difference of level 1 and 2 tsunamis and their countermeasures (based on Tokushima Prefecture, 2013).

previous large earthquakes that occurred worldwide, such as the 2011 Tohoku-oki, 2010 Chilean earthquake, and 2004 Sumatra earthquake (CDMC, 2012). The report also noted the extreme difficulty of predicting the future occurrence of such an earthquake and tsunami. This is largely because no historical or geological evidence exists to support the occurrence of such an extreme event.

To the north, prior to 2011, a tsunami hazard map for Hokkaido was produced based on the known 17th century event (Hokkaido, 2007; Satake and Nanayama, 2005). However, following the 2011 event this was renewed and tsunami heights became several times larger than the previous estimation even though they used the same pre-2011 geological dataset (Hokkaido, 2012).

Based on lessons learned from the severe accident of Fukushima Daiichi Nuclear Power Plant, the Nuclear Regulation Authority (NRA) issued a screening guidebook for use in evaluating tsunami countermeasures for each nuclear power plant in Japan (NRA, 2013). The report described how to use a source model for a benchmark maximum possible earthquake and tsunami, the outputs of which were to be used to design prevention facilities for a nuclear power plant (NRA, 2013). The guidebook also noted the potential occurrence of tsunamis generated by non-seismic hazards (e.g., submarine landslides, caldera collapse) and that models of benchmark events for both seismic and non-seismic sources should produce larger waves than those estimated from existing historical and geological evidence.

As extreme examples, source models were produced for the following three regions (1) Kuril plus Japan Trenches (approximate maximum magnitude (Mw) = 9.6), (2) Izu-Ogasawara Trench (Mw=9.2), and (3) Nankai Trough plus Ryukyu Trench (Mw=9.6), respectively (Fig. 1c), based on seismological knowledge obtained from past Mw>9 earthquakes occurring throughout the world. This is far larger than the government-level estimation. Similarly to the CDMC (2012) assumption for the Nankai Trough, the NRA (2013) also acknowledged that no evidence currently exists to support the occurrence of such large earthquakes in the past. However, they reasoned that the evaluation of the tsunami hazard for nuclear power plants should be stricter, and safe-side countermeasures are strongly required for consideration of the possible occurrence of such extremely strong earthquakes.

Perspective of tsunami geology

As stated in the previous section, it seems reasonable that the Japanese government requests scientists to estimate the maximum possible tsunami along each coast. This is not necessarily based on previous events in each region, but considers lessons learned from other tsunamis around the world. More importantly, a quick response, from months to years, has been required to reflect scientific knowledge in the ongoing improvement of tsunami countermeasures. Indeed, the estimation of maximum possible earthquake and tsunami along Nankai Trough was done swiftly - within one and half years of the 2011 event.

Then, what can tsunami geology contribute to disaster countermeasures under these circumstances? Tsunami geology is undoubtedly useful in helping to better understand both historical and paleotsunamis. Paleotsunami studies are not only useful for paleoseismology, but they can also reveal the potential occurrence of non-seismic events. Therefore, tsunami research must continue in order to improve our understanding of both historical and prehistoric tsunamis, whether the tsunami origin was seismic or non-seismic. However, for the very specific issue (exploring possible maximum earthquakes and tsunamis along the Japanese coast over a short time frame (e.g., 1-2 years)), we consider that the capabilities of tsunami geology are limited.

As the 869 Jogan tsunami studies showed, evidence-based studies usually take a lot of time to elucidate the nature of paleotsunamis. In fact, the 869 Jogan tsunami studies took more than 20 years to produce a scientific consensus. Although recent developments in tsunami geology may be sufficient to reduce the time taken for paleotsunami research, it is still probably difficult to contribute to the rapid revision of local governments' tsunami disaster mitigation plans within the next 1–2 years. Moreover, it is probably not straightforward to estimate the maximum possible earthquake and tsunami based solely on geological research because past events determined from paleotsunami research may not necessarily represent the maximum size of future events.

Estimating tsunami size from paleotsunami deposits also tends to underestimate the size of tsunamis and therefore underestimate earthquake magnitude (e.g., Goto et al., 2011; Namegaya and Satake, 2014). However, further improvement of methods are being made to estimate the sizes of paleotsunamis from geological evidence, based on field surveys (e.g. Goto et al., in press), various analyses (e.g., Goff et al., 2012; Chagué-Goff et al., 2012), and numerical modeling (e.g., Jaffe et al., 2012; Namegaya and Satake, 2014; Sugawara et al., 2014). These will better help to elucidate the nature and extent of paleotsunamis.

Equally, tsunami geology is also likely to be capable of evaluating the validity of presumed maximum tsunami inundation areas estimated though numerical modeling. For example, along the Nankai Trough, paleotsunami research at high elevations, where no historical evidence of tsunami inundation is available, but where possible inundation is suggested such as the model by CDMC (2012), would be important to test whether a maximum event that was estimated based on the seismology is an overestimation or an underestimation. However, at the moment, no results show quantitative support of the occurrence of an extremely large tsunami along the Nankai Trough estimated by CDMC (2012), although a potentially large event at around 2000 BP has been implied (e.g., Okamura et al., 2012).

It is also extremely important to continue to pursue the study of paleotsunami evidence along the coasts based on the classical style of field surveys, even if these appear to take some considerable time. As Figure 1a shows, many places exist in which no paleotsunami research has been done. Indeed, very few studies have examined areas along the coast of the Sea of Japan, even though this is an area with numerous nuclear power plants. There is no geological data along the Izu-Ogasawara Trench and thus tsunami risk along this trench is poorly understood. Potential tsunami generation by non-seismic sources is also no small issue because such events are indeed "unexpected" in most cases. Tsunami geology might help to ascertain where and when such non-seismic tsunamis might occur (e.g., Maeno and Imamura, 2007).

Physical evidence such as tsunami deposits is also an important means of educating local people about large paleotsunamis that inundated their towns in the past. This is important for local people so that they can be better aware of the tsunami risk. For example, in 2013, tsunami boulders on Ishigaki Island (Fig. 5), some of which were deposited by the 1771 Meiwa tsunami (e.g., Goto et al., 2010; Araoka et al., 2013), were designated as national monuments, which is probably the first example of geological evidence of a paleotsunami

Figure 5. Largest Porites coral boulder in eastern Ishigaki Island, Japan, which was deposited by the 1771 Meiwa tsunami based on the sedimentological observation (e.g., Goto et al., 2010) and radiocarbon dating (Araoka et al., 2013). This was designated as a national monument in Japan in 2013.

being so designated in Japan. Such evidence is important for disaster education purposes because people can be made aware of how large a tsunami was that struck an area in the past.

Another important issue is how to provide scientific results to the public. Satake and Nanayama (2005) provided maps of historical and prehistoric tsunami inundation zones for eastern Hokkaido that included the 17th century event. Alternatively, the "Japan Tsunami Trace Database" developed by Tohoku University and Japan Nuclear Energy Safety (JNES, currently NRA) is available on the web (http://tsunami-db.irides.tohoku.ac.jp/) and approx. 30,000 data points of tsunami heights based on historical records are included with validation. Database systems for tsunami deposits have been developed in the USA (Peters and Jaffe, 2010), New Zealand (Goff et al., 2010) and Australia (Goff and Chagué-Goff, 2014), but no Japanese version has yet been developed. With JNES support, we preliminary constructed a web database system for tsunami deposits, which is compatible with the Japan Tsunami Trace Database. Such a database might help local governors and the general public to better understand their local tsunami histories based on these historical and geological records.

Because of the circumstances described above, tsunami geology in Japan has become a richly interdisciplinary research field. In fact, not only geologists but researchers in other fields, along with engineers, governors, and private companies have been conducting investigations. This represents important progress in accelerating studies of how to differentiate tsunami deposits from other extreme events, how to use geological evidence for risk assessment, and how to communicate with local people because answers to these questions must be explored from various angles. Future communication between interdisciplinary researchers and governors must be carried out in order to improve the transfer of knowledge about tsunami geology efficiently and to consider how to use this scientific evidence to improve countermeasures.

Acknowledgements

Part of this study was supported by the Japan Nuclear Energy Safety (currently Nuclear Regulation Authority) and by Grants-in-Aid for Scientific Research from the Japan Society for the Promotion of Science (K. Goto, 26302007). We thank J. Goff for his valuable suggestions and comments on the manuscript.

References

Abe, H., Sugeno, Y., and Chigama, A., 1990, Estimation of the Height of the Sanriku Jogan 11 Earthquake-Tsunami (A.D. 869) in the Sendai Plain: Zishin (Journal of the Seismological Society of Japan), Second Series, v. 43 (4), pp. 513–525. (in Japanese with English abstract)

Araoka, D., Yokoyama, Y., Suzuki, A., Goto, K., Miyagi, K., Miyazawa, K., Matsuzaki, H., and Kawahata, H., 2013, Tsunami recurrence revealed by Porites coral boulders in the southern Ryukyu Islands, Japan: Geology, v. 41, pp. 919-922.

Central Disaster Management Council, 2011, Report of the Committee for Technical Investigation on Countermeasures for Earthquakes and Tsunamis Based on the Lessons Learned from the "2011 off the Pacific coast of Tohoku Earthquake". 50p. http://www.bousai.go.jp/kaigirep/chousakai/tohokukyokun/pdf/Report.pdf

Central Disaster Management Council, 2006, Report of damage estimation by the subduction zone earthquake along Japan and Kuril Trenches. 79p (in Japanese). http://www.bousai.go.jp/kaigirep/chuobou/senmon/nihonkaiko_chisimajishin/pdf/houkokusiryou1.pdf

Central Disaster Management Council, 2012, Report of investigative commission of large earthquake at Nankai Trough (second report) – tsunami fault model. 103p. (in Japanese). http://www.bousai.go.jp/jishin/nankai/nankaitrough_info.html

Chagué-Goff, C., Andrew, A., Szczucinski, W., Goff, J., and Nishimura, Y., 2012, Geochemical signatures up to the maximum inundation of the 2011 Tohoku-oki tsunami – implications for the 869 AD Jogan and other palaeotsunamis: Sedimentary Geology, v. 282, pp. 65–77.

Furumura, T., Imai, K., and Maeda, T., 2011, A revised tsunami source model for the 1707 Hoei earthquake and simulation of tsunami inundation of Ryujin Lake, Kyushu, Japan: Journal of Geophysical Research, v. 116, B02308.

Goff, J., and Chagué-Goff, C., 2014, The Australian tsunami database - A review: Progress in Physical Geography, v. 38, pp. 218–240.

Goff, J., Nichol, S., Kennedy, D., 2010, Development of a palaeotsunami database for New Zealand: Natural Hazards, v. 54, pp. 193–208.

Goff, J., Chagué-Goff, C., Dominey-Howes, D., Nichol, S., and Jaffe, B., 2012, Progress in palaeotsunami research: Sedimentary Geology, v. 243-244, pp. 70–88.

Goff, J., Terry, J. P., Chague-Goff, C., and Goto, K., What is a mega-tsunami?: Marine Geology, in press. 10.1016/j.margeo.2014.03.013

Goto, K., Miyagi, K., Kawamata, H., and Imamura, F., 2010, Discrimination of boulders deposited by tsunamis and storm waves at Ishigaki Island, Japan: Marine Geology, v. 269, pp. 34–45.

Goto, K., Chagué-Goff, C., Fujino, S., Goff, J., Jaffe, B., Nishimura, Y., Richmond, B., Sugawara, D., Szczucinski, W., Tappin, D.R., Witter, R., and Yulianto, E., 2011, New insights of tsunami hazard from the 2011 Tohoku-oki event: Marine Geology, v. 290, pp. 46–50.

Goto, K., Nishimura, Y., Sugawara, D., and Fujino, S., 2012, The Japanese tsunami deposit studies: Journal of Geological Society of Japan, v. 118, pp. 431–436. (in Japanese with English abstract)

Goto, K., Hashimoto, K., Sugawaran D., Yanagisawa, H., and Abe, T., Spatial thickness variability of the 2011 Tohoku-oki tsunami deposits along the coastline of Sendai Bay: Marine Geology, in press. doi:10.1016/j.margeo.2013.12.015

Hatori, T., 1974, Sources of large tsunamis in southwest Japan: Zishin (Journal of the Seismological Society of Japan), Second Series, v. 27, pp. 10–24. (in Japanese with English abstract)

Hatori, T., 1976, Documents of tsunami and crustal deformation in Tokai District associated with the Ansei Earthquake of Dec. 23, 1854: Bulletin of the Earthquake Research Institute, v. 51, pp. 13–28. (in Japanese with English abstract)

Headquarters for Earthquake Research Promotion, 2013, Long-term evaluation of seismic activities along the Nankai Trough (second edition): 96p. (in Japanese). http://www.jishin.go.jp/main/chousa/kaikou_pdf/nankai_2.pdf

Hirakawa, K., Nakamura, Y., and Echigo, T., 1998, Tsunami deposits on the terrace surface at Tokachi coast of Hokkaido: Programs and abstract of Seismological Society of Japan, C56. (in Japanese)

Hirakawa, K., Nakamura, Y., and Nishimura, Y., 2005, Holocene large tsunamis at the Pacific coast of Hokkaido: Comparison with the 2003 Tokachi-oki earthquake and tsunami: Chikyu Monthly, v. 49, pp. 173–180. (in Japanese)

Hokkaido, 2007, Tsunami inundation map at the Pacific coast of Hokkaido. (in Japanese). http://www.bousai-hokkaido.jp/BousaiPublic/html/common/sim_tsunami/rep/00_report_zendou.html

Hokkaido, 2012, Tsunami inundation map at the Pacific coast of Hokkaido. (in Japanese). http://www.pref.hokkaido.lg.jp/sm/ktk/bsb/tunami/index.htm

Jaffe, B., Goto, K., Fujino, S., Sugawara, D., Nishimura, Y., and Richmond, B., 2012, Flow speed estimated by inverse modeling of sandy tsunami deposits: results from the 11 March 2011 tsunami on the coastal plain near the Sendai Airport, Honshu, Japan: Sedimentary Geology, v. 282, pp. 90–109.

Maeno, F. and Imamura, F., 2007, Numerical investigations of tsunamis generated by pyroclastic flows from the Kikai caldera, Japan: Geophysical Research Letters, v. 34, L23303.

Ministry of Land, Infrastructure, Transport and Tourism, 2011, Basic guideline for implementation of regional construction with tsunami disaster prevention. (in Japanese). http://www.mlit.go.jp/common/000188287.pdf.

Miyagi Prefecture, 2004, Master plan of the beach protection along the coast of Sendai Bay: 66 pp•D(in Japanese) http://www.pref.miyagi.jp/soshiki/kasen/ka-sendaiwan.html

Mori, N., Takahashi, T., and the 2011 Tohoku earthquake tsunami joint survey group, 2012, Nationwide post event survey and analysis of the 2011 Tohoku Earthquake Tsunami: Coastal Engineering Journal, v. 54, 27 p., doi: 10.1142/S0578563412500015.

Minoura, K., 1990, Emergence and period of large-scale tsunamis in northeast Japan: Rekishi-Zishin, v. 6, pp. 61–76. (in Japanese)

Minoura, K., and Nakaya, S., 1991, Traces of tsunami preserved in inter-tidal lacustrine and marsh deposits: some examples from northeast Japan: Journal of Geology, v. 99, pp. 265–287.

Miyagi Prefecture, 2004, Report of damage estimation in Miyagi Prefecture. (in Japanese). http://www.pref.miyagi.jp/soshiki/kikitaisaku/ks-sanzihigai-houkoku.html

Miyagi Prefecture, 2011, Recurrence interval of the Miyagiken-oki earthquake. (in Japanese). http://www.city.sendai.jp/kurashi/shobo/shiryo/0053.html

Namegaya, Y., and Satake, K., Reexamination of the AD 869 Jogan earthquake size from tsunami deposit distribution, simulated flow depth, and velocity: Geophysical Research Letters, v. 41, pp. 2297–2303. doi: 10.1002/2013GL058678

Namegaya, Y., Satake, K., and Yamamoto, S., 2010, Numerical simulation of the AD 869 Jogan tsunami in Ishinomaki and Sendai plains and Ukedo river-mouth lowland: Annual Report of Active Fault and Paleoearthquake Researches, v. 10, pp. 1–21. (in Japanese, with English abstract)

Nanayama, F., and Shigeno K., 1998, Historical tsunami deposits along the Kuril Trench at eastern Hokkaido: Kaiyo Monthly, v. 15, pp. 177-182. (in Japanese)

Nanayama, F., Satake, K., Furukawa, R., Shimokawa, K., Atwater, B.F., Shigeno, K., and Yamaki, S., 2003, Unusually large earthquakes inferred from tsunami deposits along the Kuril trench: Nature, v. 424, pp. 660–663.

Normile, D., 2011, Scientific consensus on Great Quake came too late: Science, v. 332, pp. 22–23.

Nuclear Regulation Authority, 2013, Review guide for design-basis tsunami and design policy against tsunami. 42p. (in Japanese)

Okamura, M., and Matsuoka, H., 2012, Recurrence of Nankai earthquake based on the tsunami deposit. Kagaku, v. 82, 182–191. (in Japanese)

Ozawa, S., Nishimura, T., Suito, H., Kobayashi, T., Tobita, M., and Imakiire, T., 2011, Coseismic and postseismic slip of the 2011 magnitude-9 Tohoku-Oki earthquake: Nature, v. 475, pp. 373–376.

Peterson, C.D., Clague, J.J., Carver, G.A., and Cruikshank, K.M., 2013, Recurrence intervals of major paleotsunamis as calibrated by historic tsunami deposits in three localities: Port Alberni, Cannon Beach, and Crescent City, along the Cascadia margin, Canada and USA: Natural Hazards, v. 68, pp. 321–336.

Peters, R., and Jaffe, B.E., 2010, Database of recent tsunami deposits: US Geological Survey Open-File Report 2010–1172 (12 pp.).

Satake, K., and Nanayama, F., 2005, Records of tsunami reach on the Hokkaido pacific coast: Geological Survey of Japan, National Institute of Advanced Industrial Science and Technology, CD-ROM. (in Japanese).

Satake, K., Namegaya, Y., and Yamaki, S., 2008a, Numerical simulation of the AD 869 Jogan tsunami in Ishinomaki and Sendai plains: Annual Report of Active Fault and Palaeoearthquake Researches, v. 8, pp. 71–89 (in Japanese with English abstract).

Satake, K., Nanayama, F., and Yamaki, S., 2008b, Fault models of unusual tsunami in the 17th century along the Kuril Trench: Earth Planets Space, v. 60, pp. 925–935.

Sawai, Y., Shishikura, M., Okamura, Y., Takada, K., Matsu'ura, T., Aung, T.T., Komatsubara, J., Fujii, Y., Fujiwara, O., Satake, K., Kamataki, T., and Sato, N., 2007, A study of paleotsunami using handy geoslicer in Sendai Plain (Sendai, Natori, Iwanuma, Watari, and Yamamoto), Miyagi, Japan: Annual Report on Active Fault and Paleoearthquake Researches, v. 7, pp. 47–80. (in Japanese with English abstract).

Sawai, Y., Kamataki, T., Shishikura, M., Nasu, H., Okamura, Y., Satake, K., Thomson, K.H., Matsumoto, D., Fujii, Y., Komatsubara, J., and Aung, T.T., 2009, Aperiodic recurrence of geologically recorded tsunamis during the past 5500 years in eastern Hokkaido, Japan: Journal of Geophysical Research, v. 114, B013191.

Sawai, Y., Namegaya, Y., Okamura, Y., Satake, K., and Shishikura, M., 2012, Challenges of anticipating the 2011 Tohoku earthquake and tsunami using coastal geology: Geophysical Research Letters, v. 39, L21309.

Seno, T., 2012, Great earthquakes along the Nankai Trough –A new idea for their rupture mode and time series: Zishin (Journal of Seismological Society of Japan), Second Series, v. 64, pp. 97–116. (in Japanese with English abstract)

Sugawara, D., Imamura, F., Matsumoto, H., Goto, K., and Minoura, K., 2011, Reconstruction of the AD869 Jogan earthquake induced tsunami by using the geological data: Journal of Natural Disaster Science, v. 29 (4), pp. 501–516. (in Japanese with English abstract)

Sugawara, D., Imamura, F., Goto, K., Matsumoto, H., and Minoura, K., 2013, The 2011 Tohoku-oki Earthquake Tsunami: Similarities and Differences between the 869 Jogan Tsunami on the Sendai Plain: Pure and Applied Geophysics, v. 70(5), pp. 831–845.

Sugawara, D., Goto, K., and Jaffe, B., 2014, Numerical models of tsunami sediment transport -Current understanding and future directions: Marine Geology, v. 352, pp. 295–320.

Takashimizu, Y., 2013, Review of previous studies on tsunami deposits in Hokkaido, northern Japan: Focusing on the studies of deposits from 17th Century large tsunamis and others: Journal of Geological Society of Japan, v. 119, pp. 599–612. (in Japanese with English abstract)

Tokushima Prefecture, 2013, Sea level of the designed tsunami. (in Japanese) http://www.pref.tokushima.jp/docs/2013032900154/

Watanabe, H., 2001. Is it possible to clarify the real state of past earthquakes and tsunamis on the basis of legends? As an example of the 869 Jogan earthquake and tsunami: Rekishi-Zishin, v. 17, pp. 130–146. (in Japanese)

NOTE: English titles of Japanese papers were translated by authors.

by Akifumi Hisamatsu[1], Kazuhisa Goto [2] and Fumihiko Imamura [2]

Local paleo-tsunami size evaluation using numerical modeling for boulder transport at Ishigaki Island, Japan

1 Department of Civil and Environmental Engineering, Graduate School of Engineering, Tohoku University, 468-1-305 Aza-Aoba, Aramaki, Aoba-ku, Sendai 980-0845, Japan. *E-mail: Hisamatsu@tsunami2.civil.tohoku.ac.jp*

2 International Research Institute of Disaster Science (IRIDeS), Tohoku University, 468-1 Aza-Aoba, Aramaki, Aoba-ku, Sendai 980-0845, Japan

In this study, we simulated the transport of a large coralline boulder on southern Ishigaki Island of the Sakishima Islands, Japan, to evaluate local paleo-tsunami size in comparison to a well-known historical event (the 1771 Meiwa tsunami). According to the geological evidence, the boulder was deposited at 10 m elevation by two paleo-tsunami events. We assumed two types of fault models and eight dislocations for each fault. Then we investigated whether there are any combinations of the fault models that can satisfy the movement of the boulder from its presumed initial position to the present position by two tsunamis. Results show that several combinations of tsunami source models can satisfy the geological constraints. Our results revealed that at least one tsunami event during the prehistoric age was equivalent to or even larger than the 1771 tsunami in terms of the flow depth at the southeastern coast of the Ishigaki Island. Although the accuracy of this method depends strongly on the available geological evidence, we infer that the numerical modeling for boulder transport will have great value for evaluation of the local tsunami size, which is important for local tsunami risk assessment.

Introduction

For better future tsunami risk assessment, it is extremely important to elucidate the local tsunami history in terms of parameters such as the size and recurrence interval of tsunamis that occurred during historical and prehistoric ages. Historical and geological records are useful to estimate the inundation areas and sources of paleo-tsunamis (e.g., Sawai et al., 2012). Many works have been done to estimate the size and recurrence interval of paleo-tsunamis based on such records (e.g., Atwater et al., 2005; Cisternas et al., 2005; Jankaew et al., 2008). Numerical modeling based on geological records is also useful to improve estimation of the size of local tsunamis as well as the source model (e.g., Koshimura et al., 2002; Nanayama et al., 2003). However, many of these works used sandy tsunami deposits because sandy tsunami deposits are useful to estimate minimum tsunami inundation areas (e.g., MacInnes et al., 2009; Morton et al., 2007). Although various sizes of tsunami deposits from mud to boulders have been reported (e.g., Clague et al., 2000; Dawson and Shi, 2000; Gelfenbaum and Jaffe, 2003; Goff et al., 2010, 2012; Goto et al., 2010a; Sheffers, 2008; Sugawara et al., 2012; Yamada et al., in press), very few studies have used deposits other than sandy ones to estimate the paleo-tsunami size.

Tsunami boulders have recently been recognized as important geological evidence of paleo-tsunamis (Etienne et al., 2011). These boulders are deposited along coastal areas throughout the world (Goto et al., 2010a). The size and source model of paleo-tsunamis has been assessed based on boulder deposits (e.g., Frohlich et al., 2009). For example, Tonga has one of the largest deposited boulders in the world, estimated as weighing more than 1600 tons (Frohlich et al., 2009). Using numerical modeling with an equation reported by Nott and Bryant (2003), Frohlich et al. (2009) calculated the required tsunami height sufficient to cast this boulder ashore to its present position. They found that volcanic flank collapse or submarine slumps are the plausible tsunami sources providing sufficient tsunami height. However, the equation reported by Nott and Bryant (2003) calculates the minimum current velocity to move the boulder. For that reason, it is probable that the estimated size and source model are markedly underestimated. To estimate the size and source model of paleo-tsunamis better using boulder deposits, forward modeling of boulder transport by the tsunami (e.g., Imamura et al., 2008; Nandasena et al., 2013; Sugawara et al., 2014) may be more appropriate, because the forward modeling can evaluate whether large boulders can be moved from the initial position to the present position by the arbitrary size of the tsunami.

In the Sakishima Islands at the southeastern end of Japan (Fig. 1), numerous coralline and reef boulders are believed to have been deposited by paleo-tsunamis (Goto et al., 2010a). Araoka et al. (2013) conducted radiocarbon dating of 92 *Porites* tsunami boulders and reported that eight tsunamis would have struck the Sakishima Islands during the last approximately 2400 years (250±100 B.C., A.D. 200±100, A.D. 550±100, A.D. 800±100, A.D. 1100±100, A.D. 1400±100, A.D. 1600±100, A.D. 1800±100). The latter two events are probably consistent with historically recorded events occurring in 1625 and 1771 (Fig. 2, Araoka et al., 2013). Among them, the 1771 tsunami, the so-called the Meiwa tsunami, is remarkable because

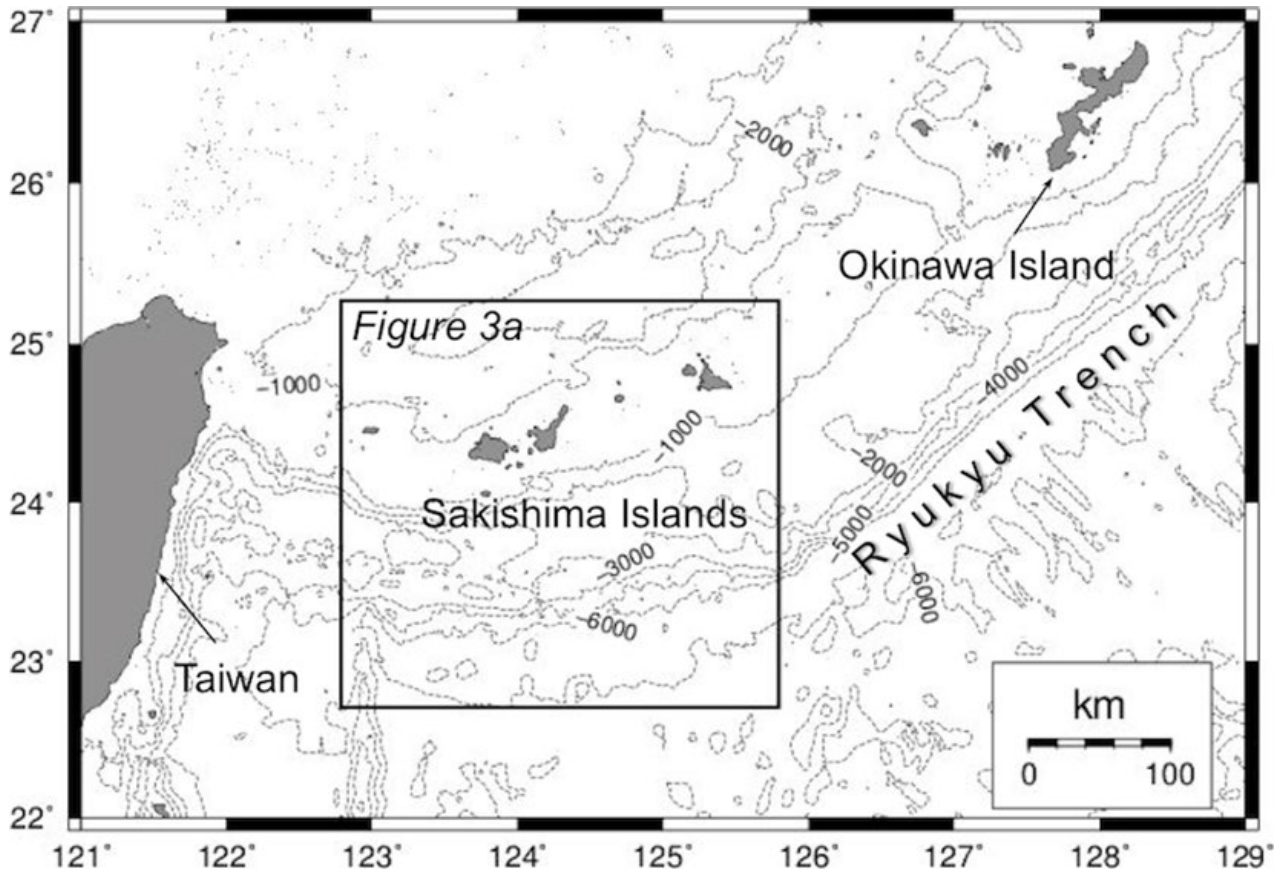

Figure 1. Location of the Sakishima Islands.

great amounts of historical and geological evidence, including tsunami boulders, are available (e.g., Goto et al., 2010a; Kawana and Nakata, 1994). Nevertheless, the tsunami source model of the 1771 event has remained controversial: a fault plus a submarine landslide (Imamura et al., 2001, 2008; Miyazawa et al., 2012) and a tsunami earthquake assuming a thrust fault along the plate boundary (Nakamura, 2009) have been proposed as possible causes.

The potential usefulness of tsunami boulders to improve estimation of the size and source model of the 1771 tsunami as well as the past events before 1771 was reported by Imamura et al. (2008). However, tsunami boulders have never been used to evaluate paleo-tsunami size. Therefore, it remains uncertain whether large tsunami(s) that are equivalent to or even larger than the 1771 event occurred repeatedly before 1771 or not. Nevertheless, this presents an extremely important question for local tsunami risk assessment.

This study was conducted to explore methods to use tsunami boulders to improve paleo-tsunami size estimation based on the forward model of boulder transport. To achieve this objective and to simplify the discussion, we examine only a single large coralline boulder deposited on the Ishigaki Island in the Sakishima Islands (detailed information about the boulder will be described in Geological setting). Using this boulder, we investigated local paleo-tsunami sizes at southeastern coast of the Ishigaki Island during the past 2400 years. Results suggest that at least one large tsunami equivalent to the 1771 event occurred before 1771.

Geological setting

The Ishigaki Island, located approximately 400 km southwest from the Okinawa Island, is surrounded by fringing reefs and the maximum distance between the coastline and reef edge is about 1.5 km (Goto et al., 2010a). The tide is semidiurnal, with a maximal range at spring tide of 2.0 m and mean low tide level that is 1.0 m below mean sea level (Iryu et al., 1995). The Ryukyu trench lies about 100 km south of the Ishigaki Island. The relative plate motion is 67 mm/yr (Rhea et al., 2010).

Goto et al. (2010a) investigated the distribution of boulders in the Ryukyu Islands. They reported that boulders transported by typhoon-generated storm wave were distributed only on the reef crest (within approximately 300 m inland from reef edge), although tsunami-transported boulders reached the beach and further inland after crossing over the 1.5 km reef flat.

The largest coralline boulder on the Ishigaki Island, the so-called "*Tsunami ufu-ishi*" boulder (Fig. 4c, hereinafter designated as the TU boulder), was deposited approximately 100 m inland from the present shoreline (approximately 10 m a.s.l.) at the southern coast of the island (Figs. 4a and 4b). The boulder dimensions are approximately 12.4 × 10.8 × 5.9 m. It weighs more than 500 tons, as inferred from its material and ellipsoidal shape (coral density was 1.62 ton/m^3). The boulder porosity was assumed as 20%, based on Kawana (2008). This study used this boulder for the numerical modeling because the boulder is the largest prehistoric tsunami boulder in the Sakishima Islands whose depositional age and rotation history was estimated from the radiocarbon dating (Kawana and Nakata, 1994) and paleo-magnetic analysis (Sato et al., 2013). Moreover, the original location can be estimated from the coral assemblage (Kawana et al., 1987) as described below. Therefore, the boulder is adequate to evaluate sizes of paleo-tsunamis in the Ishigaki Island.

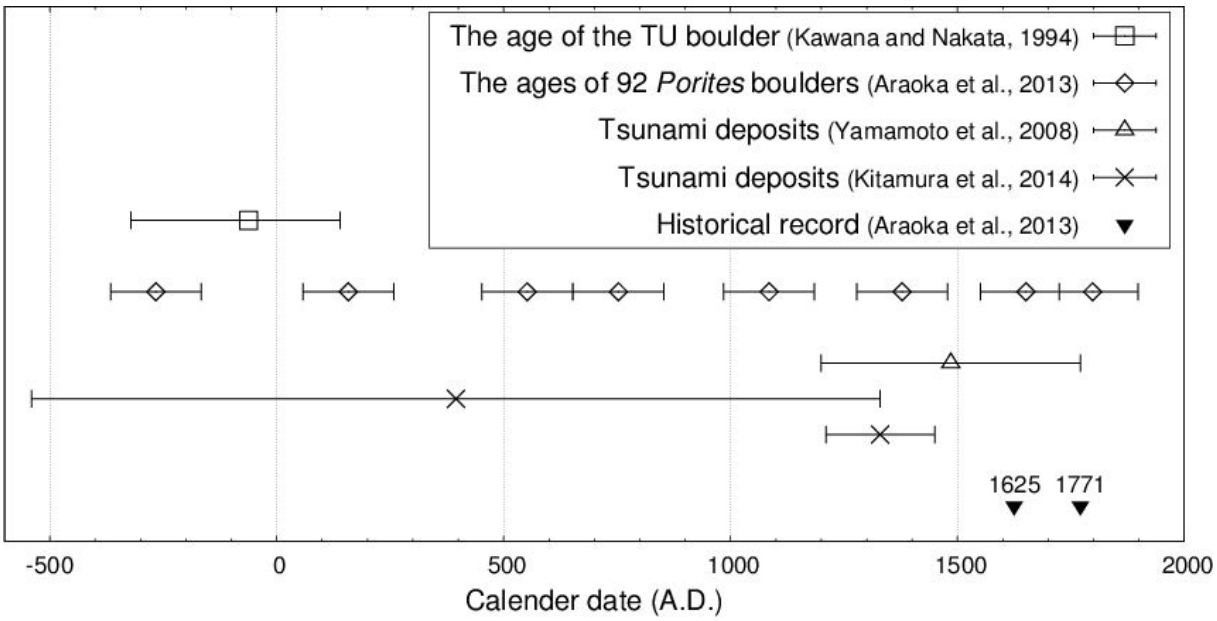

Figure 2. Tsunami occurrence according to the radiocarbon age of the TU boulder (Tsunami ufu-ishi)(Kawana and Nakata, 1994), the ages of 92 Porites boulders in the Sakishima Islands (Araoka et al., 2013), historical records (Araoka et al., 2013), and the ages of tsunami deposits (Yamamoto et al. 2008 and Kitamura et al., 2014).

The original position of the boulder is estimated as shallower than 10 m water depth of the reef slope, based on coral assemblages (*Favia, Favites, Acropora, Goniastrea, Platygra*) (Kawana et al., 1987). Moreover, considering the boulder height (approximately 6 m) and tidal range ±1 m, the boulder is expected to have been located in deeper than 7 m of water depth because corals cannot grow above the lowest tide level. The radiocarbon age of a coral taken at the youngest part of the boulder showed 1980±80 yrBP (Kawana and Nakata, 1994). Consequently, it is likely that the boulder emerged above sea level from the water during 321 B.C.–A.D. 140 (2σ) (see Appendix 1).

Kawana and Nakata (1994) and Goto et al. (2010a) proposed that the TU boulder was likely to have been deposited by the paleo-tsunami at around 321 B.C.–A.D. 140 because (1) it should have been relocated from somewhere by the wave when the tide level was, at that time, almost equal to the present level (Kawana, 2006). Therefore, the boulder presence at 10 m elevation cannot be explained by the sea level change. (2) The distance from the nearest reef edge is about 450 m, which is far greater than the transport limit of storm wave boulders as estimated by Goto et al. (2010a). In fact, Goto et al. (2010a) reported that the boulder was not moved from its present position even by the 1771 event because no historical description exists of movement of the boulder. Movement of much smaller boulders near the TU boulder was described, which also suggests that the TU boulder was deposited in its present location by a large tsunami before 1771.

Rotation history of the TU boulder is also well studied (Sato et al., 2013). Boulders originally grew as corals on the reef before the tsunami. The corals acquired depositional remanent magnetization parallel to Earth's current magnetic field as natural remanent magnetization, and after the corals were transported by tsunami, new remanence was superimposed as viscous remanent magnetization parallel to Earth's current magnetic field (Sato et al., 2014). Vector component changes can be seen in vector plots for successive thermal demagnetization steps, if the boulder had been rotated (Sato et al., 2014). Based on this idea, Sato et al. (2013) reported that the TU boulder was rotated twice in the past by two paleo-tsunamis.

Alternatively, it is possible that the boulder was rotated once by a typhoon-generated storm wave at the source on the reef slope and then displaced to the present position by one large tsunami. However, this boulder is extremely heavy (approximately 500 tons) and it is far heavier than the known storm wave boulders at Ryukyu Islands (<200 tons, Goto et al., 2013). Moreover, if the boulder can be rotated by storm waves, it should have been rotated many times because many large typhoons attack the Ishigaki Island every year. Considering that the boulder was rotated only twice during the last 2000 years (Sato et al., 2013), it is unlikely that the boulder was rotated by such high frequency typhoon-generated storm wave and we prefer the interpretation proposed by Sato et al. (2013) that it was rotated by two large tsunami events.

Yamamoto et al. (2008) reported a sandy tsunami deposit on the eastern coast of the Ishigaki Island that was deposited after A.D. 1200 but before A.D. 1771 (Fig. 2). Kitamura et al. (2014) reported two possible tsunami deposits that were probably deposited by the tsunami in 540 B.C.–A.D. 1330 and A.D. 1210–1450 at an eastern coastal area of the Ishigaki Island (Fig. 2). The former tsunami event might be of comparable age to the emergence of the TU boulder.

In summary, the geological evidence presented above suggests that (1) the TU boulder emerged above the lowest sea level by the tsunami at around 321 B.C.–A.D. 140 and that (2) it was moved (or rotated) again by the tsunami occurring after that event but before 1771. It reached its present position, and (3) it remained unmoved by the 1771 Meiwa tsunami. These three geological implications are used as constraint conditions for our numerical modeling.

Numerical method

In this study, we assumed that the TU boulder was moved twice by two tsunamis based on Sato et al. (2013). We calculated the boulder transport by the first tsunami and estimated its stop position. Then,

the final stop position after the first tsunami was used as the initial position of the second tsunami event. If the boulder stopped within the 50 m radius circle, we infer that the modeling result satisfies the constraint conditions. Detail numerical methods and constraint conditions are explained below.

Numerical calculation for boulder transport by tsunami

Numerical modeling for the tsunami inundation fundamentally follows that of Miyazawa et al. (2012). A nested grid system constructed by Miyazawa et al. (2012) was used across a wide area (regions 1 and 2) to the coast of each island (region 3). Spatial grid sizes of each region are, 300 m for region 1 (Fig. 3a), 100 m for region 2 (Fig. 3a) and 50 m for region 3 (Fig. 3b), respectively (Miyazawa et al., 2012). We also added region 4 with a 10 m grid (Fig. 3c) for detailed modeling of boulder transport by the tsunami. Our preliminary modeling revealed no effect of the third and later waves for the movement of the TU boulder. Therefore, we calculated up to 30 min after the tsunami generation to simulate the boulder movement by the end of the second backwash.

The Boulder Transport by Tsunami model (hereinafter the BTT model, see Appendix 2 for the method) developed by Imamura et al. (2008) was used to calculate the boulder movement by the tsunami in region 4. The model validity was well confirmed by several examples such as the 2004 Indian Ocean tsunami (Goto et al., 2010b) and the 1771 Meiwa tsunami (Imamura et al., 2008).

Source models for evaluating paleo-tsunami size at the TU boulder

As stated in Geological setting, the TU boulder was likely to have been moved to its present position by two tsunami events before 1771 (Sato et al., 2013). Then, the question is whether the sizes of these two paleo-tsunamis were equivalent to or greater than that of the 1771 event. To explore the answer to this question, we evaluate the sizes of two paleo-tsunamis before 1771 using the BTT model. However, to adopt the BTT model, the tsunami source should be assumed, but geological evidence of prehistoric tsunamis is insufficient to evaluate the tsunami source. Therefore, we assume the source model of the 1771 event, which is well estimated, as the basis of the source of paleo-tsunamis and discuss whether the local tsunami heights of paleo-tsunamis were larger than the 1771 event or not.

Two tsunami source models for the 1771 event were used for our analysis (Table 1). Nakamura (2009) proposed a Mw=8.0 inter-plate earthquake along the Ryukyu trench (hereinafter called the NK model), whereas Miyazawa et al. (2012) proposed a combination of a Mw=8.2 intra-plate earthquake and submarine landslide, the latter of which is imitated by a fault model (hereinafter called the MY model) (Fig.

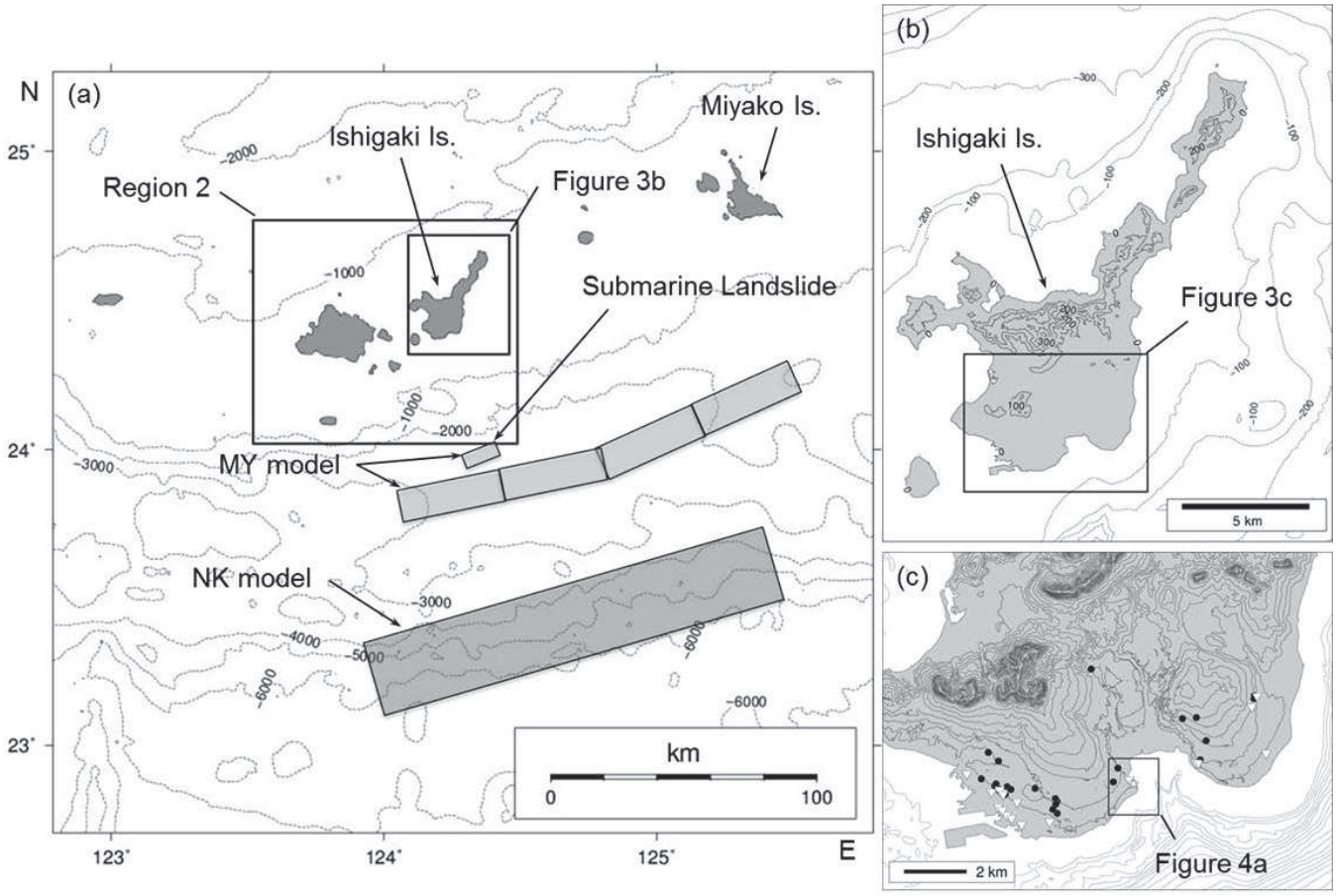

Figure 3. Regions 1–4 for numerical calculations. (a) Region 1 for numerical calculation. NK and MY model in the figure respectivelyshow the 1771 Meiwa tsunami model proposed by Nakamura (2009) and Miyazawa (personal communication). (b) Region 3 for numerical calculation. (c) Region 4 for numerical calculation and 45 instances of historical evidence related to the Meiwa tsunami. White triangles show sites inundated by the Meiwa tsunami. Black dots show non-inundated sites.

Table 1. Fault parameters of tsunami source models for the 1771 Meiwa tsunami. The NK model was proposed by Nakamura (2009). The MY model was proposed by Miyazawa (personal communication) and we slightly revised it from Miyazawa et al. (2012).

Model	Tsunami source	Latitute (deg)	Longitude (deg)	Depth (km)	Length (km)	Width (km)	Dislocation (m)	Strike (deg)	Dip (deg)	Rake (deg)
NK model (Mw=8.0)	Fault 1	23.5000	125.4500	5	150	30	16	255	12	90
MY model (Mw=8.2)	Fault 1	24.2018	125.5184	5	41	35	14	245	70	90
	Fault 2	24.0526	125.1497	5	40	35	14	246	70	90
	Fault 3	23.9100	124.8000	5	35	35	13	259	70	90
	Fault 4	23.8421	124.4576	5	36	35	14	261	70	90
	Landslide	24.0036	124.2640	0.1	12	8	90	76	70	90

3a). These models are well consistent with the measured run-up heights at many places in the Sakishima Islands. However, both models underestimated the tsunami run-up heights in the southern part of the Ishigaki Island (Miyazawa et al., 2012), where the maximum run-up height (approximately 30 m) was recorded (Goto et al., 2010a). Therefore, we first improve the NK and MY models by changing the dislocation of the fault in case of the NK model, and the dislocation of landslide-imitated fault in case of MY model to satisfy the run-up heights along the southeastern part of the Ishigaki Island based on 45 instances of historical evidence that indicate inundated (19 sites) and non-inundated (26 sites) area by the 1771 tsunami (Fig. 3c). It is noteworthy that the model estimated for this study is not necessarily the actual model of the 1771 event because we consider only the historical records along the southeast coast of the Ishigaki Island and thus this fault model may not fit to the inundation area or run-up heights at other islands. In this sense, we do not regard this model as the source model of the 1771 event but, rather, regard it as the benchmark tsunami source model that satisfies the inundation area and run-up height specifically at the southeastern coast of the Ishigaki Island.

It is important to note that many combinations of tsunami source models may satisfy the constraint conditions in Geological setting. Moreover, it is uncertain whether large submarine landslides were repeatedly generated at the same location. Considering the paleo-tsunami traces are very scarce, it is not realistic to explore the source model of paleo-tsunamis. Our main objective is to find whether there were any paleo-tsunamis that were equivalent or larger size than the 1771 event in terms of the flow depth at the southeast coast of the Ishigaki Island. For this particular objective, we limited the modeling cases.We changed the dislocation of the fault of NK model and the dislocation of landslide-imitated fault in the case of the MY model (Table 2), respectively, to generate tsunamis with flow depths smaller or larger than the benchmark tsunami at the TU boulder position. We changed only the dislocation of the landslide-imitated fault in case of the MY model because the landslide-imitated fault may generate a tsunami with high amplitude but short wave length, which may be very different from the tsunami generated by the usual fault model (low amplitude and long wavelength). On the other hand, we did not change the slip amount of the fault in the MY model because the effect of the slip amount of the fault model is probably similar to that of the NK model and thus it is not necessary to change this in the MY model. Eight models with different fault dislocations were assumed for the NK model and MY model, respectively, to make the maximum flow depths at the present TU boulder position 1–8 m in every 1 m interval (within 0.2 m error). Based on this assumption, the relative sizes of paleo-tsunamis can be evaluated in comparison with the flow depth of the benchmark tsunami at the present TU boulder position.

Initial setting of the TU boulder and constraint conditions

Because the exact initial position of the TU boulder is uncertain, we set 100 boulders in the area at 20 m intervals in 7–10 m water depth along the reef slope (Figs. 4a and 4b) based on the geological evidence (see Geological setting). Interaction among boulders (e.g. collision) and wave reflection by the boulders were not considered. We assumed that the boulder had already been detached from the reef before the tsunami struck. Although the validity of this assumption cannot be confirmed, it is likely because severe typhoons frequently strike the reef, as frequently as every year, and many fragments of reef rocks remain on the slope of the present reef. The average distance between the present and initial positions of the TU boulder was approximately 970 m (the shortest distance was 826 m and the longest distance was 1104 m). The vertical elevation distance is approximately 19.0 m, on average (Figs. 4a and 4b).

Considering the uncertainties and errors of the model, we evaluated the size of tsunamis according to whether the boulder reaches a circle with 50 m (100 m diameter) radius from the TU

Table 2. Fault parameters of tsunami source models for evaluating the paleo-tsunami size. Fault dislocation of MY model is the dislocation of landslide-imitated fault.

Model	Fault dislocation (m)	Maximum flow depth at the TU boulder present position (m)
NK1	16.0	1.00
NK2	19.0	1.98
NK3	22.0	2.98
NK4	23.5	4.08
NK5	25.0	5.14
NK6	26.5	5.96
NK7	28.5	7.02
NK8	31.0	8.06
MY1	35.0	0.81
MY2	60.0	2.18
MY3	90.0	3.15
MY4	120	4.10
MY5	150	5.06
MY6	180	5.93
MY7	240	7.02
MY8	300	7.98

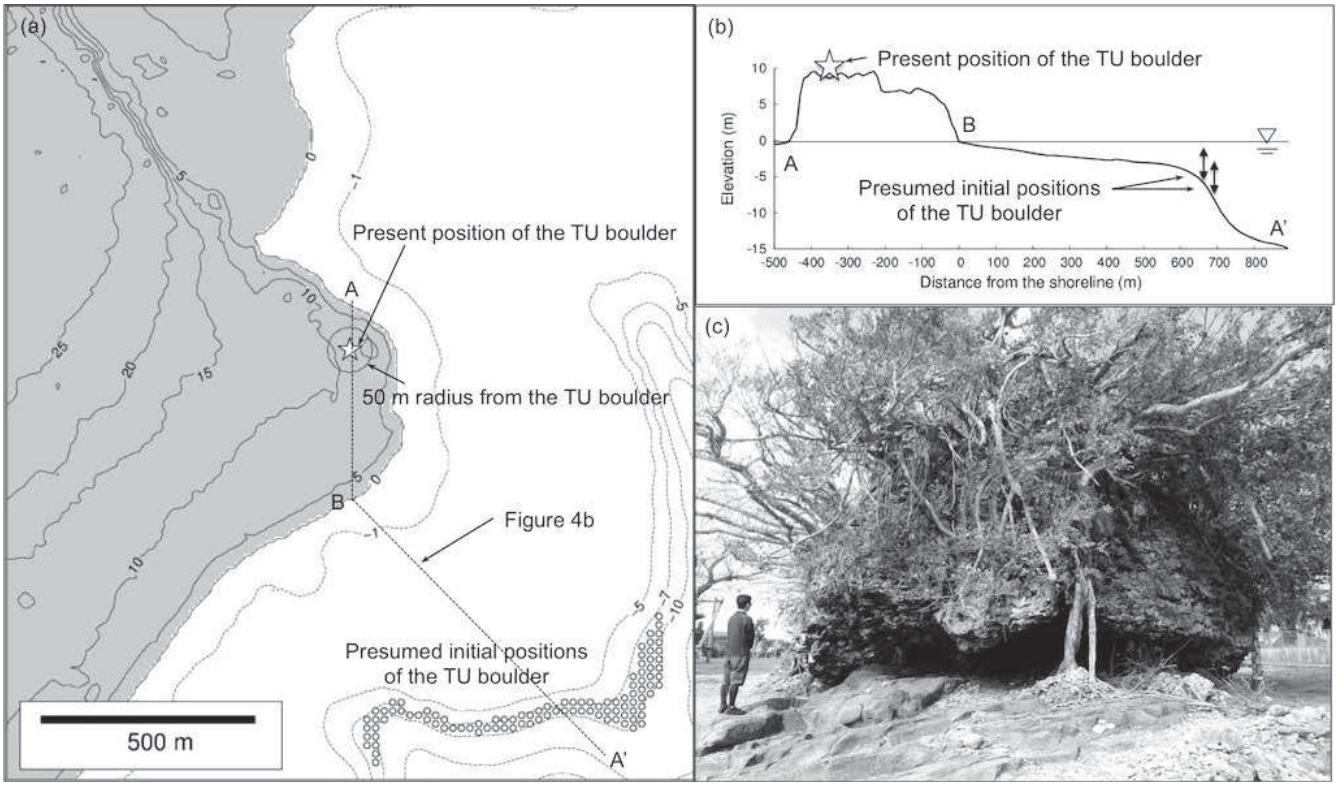

Figure 4. (a) The present position and the presumed initial positions of the TU boulder (Tsunami ufu-ishi) and their surrounding bathymetry. (b) Transect A-A'. (c) Picture of the TU boulder.

boulder's present position (Fig. 4a), which is equivalent to a 2 m difference in elevation. The 100 m distance is approximately 10 % of the average distance from the TU boulder initial and present positions. Petroff et al. (2001) reported an error of approximately 20% of the final stop position of a boulder, even in the case of a well-controlled water tank experiment. Our assumption is stricter than that used for the results reported by Petroff et al. (2001).

Results

Tsunami propagation and inundation

The first wave of the tsunami reached the southern part of the Ishigaki Island at approximately 15 and 10 min respectively for the NK and MY models (Figs. 5c and 5e). In both cases, the wave trough reached the coast first. Then the wave crest marked the highest run-up and the largest inundation (Fig. 5). For example, for the NK6 model, the first wave reached the initial position of the TU boulder about 16 min after the tsunami generation (Fig. 6a) and the maximum water elevation was recorded about 2 min later (Fig. 6c). After the maximum inundation, the wave direction changed 45–90 deg because of wave reflection by the steep slope (Fig. 6c). The backwash started about 2 min later (Fig. 6d). Those changes of current direction seemed to have affected the boulder movement direction.

Among the modeling cases, we first evaluate the tsunami source model, which was determined to specifically satisfy the inundation area and run-up heights of the 1771 event at southeastern coast of the Ishigaki Island, to determine the benchmark tsunami (Table 3). The inundation area increased with increasing dislocation of the fault in the NK model, and with increasing dislocation of landslide-imitated

Table 3. Numerical results for reproducibility of the 45 instances of historical evidence of the Meiwa tsunami, with inundated/non-inundated number, rate and inundation area in region 4 of each model.

Historical record	Number				
	Inundated sites	Non-inundated sites	Total		
	19	26	45		
	Reproducibility				
Model	Inundated sites	Non-inundated sites	Total	Rate (%)	Inundation area in region 4 (km^2)
NK1	9/19	26/26	35/45	77.8	13.7
NK2	11/19	26/26	37/45	82.2	16.5
NK3	12/19	26/26	38/45	84.4	18.6
NK4	14/19	25/26	39/45	86.7	19.5
NK5	14/19	23/26	37/45	82.2	20.4
NK6	14/19	23/26	37/45	82.2	21.4
NK7	15/19	20/26	35/45	77.8	22.9
NK8	16/19	19/26	35/45	77.8	24.6
MY1	8/19	26/26	34/45	75.6	11.7
MY2	10/19	26/26	36/45	80.0	14.1
MY3	10/19	26/26	36/45	80.0	16.6
MY4	12/19	25/26	37/45	82.2	18.4
MY5	14/19	23/26	37/45	82.2	20.2
MY6	14/19	21/26	35/45	77.8	22.1
MY7	17/19	15/26	32/45	71.1	25.7
MY8	17/19	12/19	29/45	64.4	28.9

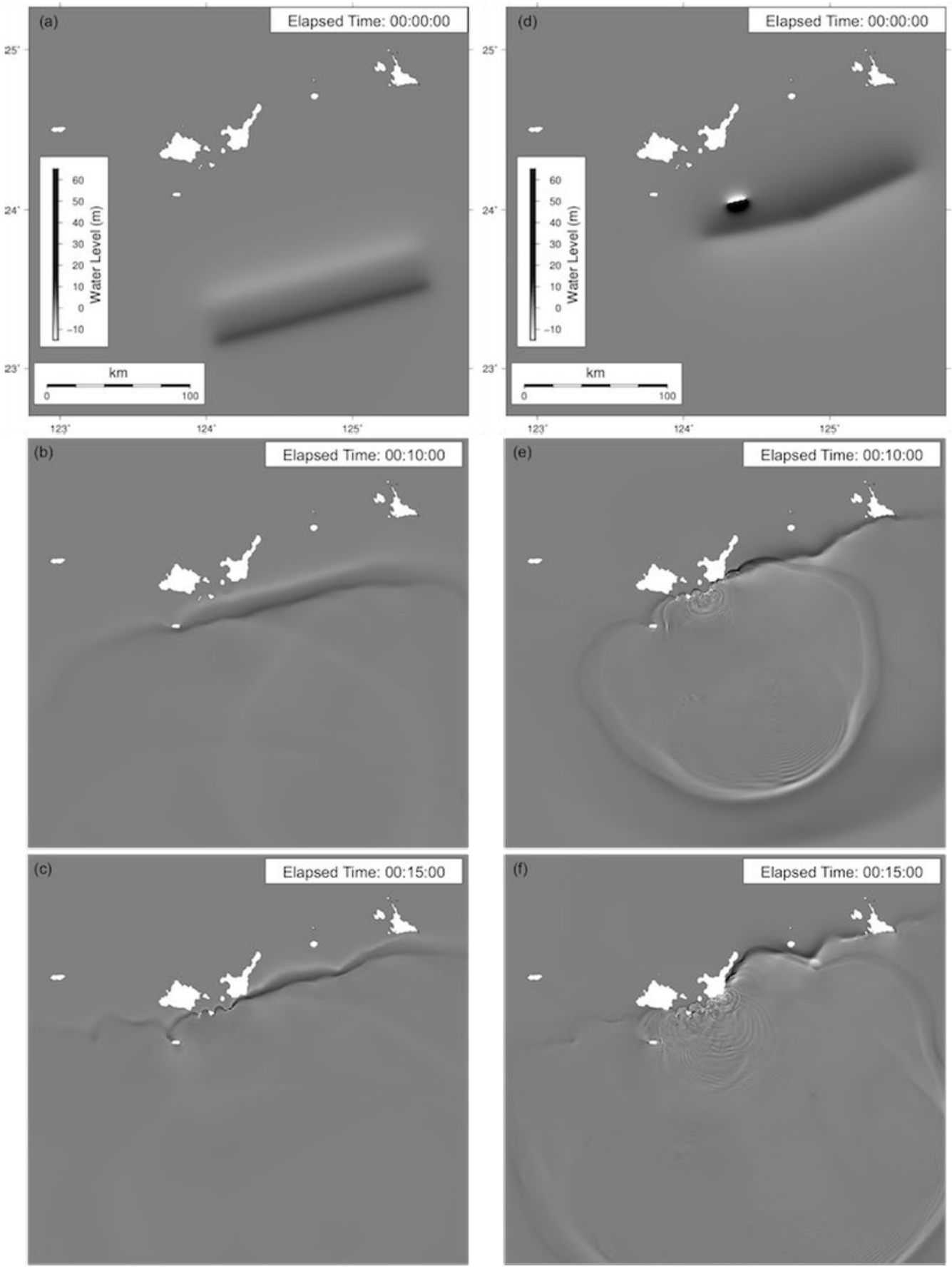

Figure 5. Snap-shots of numerical results for propagation of the 1771 Meiwa tsunami models proposed by Nakamura (2009) (left) and by Miyazawa (personal communication) (right). The images show the deformation, 10 and 15 minutes after the deformation.

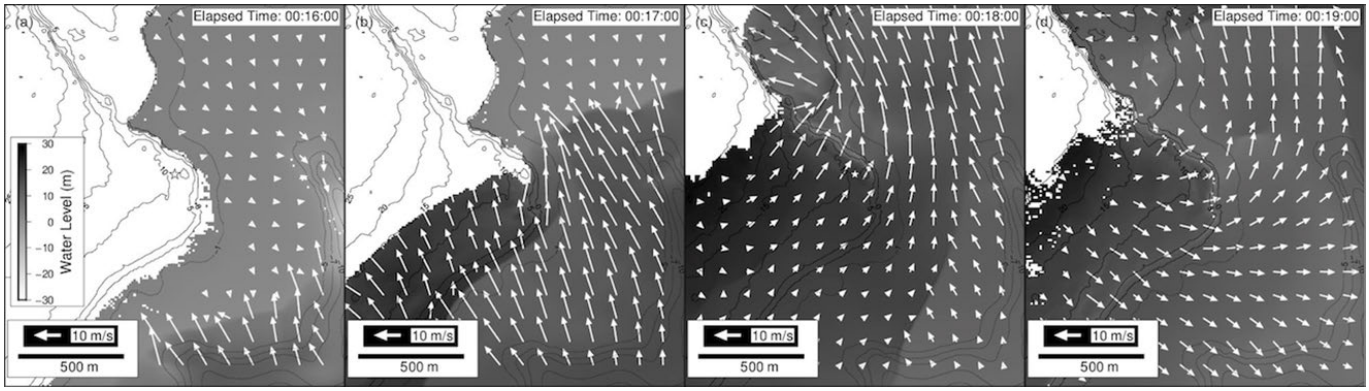

Figure 6. Snap-shots of numerical results for inundation of NK6 model. Each snap shows the wave height and current direction of (a) 16, (b) 17, (c) 18, and (d) 19 minutes after the tsunami generation.

fault of the MY model. We determined the NK4 model (86.7% accuracy) and MY4 model (82.2% accuracy) as the benchmark tsunami of each model, respectively. Actually, the MY5 model can also give the same accuracy as the MY4 model. However, the tsunami generated by the MY5 model is too strong and thus the TU boulder was displaced from the present position by the latest event (i.e. the 1771 event). This is not consistent with the historical and geological evidence that suggest the TU boulder was located in its present location before the 1771 event and was not moved by the 1771 event (e.g., Kawana and Nakata, 1994; Goto et al., 2010). In contrast, the MY4 model moved the boulder less than 50 m, which is within the range of uncertainty for this calculation. Therefore, we adopt the MY4 model as the benchmark tsunami.

Boulder transport

For NK models, six cases satisfied the constraint conditions (see Geological setting): (1) NK2 (first tsunami event) + NK6 (second tsunami event) models (Fig. 7a), (2) NK4 + NK6 models, (3) NK5 + NK6 models, (4) NK6 + NK6 models, (5) NK7 + NK5 models (Fig. 7b), and (6) NK7 + NK6 models. Considering that NK4 is the benchmark tsunami equivalent to the 1771 Meiwa tsunami, these results indicate that the second tsunami event was larger than the benchmark tsunami to move the boulder to its present position, but that the first tsunami can be either smaller or larger than the benchmark.

For MY models, six cases satisfied the constraint conditions: (1) MY4 + MY5 models, (2) MY5 + MY4 models, (3) MY6 + MY4 models, (4) MY6 + MY5 models, (5) MY7 + MY4 models, and (6) MY7 + MY5 models. Considering that MY4 model is the benchmark tsunami equivalent to the 1771 Meiwa tsunami, these results indicate that both the first and second tsunamis were equivalent to or larger than the benchmark tsunami.

Discussion

Potential occurrence of paleo-tsunami larger than the 1771 event

As summarized in Geological setting, geological evidence suggests that (1) the TU boulder emerged above the lowest sea level because of a tsunami occurring at around 321 B.C.-A.D. 140; that (2) it was moved (or rotated) again by a tsunami occurring after that event but before 1771, reaching its present position; and (3) it was not moved by the 1771 Meiwa tsunami.

Many cases satisfy constraint condition (1). In fact, as Table 4 shows, the tsunami size of the first event can be either smaller or larger than the benchmark tsunami (equivalent to the 1771 Meiwa tsunami), although the MY1 model and MY2 model can be excluded because no boulder would be able to emerge above sea level in these cases. Therefore, we infer that at least the second tsunami was equivalent to or larger than the benchmark tsunami (Table 4), irrespective of its original position that was changed somewhere by the first tsunami event.

According to Yamamoto et al. (2008), a sandy tsunami deposit was reported on the eastern coast of the Ishigaki Island. Its age was estimated after A.D. 1200, but before A.D. 1771. Kitamura et al. (2014) also suggested the potential occurrence of the tsunami, which was sufficiently large to leave sandy deposits at 8 m in elevation, in A.D. 1210–1450. These results might be compatible with the tsunami event

Table 4. Numerical results for boulder transport. O signifies that at least one boulder stopped within the 50 m radius circle, x means that no boulder stopped within the circle. Therefore we did not need to simulate the transport because the result will be expected.

		Second Tsunami							
First Tsunami	Model	NK1	NK2	NK3	NK4	NK5	NK6	NK7	NK8
	NK1	x	-	-	-	-	x	x	-
	NK2	-	x	-	-	-	O	x	-
	NK3	-	-	x	-	-	x	x	-
	NK4	-	-	-	x	x	O	x	-
	NK5	-	-	-	-	x	O	x	-
	NK6	-	-	-	-	x	O	x	-
	NK7	-	-	-	-	O	O	x	x
	NK8	-	-	-	-	-	-	-	x

		Second Tsunami							
First Tsunami	Model	MY1	MY2	MY3	MY4	MY5	MY6	MY7	MY8
	MY1	x	-	-	-	-	-	-	-
	MY2	-	x	-	-	-	-	-	-
	MY3	-	-	x	-	x	x	x	-
	MY4	-	-	-	x	O	x	x	-
	MY5	-	-	-	O	x	x	x	-
	MY6	-	-	-	O	O	x	-	-
	MY7	-	-	-	O	O	x	x	x
	MY8	-	-	-	x	x	-	-	x

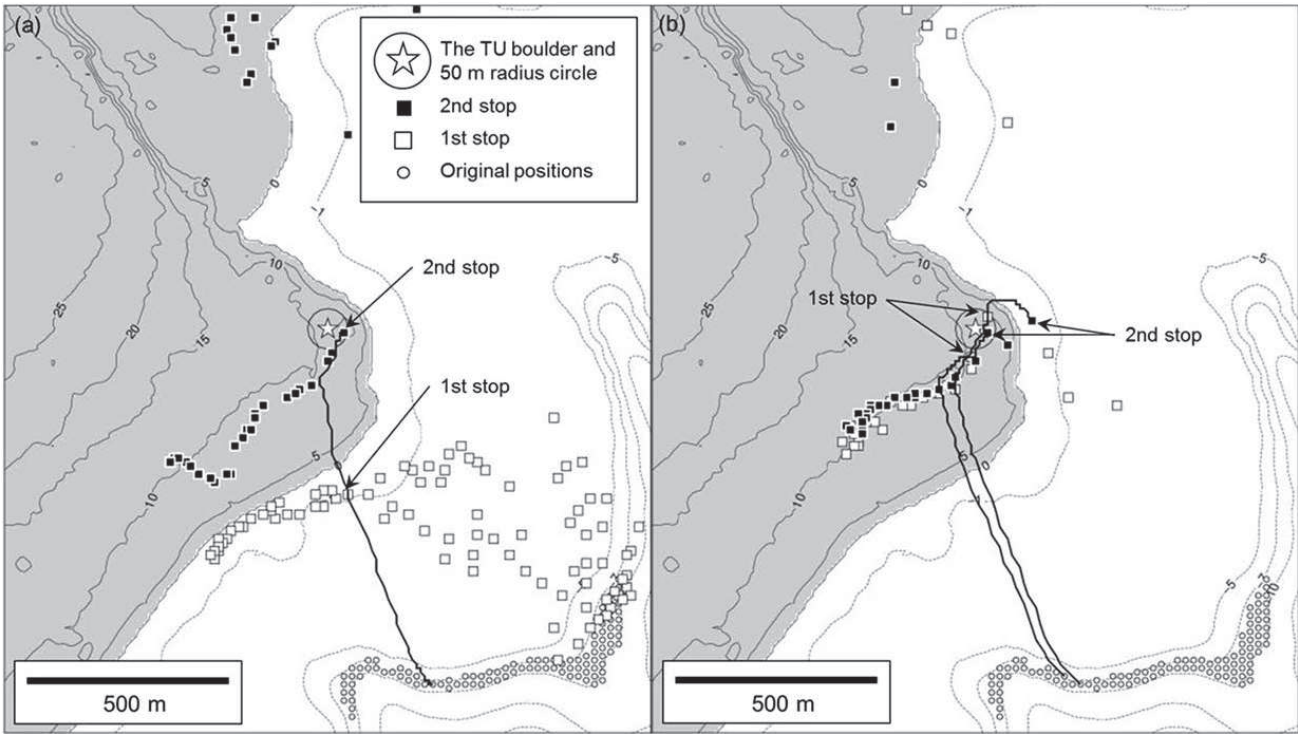

Figure 7. Numerical results for boulder transport by (a) NK2 + NK6 models and (b) NK7 + NK5 models.

on A.D. 1400±100, as estimated by Araoka et al. (2013). Although additional careful research is required, our results support the potential occurrence at around this age of a tsunami that could have been larger than the 1771 Meiwa tsunami at the southern coast of the Ishigaki Island.

Tsunami boulders as useful evidence to evaluate paleo-tsunami size

As demonstrated in this study, tsunami boulders are extremely useful to evaluate the local size of paleo-tsunamis based on numerical modeling, even if it is a single isolated boulder. However, the estimation accuracy is strongly dependent on the available geological evidence.

We assumed that two tsunami events were sufficiently large to move the TU boulder based on Sato et al. (2013). However, Araoka et al. (2013) reported occurrence of seven tsunami events after 250 B.C. but before A.D. 1771, which in turn suggests that five tsunami events should have been small enough not to move (or rotate) the TU boulder. If we had no rotation history based on the paleo-magnetic information, then many combinations of tsunami sizes could be considered given the seven tsunami events. Even in that case, it would be possible to infer that at least one tsunami event before 1771 was equivalent to or larger than the benchmark tsunami and would move the TU boulder to its present position.

Moreover, it is noteworthy that the tsunami boulders in the Ishigaki Island were well studied and that paleo-tsunami recurrence was estimated (e.g., Araoka et al., 2013). However, in other areas of the world, it is not always possible to ascertain paleo-tsunami recurrence as we did at the Ishigaki Island. In fact, depositional ages of boulders are usually difficult to estimate if the boulders do not consist of bioclastic materials such as corals. Even in such cases, it seems possible to estimate the size of the paleo-tsunami which deposited the boulder at its present position. This is the fundamental idea underlying reconstruction of the tsunami size based on inverse modeling (e.g., Nandasena et al., 2011; Nott, 1997, 2003), but flow depth estimation by inverse modeling is not straightforward (e.g., Morton et al., 2006). Instead, forward modeling of boulder transport might useful to estimate the tsunami flow depth better at the boulder's position or to estimate offshore wave properties (Goto et al., 2014).

Further development of the method to elucidate the rotation history of boulders and numerical modeling is expected to be extremely useful for tsunami risk assessment in areas throughout the world where many coastal boulders are deposited.

Conclusions

Estimation of the paleo-tsunami size according to numerical modeling of boulder transport was tested in this study. We used only a single large coralline boulder in the Ishigaki Island and explored sizes of repeated paleo-tsunamis during the past 2400 years. Boulder transport by tsunamis of various sizes was simulated. Several combinations of tsunami sizes satisfying the geological conditions were obtained. Results suggest that at least one large tsunami equivalent to or larger than the 1771 Meiwa tsunami struck the area before 1771. Although the accuracy of this method depends greatly on the available geological evidence, we infer that numerical modeling of boulder transport will have great value for evaluation of the local tsunami size, which is important for local tsunami risk assessment.

Acknowledgements

This research was supported by Grants-in-Aid from the Japanese Ministry of Education, Culture, Sports, Science, and Technology to Goto (23684041) and a Grant-in-Aids from the Japan Society for the Promotion of Science (22241042, 26242033) and from IRIDeS,

Tohoku University to Imamura. We thank D. Sugawara, C. Hongo and D. Araoka for their kind advice related to field surveys and numerical modeling.We also thank S. Fujino and Y. Ogawa for their valuable suggestions and comments.

References

Araoka, D., Yokoyama, Y., Suzuki, A., Goto, K., Miyagi, K., Miyazawa, K., Matsuzaki, H., and Kawahata, H., 2013, Tsunami recurrence revealed by *Porites* coral boulders in the southern Ryukyu Islands, Japan, Geology: v. 41, pp. 919–922.

Atwater, B.F., Musumi-Rokkaku, S., Satake, K., Tsuji, Y., Ueda, K., and Yamaguchi, D.K., 2005, The Orphan Tsunami of 1700 Japanese Clues to a Parent Earthquake in North America: U.S Geological Survey Professional Paper,v. 1707, p. 133.

Cisternas, M., Atwater, B.F., Torrejón, F., Sawai, Y., Machuca, G., Lagos, M., Eipert, A., Youlton, C., Salgado, I., Kamataki, T., Shishikura, M., Rajendran, C.P., Malik, J.K., Rizal, Y., and Husni, M., 2005, Predecessors to the giant 1960 Chile earthquake: Nature, v. 437, pp. 404-407.

Clague, J.J., Bobrowsky, P.T., and Hutchinson, I., 2000, A review of geological records of large tsunamis at Vancouver Island, British Columbia, and implications for hazard: Quaternary Science Reviews, v. 19, pp. 849-863.

Dawson, S., and Shi, S., 2000, Tsunami Deposits: Pure and Applied Geophysics, v. 157, pp. 875-897.

Etienne, S., Buckley, M., Paris, P., Nandasena, N.A.K., Clark, K., Strotz, L., Chague-Goff, C., Goff, J., and Richmond, R., 2011, The use of boulders for characterising past tsunamis: lessons from the 2004 Indian Ocean and 2009 South Pacific tsunamis: Earth-Science Reviews, v. 107, pp. 76-90.

Frohlich, C., Hornbach, M.J., Taylor, F.W., Shen, C.-C., Moala, A., Morton, A.E., and Kruger, J., 2009, Huge erratic boulders in Tonga deposited by a prehistoric tsunami: Geology, v. 37, pp. 131-134.

Gelfenbaum, G., and Jaffe, B., 2003, Erosion and Sedimentation from the 17 July, 1998 Papua New Guinea Tsunami: Pure and Applied Geophysics, v. 160, pp. 1696-1999.

Goff, J., Chagué-Goff, C., Dominey-Howes, D., McAdoo, B., Cronin, S., Bonté-Grapetin, M., Nichol, S., Horrocks, M., Cisternas, M., Lamarche, G., Pelletier, B., Jaffe, B., and Dudley, W., 2010, Palaeotsunamis in the Pacific Islands: Earth-Science Reviews, v. 107, pp. 141-146.

Goff, J., and Chagué-Goff, C., 2012, A review of palaeo-tsunamis for the Christchurch region, New Zealand: Quaternary Science Reviews, v. 57, pp. 136-156.

Goto, K., Kawana, T., and Imamura, F., 2010a, Historical and geological evidence of boulders deposited by tsunamis, southern Ryukyu Islands, Japan: Earth-Science Reviews, v. 102, pp. 77-99.

Goto, K., Okada, K., and Imamura, F., 2010b, Numerical analysis of boulder transport by the 2004 Indian Ocean tsunami at Pakarang Cape, Thailand: Marine Geology, v. 268, pp. 97-105.

Goto, K., Miyagi, K., Kawana, T., Takahashi, J., and Imamura, F., 2011, Emplacement and movement of boulders by known storm waves – Field evidence from the Okinawa Islands, Japan: Marine Geology, v. 283, pp. 66-78.

Goto, K., Miyagi, K., Imamura, F., 2013, Localized tsunamigenic earthquakes inferred from preferential distribution of coastal boulders on the Ryukyu Islands, Japan: Geology, v. 41, pp. 1139-1142.

Goto, K., Hashimoto, K., Sugawara, D., Yanagisawa, H., and Abe, T, 2014, Spatial thickness variability of the 2011 Tohoku-oki tsunami deposits along the coastline of Sendai Bay: Marine Geology, in press.

Imamura, F., Yoshida, I., and Moore, A., 2001, Numerical study of the 1771 Meiwa tsunami at Ishigaki Island, Okinawa and the movement of the tsunami stones: Proceedings of Coastal Engineering, JSCE, v. 48, pp. 346-350.

Imamura, F., Goto, K., and Ohkubo, S., 2008, A numerical model for the transport of a boulder by tsunami: Journal of Geophysical Research – Ocean, v. 113, C01008.

Iryu, Y., Nakamori, T., Matsuda, S., and Abe, O., 1995, Distribution of marine organisms and its geological significance in the modern reef complex of the Ryukyu Islands: Sedimentary Geology, v. 99, pp. 243-258.

Jankaew, K., Atwater, B., Sawai, Y., Choowong, M., Charoentitirat, T., Martin, M., and Prendergast, A., 2008, Medieval forewarning of the 2004 Indian Ocean tsunami in Thailand: Nature, v. 455, pp. 1228-1231.

Kawana, T., Nakata, K., and Omura, A., 1987, Age of the Fossil Coral from the “Tsunami-ufuishi” on Ohama of Ishigaki Island, the South Ryukyus, Japan: The Quaternary Research, v. 26, no, 2, pp. 155-158 (in Japanese with English title).

Kawana, T., and Nakata, K., 1994, Timing of Late Holocene tsunamis originated around the southern Ryukyu Islands, Japan, deduced from coralline tsunami deposits: Journal of Geography Japan, v. 103, p. 352-376 (in Japanese with English abstract).

Kawana, T., 2006, Invasion of about 3400 cal BP large wave in the southeastern Okinawa Island and the surroundings, the Ryukyus, Japan, as deduced from coralline deposits: Bulletin of Department of Education University of Ryukyu, v. 68, pp. 265-271 (in Japanese with English title).

Kawana, T., 2008, Yuisa-Ishi on the reef crest off Chinen, Nanjo City, Okinawa Island: coralline block transported by the Ruth Typhoon in 1951: Bulletin of Faculty of Education, University of the Ryukyus, v. 72, 135–139 (in Japanese).

Kitamura, A., Ando, M., Tu, Y., Ohashi, Y., Nakamura, M., Miyagi, Y., Yokoyama, Y., Shiga, S., and Ikuta, R., 2014, Tsunami deposits in eastern coast area of Ishigaki Island, Japan (abs): Japan Geoscience Union Meeting 2014, MIS23-P11.

Koshimura, S., Mofjeld, H.O., Gonzalez, F.I., and Moore, A.L., 2002, Modeling the 1100 bppaleotsunami in Puget Sound, Washington: Geophysical Research Letters, v. 29, 1948.

MacInnes, B.T., Bourgeois, J., Pinegina, T.K., and Kravchunovskaya, E.A., 2009, Tsunami geo- morphology: Erosion and deposition from the 15 November 2006 Kuril Island tsunami: Geology, v. 37, pp. 995-998.

Miyazawa, K., Goto K., and Imamura, F., 2012, Re-evaluation of the 1771 Meiwa Tsunami source model, southern Ryukyu Islands, Japan: Submarine Mass Movements and Their Consequences, Advances in Natural and Technological Hazards Research, v. 31, pp. 497-506.

Morton, R.A., Richmond, B.M., Jaffe, B.E., Gelfenbaum, G., 2006, Reconnaissance investigation of Caribbean extreme wave deposits — preliminary observations, interpretations, and research directions: Open-File Report 2006-1293, USGS,p. 46.

Morton, R.A., Gelfenbaum, G., and Jaffe, B.E., 2007, Physical criteria for distinguishing sandy tsunami and storm deposits using modern examples: Sedimentary Geology, v. 200, pp. 184-207.

Nakamura, M., 2009, Fault model of the 1771 Yaeyama earthquake along the Ryukyu Trench estimated from the devastating tsunami: Geophys. Res. Lett., v. 36, L19307.

Nanayama, F., Satake,K., Furukawa,R.,Shimokawa,K., Atwater, B.F., Shigeno,K., and Yamaki,S., 2003, Unusually large earthquake inferred from tsunami deposits along the Kuril trench: Nature, v. 424, pp. 6606-6663.

Nandasena, N.A.K., Paris, R., and Tanaka, N., 2011, Reassessment of hydrodynamic equations: minimum flow velocity to initiate boulder transport by high energy events (storms, tsunamis): Marine Geology, v. 281, pp. 70-84.

Nandasena, N.A.K., and Tanaka, N., 2013, Boulder transport by high energy: numerical model-fitting experimental observations: Ocean Engineering, v. 57, pp. 163-179.

Nott, J., 1997, Extremely high-energy wave deposits inside the Great Barrier Reef, Australia: determining the cause – tsunami or tropical cyclone: Marine Geology, v. 141, pp. 193-207.

Nott, J., 2003, Waves, coastal boulders and the importance of the pre-transport setting: Earth and Planetary Science Letters, v. 210, pp. 269-276.

Nott, J., and Bryant, E., 2003, Extreme marine inundations (tsunamis?) of coastal western Australia: Journal of Geology, v. 111, pp. 691-706.

Petroff, C.M., Moore, A.L., and Árnason, H., 2001, Particle advection by turbulent bore – Orientation effects: ITS Proceedings, pp. 897-904.

Rhea, S., Tarr, A.C., Hayes, G., Villaseñor, A., and Benzl, H., 2010, Seismicity of the earth 1900–2007, Japan and vicinity. U.S.: Geological Survey Open-File Report, 2010–1083-D. pubs.usgs.gov/of/2010/1083/d/pdf/OF10-1083D.pdf

Sato, T., Nakamura, N., Goto, K., Minoura, K., and Nagahama, H., 2013, Viscous remanent magnetization of individual boulders in Ishigaki Island and its application to estimate the paleotsunami histories (abs): AGU Fall meeting 2013, GP41A-1104.

Sato, T., Nakamura, N., Goto, K., Kumagai, Y., Nagahama, H., and Minoura, K., 2014, Paleomagnetism reveals the emplacement age of tsunamigenic: Geology, v. 42, pp. 603-606.

Sawai, Y., 2012, Evidence of past crustal movements and tsunamis recorded in geological deposits: AIST Today (International Edition), v. 45, pp. 10-11.

Scheffers, A., 2008. Tsunami boulder deposits, in Shiki, T., Tsuji, Y., Yamazaki, T., Minoura, K. eds., Tsunamiites – Features and Implications: Berlin, Elsevier, pp. 299-318.

Sugawara, D., Goto, K., Imamura, F., Matsumoto, H., and Minoura, H., 2012, Assessing the magnitude of the 869 Jogan tsunami using sedimentary deposits: Prediction and consequence of the 2011 Tohoku-oki tsunami: Sedimentary Geology, v. 282, pp. 14-26.

Sugawara, D., Goto, K., and Jaffe, B.E., 2014, Numerical models of tsunami sediment transport – Current understanding and future directions: Marine Geology, v. 352, pp. 259-320.

Yamada, M., Fujino, S., Goto, K., in press, Deposition of sediments of diverse sizes by the 2011 Tohoku-oki tsunami at Miyako City, Japan: Marine Geology,doi: 10.1016/j.margeo.2014.05.019

Yamamoto, M., Hayata, T., and Kawana, T., 2008, Evidence of earthquake and tsunami in Ishigaki Island – Okinawa prefecture Karadake east shell mount / Karadake east tumuluses: Archaeology Quarterly, v. 106, pp. 91-92.

Appendices

Appendix 1: Calibration method for measured radiocarbon age

The measured radiocarbon age of the TU boulder (*Tsunami ufu-ishi*) by Kawana and Nakata (1994) was calibrated using the online CALIB program ver. 6.0 (http://calib.qub.ac.uk/calib/) and the MARINE09 calibration curve presented by Reimer et al. (2009), along with the local marine reservoir correction value for this region (ΔR = 10 ± 37, Araoka et al., 2010).

Appendix 2: Equations of numerical calculation

With the tsunami inundation program, we conducted connection calculations from the first region to the fourth region. Linear long wave theory on a spherical earth (Equations (1)–(3)) was used for numerical calculations of tsunami propagation in region 1 (Fig. 3a, 300 m grid) with allowance made for the Coriolis force. Deformation attributable to faults and landslides was calculated according to the method explained by Mansinha and Smylie (1971).

$$\frac{\partial \eta}{\partial t}+\frac{1}{\partial R\cos\theta}\left[\frac{\partial M}{\partial \lambda}+\frac{\partial\left(N\cos\theta\right)}{\partial \theta}\right]=0 \tag{1}$$

$$\frac{\partial M}{\partial t}+\frac{gh}{R\cos\theta}\frac{\partial \eta}{\partial \lambda}=fN \tag{2}$$

$$\frac{\partial N}{\partial t}+\frac{gh}{R}\frac{\partial \eta}{\partial \theta}=-fM \tag{3}$$

Therein, η stands for the vertical displacement of water surface above the still water surface, R signifies the radius of the earth, λ and θ respectively represent longitude and latitude directions, M and N respectively denote discharge fluxes in the λ and θ direction, g represents the gravitational constant, h stands for static depth of water, and $f = 2\ \omega \sin\ \theta$ denotes Coriolis's coefficient (ω = the angular velocity of the earth rotation).

In region 2 (Fig. 3a, 100 m grid), region 3 (Fig. 3b, 50 m grid), and region 4 (Fig. 3c, 10 m grid), shallow-water theory on a Cartesian coordinate (Equations (4)–(6)) was used for tsunami propagation and run-up. The Staggered Leap-Frog scheme is used to solve equations numerically (Goto et al. 1997; Kotani et al., 1998).

$$\frac{\partial \eta}{\partial t}+\frac{\partial M}{\partial x}+\frac{\partial N}{\partial y}=0 \tag{4}$$

$$\frac{\partial \eta}{\partial t}+\frac{\partial}{\partial x}\left(\frac{M^2}{D}\right)+\frac{\partial}{\partial y}\left(\frac{MN}{D}\right)+gD\frac{\partial \eta}{\partial x}+\frac{gn^2}{D^{7/3}}M\sqrt{M^2+N^2}=0 \tag{5}$$

$$\frac{\partial \eta}{\partial t}+\frac{\partial}{\partial x}\left(\frac{MN}{D}\right)+\frac{\partial}{\partial y}\left(\frac{N^2}{D}\right)+gD\frac{\partial \eta}{\partial y}+\frac{gn^2}{D^{7/3}}N\sqrt{M^2+N^2}=0 \tag{6}$$

Therein, M and N respectively denote discharge fluxes in the x and y directions, D stands for the total water depth (= $h + \eta$), and n is the Manning's roughness coefficient.

In the boulder transport program, external forces, including those induced by the tsunami wave current, acting on the boulder are represented by the hydraulic force F_m, following the Morison formula, the friction force at the bottom F_b, and the component of the gravitational force F_g along the slope (Noji et al., 1993).

$$\rho_s V\ddot{x} = F_{mx} - F_{bx} - F_{gx} \tag{7}$$

$$\rho_s V\ddot{y} = F_{my} - F_{by} - F_{gy} \tag{8}$$

In those equations, ρ_s stands for the boulder density, V is the boulder volume. F_{bx} and F_{by} respectively denote x and y components of F_b, and F_{gx} and F_{by} respectively stand for the x and y components of F_g, F_{mx}, F_{my}, F_b and F_g are determined as shown below.

$$F_{mx} = C_D\frac{1}{2}\rho_f A\left(u-\dot{x}\right)\sqrt{\left(u-\dot{x}\right)^2+\left(u-\dot{y}\right)^2}+C_M\rho_f V\dot{u}-\left(C_M-1\right)\rho_f V\ddot{x} \tag{9}$$

$$F_{my} = C_D\frac{1}{2}\rho_f A\left(u-\dot{y}\right)\sqrt{\left(u-\dot{x}\right)^2+\left(u-\dot{y}\right)^2}+C_M\rho_f V\dot{v}-\left(C_M-1\right)\rho_f V\ddot{y} \tag{10}$$

$$F_b = \mu\left(\rho_s-\rho_f\right)Vg\cos\theta \tag{11}$$

$$F_g = \left(\rho_s-\rho_f\right)Vg\sin\theta \tag{12}$$

Therein, C_D and C_M respectively represent coefficients of drag and mass, ρ_f is the water density, A is the projected area of the boulder against the current, u and v respectively denote the current velocity at the boulder position in the x and y direction, as obtained from tsunami inundation calculations in region 4. θ is the angle of the slope at the boulder position. We calculated the values of V and A by approaching the shape of the boulder as an ellipsoid body.

In the Boulder Transport by Tsunami model, the empirical variable coefficient of friction $\mu(t)$ is innovated (Imamura et al., 2008). They are assuming that the coefficient decreases as ground contact time become short when the boulder is transported by rolling or saltation related to the current velocity increase.

$$\mu = \frac{2.2}{\beta^2+2.2}\mu_0 \tag{13}$$

$$\beta^2 = \frac{\dot{x}^2+\dot{y}^2}{(1-\rho_f/\rho_s)gd} \tag{14}$$

In those equations, β denotes the degree of contact between the boulder and the floor, μ_0 is the coefficient of dynamic friction during sliding, and d is short-axis boulder length.

References

Araoka, D., Inoue, M., Suzuki, A., Yokoyama, Y., Edwards, R.L., Cheng, H., Matsuzaki, H., Kan, H., Shikazono, N., and Kawahata, H., 2010, Historic 1771 Meiwa tsunami confirmed by high-resolution U/Th dating of massive Porites coral boulders at The Ishigaki Island in the Ryukyus, Japan: Geochemistry Geophysics Geosystems, v. 11, no. 6, Q06014.

Goto, C., Ogawa, Y., Shuto, N., and Imamura, F., 1997, IUGG/IOC Time Project, Numerical Method of Tsunami Simulation with the Leap-Frog Scheme:IOC Manuals and Guides, v. 35, p. 130.

Imamura, F., Goto, K., and Ohkubo, S., 2008, A numerical model for the transport of a boulder by tsunami: Journal of Geophysical Research – Ocean, v. 113, C01008.

Kotani, M., Imamura, F., and Shuto, N., 1998. Tsunami run-up simulation and damage estimation by using GIS: Proceedings of Coastal Engineering JSCE, v. 45, pp. 356-360 (in Japanese).

Mansinha, L., and Staylie, D.E., 1971, The displacement fields of inclined faults: Bulletin ofthe Seismological Society of America, v. 61, pp. 1433-1440.

Noji, M., Imamura, F., and Shuto, N., 1993, Numerical simulation of movement of large rocks transported by tsunamis: Proceedings of IUGG/IOC International Tsunami Symposium, pp. 189-197.

Reimer, P.J., and 27 others, 2009, INTCAL09 and MARINE09 radiocarbon age calibration curves, 0–50,000 years cal BP: Radiocarbon, v. 51, no. 4, pp. 1111-1150.

by Ren Yefei, Wen Ruizhi and Song Yuying

Recent progress of tsunami hazard mitigation in China

Institute of Engineering Mechanics, China Earthquake Administration, Harbin 150080, China. *E-mail: ruizhi@iem.ac.cn*

Since the disastrous aftermath of the 2004 Sumatra Tsunami (Indonesia) and the 2011 Tohoku Tsunami (Japan), China has made much effort to mitigate tsunami hazards. We briefly reviewed the progress of cataloguing, modeling, early warning and hazard analysis for tsunamis in China. Compiling a Chinese tsunami catalogue is a challenge at present due to a large number of inconsistent research results. In China, the numerical models widely used in engineering and related studies are developed by other countries, and the development of a domestic model is being funded by the Chinese government. The tsunami early warning system has been set up and used during the recent tsunami events, such as the Chile earthquake on February 27, 2010, and the Tohoku earthquake on March 11, 2011. Probabilistic tsunami hazard analysis (PTHA) in China has been used for the national zonation map. A test case of PTHA at Mirs Bay of South China was demonstrated. The test case supported the general view that a regional tsunami could be a great hazard to the south China coast.

Introduction

Recently, many large infrastructures have emerged along the Chinese coast, necessitating a rigorous tsunami risk assessment, because the Chinese coast cannot be immune to tsunami hazards. Therefore, China began to keep track of the potential tsunami hazards emanating from the Pacific Ocean after the 2004 Sumatra Tsunami. On March 11, 2011, the Japanese Tohoku Earthquake triggered a destructive tsunami that swept over cities and farmlands along the northern part of Japan and threatened coastal areas throughout the Pacific. This event led to a reconsideration of the safety of coastal nuclear power plant (NPP) sites and other infrastructures. There are 13 NPP sites along the coast of the Chinese mainland at present, with 15 nuclear units in operation and 26 units under construction (Chang et al., 2013). After the Japanese Fukushima NPP accident in 2011, which was caused by an earthquake and tsunami, Chinese NPP safety from extreme external events, including events beyond the design basis, such as tsunamis, was reevaluated. In addition, the coastal area is the most economically developed zone in China. Based on 1:100 m digital elevation models (DEM) and national GDP data in 2004, the statistical analysis shows that 25% of the Chinese GDP is produced along the coastal areas at elevations below 5 meters (Chen et al., 2007).

The lessons from the 2004 Sumatra Tsunami and 2011 Tohoku Tsunami have increased the awareness of tsunami risks in China. In this paper, we briefly review the recent progress of tsunami hazard mitigation in the Chinese mainland, not including Taiwan and Hong Kong. This study focuses on a Chinese historical tsunami event catalogue, a numerical tsunami model, and tsunami early warning system as well as the tsunami hazard analysis methodology.

Chinese tsunami research before 2004

China is located at the eastern edge of Asia adjacent to the northwestern segment of the circum-Pacific earthquake belt. From north to south, the seas bordering China are the Bohai Sea, the Yellow Sea, the East China Sea and the South China Sea. In the Bohai and Yellow Seas, the average depth is 18 m and 44 m, with a maximum depth of only 100 m. However, in the East China Sea and the South China Sea, the average depth is 340 m and 1200 m, respectively, as shown in Figure 1.

The Great Tangshan Earthquake (epicenter is shown in Figure 1) on July 28, 1978, raised concerns about the exposure to natural hazards along the Chinese coast. In 1982, it was commonly suggested that the Chinese coast would be little affected by a tsunami (Li, 1982), and this advice was regarded by the China Seismological Bureau (CSB), which is now the China Earthquake Administration (CEA). In fact, from 1904 to 1968 approximately 350 earthquakes with magnitudes greater than 7.0 occurred in the northwest Pacific Ocean; 33 of these earthquakes, approximately 10% of the total number, occurred off the Chinese coast, but only two of them generated tsunamis with low wave amplitudes (Zhou and Adams, 1986; 1988; Wang et al., 2005).

In 1986, a book named Earthquake Countermeasure was published. One of the chapters of this book reconsiders the tsunami disaster countermeasures that should be used in China (Guo, 1986). In the same year, Zhou and Adams (1986) investigated the historical events of Chinese tsunamigenic earthquakes and suggested that the historical data could provide a basis for the development of Chinese tsunami hazard zonation maps considering the geological and geophysical characteristics of three prominent seismic zones for China.

Zhou and Adams (1986) paper could be the first in which Chinese researchers showed their opinions in an international journal. Later, a preliminary tsunami risk analysis was performed for the coast of China, stating that the ratio of risk among the East Taiwan Coast, Continental Shelf and Bohai Sea was approximately 16:4:1, and the

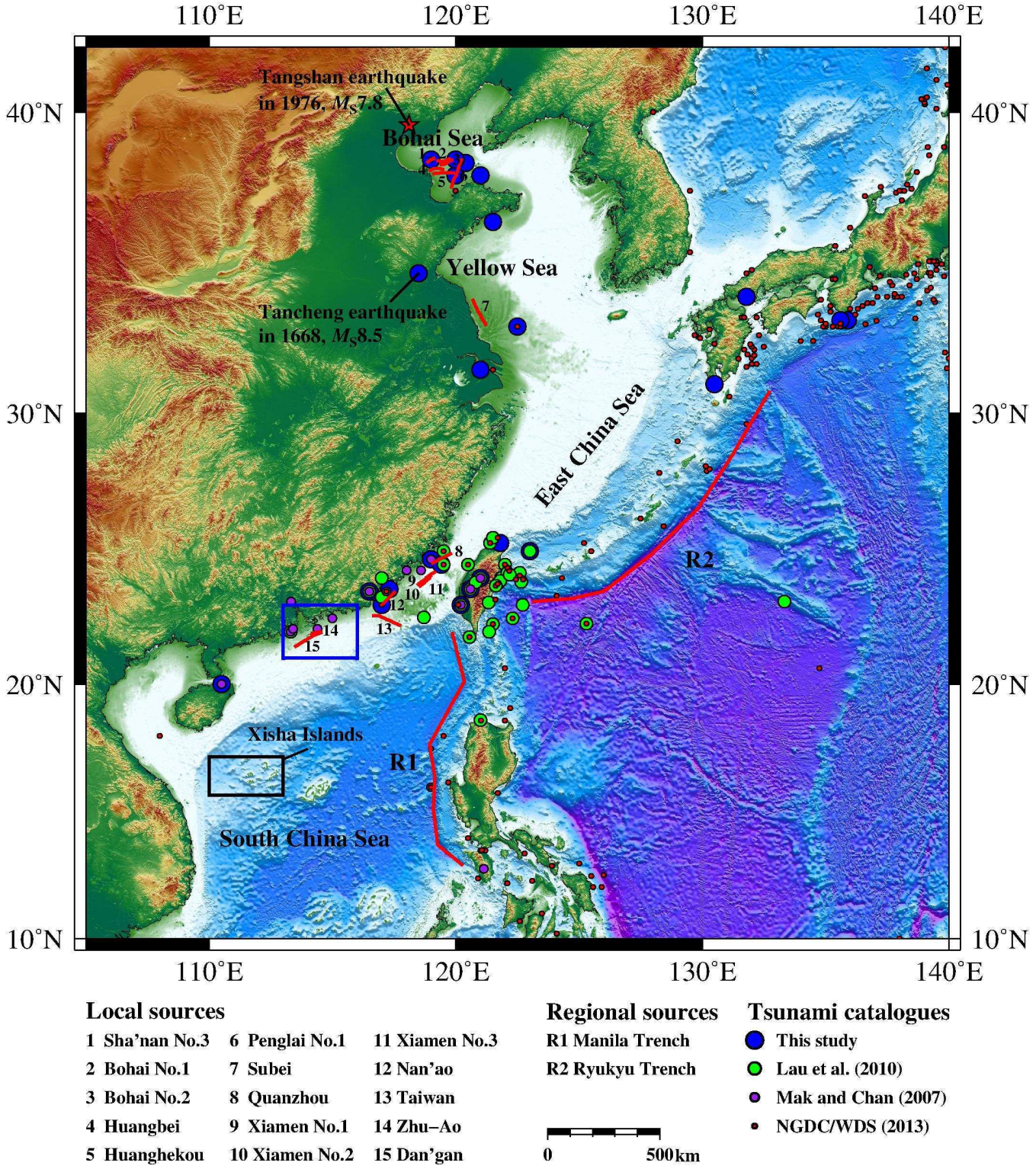

Figure 1. Locations of historical tsunamigenic earthquakes in China derived from several catalogues. The trans-oceanic events are out of this range. The blue circles represent the events from the catalogue developed by this study based on the historical earthquake catalogues (CSB, 1995; 1999) from 23 BC to AD 1990. The green circles represent the events from Lau et al. (2010). The purple circles are from Mak and Chan (2007). The red circles are from the NOAA worldwide database without the inland events (NGDC/WDS, 2013). The potential local tsunami sources are indexed by No. 1-15, and the regional ones are listed by R1 and R2. The epicenter of Great Tangshan Earthquake on July 28, 1978 is also plotted in this figure which first raised concerns about the exposure to natural hazards along the Chinese coast. Blue box bounds the area shown in Figure 3 and black box indicates the locations of the Xisha Islands where evidence of deposits from a possible tsunami was found by Sun et al. (2013). The Bathymetry data are derived from SRTM30 PLUS given by Beker et al. (2009).

tsunami hazard zonation of China with three levels was then suggested (Zhou and Adams, 1988). At the end of 1990, the State Oceanic Administration of China (SOA) launched a research program for collecting historical tsunami data, developing teletsunami and local tsunami propagation models. Both models were then applied to the tsunami hazard assessment in five early NPP sites: Dayawan, Qinshan, Sanmen, Lianyungang and Hui'an (Yu et al., 2001).

The knowledge of tsunami hazards at that time was not completely recognized, and the research was only limited to meet the construction of certain NPP sites. Most of the opinions at that time stated that there was an extremely low probability of the recurrence frequency for tsunamigenic earthquakes near the Chinese coast. On December 26, 2004, the tsunami event in the Indian Ocean became known to the public, leading to a new round of tsunami research and hazard mitigation in China.

Chinese tsunami catalogue

Historical tsunami catalogues have been compiled for many regions in the world, highlighting the occurrence and geographical extent of several large tsunamis. These catalogues may also support an elementary statistical analysis of the recurrence intervals of tsunamis of different magnitudes. Throughout Chinese history over approximately the past 3,000 years, tsunami events and runup data could be found in the literature. To identify a tsunami event, a catalogue needs to collect the information on the location, date and time, event magnitude, maximum water height, total number of deaths and injuries, and total damage. However, many written records seem to be inconsistent and fragmented. As a result, different studies developed tsunami catalogues based on the different data sources and obtained different results. Lu (1984) compiled the historical documents with descriptions of marine disasters, including approximately 227 possible tsunami events, covering the years from 47 BC to AD 1978. However, Chau (2008) believed that this catalogue had been overlooked or ignored by previous authors, and the total number of tsunami associated with definite earthquake events was only four, the number of tsunami induced by meteorological impact was only one, and the remaining 222 events were of unknown origin. Mak and Chan (2007) documented the historical tsunamis of South China, and only two events had been identified as credible reports of tsunamis, and certain events that were previously considered as tsunamis, including a few with many reported casualties, were found to be unsubstantial. Based on 15 previously published regional databases incorporating more than 100 sources for the northeastern region of the South China Sea, Lau et al. (2010) built a database identifying 58 recorded tsunami events between AD 1076 and 2009.

These two catalogues focused on the South China Sea. In the present study, we attempt to develop a tsunami catalogue characterizing the whole Chinese coast. As we know, tsunamis are mainly triggered by large earthquakes, and a simple way to find the historical tsunami events is to search statements about the inundation phenomenon in currently recognized earthquake catalogues. We took a closer look into the Chinese Historical Strong Earthquake Catalogue from 23 BC to AD 1911 and the Chinese Modern Earthquake Catalogue from 1912 to 1990 (CSB, 1995; 1999). We have indentified 25 events as the tsunamigenic earthquakes during approximately the past 2000 years along the Chinese coast, as shown in Figure 1. However, some of the events are still arguable, such as the Tancheng earthquake in 1668, which had an epicenter located inland (Figure 1), but some studies stated that this giant earthquake caused a tsunami that affected the Korean Peninsula (Li et al, 2003). Note that four events generated in Japan also affected the Chinese coast. These are the Meio Earthquake in 1498, Hoei Earthquake in 1707, Ansei-Nankai Earthquake in 1854, and Ryukyu Earthquake in 1923. Many Chinese historical documents recorded the phenomena of rising tide at different locations for each event. However, the flood and inundation associated with injuries and deaths were recorded only in the Ansei-Nankai Earthquake. In general, tsunamis generated in Japan have little effect on the Chinese coast.

Figure 1 shows the event locations of the three above mentioned catalogues. The events from the NOAA tsunami database, which is a list of historical tsunami events and runup locations throughout the world that range in date from 2000 BC to the present, are also shown in Figure 1 (NGDC/WDS, 2013). Until now, there has been no evaluation of the different tsunami catalogues in China. Figure 1 clearly shows that there is still not a consistent list of events along the Chinese coast due to the different literature and identification rules. The compilation of a Chinese tsunami catalogue is still a great challenge.

Furthermore, paleo-tsunami research, which is the investigation of geological deposits, is another way to identify past tsunami events. For a major tsunami that causes extensive inundation and reaches multiple kilometers inland, a unique geological deposit would be produced. The identification of paleo-tsunami deposits in China was performed in recent years. Shi et al. (2012) surveyed 55 coastal sites on the Chinese coast to look for evidence of tsunami-generated geological deposits. Unfortunately, no visual evidence was found. Considering the tectonic setting, the study concluded that "the sea-overflow" described in Chinese ancient books could be not considered as tsunami events (Shi et al., 2012). However, Sun et al. (2013) recently reported preliminary research results from the Xisha Islands (location is shown in Figure 1) in the South China Sea, investigating a large tsunami that may have occurred around AD 1024. Sand layers in lake sediment cores and the geochemical characteristics indicate a sudden deposition event around AD 1024, which is temporally consistent with the written record of a disastrous event, characterized by high waves in AD 1076. This study presents evidence of deposits from a possible tsunami in this area and calls for awareness of the potential risk of tsunamis in the South China Sea.

Paleo-tsunami information could help to expand the time span of the tsunami catalogue. Studies on historical documents and tsunami deposits are the two key ways to understand much more about the magnitude and return period of great events in the past. Results from these two topics will help to improve the later studies such as PTHA. Therefore, we suggest a complete tsunami catalogue should be authoritatively published, and many more field surveys on the identification of tsunami geological deposits should be performed along the whole Chinese coast.

Tsunami modeling and its application

The National Marine Environmental Forecasting Center (NMEFC) of SOA is an early institution in China to develop numerical models for simulating the process of tsunami generation and propagation in the 1980s with reference to the TUNAMI (Tohoku University's Numerical Analysis Model for Investigation of near and far field tsunamis) code (Yu et al., 2001; Imamura et al., 1988). The Chinese Tsunami Model (CTM) was established and has run since

2005, just after the 2004 Sumatra Tsunami. For this model, the geometrical displacement of the seafloor is assumed to be the same as the initial tsunami wave field, and the formula of fault dislocation in elastic anisotropic half-space is deployed (Mansinha and Smylie, 1971). The finite difference method is used to solve linear and non-linear shallow-water equations, and the leap-frog scheme is used to improve the model's high-speed computation. After 2009, this model was updated to a parallel version based on the OPENMP (Open Multi-Processing) system and was used to estimate the probable maximum tsunami waves for several NPP sites. Recently, several researchers from universities and institutions have become interested in studies on tsunami simulation that emphasize the fundamental physical theory (Zhu et al., 2006).

Most engineers and scientists in the Chinese mainland prefer to use popular international models for engineering applications and scientific studies related to tsunami hazards. For instance, Pan et al. (2009) used the COMCOT (Cornell Multi-grid Coupled Tsunami Model) to simulate scenario tsunamis in the South China Sea and showed that there would be an approximate 0.3-0.5 m tsunami wave height along the coastline where the water depth is 20 m in the case of an M8.0 earthquake, and above 3 m in the case of an M9.0 earthquake. Wen et al. (2008) also used the COMCOT to simulate the tsunami propagation generated by a scenario M8.5 earthquake near the Okinawa Trough and showed that the maximum initial tsunami wave height was estimated to be 4.3 m. It would take approximately 4 hours for a tsunami wave to propagate from the source to the coast of Zhejiang Province in this case, with a maximum height of approximately 2.0 m, and 8 hours to reach to the shoreline of Shanghai. Using the TUNAMI-N2-NUS model, Dao et al. (2008) studied various tsunami scenarios in the South China Sea, and the maximum tsunami wave height reached 8 m in the coastal area of Guangdong Province for the worst-case scenario. Yu et al. (2011a) used the GeoClaw model to simulate the propagation process and characteristics of the 2010 Chile Tsunami around China coastal areas and quantitatively analyzed the impact of this tsunami on Chinese coast.

In general, engineers and scientists in China apply commonly used numerical tsunami models to accomplish their engineering or research tasks. However, we hope a domestic model will be developed in the future supported by more funds from the Chinese government.

Chinese tsunami early warning system

In 1994, when tsunami waves were observed by tide gauges around Hainan Island in China, the development of a Chinese tsunami warning service system was proposed (Ye et al., 1994). After the 2004 Sumatra earthquake, Wen et al. (2006) suggested the integration of the Chinese seismic monitoring network and the tsunami simulation model to build the tsunami early warning system in China. Liu et al. (2009) proposed a procedure to establish a tsunami early warning system for the South China Sea region focusing on the characteristics of tsunamis generated from earthquakes along the Manila subduction zone. In 2010, the Regional South China Tsunami System (RSCTS) was established by the Earthquake Administration of Guangdong Province, which is in charge of backing up the data of the Chinese seismic monitoring network. The seismic monitoring data can be easily integrated into RSCTS, and this system is mainly responsible for tsunami warning for the coast of the Guangdong and Hainan Provinces (Chen and Ye, 2010).

The China Tsunami Early Warning Center (CTEWC) was established in 2013 and is the only national agency responsible for producing and issuing tsunami warnings. Based on the earthquake information provided by the Chinese Earthquake Networks Centre (CENC) and the tsunami information provided by the Pacific Tsunami Warning Center (PTWC), CTEWC has the ability to evaluate the maximum wave height in the Chinese coastal area using a CTM model and to release tsunami warning information to the public in 20 minutes after the earthquake occurs. CTEWC releases the tsunami early warning to their local agencies first; then the agencies release it to local people who may be affected by the coming tsunami waves. Meanwhile, the warning information would be pasted on the CTEWC's webpage where anyone can access it. The Chinese Tsunami Travel Time Model (CTTTM) can also provide an estimation of the wave arrival time after a tsunami event. This model was implemented in 2005 by CTEWC, covering the entire Chinese sea with the 2′ resolution bathymetry data.

The color-coded warning class is used in China based on tsunami heights and the seriousness of the potential hazard. Tsunami warnings are classified into four classes: I, II, III and IV, with red, orange, yellow and blue color codes, corresponding to the tide height ranges of approximately > 3.0 m, 2.0-3.0 m, 1.0-2.0 m and less than 1.0 m, respectively. Half an hour after the occurrence of the Chile earthquake on February 27, 2010, CTEWC released a blue warning and predicted that the tsunami could have a height of approximately 0.2 m and would not cause damage along the Chinese coast. The wave heights retrieved from tide gauges along Chinese coast are shown in Figure 2 and imply an agreement with the predicted height (Yu et al., 2011b). Three hours after the start of the Tohoku earthquake on March 11, 2011, CTEWC issued a blue tsunami warning and predicted that the leading wave would arrive at Shanghai in 10 hours with a maximum height of 0.5 m. The recorded maximum wave height near a tide station of Zhoushan Island close to Shanghai was approximately 0.55 m (NGDC/WDS, 2013). In addition, CTEWC also issued a safety warning for some moderate and small tsunamis, such as the Chile tsunami on April 1, 2014. The warning information showed that the tsunami wave would not reach the coastline of China. Correspondingly, there is not any record from tide gauges along the Chinese coast.

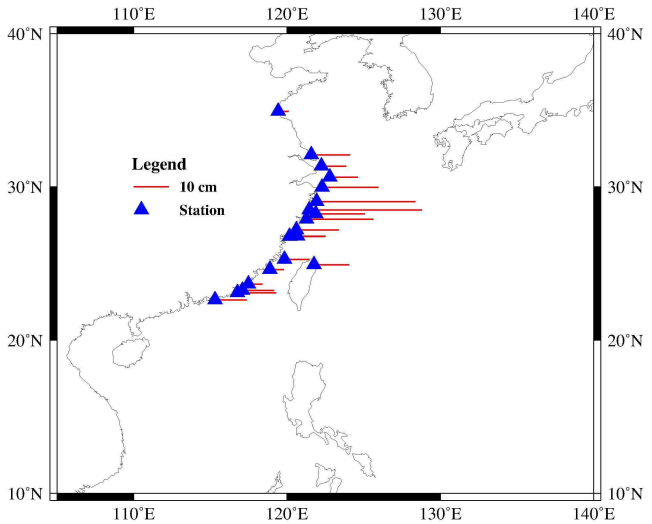

Figure 2. Observed tsunami wave heights along the Chinese coast for the 2010 Chile Earthquake (Yu et al., 2011b)

CTEWC, which is now attached to NMEFC, is collaborating with the U.S. Pacific Marine Environmental Laboratory (PMEL) to build a real-time tsunami forecasting system in the South China Sea. To monitor potential tsunami waves generated by a submarine earthquake in the Manila Trench and to provide early warning for the southern China coast, SOA deployed two buoys in the South China Sea that can monitor tsunami waves within 15-30 min if the tsunami is generated by an earthquake in the Manila Trench, and the real-time buoy data could also be accessed (Zhao et al., 2013).

The Chinese seismic monitoring network consists of many seismic stations, and SOA manages more than 100 marine gauges, most of which collect and transmit real-time data. Recent advanced numerical modeling technologies are being integrated with both earthquake and tsunami monitoring networks to create a more effective tsunami early warning system. Automatic collection of earthquake information data could be processed. We believe that the tsunami warning bulletin could also be automatically generated in the future based on predefined templates.

Probabilistic Tsunami Hazard Analysis (PTHA) in China and a test case

Deterministic Tsunami Hazard Analysis (DTHA) is a simple way to qualitatively assess the tsunami hazard for a site of interest and has been widely used in China (e.g., Zhou and Adams, 1988; Yang and Wei, 2005; Wen et al., 2008; Ren et al., 2010). However, the preferred method for evaluating the tsunami hazard in China is starting to shift from DTHA to Probabilistic Tsunami Hazard Analysis (PTHA). Liu et al. (2007) performed a PTHA for the southern China coast affected by the potential sources in the Manila Trench. The results show that the probability that a tsunami wave with a height over 2.0 m will hit coastal areas in Hong Kong and Macau is approximately 10%, and the cities in Taiwan are less vulnerable than those on the mainland coast. The authors of this paper are devoted to pushing the PTHA forward in China under the funding supported by the National Natural Science Foundation of China (NSFC). We have proposed a Chinese PTHA method by following the regular seismic hazard analysis methods in China and gave a detailed description of the framework (Wen et al., 2011).

PTHA is derived from Probabilistic Seismic Hazard Analysis (PSHA). If we assume a Poisson time process, the probability that a tsunami with amplitude H greater than a given height h (i.e., $H \geq h$) occurs per year at a coastal site is given by the function:

$$P(H \geq h) = 1 - \prod_{n=1}^{N} (1 - P_n(H \geq h)) \qquad (1)$$

where P_n represents that the probability of amplitude $H \geq h$ when the tsunami is generated by the n^{th} source. The following is a trial case applied at the site in Mirs Bay (114.77°E, 22.59°N) near Guangzhou and Hong Kong, as shown in Figure 3.

The ring of subduction zones around the Pacific Ocean is responsible for most tsunami sources for China. The distant sources were not considered in this paper because they have minor effect on China. For example, tsunami sources in Chile and Japan, where the tsunamis were generated by great earthquakes in 2010 and 2011, had almost no effect on the Chinese coast, as mentioned earlier. The potential regional tsunami sources for China are typically along the Korean Peninsula, the Sea of Japan, and the Ryukyu Islands as well as along Taiwan and the Philippines. For this evaluated site, only three potential tsunami sources are considered: the Manila Trench, which is a regional source, and the Zhu-Ao Fault and the Dangan Fault, which are the local sources. All of the related parameters of these sources are listed in Table 1.

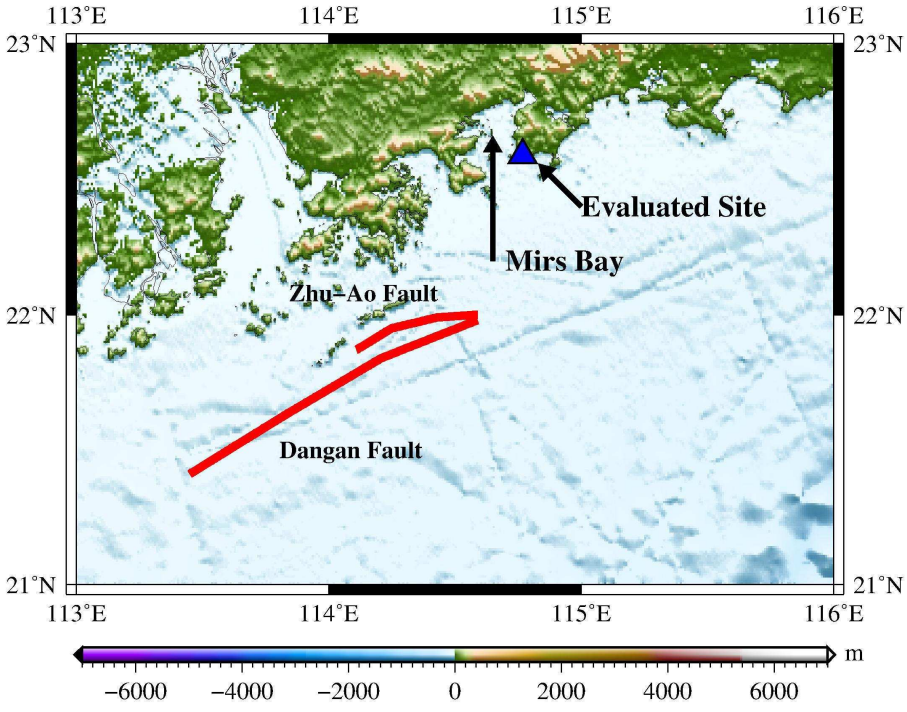

Figure 3. Geographical locations of the PTHA-evaluated site with two local potential sources, Zhu-Ao Fault and Dangan Fault, which are No. 14 and No. 15 in Figure 1. A regional source, the Manila Trench, is shown in Figure 1. A large-scale map of the area is also shown in Figure 1 as a blue box.

First, the seismic activities should be evaluated for these three sources. For the Manila Trench, constant b (slope of Gutenberg–Richter relationship of frequency vs. magnitude) was determined as b=0.89 or 0.98 for different fault segments given by Liu et al. (2007), as shown in Table 1. For the other potential tsunami sources, we used b=0.73, which was given by Chan and Zhao (1996). Then the numerical model COMCOT was applied to evaluate the wave heights at the given site in each computational tsunami case with various earthquake magnitudes.

From the simulated results, we find that the tsunami hazard for this site is dominated by the Manila Trench; both local sources contribute a small amount due to their small values of upper bound magnitude M_u and fault sizes. Tsunami waves generated by the Manila Trench region can reach this site with little loss in energy. We did not consider another regional potential tsunami source, the Ryukyu Islands, for this site. We believe that tsunami waves from this region could be blocked by Taiwan

Table 1. Seismic parameters of three potential tsunami sources for the PTHA evaluated site in this study

Source Name	Node Coordinates	Length (km)	Width (km)	Average Depth (km)	Strike (°)	Dip (°)	Rake (°)	Slip (m)	Upper M (M_u)	b
Manila Trench	(119.85, 21.97), (120.35, 20.10)	210	82	20	350	14	110	2.94	8.2	0.89
	(120.35, 20.10), (118.93, 17.67)	310	109	20	29	20	110	5.3	8.6	0.98
	(118.93, 17.67), (119.15, 16.40)	135	66	20	3	20	90	1.89	7.9	0.98
	(119.15, 16.40), (119.08, 15.20)	140	66	20	351	20	90	1.89	7.9	0.98
	(119.08, 15.20), (119.27, 13.73)	166	71	20	353	30	50	2.19	8.0	0.98
	(119.27, 13.73), (120.28, 12.92)	142	66	20	308	30	50	1.89	7.9	0.98
Zhu-Ao Fault	(114.11, 21.87), (114.25, 21.95) (114.43, 21.99), (114.59, 22.00)	52	50	20	74	60	90	1.00	7.5	0.73
Dangan Fault	(113.45, 21.41), (113.83, 21.63) (114.21, 21.84), (114.59, 21.98)	135	50	20	63	60	90	1.00	7.5	0.73

Island and cannot impose a tremendous tsunami hazard to this site.

Figure 4 shows the calculated exceeding probability curves at the site in Mirs Bay for 1 year, 50 years and 100 years. Because the upper bound magnitude, M_u, is only 8.6 for the Manila Trench and 7.5 for the local sources (see Table 1), the maximum wave height only reaches 2.3 m, which leads to a convergence for the exceeding probability curves for 50 years and 100 years at 2.3 m, as shown in Figure 4. Our results are similar to the analysis result given by Liu et al. (2007), who only considered the regional source of the Manila Trench, for which, in the next century, the probability that a wave with a height of over 2.0 m will hit the near-coast ocean of Hong Kong and Macau was approximately 10%.

We have already launched a project funded by NSFC to compile the national tsunami zonation map. The test case above only shows

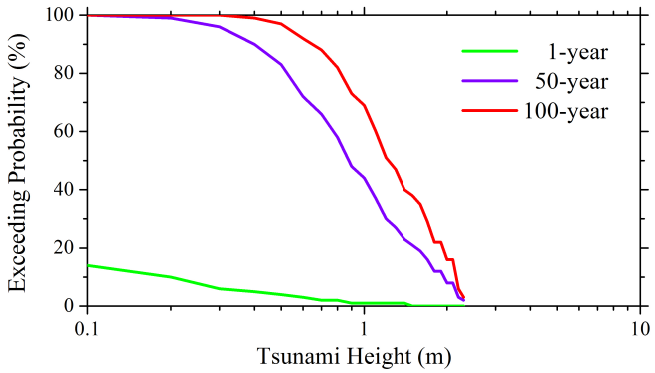

Figure 4. Exceeding probability curve for 1 year, 50 years and 100 years at the site evaluated by PTHA in this study.

the beginning of the use of PTHA in China, and more tsunami sources will be included in PTHA for other sites along the Chinese coast. Furthermore, PTHA with the identification of all possible uncertainties in tsunami source parameters will be considered in the following step. As discussed in Geist and Parsons (2006), the uncertainties associated with PTHA calculations must be included in the processes of generation, propagation and runup.

Conclusions

We introduce the recent progress of tsunami hazard mitigation, including the compilation of a Chinese tsunami catalogue, the development of a tsunami model, the construction of a tsunami early warning system and the validation of a tsunami hazard analysis methodology in China. Following are several conclusions and remarks:

1 There is still not an approved tsunami catalogue for the Chinese coast. Increased funding has led to an increase in people's awareness of tsunami hazards in China that may have previously been underestimated. There is a need to reevaluate all of the related ancient literatures to improve the completeness of the tsunami catalogue so that the recurrence intervals of tsunamis can be estimated accurately. Information from paleo-tsunami studies could help to expand the time span of the tsunami catalogue. Therefore, many more field surveys on the identification of tsunami geological deposit should be performed. Meanwhile, numerical inundation modeling could be used to validate the findings in those paleo-tsunami surveys.

2 Several popular numerical models for tsunami simulation have been commonly used in China. However, with a high-performance computation technique, a pre-computed database of simulated heights and arrival times could be developed for a large number of tsunami scenarios, which has been accepted as an effective way to issue timely tsunami warning information. In addition, raising the awareness of tsunami hazards for people who live in the coastal areas and disseminating the knowledge of tsunami early warning systems and evacuation guidance are suggested.

3 The calculation of the PTHA test case at the site of southern China coast shows relatively acceptable results. We stress that this test case is an initial step towards a nationwide tsunami hazard assessment. The uncertainty analysis for PTHA should be considered in future work. The final goal of PTHA is to provide a national zonation map of tsunami inundation.

Establishing a national tsunami hazard program in China to mitigate the impact of tsunamis through hazard assessment, early warning, and other means should be the main goal in the future, and collaboration between corporations and international programs is also important.

Acknowledgements

We thank the anonymous reviewer for his or her valuable suggestions and constructive comments, which helped us improve the manuscript. This work is supported by the National Natural Science Fund No. 51278473, the Environmental Protection Research Fund

for Public Interest No. 201209040 and the northeast Asia (China-Japan-Korea) cooperative research project of earthquake, tsunami and volcano No. ZRH2014-11. We thank Dr. Shinji Takarada and Dr. Tadashi Maruyama from the Geological Survey of Japan and Yujiro Ogawa, Professor Emeritus of the University of Tsukuba for their help in preparing this manuscript.

References

Becker, J.J., Sandwell, D.T., Smith, W.H.F., Braud, J., Binder, J., Depner, J., Fabre, D., Factor, J., Ingalls, S., Kim, S-H., Ladner, R., Marks, K., Nelson, S., Pharaoh, A., Trimmer, R., Von Rosenberg, J., Wallace, G., and Weatherall, P., 2009, Global Bathymetry and Elevation Data at 30 Arc Seconds Resolution: SRTM30_PLUS. Marine Geodesy, v. 32(4), pp. 355-371.

Chan, L.S., and Zhao, A., 1996, Frequency and time series analysis of recent earthquakes in the vicinity of Hong Kong. Hong Kong Geologist, v. 2, pp. 11-19.

Chang, X.D., Zhou, B.G., and Zhao, L.D., 2013, Checking of seismic and tsunami hazard for coastal NPP of Chinese continent after Fukushima nuclear accident. Engineering Sciences, v. 11(3), pp. 60-65.

Chau, K.T., 2008, Tsunami hazard along coasts of China: a re-examination of historical data. The 14th World Conference on Earthquake Engineering October 12-17, Beijing, China.

Chen, J.T., and Ye, C.M., 2010, Discussion on the Construction of the Tsunami Monitoring and Warning System in the South China Sea. South China Journal Of Seismology, v. 30(z1), pp. 145-152. (in Chinese)

Chen, R., Chen, Q.F., and Zhang, W., 2007, Tsunami disaster in China. Journal of Natural Disasters, v. 16(2), pp. 1-6. (in Chinese)

China Seismological Bureau (CSB), 1995, The catalogue of historical earthquake in China (23 B.C. - A.D. 1911), Beijing: Seismological Press. (in Chinese)

China of Seismological Bureau (CSB), 1999, The catalogue of modern earthquakes in China (A.D. 1912 -A.D. 1990) (in Chinese), Beijing: China Science and Technology Press. (in Chinese)

Dao, M.H., Pavel, T., Chan, E.S., and Kusnowid, M., 2008, Tsunami propagation scenarios in the South China Sea. Journal of Asian Earth Sciences, v. 36(1), pp. 67-73.

Geist, E.L., and Parsons, T., 2006, Probabilistic Analysis of Tsunami Hazards. Natural Hazards, v. 37(3), pp. 277-314.

Guo, Z.J., 1986, Earthquake Countermeasure. Beijing: Seismological Press. (in Chinese)

Imamura, F., Shuto, N., and GOTO, C., 1988, Numerical simulations of the transoceanic propagation of tsunamis. 6th Congress APD-IAHR, Kyoto, Japan.

Lau, A.Y.A., Switzer, A.D., Dominey-Howes, D., Aitchison1, J.C., and Zong, Y., 2010, Written records of historical tsunamis in the northeastern South China Sea - challenges associated with developing a new integrated database. Nat. Hazards Earth Syst. Sci., v. 10, pp. 1793-1806.

Li, C., 1982, On Earthquake tsunami. Marine Science Bulletin, v. 1(2), pp. 16-23. (in Chinese)

Li, Y.C., Lee, D.K., Oh, S.H., and Yoon, Y.H., 2003, The Felt Area and Tsunami of the 1668 Tancheng Great Earthquake with M8.5 in the Korean Peninsula. Chinese Earthquake, v. 19(2), pp. 184-187. (in Chinese)

Liu, P.L.F., Wang, X.M., and Salisbury, A.J., 2009, Tsunami hazard and early warning system in South China Sea. Journal of Asian Earth Sciences, v. 36(1), pp. 2-12.

Liu, Y., Santos, A., Wang, S.M., Shi, Y.L., Liu, H.L., and Yuen, D.A., 2007, Tsunami hazards along Chinese coast from potential earthquakes in South China Sea. Physics of the Earth and Planetary Interiors, v. 163(4), pp. 233-244.

Lu, R., 1984, Historical Tsunami and Related Events in China, Beijing, Oceanic Press. (in Chinese)

Mak, S., and Chan, L.S., 2007, Historical tsunamis in South China. Nature Hazards, v. 43, pp. 147-164.

Mansinha, L., and Smylie, D., 1971, The displacement field of inclined faults. Bulletin Seismology Society America, v. 61(5), pp. 1433-1440.

National Geophysical Data Center / World Data Service (NGDC/WDS), 2013, Global Historical Tsunami Database. National Geophysical Data Center, NOAA.

Pan, W.L., Wang, S.A., and Cai, S.Q., 2009, Simulation of potential tsunami hazards in the South China Sea. Journal of Tropical Oceanography, v. 28(6), pp. 7-14. (in Chinese)

Ren, Y.F., Wen, R.Z., Zhou, B.F., and Shi, D.C., 2010, Deterministic analysis of the tsunami hazard in China. Science of Tsunami Hazards, v. 29(1), pp. 32-42.

Shi, F., Bi, L.S., Tan, X.W., Wei, Z.Y., and He, H.L., 2012, Did earthquake tsunami in Bohai Sea in history? Chinese Journal of Geophysics, v. 55(9), pp. 3097-3104.(in Chinese)

Sun, L.G., Zhou, X., Huang, W., Liu, X.D., Yan, H., Xie, Z.Q., Wu, Z.J., Zhao, S.P., Shao, D., and Yang, W.Q., 2013, Preliminary evidence for a 1000-year-old tsunami in the South China Sea. Science Report 3, Article number: 1655.

Wang, F., Liu, C.S., and Zhang, Z.Q., 2005, Earthquake tsunami record in Chinese ancient books. Earthquake research in China, v. 21(3), pp. 437-443. (in Chinese)

Wen, R.Z., Ren, Y.F., Li, X.J. and Pan, R., 2011, Probability Analysis Method of Earthquake-induced Tsunami Risk in China. South China Journal of Seismology, v. 31(4), pp. 1-13. (in Chinese)

Wen, R.Z., Zhou, Z.H., and Xie, L.L., 2006, A numerical study on tsunami travel time for China seashore based on strong ground motion network. Journal of Earthquake Engineering and Engineering Vibration, v. 26(2), pp. 20-24. (in Chinese)

Wen, Y.L., Zhu, Y.Q., Song, Z.P., Xue, Y., Liu, S.Q., and Dong, F.F., 2008, Preliminary numerical simulation of potential earthquake—induced tsunami in East China Sea. Acta Seismologica Sinica, v. 30(5), pp. 456-463. (in Chinese)

Yang, M.L., and Wei, B.L., 2005, The potential seismic tsunami risk in South China Sea and it's surrounding region. Journal of Catastrophology, v. 20(3), pp. 41-47. (in Chinese)

Ye, L., Wang, X.N., and Bao, C. L., 1994, Tsunami in China Seas and its warning service. Journal of Natural Disasters, v. 3(1), pp. 100-103. (in Chinese)

Yu, F.J., Ye, L., and Wang, X.N., 2001, The simulation of tsunami happened in the Taiwan Strait in 1994. Acta Oceanological Sinica, v. 23(6), pp. 32-39. (in Chinese)

Yu, F.J., Wang, P.T., Zhao, L.D., and Yuan, Y., 2011a, Numerical simulation of 2010 Chile tsunami and its impact on Chinese coasts. Chinese Journal of Geophysics, v. 54(4), pp. 918-925. (in Chinese)

Yu, F.J., Yuan, Y., Zhao, L.D., and Wang, P.T., 2011b, Evaluation of potential hazards from teletsunami in China: Tidal observations of a teletsunami generated by the Chile Mw8.8 earthquake. Chinese Science Bulletin, v. 59(3), pp. 239-246. (in Chinese)

Zhao, L.D., Yu, F.J., Hou, J.M., Wang, P.T., and Fan, T.T., 2013, The role of tsunami buoy played in tsunami warning and its application in South China Sea. Theoretical and Applied Mechanics Letters, v. 3(3), pp. 23-26.

Zhou, Q., and Adams, W.M., 1986, Tsunamigenic Earthquakes in China, 1831 BC to 1980 AD. Science of Tsunami Hazards, v. 4(3), pp. 131-148.

Zhou, Q., and Adams, W.M., 1988, Tsunami Risk Analysis for China. Natural Hazards, v. 1(2), pp. 181-195.

Zhu, H.B., Yu, Y. and Dai, S.Q., 2006, The research progress in numerical simulation of tsunami models, Journal of Hydrodynamics. v. 21(6), pp. 714-723. (in Chinese)

by Masahiro Chigira

Geological and geomorphological features of deep-seated catastrophic landslides in tectonically active regions of Asia and implications for hazard mapping

Disaster Prevention Research Institute, Kyoto University, Gokasho, Uji 611-001, Kyoto, Japan. *E-mail: chigira@slope.dpri.kyoto-u.ac.jp*

Deep-seated catastrophic landslides, particularly rock or debris avalanches, travel extremely rapidly for long distances, causing severe damage over wide areas. This paper summarizes the geological and geomorphological features of such events, which were induced by earthquakes and rainstorms in Asia, and then uses these features to predict future potential sites of failures. Most of the rock avalanches are preceded by gravitational slope deformation with topographic features, in which small scarps along future head of landslide are the most representative; the scarps can be identified in topographic images made by high-resolution airborne LiDAR DEMs and may suggest the instability just before catastrophic failure. Earthquake-induced debris avalanches of pyroclastic fall deposits are not preceded by gravitational slope deformation but are of specific type and sequence of deposits, in which resilicified paleosol with halloysite may be the most important to accommodate a sliding surface.

Introduction

The numbers of lives lost in landslides in tectonically active regions is generally constantly large in comparison with those resulting from episodic earthquakes or volcanic eruptions (Petley, 2012), although the latter have received more attention as fatal natural hazards. In recognition of the fatal nature of landslides in such regions, the Japanese government changed its policies regarding earthquake prediction research after the 2011 Tohoku earthquake, to also include earthquake-induced hazards such as landslides, since research only on earthquakes cannot mitigate the associated hazards that contribute to the scale of such disasters. Most Asian countries are located in tectonically active, high-rainfall areas, and devastating landslides triggered by rainstorms, earthquakes, and snowmelt are frequent in many locations. Recent notable triggers include the 2011 typhoon Talas (Chigira et al., 2013b), 2011 Tohoku earthquake in Japan, 2009 typhoon Molakot in Taiwan (Tsou et al., 2011), 2009 Padang earthquake in Indonesia (Nakano et al., 2013), and 2008 Wenchuan earthquake and subsequent rainstorms in China (Chigira et al., 2010; Chigira et al., 2012a) (Table 1).

To mitigate landslide-induced disasters, it is necessary to know where and when landslides are likely to occur, and how and when to evacuate threatened areas prior to an event. Rock or debris slide avalanches are especially hazardous, and such events must be anticipated and prepared for, as they generally occur suddenly and travel quickly over long distances, affecting large areas. This paper focuses on the geological and geomorphological features of potential sites of rock or debris slide avalanches with respect to predicting the locations of these types of landslides.

Several approaches have been developed to predict potential sites of landslides, including those of physical modeling, stochastic modeling, and the indexing of geological and geomorphological features (Guzzetti et al., 1999). Physical modeling, such as slope stability analysis under conditions of heavy rainfall or an earthquake, requires information related for example to hydrological or geotechnical factors and subsurface structures, which are unavailable in many areas (Jibson et al., 1998; Montgomery et al., 2000). Stochastic modeling can be effective for investigating rather shallow landslides, which usually occur repeatedly in areas with particular geological characteristics, such as particular types of weathering profiles. In contrast, the occurrence of deep-seated catastrophic landslides is highly dependent on local and specific geological and/or geomorphological conditions. Therefore, an understanding of the typology of these specific conditions may allow predictions regarding potential sites of rock and debris slides.

On the basis of our studies on the geological and geomorphological features of catastrophic rock and debris-slide avalanches in Asian countries, I have reached the conclusion that it is possible to predict at least the potential sites of such events. Most of the catastrophic rock-slide avalanches induced by either rainstorms or earthquakes are preceded by a particular type of gravitational slope deformation (Chigira, 1992; Dramis and Sorrisovalvo, 1994; Kilburn and Petley, 2003; Crosta et al., 2006; Chigira, 2009), whereas debris-slide avalanches caused by earthquake-induced failure of pyroclastic fall deposits are not (Chigira, 1982; Chigira et al., 2014). The latter, however, occur in areas of a particular type of pyroclastic succession characterized by heavily weathered pyroclastics or paleosol(s) at depth.

In this paper, I summarize the geological and geomorphological features of potential sites of deep-seated catastrophic landslides as a basis for establishing a methodology of landslide hazard mapping.

Table 1. Recent landslide hazards in Asia

Country	Trigger	Type of landslide	Fatality by landslides	References
China	2008 Wenchuan earthquake	Landslide on natural slopes	>20000	Huang and Fan (2013)
	Rainstorms after the 2008 Wenchuan earthquake	Debris flows	3029	Chuan Tang (oral communication)
Taiwan	1999 Chi-Chi earthquake	Landslide on natural and valley fills of residential houses	39/Chiu-fen-erh-shan 29/Tsaoling	Chigira et al. (2003) Wang et al. (2003)
	Typhoon Molakot, 2009	Landslide on natural slopes	More than 400 by the Shiaolin landslide	Tsou et al. (2011)
Malaysia	Typhoon Greg, 1996	Landslide on natural slope	302	Lim Chounsian (oral communication)
Indonesia	2009 Padang earthquake	Landslide on natural slopes	More than 400	Nakano et al. (2013)
Phillipines	2006 Rain	Landslide on natural slopes	1100 by Ginsaugon landslide	Guthrie et al. (2009) Evans et al. (2007)
Japan	2011 Tohoku earthquake	Landslide on natural and valley fills for residential houses	12 by landslides (mostly by tsunami)	Chigira et al. (2014)
	Typhoon Talas, 2011	Landslide of natural slopes	56 by landslides	Chigira et al. (2013)

Catastrophic earthquake-induced landslides, such as those that have occurred in North America as a result of quick clay produced by glaciers (Hansen, 1965; Seed and Wilson, 1967), do not occur along the coastal regions of east or Southeast Asia, and therefore this type of landslide is not discussed here. Similarly, landslides induced by the collapse of large volcanic edifices, such as occurred during the 1982 Mt. Saint Helens event (Voight et al., 1983; Waitt et al., 1983), are related to volcanic activity, not rainfall or earthquakes, and therefore also lie outside the scope of this paper.

Earthquake-induced landslides

Recent earthquakes, such as the 2011 Tohoku earthquake in Japan, 2009 Padang earthquake in Indonesia, 2008 Wenchuan earthquake

Figure 1. A typical catastrophic landslide induced by an earthquake on a slope of pyroclastic fall deposits. The Hanokidaira landslide induced by the 2011 Tohoku earthquake. (Photo courtesy: National Institute for Land and Infrastructure Management and Public Works Research Institute).

in China, 2008 Iwate–Miyagi inland earthquake in Japan, 2005 northern Pakistan earthquake, and 2004 Mid-Niigata Prefecture earthquake in Japan, have proved of use in understanding where and why large catastrophic landslides are induced by earthquakes. These landslides have generally occurred where chemical weathering or gravitational deformation of rocks have preceded and reached near-threshold conditions just prior to the catastrophic failure induced by earthquakes.

Landslides prepared by chemical weathering processes

Pyroclastic fall deposits

The 2011 Tohoku earthquake induced long-run-out catastrophic landslides in pyroclastic fall deposits with sliding surfaces in a halloysite-rich paleosol (Figure 1), which was originally formed by chemical weathering and then buried by subsequent pyroclastics. The paleosol, which had been formed by the leaching out of silica, alkali, and alkaline earth elements, reacted with percolating rainwater that had obtained silica during its infiltration through the new deposits, then resilicified and formed halloysite. This process is understood to be the primary reason for the occurrence of halloysite in these buried paleosols (Chigira, 1982; Kleber et al., 2007; Chigira et al., 2014). Similar landslides involving a sliding surface in a paleosol have occurred during many other earthquakes (Table 2), including the 2009 Padang earthquake. The largest landslide of pyroclastic fall deposits was the 1984 Ontake landslide induced by the Naganoken–Seibu earthquake in Japan with a volume of 36×10^6 m^3 (Okuda et al., 1985). It had a sliding surface in halloysite-rich weathered pumice bed (Tanaka, 1985). The next largest was the Las Colinas landside, which had a volume of 1.83×10^5 m^3, and which was induced by the 2001 El Salvador earthquake (Evans and Bent, 2004; Crosta et al., 2005); this landslide had a sliding surface in a paleosol even though clay minerals were not actually identified in that case. The distribution of halloysite-rich soil could be predicted by the study of both volcano-stratigraphic characteristics and weathering mechanisms.

Landslides of this type do not occur on steep slopes because the pyroclastic fall deposits themselves do not form slopes steeper than the angle of repose, and such landslides may occur on gentle slopes even shallower than 20° (Figure 2); these landslides are commonly very mobile with low equivalent coefficients of friction (Figure 2). Equivalent coefficients of friction are known to decrease with increasing landslide volume (Scheidegger, 1973; Hsu, 1975), but landslides of this type have exceptionally low values even for small-volume landslides (Figure 3).

Table 2. A list of catastrophic landslides of pyroclastic fall deposits

Earthquake		1949 Imaichi	1968 Tokachi-Oki	1978 Izu-Oshima-Kinkai	1984 Naganoken-Seibu	2011 Tohoku	2001 El Salvador	2009 Padang	2008 Iwate Miyagi Inland
Date		26 Dec.	16 May	14 Jan.	14 Sept.	11 March	13 Jan.	30 Sept.	14 June
Magnitude		Mjma 6.4	Mjma7.9 (Mw8.2)	Mjma 7.0	Mjma 6.8	Mw 9.0	Mw 7.7	Mw 7.5	Mjma 7.2
Seismic Intensity at landslide sites (JMA)		5~6	5	5–6	6	6-~6+	MM 6, 7 4, 5- (JMA)	MM 8 (USGS) 5+ (JMA)	5+~ 6+
Antecedent rain (mm)	Rain gauge	Utsunomiya	Hachinohe	Inatori	Ontakesan	Shirakawa			Komanoyu
	10 days	22.5	181	12	183	12.5	no data (Nov.-Apr.: dry season)[h)]	Unknown (occurred during heavy rain)	89
	30 days	80.8	292	172	555	83.5			284.5
	60 days	255	307	334	839	93.5			388
Number of collapsing landslide		88[a)]	152[b)]	7[d)] (controlled by the material distribution)	5[i)]	<10[e)]	>1000[g)]	160[i)]	>100
Sliding surface		Weathered pumice Halloysite[a)] Paleosol[m)]	Paleosol (Sandy ash) Halloysite[c)]	Paleosol Halloysite[d)]	Weathered pumice and scoria Halloysite[k)]	Paleosol Halloysite[e)]	Paleosol[f)] No report of clay minerals	Mixed layer of paleosol and pumice Halloysite[i)]	Various Many in weathered pumice
Slid material		Shichihonzakura pumice and Imaichi pumice[l)]	Towada-Hachinohe tephra[b,c)]	East Izu monogenic volcanic tephra[d)]	Scoria, lava, agglutinate, aterrace deposits,	Tephra from Nasu Volcano[e)]	Pumice etc.	Pumice (Qhpt)	Various
Source of the slid materials		Nantai volcano	Towada Volcano volcanoes	Higashi-Izu monogenetic	Ontake Volcano	Nasu Volcano[1)]	?	Tandikat Volcano[i)]	Various
Sliding surface depth (m)		3~5 m[a)]	<3 m[b)], 01~2.5 m[c)]	2~6 m[d)]	5 m~200 m (Ontake)[j)]	3~9 m[e)]	50~70 m (Las Colinas)[f)]	3.5~5.5 m[i)]	–
Slope-parallel bedding		O	O	O	O	O	O	O	No
Undercut		Unknown	Unknown	O	O	O	O	Mostly	Various
Fatality		8	33	7	29	13	844[g)]	600?	O

Reference: a: Morimoto (1951); b: Inoue et al. (1970); c: Yoshida and Chigira (2012); d: Chigira (1982); e:Chigira et al. (2012); f: Crosta et al. (2005); g: Jibson et al. (2004); h: Evans and Bent (2004); i: Nakano et al. (2013); j: Hirano et al. (1985); k: Tanaka (1985); l: Suzuki (1993); m: Chigira (unpublished data)

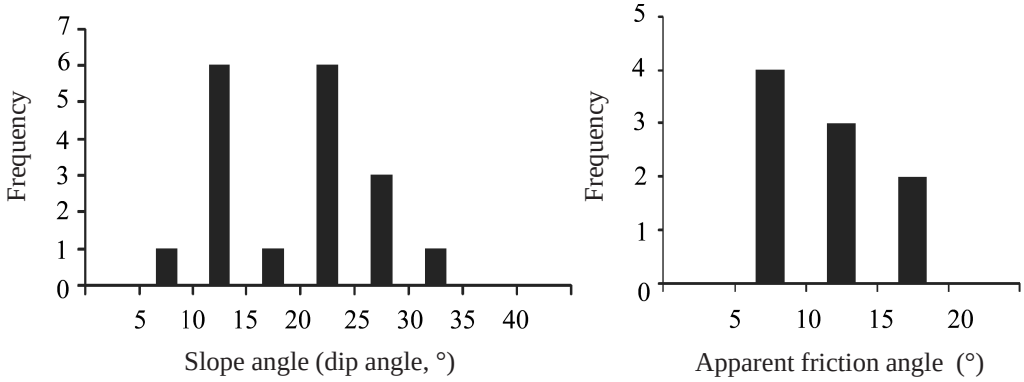

Figure 2. Slope angles and apparent friction angles of soilslide-avalanches of pyroclastic fall deposits. Data: 1923 Kanto earthquake (Kamai, 1990), 1968 Off Tokachi earthquake (Inoue et al., 1970), 1978 Izu-Oshima Kinkai earthquake (Chigira, 1982), 1984 Naganoken-Seibu earthquake (Tanaka, 1985; Hirano et al., 1985), and 2011 off the Pacific coast of Tohoku earthquake.

Carbonate rocks

Carbonate rocks are easily dissolved by carbonic acid in groundwater, thereby leading to the formation of karstic landscapes with features such as caverns and dolines. The 2008 Wenchuan earthquake induced numerous landslides of carbonate rocks (Table 3; Huang, 2011; Huang and Fan, 2013). Many of these landslides occurred on the dip slopes of well-stratified carbonate rocks with sliding surfaces developed along bedding planes. The sliding surfaces commonly have rough surfaces with dimple-like depressions and fractured protrusions, with the depressions being formed by the dissolution of carbonates (Chigira et al., 2010) and fractured protrusions being formed at the contact between the overlying slide rock and the rock beneath. Groundwater flow along a bedding plane dissolves carbonates and decreases the areas of contact between rock masses above and below the surface; these contacts are finally broken by seismic shaking. The enlargement of pore spaces, in contrast, drains groundwater, and hence pore-water pressure build up is unlikely to occur during rainfall events. Catastrophic landslides of carbonate rocks were also induced in many places during the 2005 Kashmir earthquake (Sato et al., 2007).

Mudstone

Many slow-moving landslides in weak mudstone have been recorded in Japan, Malaysia, and Indonesia. These landslides are generally induced by melting snow or rainfall (Matsuura et al., 2008). Although rapid and catastrophic landslides of mudstone are generally not reactivated or newly induced by earthquakes, the 2004 mid-Niigata Prefecture earthquake triggered many such landslides in Neogene marine mudstone areas as well as in sandstone areas (Chigira and Yagi, 2005). Landslides in these areas may be related to the weathering of marine mudstone, whose weathering is dominated by the oxidation of pyrite (Chigira, 1990). Pyrite oxidation forms sulfuric acid, which in turn dissolves microfossils as well as other acid-labile minerals, and acts to deteriorate mudstone and to form micropores. Thus, weakened mudstone with many micropores might be sheared during an earthquake, generating abnormally high pore pressures, in turn leading to liquefaction of the sliding surface (Sassa et al., 1996). This may be a reasonable cause of a catastrophic landslide in mudstone.

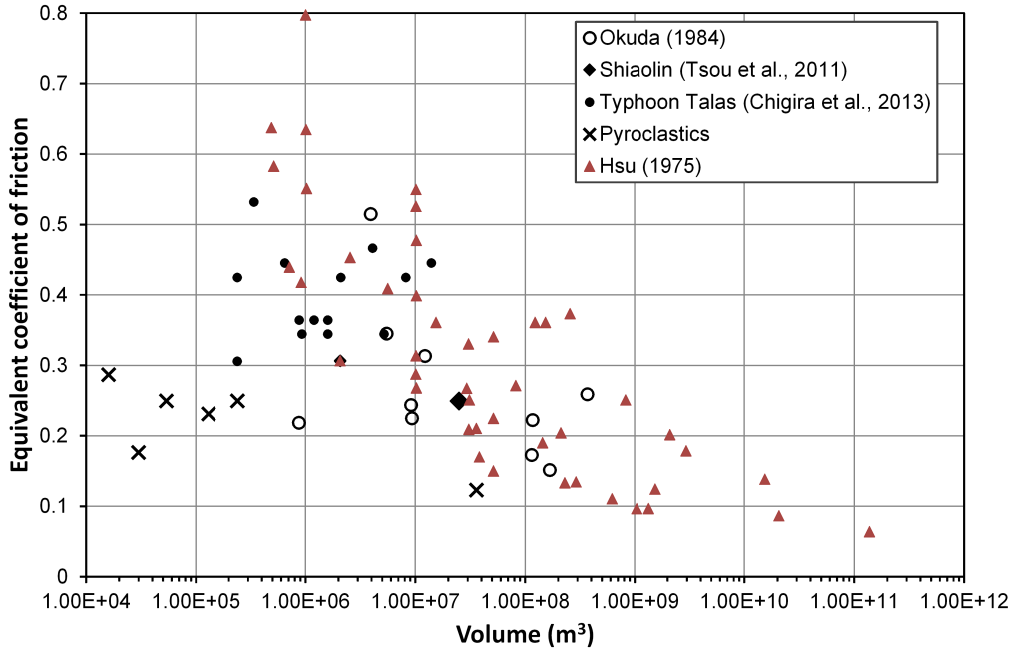

Figure 3. Equivalent coefficients of friction and landslide volumes. Landslides of pyroclastic fall deposits are plotted far below the trend of the other landslides.

Mechanical preparation

The mechanical preparation for large earthquake-induced landslides is deep-seated gravitational slope deformation, which has preceded many landslides. Such landslides include the Daguanbao landslide, which was triggered by the Wenchuan earthquake and is one of the largest historic landslides (Chigira et al., 2012b), and the Chiu–fen–erh–shan and Tsaoling landslides, which occurred during

Table 3. List of earthquake-induced landslides of various rocks with special references to geologic structures and precursory landforms.

Earthquake	Country	Magnitude	Seismic intensity at the landslide site	Landslide	Volume (10^6 m^3)	Rock type	dip (°)	Structure*		Precursory landform	Reference Chigira
715 earthquake	Japan	M 6.5-7.5**	Unknown	Ikeguchi	93	Sandstone, mixed rocks, green stone	50-60	UC	Bt	Head scarp	(2013)
1707 Hoei	Japan	M 8.4	5-6(JMA)**	Kanagi	8.5	Sandstone, mudstone	60-90	A	FT	Furrows	Chigira (2000)
1985 Papua New Guinea	Papua New Guinea	M 7.1	MM 8? (14 km from the epicenter)	Bairaman	200	Limestone	8	OC	U	Linear depression	King et al. (1989)
1999 Chi-Chi	Taiwan	Mw 7.6	465.3 gal EW 370.5 gal NS, and 274.7 gal UD 6 km north of the site	Chiu-fen-erh-shan	50	Sandstone, mudstone, shale	20-36	UC	B	Linear depression, steps	Wang et al. (2003)
				Tsaoling	125	ditto	14	OC	U	V-shaped linear depression	Chigira et al. (2003)
2004 Mid Niigata Prefecture	Japan	Mw 6.6 (Mj 6.8)	6+, 6-, 7 (JMA)	Higashitake-zawa	2	Sandstone, mudstone	20	OC	CU	Head scarp	Chigira and Yagi (2005)
				Shiono	5	ditto	14	OC	CU	Head scarp	
				Terano	0.5	ditto	14	OC	CU	Head scarp	
				Kazefukitoge	0.09	ditto	30-42	UC	B	Unknown	
2005 Northern Pakistan	Pakistan	Mw 7.6	MM 8	Dandbeh	65	Sandstone, mudstone	20 (plunge of a syncline)	OC	CU	Small scarps	Chigira (2007), Schneider (2008)
				Pir Bandiwala	1	Sandstone, mudstone	Unknown	Unknown	CU	Head scarp	
2008 Wenchuan	China	Mw 7.9	824.1 gal EW, 802.7 gal NS and 622.9 gal UD	Daguanbao	837	Carbonate rocks	35-38 (oblique)	UC	B	Linear depression	Chigira (2010)
				Yinxinggou	Unknown	Carbonate rocks	25?	OC	U	Unknown	
2008 Iwate Miyagi Inland	Japan	Mw 6.9 (Mj 7.2)	328 gal EW, 413 gal NS	Aratozawa	67	Sandstone, siltstone, tuff, welded tuff	0-2	OC	CU	Linear depression	Ohno et al. (2010)

*: OC: overdip cataclinal; UC: underdip cataclinal; A: anaclinal: Bt: buttress; B: buckling; FT: flexural toppling; U: undercut; CU: collided the opposite slope then undercut
**: Usami (2003)

the 1999 Chi–Chi earthquake (Chigira et al., 2003; Wang et al., 2003). Deep-seated gravitational slope deformation reduces the strength of rocks forming the slope, which would then become more susceptible to mass movement triggered by earthquake tremors.

Gravitational slope deformations that precede and prepare a site for earthquake-induced catastrophic landslide failure include several particular types (Table 3). The Chiu–fen–erh–shan landslide was preceded by buckle folding on a convex dip slope (Wang et al., 2003, B in Table 3); deformation on this slope was expressed topographically as linear depressions and steps. Buckle folding occurs on underdip cataclinal slopes (Cruden, 1989), in which the slope dips in the same direction as the dip of the foliation but with a gentler angle. Buckle folding can significantly destabilize a slope when it proceeds with the overturning of the lower limb of the fold, because when the lower limb is broken the whole slope loses its support at the foot. Landslides of this type, such as the Kazefukitoge landslide, also occurred during the 2004 Mid-Niigata Prefecture earthquake (Chigira and Yagi, 2005), and are also reported to have preceded the Daguanbao landslide, the largest landslide induced by the 2008 Wenchuan earthquake (Chigira et al., 2010). The Qingping landslide induced by the Wenchuan earthquake occurred on an underdip cataclinal slope and formed a landslide dam. This landslide left clearly observed buckle folding on the landslide scar (Figure 4).

A special type of underdip cataclinal slope that may become the site of an earthquake-induced landslide is a buttress-type structure, in which resistant beds at the foot of the slope support the upper part of the slope (Bt in Table 3). A well-known case is the Madison landslide, which was triggered by the 1959 Hebgen Lake earthquake in the USA (Hadley, 1964). In that case, heavily weathered gneiss and schist were supported by dolomite in the lower part of the slope, but the shaking of the earthquake broke the support and the whole slope failed. Whether gravitational slope deformation occurred before the event is not known. An earthquake-induced landslide with a similar buttress structure was the Ikeguchi landslide induced by the AD 715 earthquake in central Japan (Chigira, 2013). On the slope that hosted the landslide, beds of mixed rock and greenstone were supported by a thick, massive sandstone bed at the foot, which eventually failed because of seismic motion. The topography prior to the landslide is inferred from an adjacent slope, where the mixed rocks and greenstone

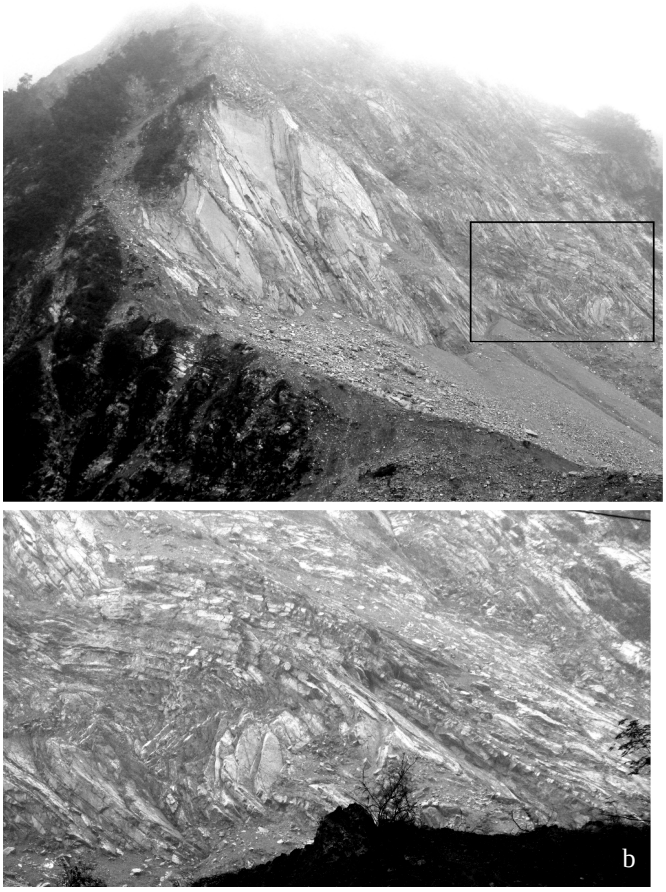

Figure 4. A buckle fold on the landslide scar of the Qingping landslide, which was induced by the 2008 Wenchuan earthquake and formed a landslide dam.

beds have been displaced downslope but remain supported by a thick sandstone bed, leaving a small scarp along the ridge. Gravitational slope deformation almost certainly preceded the catastrophic failure in AD 715.

An overdip cataclinal slope, in which a slope dips in the same direction as the bedding but more steeply (OC in Table 3), may be subject to gradual sliding, forming a linear depression or a scarp upslope. The Tsaoling landslide induced by the 1999 Chi–Chi earthquake had an overdip cataclinal slop structure, and linear depressions had developed along the position of its future crown before the earthquake. The Bairaman landslide induced by the 1985 earthquake in Papua New Guinea had a structure and linear depression upslope similar to that of the Tsaoling landslide (King et al., 1989).

Another type of landslide frequently triggered by earthquakes is the reactivation of a previous landslide that ran out across a river from one side of the valley and collided with the opposing slope, and which was subsequently undercut by erosion (CU in Table 3). The reactivation occurs because the support of the upslope material is removed, and therefore the landslide body becomes unstable. This type of landslide occurred in many locations during the 2004 Mid-Niigata Prefecture earthquake in Japan (Chigira and Yagi, 2005). The Hattian landslide, which was triggered by the 2005 northern Pakistan earthquake, had similar characteristics (Chigira, 2007; Dunning et al., 2007; Schneider, 2008).

Landslides induced by water blow-out during earthquakes

A distinctive type of landslide was induced by the 1966 Matsushiro earthquake, which caused groundwater to gush out along seismogenic faults, with the rise in water pressure inducing rotational landslides (Morimoto et al., 1967). Faults may locally cause groundwater pressure to build up by the accumulation of tectonic strain on them (Sibson, 1996), and the affected areas are in some situations more than 100 km away from the source fault (Toda et al., 1995). The locations of induced landslides are, however, limited to those areas close to surface fault ruptures.

Preceding rainfall

Rainfall that precedes an earthquake (antecedent rainfall) is known to be a significant influence on the occurrence of landslides, because the groundwater level can rise and decrease the suction forces within soil through the development of positive pore water pressure. The 2004 mid-Niigata Prefecture earthquake, Japan, triggered about 100 landslides with volumes exceeding 10^5 m^3 (Chigira and Yagi, 2005), but the 2007 Noto–hanto and the 2007 off-mid-Niigata Prefecture earthquakes induced very low numbers of landslides, even though these earthquakes had similar seismic intensities in the areas with similar geological and geomorphological settings to those of the 2004 mid-Niigata Prefecture earthquake (Table 4). The observed difference in landslide occurrence has been explained in terms of the rainfalls preceding these earthquakes (Chigira, 2007): the 2004 mid-Niigata Prefecture earthquake was preceded by more than 100 mm of rainfall within the three days prior to the earthquake, but the other two earthquakes were preceded by much smaller amounts of rainfall (Figure 5).

The occurrence of landslides in pyroclastic fall deposits is also strongly influenced by antecedent rainfall. The 2011 Tohoku earthquake caused shaking with intensities of >6 on the Japan Meteorological Agency scale over wide areas, but triggered fewer than 10 landslides on slopes formed from pyroclastic fall deposits. Comparing the rainfall amounts for 10, 30, and 60 days before the earthquakes that induced landslides in pyroclastic fall deposits (Table 2, Figure 6), the 2011 Tohoku earthquake was characterized by having the smallest amounts in all three intervals. The 1949 Imaichi earthquake had similar rainfall amounts during the 10- and 30-day intervals to those of the 2011 Tohoku earthquake, but induced 88 landslides in pyroclastic fall deposits. The materials of landslides induced by both of these earthquakes are widely distributed (Suzuki, 1993), so more landslides would have been triggered if factors other than seismic shaking had been close to their critical values for slope instability. These factors include antecedent rainfall, slope direction, undercutting conditions, and seismic behavior (Chigira, 1982); of these factors, antecedent rainfall is likely to be the most influential when a large area is considered. The 1978 Izu–Oshima–Kinkai earthquake induced only seven landslides, but these landslides were densely packed within an area of 1.5 km^2, wherein materials sourced from nearby monogenic volcanoes were distributed (Chigira, 1982). The 1984 Naganoken–Seibu earthquake induced only five landslides, but these were huge and the largest landslide had a volume of 36 million m^3 (Okuda et al., 1985). Notably, the Naganoken–Seibu earthquake was preceded by a much greater amount of rainfall than those earthquakes listed in Table 2.

Table 4. A comparison among the earthquakes that affected the areas with similar geologic and topographic settings. Only 2004 the Mid Niigata Prefecture earthquake induced many large landslides.

Earthquake	Date	Magnitude (Mj)	Seismic intensity (JMA)	Fault type	Rock types	Age	Landslide numbers	Reference
Mid Niigata Prefecture EQ in 2004	23 Oct.	6.8	6-~7	Reverse	Sedimentary rocks	Neogene and younger	More than 100 large landslides	Chigira and Yagi (2006)
Noto Peninsula EQ in 2007	25 March	6.9	6-~6+	Reverse	Sedimentary rocks Volcanic rocks	Neogene and younger	A few large landslides	
Off Mid Niigata Prefecture EQ in 2007	16 July	6.8	6+	Reverse	Sedimentary rocks	Neogene and younger	A few large landslides	

The effects of antecedent rainfall on earthquake-induced landslides have also been reported from New Zealand (Dellow and Hancox, 2006). The 1929 Buller and the 1931 Hawke's Bay earthquakes were both of Ms 7.8 and induced landslides in areas of intensities of 9 and 10 on the Modified Mercalli Intensity scale, but the former earthquake induced much larger and greater numbers of landslides. The Buller earthquake was preceded by 183.9 mm of rainfall over 10 days but the Hawke's Bay earthquake by only 8.4 mm. The geological and physiographical settings differed between these two areas, but soil moisture conditions are likely to have accounted for at least some of the difference in landslide occurrence between these two events. In Pakistan, Petley et al. (2006) reported that the 2005 northern Pakistan earthquake induced rather a low number of landslides because the amount of antecedent rainfall was small.

The effects of antecedent rainfall on landslide occurrence, as discussed above, must be considered when a landslide hazard map is constructed on the basis of historical records, because the pattern and number of landslides induced by previous earthquakes might have been very different if those earthquakes had been preceded by smaller or larger amounts of rainfall. The time intervals for the evaluation of antecedent rainfall that must be accounted for may depend on geological conditions. For example, weathered pyroclastic materials should retain water for much longer than sandy materials.

Table 5. A list of rainstorms that induced deep-seated catastrophic landslides or many shallow landslides in Japan.

Year	Date	Trigger(T: typhoon)	Place (Prefecture)	Geology	Deep-seated landslide	Many Shallow landslides
1998	26 to 31 August	Rain (Front)	Fukushima	Vapor-phase crystallized ignimbrite	–	O
1999	29 June	Rain (Baiu front)	Hiroshima	Granite	–	O
2000	28-29 July	Rain (Front)	Rumoi (Hokkaido)	Soft sedimentary rocks	–	O
	11-12 Sept.	Rain (Front+T14)	Tokai (Aichi)	Granite	–	O
2003	20 July	Rain (Baiu Front)	Minamata (Kumamoto) Hishikari (Kagoshima)	Andesite lava and pyroclastics	O	O
	9-10 August	Rain (T10)	Hidaka (Hokkaido)	Sandstone and conglomerate	–	O
	Ditto	Ditto	Ditto	Melange	–	O
2004	13 July	Rain (Baiu front)	Nagaoka (Niigata)	Weak mudstone	–	O
	Ditto	Ditto	Fukui	Volcanic rocks	–	O
	28-29 Sept.	Rain (T21)	Miyagawa (Mie)	Accretional complex (Hard sedimentary rocks)	O	–
	1 Aug.	Rain (T10)	Kisawa (Tokushima)	Accretional complex (Greeenstone and hard sedimentary rocks)	O	–
	29 Sept.	Rain (T21)	Ehime-Kagawa	Heavily weathered hard sandstone and mudstone	–	O
	29 Sept.	Rain (T21)	Saijo (Ehime)	Schist	O	O
2005	6 Sept.	Rain (T14 (Nabi))	Mimikawa (Miyazaki)	Accretional complex (Hard sedimentary rocks)	O	–
2006	19 July	Rain (Baiu front)	Okaya (Nagano)	Loam	–	O
2009	21 July	Rain (Baiu front)	Hofu (Yamaguchi)	Granite	–	O
2010	16 July	Rain (Baiu front)	Shobara (Hiroshima)	Soil	–	O
2011	4 Sept.	Rain (T12 - Talas)	Kii Mountains (Nara Wakayama)	Accretional complex (Hard sedimentary rocks)	O	–
2012	12 July	Rain (Baiu front)	Aso (Kumanoto)	Volcanic ash	–	O
2013	16 Oct.	Rain (T26 - Wipha)	Izu-Oshima (Tokyo)	Volcanic ash	–	O

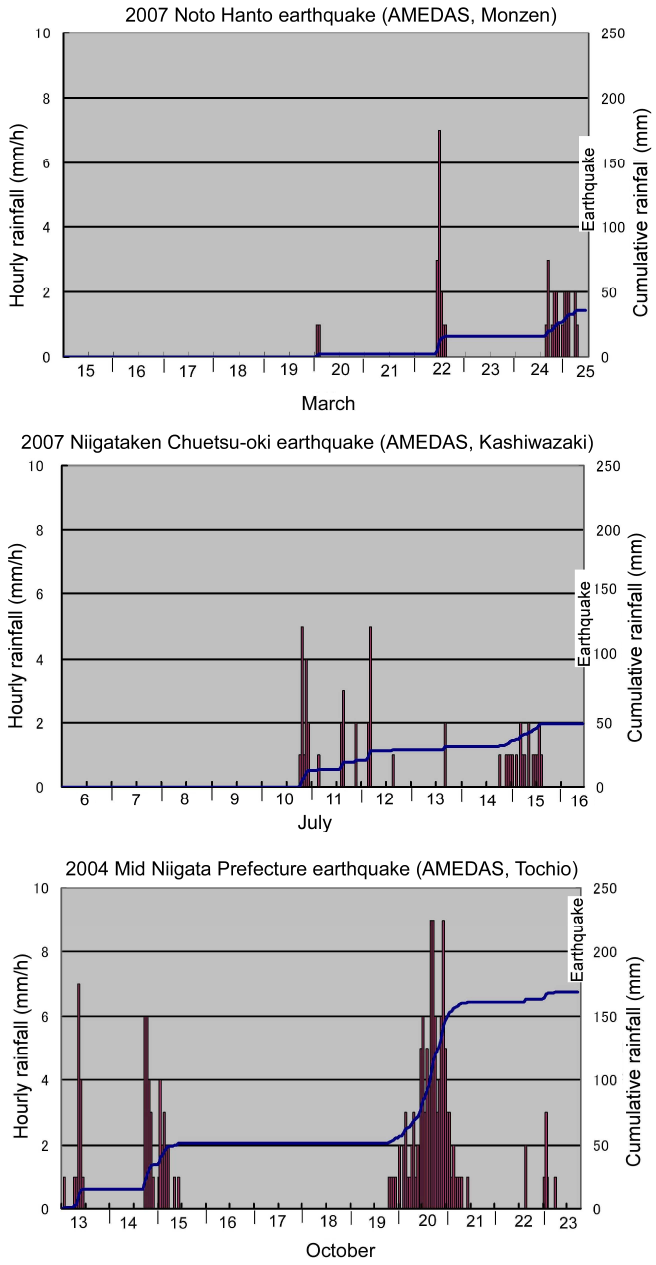

Figure 5. Antecedent rainfalls before the 2005 Mid Niigata Prefecture earthquake that induced many deep-seated landslides and other two earthquakes that induced much less numbers of landslides. See text for the details.

Thus, a longer time frame for considering the effects of antecedent rainfall may need to be considered when evaluating the effects of antecedent rainfall and earthquakes with respect to mapping landslide hazards.

Rainfall-induced landslides

In addition to the occurrence of earthquakes, most Asian countries are located in rainy areas, where large amounts of precipitation increase the probability of landslide occurrence. To predict the potential sites of shallow landslides, the effects of rainstorms have been studied deterministically using physical models (Montgomery and Dietrich, 1994; Montgomery et al., 2000). However, such

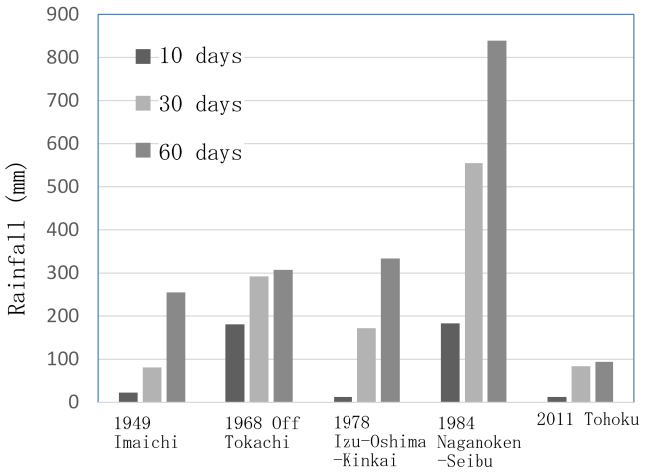

Figure 6. Antecedent rainfalls before the earthquakes that induced catastrophic landslides of pyroclastic fall deposits.

modeling needs data on both slope geometry and mechanical properties, which vary widely and are often not able to be estimated appropriately. Potential sites of shallow landslides may thus not be easily identified. In contrast, deep-seated landslides occur on slopes with very site-specific geological and geomorphological conditions; many such landslides are characterized by prior gravitational slope deformation (Chigira, 2009; Chigira et al., 2013b).

Deep-seated catastrophic landslides induced by typhoon Talas 2011 in Japan were significant, because ten were surveyed using 1-m high-resolution digital elevation models (DEMs) before the landslide events (Chigira et al., 2013b). These landslides occurred mainly in the Shimanto Belt, which is underlain by Cretaceous to Paleogene accretion complexes represented by mixed rocks and broken formations. In a recent study, Chigira et al. (2013b) analyzed the topography existing prior to the catastrophic failures triggered by typhoon Talas, and the results have shown that the catastrophic failures were preceded by gravitational slope deformation. Chigira (2013) analyzed the pre–typhoon Talas topography for an additional 29 catastrophic landslides using high-resolution DEMs and found that they were all preceded by gravitational deformation. Twentysix of the total of 39 deep-seated catastrophic landslides had small scarps marking the positions of the heads of the subsequent landslides (Figure 7, Chigira, 2013). These scarps were caused by gravitational slope deformation that preceded the catastrophic failure. Although the scarps may have been enlarged by degradation, their sizes relative to the whole slopes suggest that minimal amounts of slope deformation had occurred in the period immediately before the catastrophic failure. The scarp ratio, defined as the ratio of the length of a scarp to that of the whole slope, both measured along the slope line, ranged from 1% to 23%. Amongst landslides with small scarps, 38% had scarp ratios of <4% and 50% had scarp ratios of <8%. These data suggest that the gravitational slope deformations that preceded catastrophic failures were relatively small, and indicate that the slopes involved were likely to have been at critical condition just prior to catastrophic failure. Typical landslides featuring these small scarps occurred on slopes with wedge-shaped discontinuities dominated by thrust surfaces that were undulating and which discontinuously sandwiched competent rocks of sandstone, chert, or greenstone. The sliding surfaces that appeared just after catastrophic failure had undulating and stepped surfaces, which strongly suggests that the slopes before failure included materials that resisted whole-slope sliding. These stepped

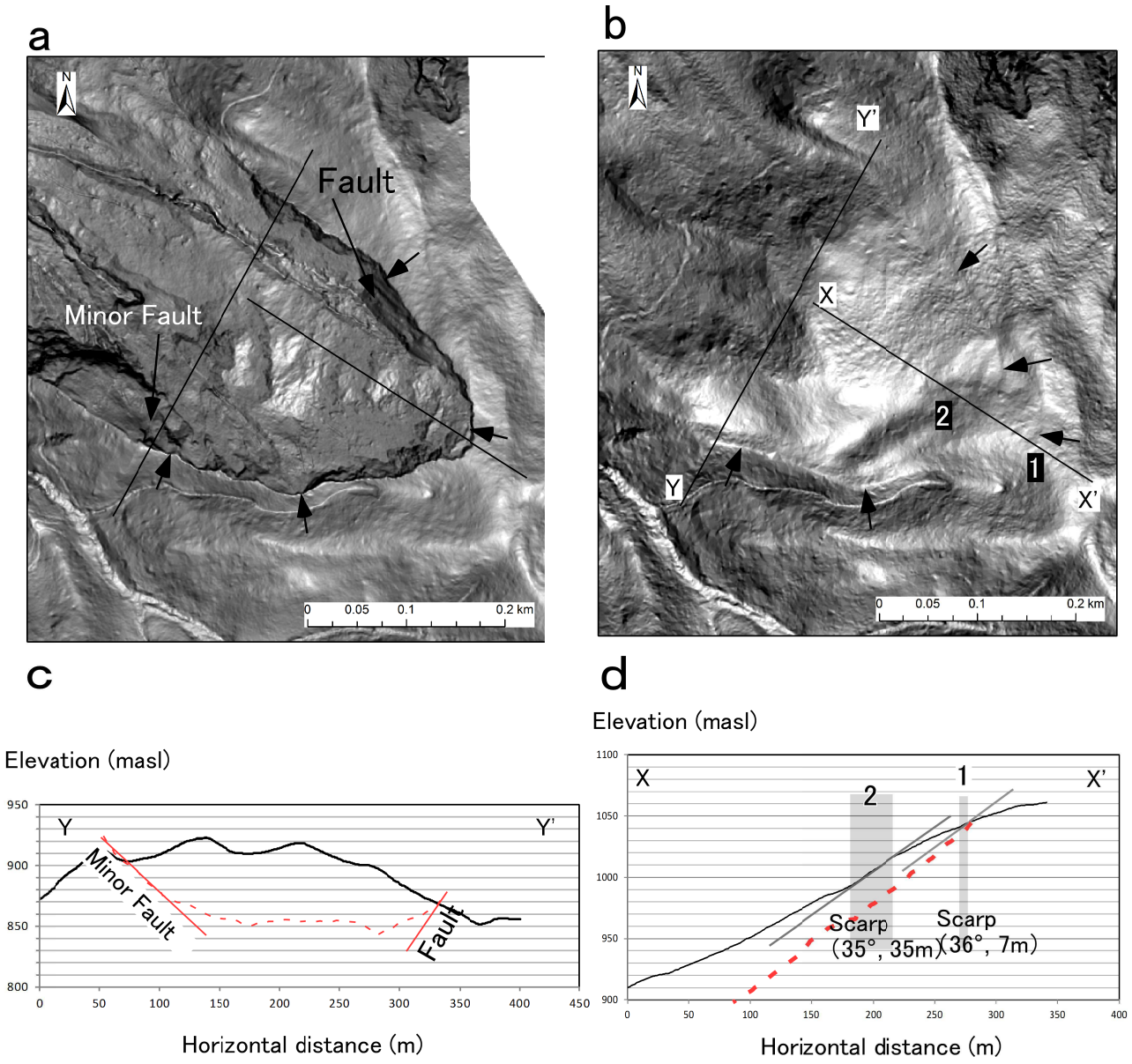

Figure 7. Slope images and cross sections of the upper part of the Akatani landslide induced by the 2011 typhoon Talas. a) After the landslide. b) Before the landslide. c) Cross-section along Y–Y' in B before (solid line) and after (dashed line) the landslide. d) Cross section along X–X' in B before (solid line) and after (dashed line) the landslide. Numbers 1 and 2 correspond to the scarp numbers in (b). Numbers in parentheses are slope angles and horizontal lengths along the slope line. Slope images were made using high resolution DEMs by the Ministry of Land, Infrastructure, Transport and Tourism.

features are similar to the "rock bridges" described by Eberhardt et al. (2004). Chigira et al. (2013a) analyzed the internal structures of a gravitationally deformed slope with irregularly shaped depressions and protrusions, and proposed that following their nucleation gravitational shear zones develop and connect to each other to form a through-going shear zone, which appears as a small scarp on the slope surface along the head of the moving body of material. The small scarps before catastrophic failure may therefore indicate an incipient landslide.

Typhoon Talas also induced one landslide with a large headscarp on a dip slope of alternating beds of sandstone and mudstone. This landslide had been gravitationally deformed with a buckle fold downslope (Chigira et al., 2013b). Buckle folds commonly accommodate large headscarps because the support from the lower slope at the lower limb remains even after a substantial amount of deformation. However, if the lower limb is exposed to intense erosion or failure, even a small amount of gravitational deformation may be sufficient to cause a catastrophic failure of the whole slope. The Shiaolin landslide, induced by typhoon Molakot in 2009 in Taiwan (Tsou et al., 2011), is an example of this type of landslide. The Shiaolin landslide had a volume of 25 million m^3 and demolished one village, causing over 400 fatalities.

The Ginsaugon landslide in Leyte, the Philippines, occurred without a clear trigger but had been preceded by about 700 mm of rainfall within the 10-day period before the landslide event (Evans et al., 2007). There is no report of whether this landslide had distinctive precursory topography, but judging from the nearby slopes and the fact that the landslide had a sliding surface along a spray fault of the

creeping Philippine Fault (Evans et al., 2007), it is very likely that there was a small headscarp before the catastrophic event.

Conclusions

The geomorphological features of deep-seated catastrophic landslides are evaluated in this paper as a basis for hazard mapping. Potential sites of shallow landslides are generally difficult to identify because of the wide variations in both subsurface structures and properties, In contrast, deep-seated landslides are predictable in many cases on the basis of specific geological and geomorphological features. Recent studies of deep-seated landslides indicate that many such landslides were preceded by gravitational slope deformation, except in the cases of earthquake-induced landslides in pyroclastic fall deposits and some mudstones and carbonate rocks. Earthquake-induced landslides in pyroclastic fall deposits, however, would be predictable by also specifying the materials that would slide or accommodate a sliding surface based on investigations of both volcanostratigraphy and material weathering. The other types of catastrophic landslide are preceded by gravitational slope deformation, which can be predicted using topographic features.

Acknowledgements

T. Kamai, Y. Matsushi, and C.-Y. Tsou of the Disaster Prevention Research Institute are thanked for helpful discussions, and some of the research results used in this paper was derived from collaborative research studies with these authors. C. Lim of the University of Kebangsaan, Malaysia and C. Tang of Chengdu University of Technology, China provided the statistics of landslide hazards in their respective countries.

References

Chigira, M., 1982, Dry debris flow of pyroclastic fall deposits triggered by the 1978 Izu-Oshima-Kinkai earthquake: the “collapsing” landslide at Nanamawari, Mitaka-Iriya, southern Izu Peninsula. Journal of Natural Disaster Science, v. 4, pp. 1-32.

Chigira, M., 1990, A mechanism of chemical weathering of mudstone in a mountainous area. Engineering Geology, v. 29, pp. 119-138.

Chigira, M., 1992, Long-term gravitational deformation of rocks by mass rock creep. Engineering Geology, v. 32, pp. 157-184.

Chigira, M., 2007, Site characteristics of gigantic landslides. Kinmiraisha, Nagoya, 256 pp.

Chigira, M., 2009, September 2005 rain-induced catastrophic rockslides on slopes affected by deep-seated gravitational deformations, Kyushu, southern Japan. . Engineering Geology, v. 108, pp. 1-15.

Chigira, M., 2013, Deep-seated catastrophic landslides - where are potential sites? Kinmiraisha, Nagoya, 231 pp.

Chigira, M., Hariyama, T., Yamasaki, S., 2013a, Development of deep-seated gravitational slope deformation on a shale dip-slope: observations from high-quality drillcores. Tectonophysics, v. 605, 104-113.

Chigira, M., Nakasuji, A., Fujiwara, S., Sakagami, M., 2014, Soil-Slide Avalanches of Pyroclastic Fall Deposits Induced by the 2011 off the Pacific Coast of Tohoku Earthquake. In: H. Kawase (Ed.), Studies on the Off the Pacific Coast of Tohoku Earthquake. Springer, Tokyo, pp. 65-86.

Chigira, M., Tsou, C.-Y., Matsushi, Y., Hiraishi, N., Matsuzawa, M., 2013b, Topographic precursors and geological structures of deep-seated catastrophic landslides caused by Typhoon Talas. Geomorphology, v. 201, pp. 479-493.

Chigira, M., Wang, G., Wu, S., 2012a, Landslides induced by the Wenchuan earthquake. In: J.J. Clague, D. Stead (Eds.), Landslides Types, Mechanisms and Modeling. Cambridge University Press, Cambridge, pp. 383-392.

Chigira, M., Wang, G., Wu, X., 2012b, Landslides induced by the Wenchuan earthquake. In: J.J. Clague, D. Stead (Eds.), Landslides: Types, mechanisms and modeling. Cambridge University Press, Cambridge, pp. 383-392.

Chigira, M., Wang, W.-N., Furuya, T., Kamai, T., 2003, Geological causes and geomorphological precursors of the Tsaoling landslide triggered by the 1999 Chi-Chi Earthquake, Taiwan. Engineering Geology, v. 68, pp. 259-273.

Chigira, M., Wu, X., Inokuchi, T., Wang, G., 2010, Landslides induced by the 2008 Wenchuan earthquake, Sichuan, China. Geomorphology, v. 118, pp. 225-238.

Chigira, M., Yagi, H., 2005, Geological and geomorphological characteristics of landslides triggered by the 2004 Mid Niigata prefecture Earthquake in Japan. Engineering Geology, v. 82, pp. 202-221.

Crosta, G.B., Chen, H., Frattini, P., 2006, Forecasting hazard scenarios and implications for the evaluation of countermeasure efficiency for large debris avalanches. Engineering Geology, v. 83, pp. 236-253.

Crosta, G.B., Imposimato, S., Roddeman, D., Chiesa, S., Moia, F., 2005, Small fast-moving f low-like landslides in volcanic deposits: The 2001 Las Colinas Landslide (El Salvador). Engineering Geology, v. 79, pp. 185-214.

Cruden, D.M., 1989, Limits to common toppling. Canadian Geotechnical Journal, v. 26, pp. 737-742.

Dellow, G.D., Hancox, G.T., 2006, The influence of rainfall on earthquake-induced landslides in New Zealand, New Zealand Geotechnical Society 2006 Symposium. Institution of Professional Engineers. Proceedings of technical groups / Institution of Professional Engineers New Zealand Nelson, New Zealand, pp. 355-368.

Dramis, F., Sorrisovalvo, M., 1994, Deep-seated gravitational slope deformations, related landslides and tectonics. Engineering Geology, v. 38(3-4), pp. 231-243.

Dunning, S.A., Mitchell, W.A., Rosser, N.J., Petley, D.N., 2007, The Hattian Bala rock avalanche and associated landslides triggered by the Kashmir Earthquake of 8 October 2005. Engineering Geology, v. 93(3-4), pp. 130-144.

Eberhardt, E., Stead, D., Coggan, J.S., 2004, Numerical analysis of initiation and progressive failure in natural rock slopes—the 1991 Randa rockslide. International Journal of Rock Mechanics and Mining Sciences, v. 41, pp. 69-87.

Evans, S.G., Bent, A.L., 2004, The Las Colinas landslide, Santa Tecla: A highly destructive flowslide triggered by the January 13, 2001, El Salvador earthquake. In: W.I. Rose, J.J. Bommer, D.L. Lopez, M.J. Carr, J.J. Major (Eds.), Natural hazards in El Salvador. Geological Society of America Special Paper, Boulder, Colorado, pp. 25-37.

Evans, S.G., Guthrie, R.H., Roberts, N.J., Bishop, N.F., 2007, The disastrous 17 February 2006 rockslide-debris avalanche on Leyte Island, Philippines: a catastrophic landslide in tropical mountain terrain. Nat. Hazards Earth Syst. Sci., v. 7, pp. 89-101.

Guzzetti, F., Carrara, A., Reichenbach, P., Cardinali, M., 1999, Landslide hazard evaluation: a review of current techniques and their application in a multi-scale study, Central Italy. Geomorphology, v. 31, pp. 181-216.

Hadley, J.B., 1964, Landslides and related phenomena accompanying the Hebgen Lake earthquake of August 17, 1959. U. S. Geol. Surv. Prof. Paper, v. 435, pp. 107-138.

Hansen, W.R., 1965, Effects of the earthquake of March 27, 1964 at Ancourage, Alaska. U. S. Geol. Surv. Prof. Paper, 542A, 68.

Hirano, M., Ishii, T., Fujita, T., Okuda, S., 1985, Geomorphological and geological characteristics of 1984 landslide hazard in Ohtaki village, Nagano Prefecture, Japan. Annuals of Disaster Preventin Research Institute, Kyoto Uiversity, v. 28, pp. 519-532.

Hsu, K.J., 1975, Catastrophic debris streams (sturzstroms) generated by rockfalls. Geological Society of America Bulletin, v. 86, pp. 129-140.

Huang, R.Q., 2011, Geo-engineering lessons learned from the 2008 Wenchuan

earthquake in Sichuan and their significance to reconstruction. Journal of Mountain Science, v. 8(2), pp. 176-189.

Huang, R.Q., Fan, X.M., 2013, The landslide story. Nature Geoscience, v. 6(5), pp. 325-326.

Inoue, Y., Honsho, S., Matsushima, M., Esashi, Y., 1970, Geological and soil mechanical studies on the slides occurred during the 1968 Toakachioki earthquake in southeastern area of Aomori Prefecture. Central Research Institute of Electric Power Industry, Report, pp. 1-27.

Jibson, R.W., Harp, E.L., Michael, J.A., 1998, A method for producing digital probabilistic seismic landslide hazard maps: An example from the Los Angeles, California, Area. U.S.Geological Survey, 98-113 pp.

Jibson, R.W., Crone, A.J., Harp, E.L., Baum, R.L., Major, J.J., Pullinger, C.R., Escobar, C.D., Martinez, M., Smith, M.E., 2004m Landslides triggered by the 13 January and 13 February 2001 earthquakes in El Salvador. In: W.I. Rose, J.J. Bommer, D.L. Lopez, M.J. Carr, J.J. Major (Eds.), Natural hazards in El Salvador. Geological Society of America, Boulder, pp. 69-88.

Kamai, T., 1990, Failure mechanism of deep-seated landslides caused by the 1923 Kanto earthquake, Japan. Proceedings of the sixth International Conference and Field Workshop on Landslides, pp. 187-198.

Kilburn, C.R.J., Petley, D.N., 2003, Forecasting giant, catastrophic slope collapse: lessons from Vajont, Northern Italy. Geomorphology, v. 54, pp. 21-32.

King, J., Loveday, I., Schuster, R.L., 1989, The 1985 Bairaman landslide dam and resulting debris flow, Papua New Guinea. Quarterly Journal of Engineering Eeology, v. 105, pp. 257-270.

Kleber, M., Schwendenmann, L., Veldkamp, E., Rössner, J., Jahn, R., 2007, Halloysite versus gibbsite: Silicon cycling as a pedogenetic process in two lowland neotropical rain forest soils of La Selva, Costa Rica. Geoderma, v. 138, pp. 1-11.

Matsuura, S., Asano, S., Okamoto, T., 2008, Relationship between rain and/or meltwater, pore-water pressure and displacement of a reactivated landslide. Engineering Geology, v. 101, pp. 49-49.

Montgomery, D.R., Dietrich, W.E., 1994, A physically based model for the topographic control on shallow landsliding. Water Resources research, v. 30-4, pp. 1153-1171.

Montgomery, D.R., Schmidt, K.M., GreenbergH.M., DietrichW.E.. 2000, Forest clearing and regional landsliding. Geology, v. 28-4, pp. 311-314.

Morimoto, R., Nakamura, K., Tsuneishi, Y., Ossaka, J., Tsunoda, N., 1967, Landslides in the epicentral area of the Matsushiro earthquake swarm - Their relation to the earthquake fault. Bull. Earthq. Res. Inst, v. 45, pp. 241-263.

Nakano, M., Chigira, M., Lim, C.-S., 2013. Landslides of pumice fall deposits induced by the 2009 Padang earthquake and the formation of halloysite, Japan Geoscience Union Meeting 2013, Makuhari, HDS06-02.

Okuda, S., Okunishi, K., Suwa, H., Yokoyama, K., Yoshioka, R., 1985, Restoration of motion of debris avalanche at Mt. Ontake in 1984 and some discussions on its moving state. Annual Report of the Disaster Prevention Research Institute, Kyoto University, v. 28, pp. 491-504.

Petley, D., 2012, Global patterns of loss of life from landslides. Geology, v. 40, pp. 927-930.

Petley, D., Dunning, S., Rosser, N., Kausar, A.B., 2006, Incipient landslides in the Jhelum Valley, Pakistan following the 8th October 2005 earthquake. Disaster Mitigation of Debris Flows,Slope Failures and Landslides, pp. 47-55.

Sassa, K., Hiroshi, F., Scarascia-Mugnozza, G., Evans, S., 1996, Earthquake-Induced-Landslides: Distribution, Motion and Mechanisms. Soil s and Foundations, pp. 53-64.

Sato, H.P., Hasegawa, H., Fujiwara, S., Tobita, M., Koarai, M., Une, H., Iwahashi, J., 2007, Interpretation of landslide distribution triggered by the 2005 Northern Pakistan earthquake using SPOT 5 imagery. Landslides, v. 4(2), pp. 113-122.

Scheidegger, A.E., 1973, On the prediction of the reach and velocity of catastrophic landslides. Rock Mechanics, v. 5, pp. 231-236.

Schneider, J.F., 2008, Seismically reactivated Hattian slide in Kashmir, Northern Pakistan. Journal of Seismology, v. 13(3), pp. 387-398.

Seed, H.B., Wilson, S.D., 1967, The Turnagain Heights landslide, Anchorage, Alaska. Journal of theSoil Mechanics and Foundations Division, Proceedings of the American Society of Civil Engineers, pp. 325-353.

Sibson, R.H., 1996, Structural permeability of fluid-driven fault-fracture meshes. Journal of Structural Geology, v. 18, pp. 1031-1042.

Suzuki, T., 1993, Stratigraphy of Middle Pleistocene tephra layers around Nasuno Plain, in north Kanto, central Japan. Journal of Geography, v. 102(1), pp. 73-90.

Tanaka, K., 1985, Features of slope failures induced by the Naganoken-Seibu Earthquake, 1984. Tsuchi-to-Kiso, v. 33(11), pp. 5-10.

Toda, S., Tanaka, K., Chigira, M., Miyakawa, K., Hasegawa, T., 1995, Coseismic behavior of groundwater by the 1995 Hyogo-ken nanbu earthquake. Jishin, v. 48, pp. 547-553.

Tsou, C.-Y., Feng, Z.-Y., Chigira, M., 2011, Catastrophic landslide induced by Typhoon Morakot, Shiaolin, Taiwan. Geomorphology, v. 127, pp. 166-178.

Voight, B., Janda, R.J., Glicken, H., Douglass, P.M., 1983, Nature and mechanics of the Mount St Helens rockslide-avalanche of 18 May 1970. Geotechnique, v. 33, pp. 243-273.

Waitt, J., R.B., Pierson, T.C., Macleod, N.S., Janda, R.J., Voight, B., Holcomb, R.T., 1983, Eruption-Triggered avalanvche, flood, and lahar at Mount St.Helens-Effects of winter snowpack. Science, v. 221, pp.1394-1397.

Wang, W.-N., Furuya, T., Chigira, M., 2003, Geomorphological Precursors of the Chiu-fen-erh-shan Landslide Triggered by the Chi-chi Earthquake in Central Taiwan. Engineering Geology, v. 69, pp. 1-13.

Yoshida, M., Chigira, M., 2012, The relation between weathering of pyroclastic fall deposits and the collapses caused by the 1968 Tokachi-Oki earthquake. Jour. Japan Soc. Eng. Geol., v. 52, pp. 213-221.

by Toshitaka Kamai

Landslides in urban residential slopes induced by strong earthquakes in Japan

Disaster Prevention Research Institute, Kyoto University, Gokasho, Uji 611-0011, Japan *(E-mail: kamai.toshitaka.3z@kyoto-u.ac.jp)*

Recent destructive earthquakes in urban regions, such as the 1978 Miyagiken-oki earthquake, the 1995 Kobe earthquake and the 2011 Tohoku earthquake have destabilized many gentle slopes in residential areas of large cities in Japan. Beyond the serious danger to residents of the earthquake affected areas, such landslides revealed the weaknesses of urban development in large cities of Japan. One of the typical large landslides, the Midorigaoka #4 landslide, occurred in residential fills in Sendai city during the 2011 Tohoku earthquake. Inclination measurements in the landslide indicate self-dumping at weak layers in ground structure. Excess pore water pressure in the landslide increased in direct proportion to horizontal peak ground velocity during after-shocks suggesting that the landslide was initiated by the complete loss of shear strength along the slip layer during the main shock. A simple analog model, the roller slider model, can discriminate stable or unstable valley fills during strong motion of past earthquakes. The results of stability analysis by the simplified 3D method based on this model explain the degree of damage in each valley fill during the 2011 Tohoku earthquake. Considering risk mitigation against such landslides in residential lots, urban development should minimize artificial changes in landforms, especially avoiding valley fills. A new concept of a "Counter line city" is proposed that includes both minimization of risk and creating a favorable natural environment.

Introduction: Brief history of landslide disasters in urban regions before 2011

Throughout Japan, large scale residential development on hillsides accompanied by massive grading operations in the suburbs of large cities started in the 1960s. According to Tamura (1977), the decision to expand residential development into hillsides did not adequately consider environmental consequences. The concept of a flat residential lot, which prevailed during the last 2000 years in Japan, was maintained. Thus, residential development into the hillsides consisted of massive grading to create flat land, including, removing hilltops and infilling valleys. Such massive grading operations often resulted in inadequate compaction of fill materials creating areas of dangerously soft and weak ground within cities throughout Japan. In recent years, a significant number of valley-fill failures and fill slope failures have been reported during large earthquakes that centered in large cities (Kamai et al., 2002). One of the first landslides in a valley-fill was recognized in a suburb of Sendai City during the Miyagi Prefecture earthquake of 1978 (Inst. Geol. Pal., Tohoku Univ., 1979). This trend followed with the Kushiro earthquake of 1993 and the Southern Hyogo Prefecture earthquake of 1995 (Kamai, 1995) (Fig. 1).

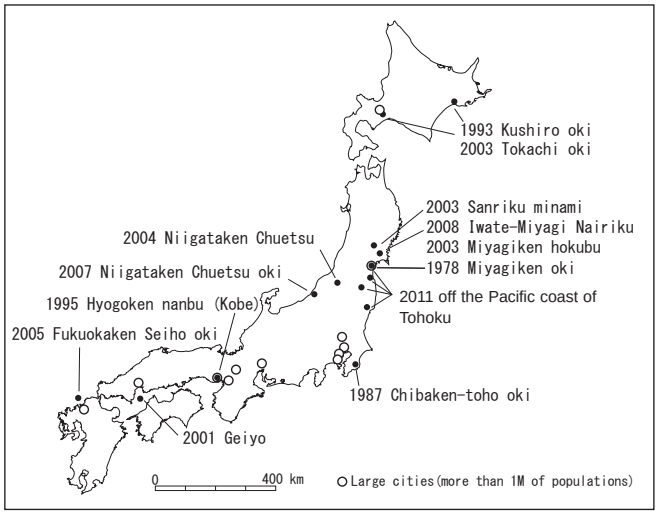

Figure 1. Earthquakes caused damage to urban residential region after WW2.

These failures include: (1) failures of most or all of the valley-fill; (2) lateral spreading associated with liquefaction; and (3) development of cracks along the cut and fill transition zones (Tamura et al., 1978; Kamai et al., 2000a; Kamai et al., 2004). These disasters revealed that: (1) many sites within cities were created, having a very high potential for failure; and (2) there is a good possibility that such sites will increase in number with future development. Thus, similar disasters could be repeated if large earthquakes occur near large cities somewhere in Japan. Based on these prior failures, the 2011 landslide disasters in urban regions could have been predicted before the earthquake.

This is a universal phenomenon associated with large scale disasters that can also be observed overseas; Ku-Lin-Ton and Chiuan-Chia-Fu during the Chi-Chi earthquake in Taiwan are some such examples (Kamai et al., 2000b). This paper discusses these highly probable future disasters that may occur under the similar conditions

and offers warnings and guidance for future urban development.

Landslides in urban regions induced by the 2011 Tohoku disaster

The events in 2011 followed similar patterns of damage by landslides in urban regions during past great earthquakes in Japan (Kamai et al., 2013). These recent landslides were distributed from southern Tohoku Province to Tokai village along the Pacific coast of the northern Kanto region; however, landslides were concentrated in the suburbs of Sendai City, the largest city in Tohoku province. In the shadow of the serious damage caused by tsunami waves, more than 200 residential lots in Sendai City were damaged. Among these, at least 50 residential lots were damaged by landslides in the urban residential region, and several hundred houses were destroyed by the landslides (Figs. 2, 3).

While great earthquakes with long recurrence intervals (M = 8) have been located off of the east coast of Japan, smaller major earthquakes with M = 7 have struck much closer to the mainland with increased frequency and have caused far more damage in these urban regions. Especially, the disaster caused by the 1978 Miyagi Prefecture earthquake is the first case when a modern large city with satellite communities was affected by a major earthquake.

Even after the 1978 Miyagi Prefecture earthquake, the urban region of Sendai City had expanded into hillsides because of population growth, especially during the economic bubble in Japan (1985-1995). In contrast, in other smaller cities, the lesser population growth precluded the need for extensive fill construction for residential lots. Thus, the population dynamics and the process of urban development in the Tohoku province during this half century are reflected in the distribution of urban landslides induced by the 2011 earthquake.

Features of ground surface deformation (i.e. cracks, subsidence, uplifting, and sand boiling) are important evidence to understand the state of landslide movements. These ground surface deformations appeared in conjunction with differences in thickness of fill, age of filling that affects the quality of fills, groundwater level, and existence or non-existence of landslide prevention works. Thus, the following five types of landslides in urban residential fills caused by the 2011 earthquake were recognized:

Type 1 “Valley-fill type landslide”
Type 2 “Widening-fill type landslide”
Type 3 “Failure and deformation in steep sloping fill”
Type 4 “Complex type of valley-fill type landslide and failure in steep sloping fill”
Type 5 “Surficial landslide”

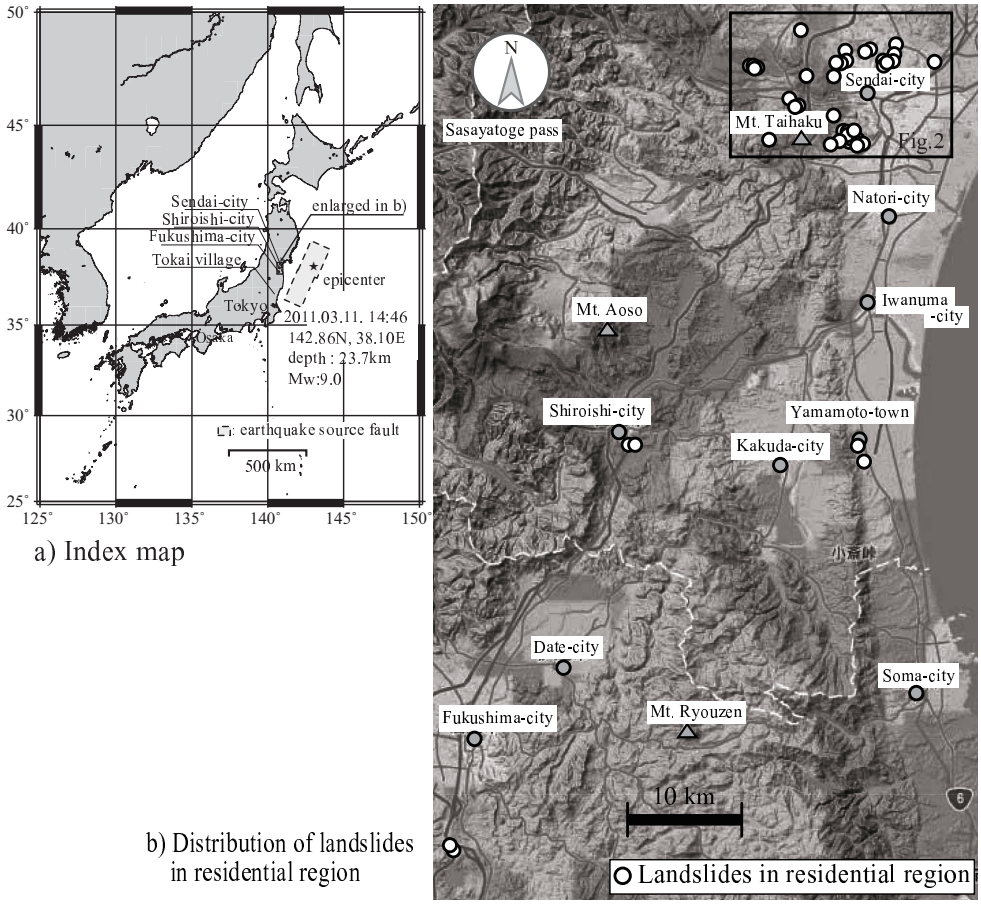

Figure 2. Distribution of landslides in urban residential region of southern Tohoku province.

Figure 4 shows slope movement classification of fill slopes from Type 1 to 5, with “thickness of movement mass” on the x-axis and “position of slip surface” on the y-axis. Among the fifty investigated sites, at least 7 sites (about 20%) are known to have been damaged by the 1978 Miyagi prefecture earthquake, indicating that the remediation of such fills was not adequate even after this disaster. Landslides also occurred in relatively newly developed housing lots that were constructed after 1990. Landsliding of fills constructed after the 1980’s

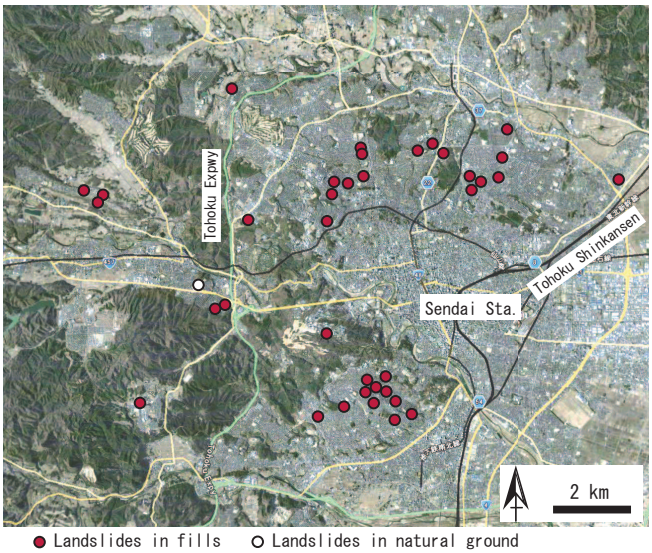

Figure 3. Distribution of landslides in Sendai urban region

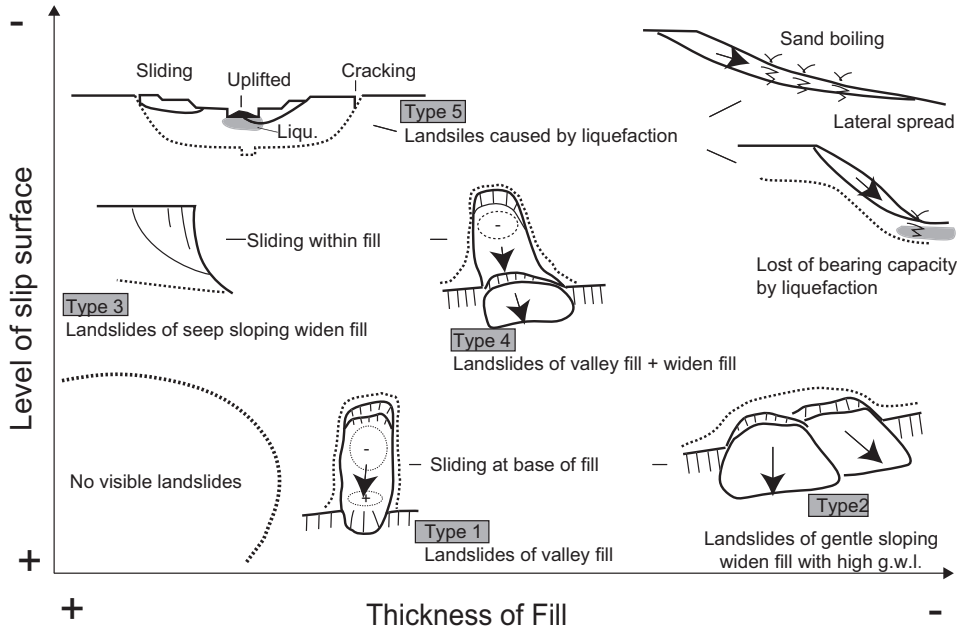

Figure 4. Types of landslides in urban region caused by the 2011 Tohoku earthquake.

were rare during past earthquake disasters, thus urban landslides in newly developed housing lots are one of the characteristic damages associated with the 2011 earthquake. Type 3 landslides were common in relatively newly developed housing lots during the 2011 earthquake, whereas Type 1 and 2 landslides were mainly distributed in areas developed before 1970. Thus, it appears that ground conditions conducive to sliding existed at the bottom of older fills and these helped generate Type 1 and 2 landslides.

The Midorigaoka #4 landslide

One typical landslide, the Midorigaoka #4 landslide, occurred in the widening fills (Type 2) of the lower part of a subdivision in the Midorigaoka District in the southern Sendai City during the 2011 Tohoku earthquake (Kamai, et.al., 2013) (Fig. 5). This is an older subdivision underlain by Pleistocene volcanic ash deposits (loam textured soils), Pleistocene marine terrace deposits and Pliocene sandstone and mudstone are the basement rocks that contributed to the construction of a staircase fashion. The grading operations consisted of balanced cuts and fills. The Midorigaoka 4-chome (Midorigaoka #4) subdivision sprawled across the flatland stretching between the terrace and valley floor. Based on comparisons of previous topographic maps, the development of the Midorigaoka #4 residential area started in 1968 by a private developer in Tokyo. The foundation ground of the upper part of the Midorigaoka #4 is cutslope; however, the lower part is typically widening fills. The large landslides occurred in the widening fills.

Figure 6 shows the geological columns with N-values of Standard Penetration Tests (SPT). The fill was loose and very soft with N-values from 0 to 4. At certain depths of N-values >5 in the columnar sections indicate the existence of large blocks of bedrock. The bedrock consists of Tertiary sedimentary material (i.e., pumice tuff, sandstone, siltstone) containing intercalated thin lignite beds. The bedrock is hard with N-values ranging from 40 to >50, except for the lignite beds.

Figure 7 shows the plan view and cross section of the Midorigaoka #4 landslide. Tension cracks were aligned along elevation counters at the boundary between the cut and fill. Contractional deformation (e.g. compression cracks, uplifting, and deformation of retaining walls) appeared at the foot of the fill slope on the alluvial valley floor. The fills consist of mixed bedrock material, sand, clay, and sandy silt with gravel. The humid top soil of the original ground surface was found at the boundary of the fill and bedrock. The ground water level was very shallow - 0.5 m to 1.1 m below the ground surface - indicating that the fills were nearly saturated by ground water. The contrast in strength between the fill and bedrock is clear, and soft topsoil exists at the boundary. Thus, the landslide is believed to move along the bottom of the fill. Observations of landslide movements, pore water pressure changes, and seismic response of fills, were conducted in this landslide.

Figure 5. Ground deformatiom induced by the Midorigaoka #4 landslide in Sendai City. (a) Tension crack at the head. (b) Compressive deformation at the toe.

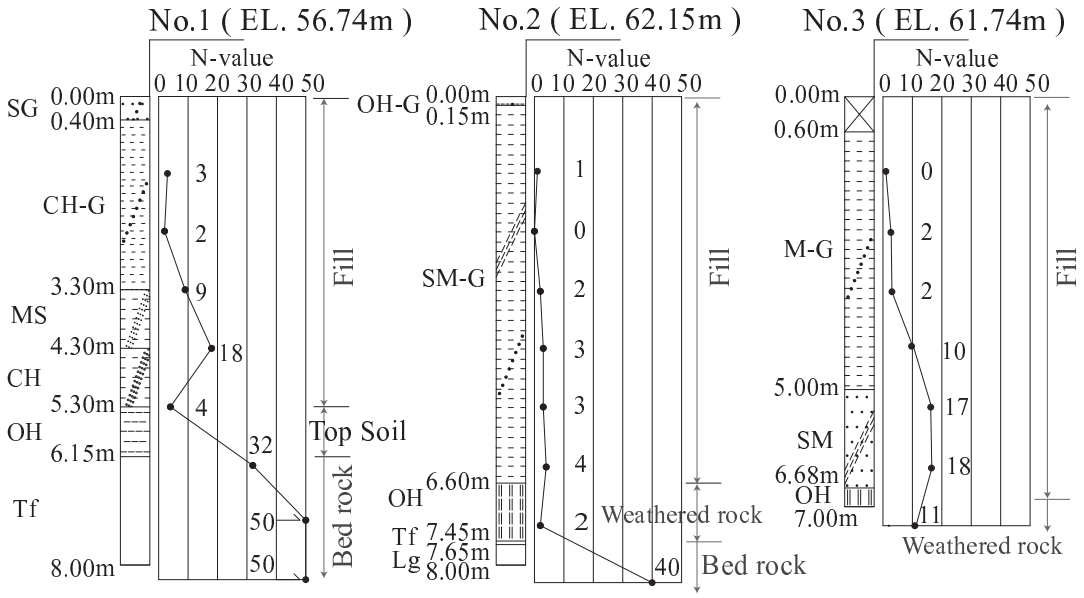

Figure 6. Columnar sections of bore holes in the Midorigaoka #4 landslide in Sendai City.

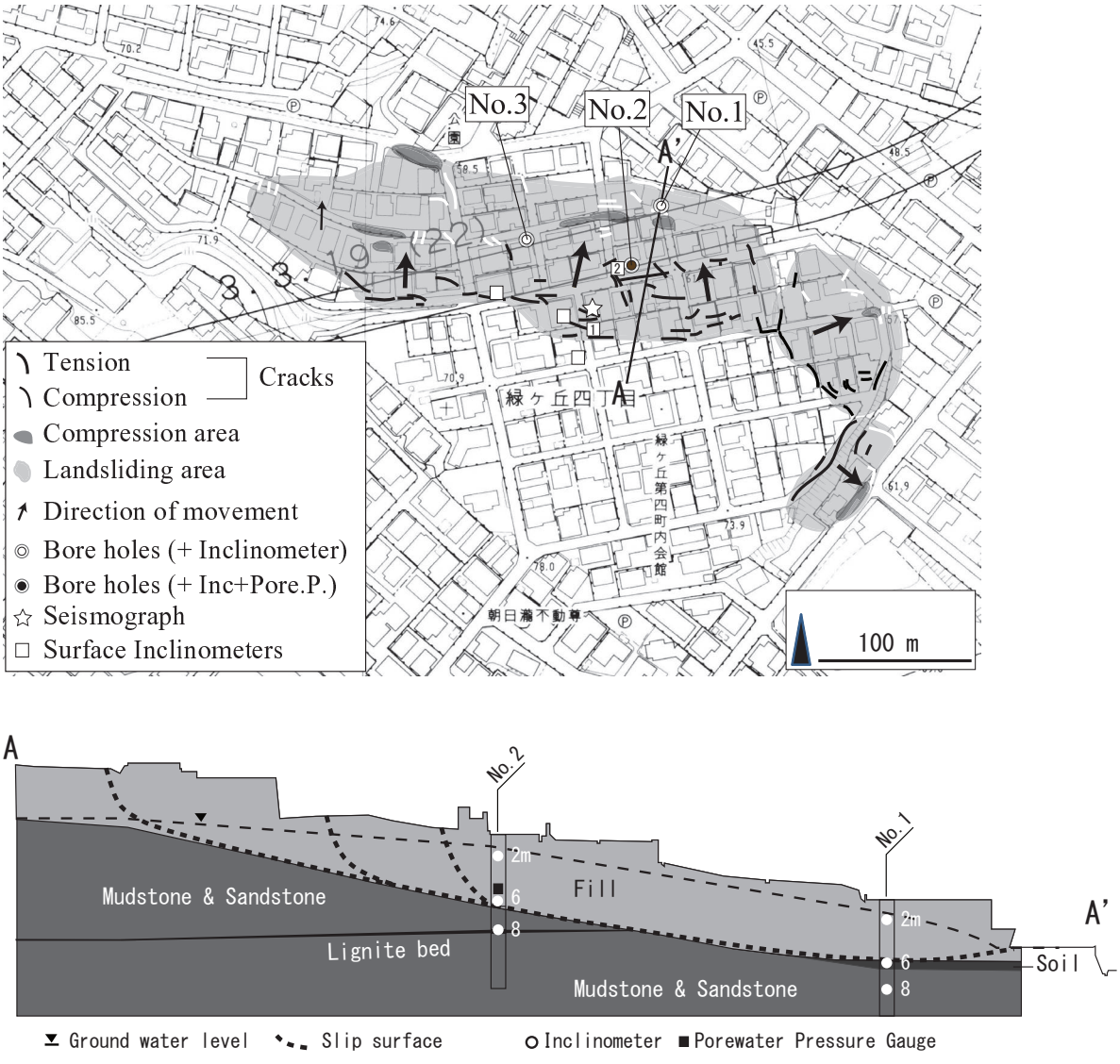

Figure 7. Plan view and cross section of the Midorigaoka #4 landslide in Sendai City.

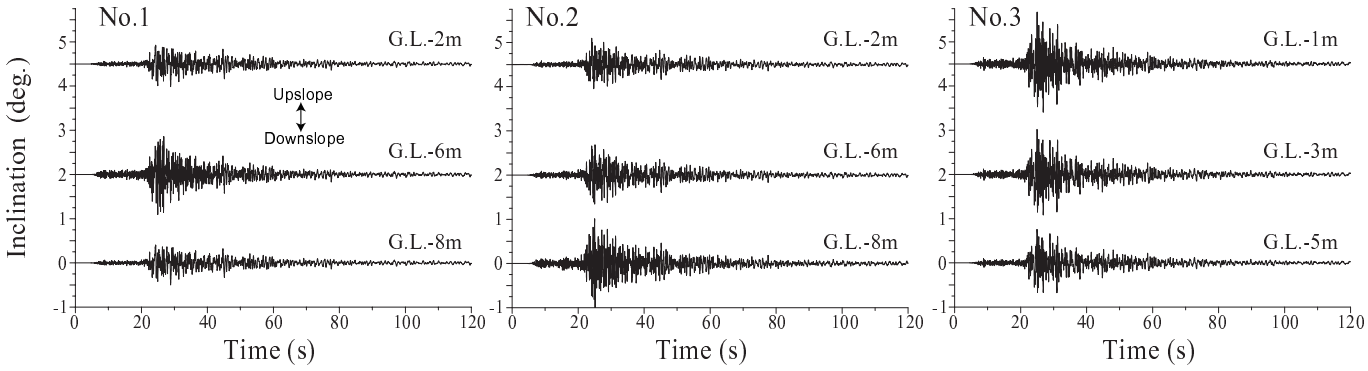

Figure 8. Co-seismic changes of inclination at 3:54 in 31th July 2011.

Landslide movements during earthquake

In the Midorigaoka #4 landslide, measurements of ground inclination using borehole inclinometers, and pore water pressure changes were made from June 2011 until June 2012 with a high precision time interval of 100 Hz. The largest seismic response of inclination was found at the weak layers in topsoils of the base of fills (GL-4m at Bore hole No.1) and in the fragile lignite layer of bedrocks (GL-8m at Bore hole No.2). In contrast, the response in the upper part of fills was small when weak layers developed at the lower portion of fills (Fig. 8). These results indicate the self-dumping effect in the weak layers of the subsurface ground structure. This effect was shown in areas where a thick weak layer developed at the bottom of the fill (borehole No.1 in Figure 8), and in the case of the aftershocks near the hypocenter. This observation indicates that the effects of self-dumping varied depending on the microstructure of landslide and local seismic response. This unique performance of landslide response during an earthquake is a significant finding related to seismic response on unstable slopes.

The horizontal peak ground velocity (PGV) of the estimated waveform of the main shock on 11th March 2011varied from 90 to 100 cm/s. Observations during aftershocks reveal that excess pore water pressure in the landslide increased in direct proportion to PGV during earthquakes less than 6 cm/s.

According to the linear relationship between PGV and excess pore water pressure in the landslide, excess pore pressure ratio, which is the effective normal stress divided by excess pore pressure during the main shock, might be almost 1.0 considering the effective overburden pressure, from 6 to 8 kPa at this site. This estimation is based on the assumption that this relationship could be applied throughout the strong motion during the main shock. The linear relationship is confirmed by smaller aftershocks until 20 cm/s of PGV (Nishikawa et al., 2002). Assuming this linear relationship during the main shock on 11th March 2011, it infer that the landslide was initiated by the complete loss of shear strength at the slip layer caused by an increase of excess pore water pressure during the strong seismic motion.

Verification of the landslide instability

The roller slider model is an analog to assess instability of valley-fill type landslides in residential regions. The advantage of this model is that it can explain the occurrence of stable valley-fills even during strong motion. This model considers friction along the side walls of valley-fills. Effects of side walls on valley-fills to constrain sliding movement should be quite important because of the significant reduction of soil strength at the bottom of fills caused by increases in pore water pressure. The analogy of a roller slider at an amusement park is effective to consider the mechanism of the sliding of valley-fills. We can more easily slide down on a wider slider as compared to a narrower one. Thus, the weak layer at the bottom of fill as shown in Fig. 9 should be necessary to represent the slider face in this analog model. There is a high potential of failure at the bottom of valley-fills during strong earthquakes because of the very weak and soft soil that has been identified at the bottoms of some fills where subsurface investigations were performed.

Fig. 10 shows plots of stiffness of fills (mean Vs) versus the ratio of width to depth of valley fills. Obviously, mean Vs of fill is not the predominant factor controlling the occurrence of landslides in fills. In contrast, ratio of width to depth is thought to be a major factor in discriminating between stable and unstable fills during strong seismic motion. It is clear from these case studies that the failure of valley fills is a phenomenon that cannot be determined by a simple 2-

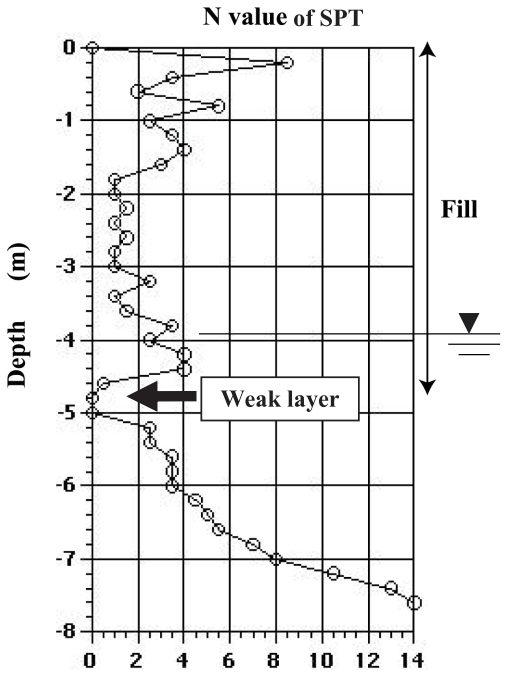

Figure 9. Typical N value of SPT changes in residential fill to original ground (in Ashiya City near Kobe).

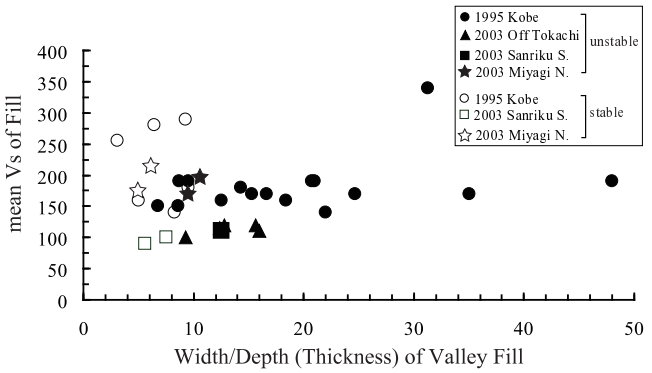

Figure 10. Stiffness of fills (mean Vs) vs. Shape ratio (Width/Depth).

dimensional mechanical analysis because the effect of the longitudinal cross-section has to be considered. Thus, the failure mechanism must be analyzed as a 3-dimenssional problem. Fig. 11 shows results of stability analyses on fills in 1978 the Miyagi Prefecture earthquake, 1993 Kushiro-oki earthquake and, 1995 Kobe earthquake by both the conventional 2D method and by the simplified 3D method that consider the roller slider model (modified after Ohta and Enokida, 2006). The method selected to assess landslide instability should be able to separate stable and unstable slopes by a factor of safety assessment; the simplified 3D method using the roller slider model (Fig. 11b) is successful in this regard, but the 2D conventional method (Fig. 11a) failed.

Table 1 shows that the factor of safety calculated by the simplified

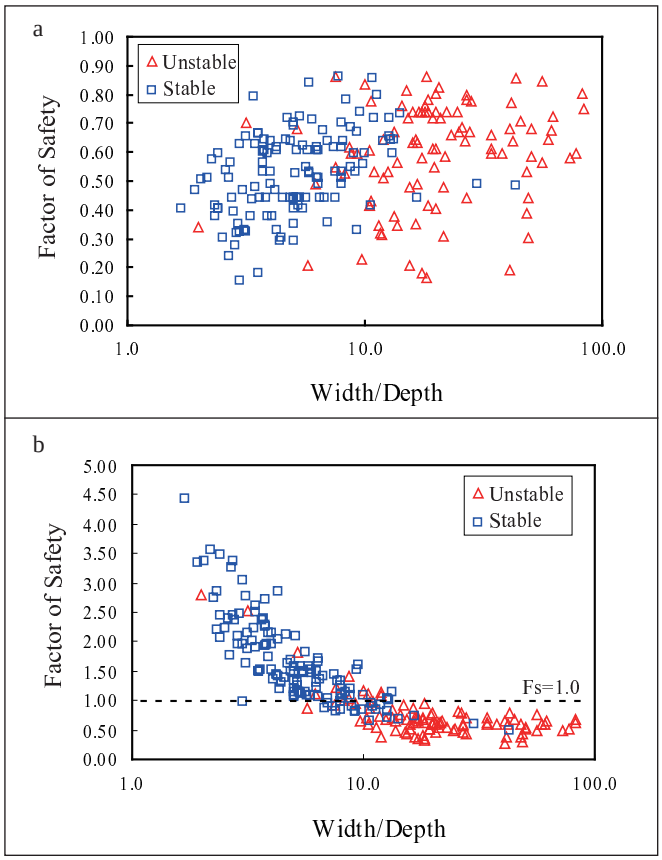

Figure 11. Results of stability analysis (factor of seismic inertia: k_h=0.25). a) 2D Fellenius method b)Simplified 3D method based on the roller slider model

Table 1. Suitability of simplified 3D analysis method based on the roller slider model in the 2011 Tohoku earthquake

Stable				Unstable			
Unit of fills	Degree of damage	Factor of safety	Rating	Unit of fills	Degree of damage	Factor of safety	Rating
A	medium	1.19	x	D	less	1.11	O
B	medium	0.88	O	J	less	1.13	O
C	serious	0.61	⊙	K	less	2.07	⊙
E	low	1.00	O	L	less	1.08	O
F	low	1.01	O	M	less	1.30	⊙
G	serious	0.86	⊙	N	less	1.10	O
H	low	1.15	x	O	less	1.50	⊙
I	low	0.84	O				

3D method could explain the degree of damage in each valley fill in Sendai City (modified after Ohta and Kamai, 2011). The roller slider model is also supported by results of stability analysis using the simplified 3D method in the case of the 2011 Tohoku earthquake.

Lessons learnt from the past earthquake disaster in 1978

A magnitude 7.4 earthquake with an epicenter off the shore of Miyagi Prefecture, northeastern Japan, struck on June 12, 1978, and caused widespread damage to Sendai City and surrounding cities and communities. Damages included 28 deaths, 11,028 injuries, and 179,255 damaged structures. Although the overall damage was moderate, there were a few notable exceptions: (1) damage to the lifelines; (2) fill and cut slope failures; and (3) failure of masonry walls. The first two types of damage occurred in all earthquakes affecting urban areas in Japan after this earthquake in 1978.

Landslides in cut and fill slopes during the 1978 earthquake occurred largely in the Midorigaoka and Nankodai Districts of Sendai City and the Kotobukiyama #4 Subdivision in Shiroishi City. These areas almost overlap with the sites of landslides in 2011. Fig. 12 shows the distribution of landslides in Midorigaoka District in 2011. In this region, landslides in 1978 were recorded in Midorigaoka #1,

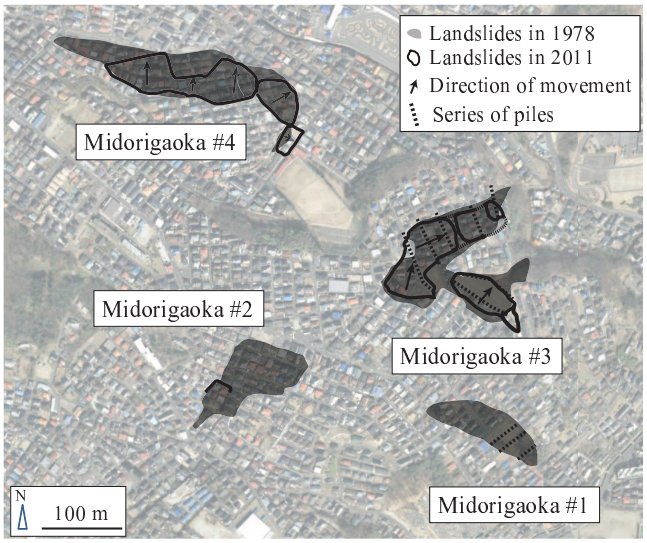

Figure 12. Distribution of landslides in the Midorigaoka area in Sendai City.

#2, #3, and #4 (Inst. Geol. Pal., Tohoku Univ., 1979). Among these areas, only the Midorigaoka #1 area was immune to landslide damage in 2011. In Midorigaoka #4, deformation of the ground in 2011, distribution of cracks, areas of subsidence, and uplifting areas experienced almost the same positions and patterns as in the 1978 earthquake. Thus, these landslides should have been expected and preventable if appropriate responses were made after the earthquake in 1978.

Contour line city

The investigation following the March 11, 2011 disaster suggests the intractability of the landslide hazard problem in urban residential fills. Even if artificial valley-fills are appropriately designed and constructed, they will continue to be at risk in urban residential regions in the future. Thus, urban residential lots should be designed to minimize artificial changes in geomorphology, especially avoiding valley fills. In other words, we have to build our houses along the counter lines of hill slopes in seismically active regions.

Fig. 13 shows a thematic drawing of the "Contour line city" (modified after Nagasaka, 2000). Winding roads connect detached houses aligned along the contour lines, and apartment and condominium complexes will be built along surface water streams that pass across artificial drainage. The foundation of buildings should be laid on the stiff original ground. Forested areas consisting of native vegetation should be planted in spaces between buildings; which will contribute rooting strength and remove some subsurface water evapotranspiration. Risk mitigation of slope disasters in urban residential regions should lead to a favorable natural environment in the "Contour line city".

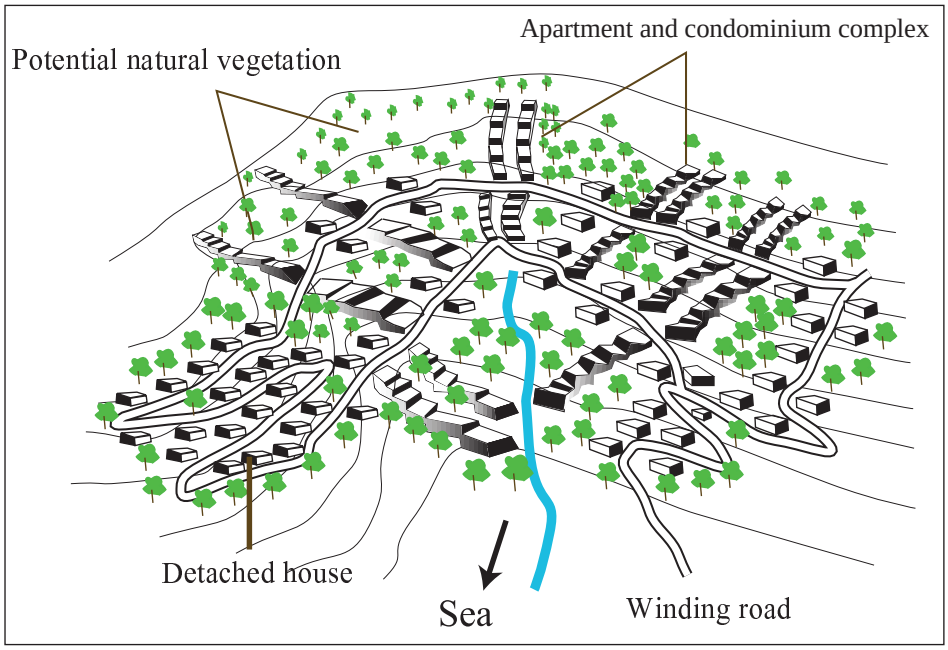

Figure 13. Thematic drawing of the "Counter line city" (the drawing was modified after Nagasaka, 2000).

Conclusions

Landslides in urban residential regions induced by earthquakes including the 2011 off the Pacific coast of Tohoku Earthquake in Japan are discussed. As the result of urbanization, most of these landslides occurred in fills of residential lots in large cities, which have been growing rapidly during the past half century. Results of the investigation of landslides in 2011 are summarized as follows:

1 Landslides of fills in residential regions induced by the 2011 earthquake are classified into five types based on the combination of "thickness of movement mass" and "position of slip surface".
2 A simple analog model, the roller slider model, was revalidated to effectively discriminate between stable and unstable valley fills in urban residential regions during strong ground-motion.
3 An unique performance of landslides during earthquakes, a self-dumping mechanism at a weak layer at the bottom of fills, was found. This effect varied depending on the microstructure of the landslide and appears to be a significant finding for seismic response on landslide slopes.
4 A rapid asymmetric increase in excess pore water pressure during strong motion suggests that the landslide was initiated by the complete loss of shear strength via liquefaction of the slip layer at the bottom of fill.
5 Some of the locations of landslides in 2011 overlapped with landslide locations in 1978. These landslides are "predictable and preventable disasters" if appropriate responses were made after the earthquake in 1978.

Considering risk mitigation against landslides in residential lots, urban development should be designed to minimize artificial changes in geomorphology, especially avoiding valley fills. A new concept of a "Counter line city" is proposed that includes both minimization of risk and creating a favorable natural environment.

Acknowledgements

I appreciate the helpful comments on an earlier draft of this manuscript from Dr. Roy C. Sidle, and review comments from Dr. Peter Bobrowsky. I wish to appreciate the support of our research by Mr. Nobuhiro Sato, Mr. Hidehiko Murao, and Hidemasa Ohta. This work was supported by KAKENHI (No. 23310125 and No. 26282110).

References

Inst. Geol. Pal., Tohoku Univ., 1979, Phenomena and Disasters Associatedwith the Miyagi-ken-Oki Earthquake of 1978 in the East-Central Part of Northeast Honshu, Japan: Tohoku Univ. Inst. Geol. Pal. Contr., no. 80, pp. 1-96.

Kamai, T., 1995, Landslides in the Hanshin Urban Region Caused by the 1995 Hyogoken-Nanbu Earthquake, Japan: Landslide News, no. 9, pp. 12-13.

Kamai,T., Kobayashi,Y., and Jinbo, C., 2000a, Earthquake risk assessments of fill slope instability in urban residential areas in Japan: Landslides (Proc. 8th Int. Symp. Landslide), Thomas Telford, London, pp. 801-806.

Kamai,T., Wang, W. N., and Shuzui, H., 2000b, The Landslides Disaster induced by Taiwan Chi-Chi earthquake of 21 September 1999: Landslide

News, no. 13, pp. 8-12.

Kamai,T, and Shuzui.H, 200, Landslides in urban region: Riko-tosho, Tokyo, pp. 1-200. (in Japanese)

Kamai, T., Shuzui, H., and Kasahara, R., 2004, Earthquake risk assessments of large residential fill-slope in urban areas: Journal of the Japan Landslide Society, no. 157, pp. 29-39. (in Japanese with English abs.)

Kamai, T., Ohta, H., Ban Y., and Murao H., 2013, Landslides in urban residential slopes induced by the 2011 off the Pacific coast of Tohoku Earthquake: "Studies on the 2011 Off the Pacific Coast of Tohoku Earthquake", DPRI Series v.1, Springer, Berlin, pp. 103-122.

Nagasaka, D., 2000, Recycled Urban Space (Nagasaki Project) model/ the project for public space in NAGASAKI /1999: SHINKENCHIKU, Tokyo, no. 4 in 2000, pp. 180-185. (in Japanese)

Nishikawa, J., Hayashi, H., Egawa, T., Miwa, S., Ikeda, T., and Mori, S., 2002, Liquefaction arrayobservations at two sites and analysis of their records: Journal of Japan Soci. Civil Engi. I, v. 59, pp. 327-343. (in Japanese with English abs)

Ohta, H. and Enokida, M., 2006, A fill-slope stability analysis method during earthquake: DS Kanto, The Japanese Geotechnical Society, pp. 21-35. (in Japanese)

Ohta, H. and Kamai, T., 2011, Landslides in residential fills by 2011 Tohoku earthquake: Symp. in Kansai, Japan Society of Engineering Geology, pp. 6-9. (in Japanese)

Tamura, T., 1977, Regional developments: Shokokusha, Tokyo, pp. 1-73. (in Japanese)

Tamura, T., Abe, T. and Miyagi T., 1978, Housing Construction in Hillside and Earthquake Disaster: General Urban Research no. 5, pp. 115-131. (in Japanese)

by Momoko Hirata, Jun Muto and Hiroyuki Nagahama

Experimental analysis on Rowe's stress-dilatancy relation and frictional instability of fault gouges

Department of Earth Science, Tohoku University, 6-3, Aramaki Aza-Aoba, Aoba-ku, Sendai, Miyagi, 980-8578, Japan.
E-mail: mhirata@dc.tohoku.ac.jp

The stress-dilatancy relation is important for understanding fault mechanics and brittle deformation of rocks, and hence the onset of frictional instability. The principle of minimum energy ratio was proposed by Rowe, and this Rowe's theory has been applied to deformation of granular materials. Rowe suggested that the energy ratio, which is the ratio of the energy dissipation rate to energy supply rate, would be a minimum and constant value. The relation between the rate of dilatancy and the maximum stress ratio can be extended to the case of a random assembly of irregular particles whereby the rate of internal work absorbed in frictional heat is a minimum as the mass dilates. According to Rowe's law, experiments show that the minimum energy criterion is closely obeyed by highly dilatant dense over-consolidated and reloaded assemblies throughout deformation. However, it is unknown whether or not the principle of minimum energy ratio can be applied to fault mechanics. The results of our friction experiments show the possibility that the energy ratio can be a new factor for evaluating frictional instability.

Introduction

Reynolds (1885) showed that dense sands expand at failure, whereas loose sands contract during shear failure. Therefore, because dilatancy is generally observed as a precursor to brittle faulting and the development of shear localization, attention has been focused on how localized failure develops in a dilatant rock (Wong et al., 2001). Dilatancy is hence closely related to earthquakes, and so to clarify the stress-dilatancy relationship is very important from the point of disaster prevention. Based on stress-dilatancy relation, the principle of minimum energy ratio was introduced by Rowe (1962) to obtain a stress-dilatancy relation for granular materials in a dense packing state under axisymmetric stress conditions. Rowe (1962) postulated that the ratio of energy dissipation by internal friction to energy supply in the direction of the major principal stress would be a constant and minimum value. The Rowe's theory can be applied not only to granular materials such as fault gouges but also to blocky materials such as lithified rocks. Niiseki (2001) and Moroto (1991) discussed Rowe's law in terms of thermodynamics and statistical mechanics of granular materials. However, there are many questions about Rowe's law, for instance, the physical meaning of an internal friction angle which is the factor of the energy ratio. Hence, it has not been utilized much for fault mechanics until now. Chappell (1979) proposed a relationship between the principal stresses in terms of the joint friction angle, whose magnitude is not only dependent on the smooth joint friction angle and roughness but also on the rotation of the blocks caused by slip.

Moreover, natural faults produce gouge due to slip, that plays an important role in controlling the stability of natural faults (e.g., Scholz et al., 1969; Marone and Scholz, 1988). Therefore, an understanding of earthquake mechanics requires the knowledge of the frictional behavior of gouge and gouge-rock systems (Marone et al., 1990). Hence, many studies about gouge have clarified that frictional instability is correlated with microstructural development of gouge (e.g., Byerlee et al., 1978; Logan et al., 1979; Marone and Kilgore, 1993; Ikari et al., 2011; Onuma et al., 2011). These studies have shown the development of shear localization in a gouge layer and possibility that the development of shear localization influences the frictional instability. However, the relationship between microstructural development and frictional instability of gouge has not yet been clear from the perspective of Rowe's law. In this study, we conducted the friction experiments using the gouge in a gas-medium apparatus in order to test whether Rowe's theory of constant energy ratio holds for frictional instability of simulated fault gouge and to clarify these relationships based on Rowe's law. The results of our friction experiments reveal that the mechanical behavior of fault gouges obeys the Rowe's law. By this law, we will effectively be able to evaluate the longitudinal shape of a slip surface in landslides or spray fault in accretionary prisms and the potential occurrences of them.

The friction experiments with a gas-medium apparatus

The friction experiments using simulated fault gouge were conducted in a gas-medium apparatus under the confining pressures (P_c) of 140-180 MPa (Figure 1). Strain rate was held constant at 10^{-3}/s. Dry quartz powders (0.1 or 0.2 g) for gouge were sandwiched into two gabbroic forcing blocks (20 mm in diameter, 40 mm in length, and cut by a 50º to their cylindrical axis). Three strain gauges glued onto a gouge layer through the Teflon jacket directly measured strain with the high-speed (sampling rate of 2 MHz) acquisition system (see Onuma et al., 2011 for details). To clarify mechanical behaviors of fault gouge, we held loads at different levels of differential stresses

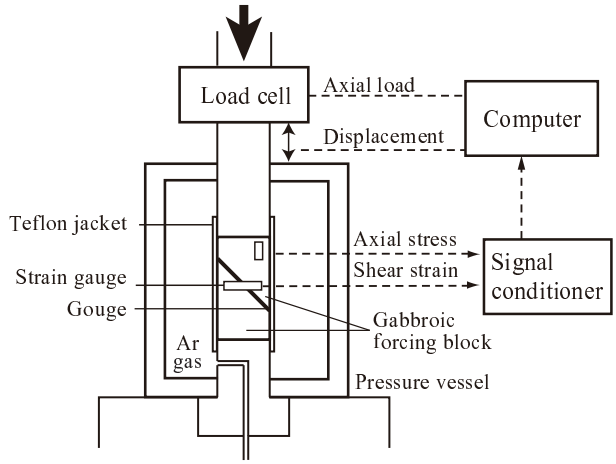

Figure 1. Schematic drawing of sample assembly and experimental setup.

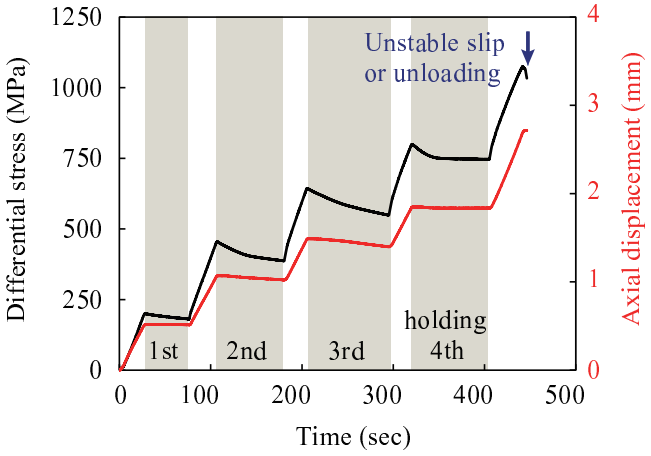

Figure 2. Operation of one cycle. After the 4th holding, the sample was loaded again until unstable slip occurred or strain gauges could not measure strains. When the latter happened, we unloaded and replaced to new strain gauges. Arrow means the end of one cycle. The gray shaded areas indicate the time ranges of holdings. The stress values are derived from the external load cell.

as shown in Figure 2 (1st holding at a differential stress of about 190 MPa, 2nd at 450 MPa, 3rd at 640 MPa, 4th at 800 MPa). When strains exceeded the measurable ranges of strain gauges, we replaced them with new ones. This succession of work, called cycle, was repeated until unstable slips occurred.

Results

We conducted 12 friction experiments at different confining pressures P_c and different weights of gouges (Table 1). From our experimental data, the number of cycles up to unstable slip increased

Table 1. Experimental parameters. Cycle means the number of experiments until unstable slip occurred at each condition.

P_c (MPa)	Weight (g)	Cycle
140	0.1	4
160	0.1	3
180	0.1	2
180	0.2	3

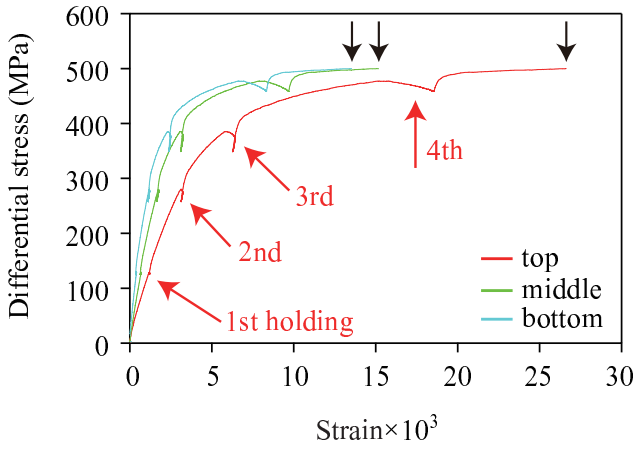

Figure 3. The representative stress-strain curve (P_c: 140 MPa, gouges: 0.1 g, cycle 4). Top, middle and bottom mean position of strain gauges. Black arrow indicates unstable slip. The stress values are determined by the vertical strain gauge.

with decreasing confining pressures and increasing weight of gouges.

Representative stress-strain curves and the mechanical behaviors of gouges during holding stages are shown in Figure 3. The positive value of strain means extension. The color means position of strain gauges (Red: top strain gauge, green: middle, blue: bottom). We obtained three different behaviors of gouges depending on differential stresses determined by the vertical strain gauge: Contraction, transition from extension to contraction and great extension from low to high stresses (Figures 3 and 4). At 1st holding, so lower stress, gouges contracted in all experiments. The behaviors of gouges show transition at 2nd or 3rd holding, and great extension at 4th holding. After repeated cycles, unstable slip took place at higher stress.

During holding stages, we also obtained the ratio of the energy rate of the major principal compressive stresses to minor compressive stresses, or the ratio of the input energy rate to output one. We obtained strain in the direction of minor principal compressive stress from three strain gauges glued onto a gouge layer. Similarly, the major principal compressive stress and strain were obtained from another gauge glued in vertical direction. The confining pressures were taken to be minor principal compressive stresses. The output energy can be expressed as a linear function of the input energy (Figure 5). This relation is expressed by

$$\sigma_1 \dot{\varepsilon}_1 = K \sigma_3 \dot{\varepsilon}_3, \quad (1)$$

where K is the ratio of energy rates, σ_1 and σ_3 are the major and minor compressive stresses, and $\dot{\varepsilon}_1$ and $\dot{\varepsilon}_3$ are strain rates of each direction, respectively. Eq. (1) can be rewritten by

$$\frac{\sigma_1}{\sigma_3} = K \frac{\dot{\varepsilon}_3}{\dot{\varepsilon}_1}. \quad (2)$$

It is revealed that the energy ratio becomes large with confining pressure as shown in Figure 5. In this figure, each color means confining pressure (Yellow: 140 MPa, green: 160 MPa and blue: 180 MPa). Moreover, because the energy ratio is slope of line, it is revealed that the energy ratio changed at each loading and holding stage (Figure 6). In Figure 6, the time passed to the direction from

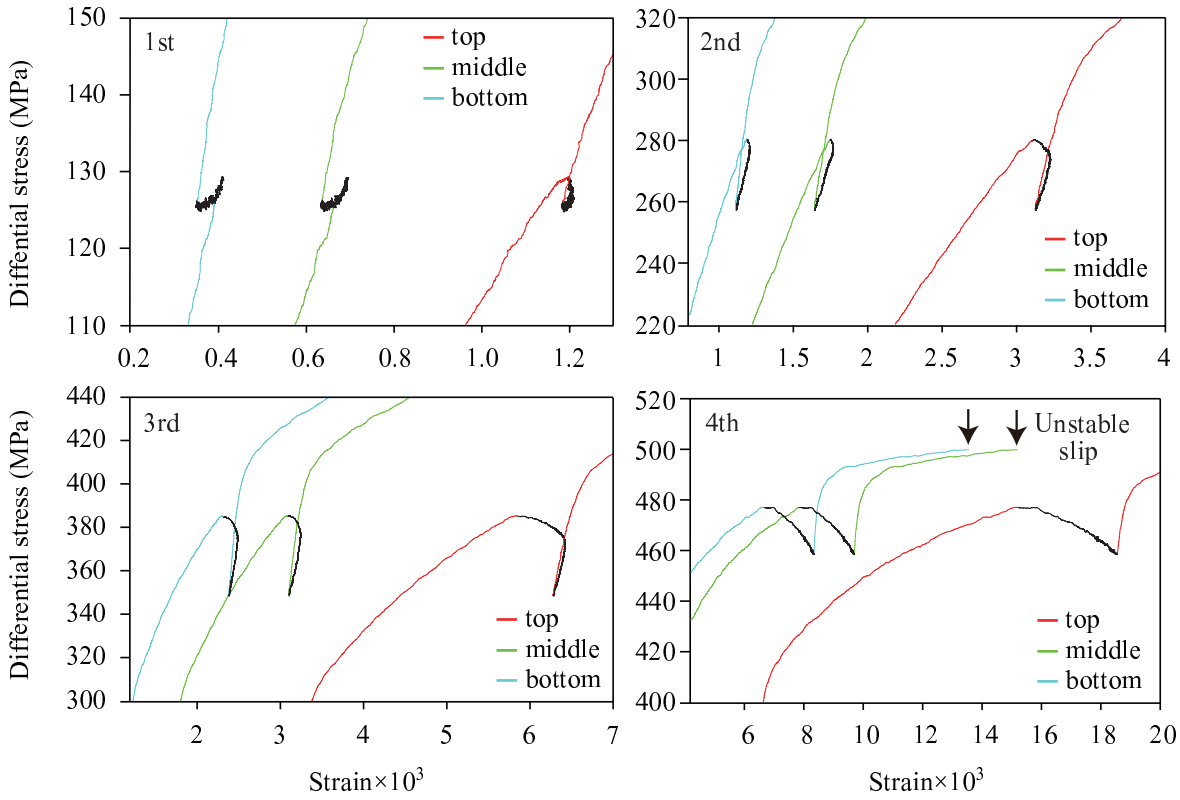

Figure 4. The enlarged diagram of Figure 3 at each holding period. Black lines mean the holding period.

the top right corner to the lower left until almost the 3rd holding stage. After that, Figure 6 shows the remarkable change in the energy ratio at the final loading stage.

Discussion

From our experiments, we consider that mechanical behaviors and the energy ratio of gouges are correlated with microstructural development. First, we discuss about the relationship between mechanical behaviors of gouges and microstructural development. After that, we mention the relationship of the energy ratio and microstructural development.

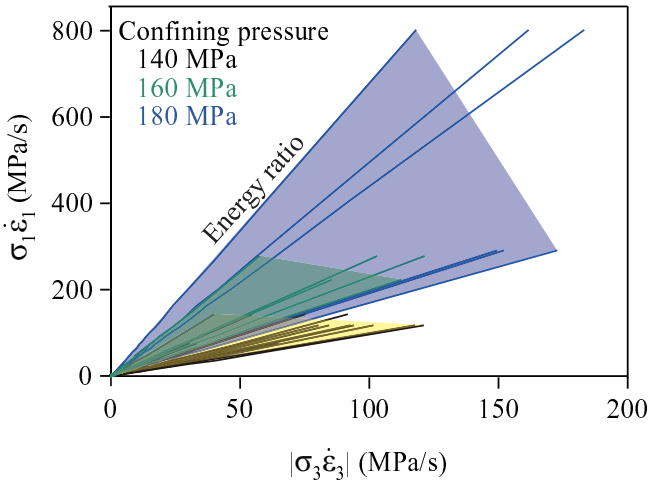

Figure 5. The ratio of the energy rate of the major principal compressive stresses to minor compressive stresses. Yellow, green and blue mean 140, 160 and 180 MPa of confining pressure, respectively. Single line was obtained by a signal of a strain gauge at each experiment.

Mechanical behaviors of gouges

Our experimental results showed three different behaviors of gouges depending on differential stresses. The contraction of gouges observed at low stress is elastic rebound. This behavior occurred without stress drop because the loading stress was still low. So, in all experiments, this behavior of gouges was commonly observed at lower stress (e.g., 1st holding in Figure 4). On the other hand, great extension at high stress means plastic deformation (4th in Figure 4). This plastic behavior implies formation of R1-shears, which appeared after peak stress (Logan et al., 1992; Marone, 1998). The difference in strain indicates microstructural heterogeneity of gouges. After this plastic behavior, the differential stress did not increase nevertheless continuous loading because plastic deformation or slip had already started. Marone et al. (1990) pointed out that compaction of gouges happens at early shear, and that unstable slip occurs after enough compaction. Thus, our results show the process until unstable slip occurs as follows; at first, gouges show elastic rebound depending on the progress of compaction. When compaction of gouges progresses fully leading to dense distribution, gouges show plastic deformation because of the formation of R1-shears. Finally, the growth from R1-shear to Y-shear results in unstable slip (e.g., Logan et al., 1992).

The energy ratio

From our experimental results, it is revealed that the energy ratio

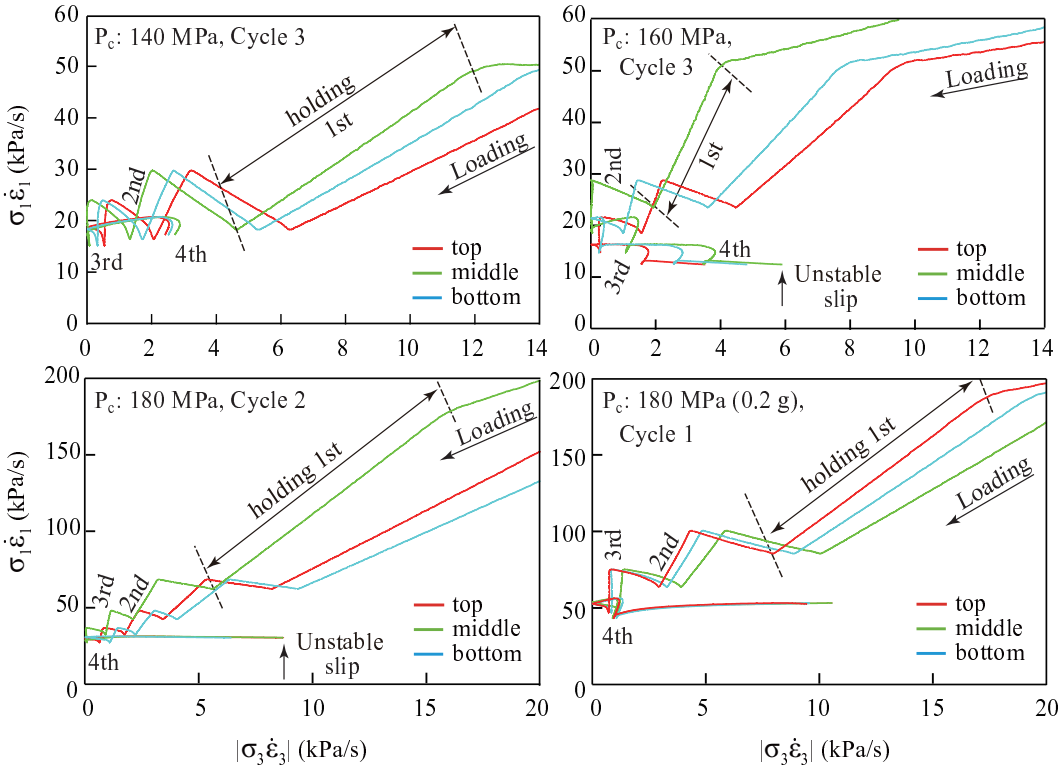

Figure 6. The enlarged diagram of Figure 5 at each experiment. The color means position of strain gauges. The remarkable change in energy ratio is shown at the final loading.

changed at each holding and loading stage, and it increased with confining pressure. Moreover, the change in the energy ratio at the final loading stage is remarkable.

The cause for the increases in the energy ratio with confining pressure is compaction. Under high confining pressure, the gouges can endure slip because they are highly dense under high confining pressure. Therefore, gouges show high strength, and the energy ratio becomes large. In the triaxial compression state, the Rowe's theory has been written as

$$\frac{\sigma_1}{\sigma_3} = \left(1 - \frac{\dot{\varepsilon}_v}{\dot{\varepsilon}_1}\right) \tan^2\left(\frac{\pi}{4} + \frac{\varphi}{2}\right), \tag{3}$$

where $\dot{\varepsilon}_v$ is the volumetric strain rate and φ is the internal friction angle (Niiseki, 2001). Eq. (3) indicates that the volumetric strain rate is related to the stress, and so it has been called the stress-dilatancy relation, which can be derived from the critical state (Schofield and Wroth, 1968) or the variational principle of granular mechanics (Niiseki, 2001). Based on the relation: $\dot{\varepsilon}_v = \dot{\varepsilon}_1 + \dot{\varepsilon}_2 + \dot{\varepsilon}_3 = \dot{\varepsilon}_1 + 2\dot{\varepsilon}_3$, the stress ratio is rewritten as.

$$\frac{\sigma_1}{\sigma_3} = -\frac{2\dot{\varepsilon}_3}{\dot{\varepsilon}_1} \tan^2\left(\frac{\pi}{4} + \frac{\varphi}{2}\right). \tag{4}$$

So, using Eq. (2) and Eq. (4), K is given by

$$K = -2\tan^2\left(\frac{\pi}{4} + \frac{\varphi}{2}\right). \tag{5}$$

Therefore, K is related to the internal friction angle φ of the fault gouges.

Riedel shear angles related to the internal friction angle decrease with shear strain in connection with microstructural development (Gu and Wong, 1994). From our experiments, it is clear that the energy ratio varied at higher stress at which gouges behaved plastically (Figures 3, 4 and 6). This remarkable change at higher stress implies frictional instability and reflection of arrangements or fabrics of gouge particles. According to Rowe's law, mechanical energy is dissipated through the process of rearranging and crushing of granular materials (Rowe, 1962). Consequently, we propose the new method to assess energetic behaviors such as frictional instability using the energy ratio.

Unconsolidated materials such as fault gouges and soft sediments exist in shallower parts of active faults and accretionary wedges in subduction zones. From our experimental results, the fault gouges are proved to obey Rowe's theory of the constant energy ratio until frictional instability occurs. Moreover, it has been known that this Rowe's theory can be applied not only to granular materials but also to blocky materials (Chappell, 1979). This indicates that the Rowe's theory can be applied to seismogenesis in active faults and subduction zone plate boundaries. Based the theory of passive or active earth pressure in the soil mechanics, the internal friction angles of geomaterials like soft sediments determine the longitudinal shape of a slip surface in landslides or spray faults in accretionary prisms (e.g., Terada and Miyabe, 1929). From our experimental results (Eq. 5), the internal friction angle of geomaterials is related to the energy ratio according to Rowe's law. So, using Rowe's law and the monitoring of energy ratio (i.e., stress ratio and volumetric strain) in situ (e.g., in the borehole), we will be able to predict the longitudinal shape of a slip surface in landslides or spray faults in accretionary

prisms. Therefore, various natural geohazards related to frictional or mechanical instability of granular and blocky geomaterials, such as earthquakes and landslides, can be evaluated with Rowe's theory of constant energy ratio.

Conclusion

We conducted 12 friction experiments using simulated fault gouges and concluded as follows. The Rowe's theory of the constant energy ratio is proved to hold for fault gouges, for instance quartz in our study. Thus, Rowe's theory can be applied to fault mechanics. The occurrence of natural disasters such as earthquakes and landslides can be assessed by Rowe's theory of constant energy ratio. These experimental observations provide us better understanding on the relationship among microstructural development, frictional instability and the energy ratio of geomaterials based on Rowe's law on seismogenic process or landslides.

Acknowledgements

We thank Professor Emeritus K. Otsuki for his assistance in experiments and many discussions. This study was funded by a Grant-in-Air for Scientific Research (24244077).

References

Byerlee, J., Mjachkin, V., Summers, R., and Voevoda, O., 1978, Structures developed in fault gouge during stable sliding and stick-slip, Tectonophysics, v. 44, pp. 161-171.

Chappell, B. A., 1979, Deformational response in discontinua, International Journal of Rock Mechanics and Mining Sciences & Geomechanics Abstracts, v. 16, pp. 377-390.

Gu, Y. and Wong, T.-f., 1994, Development of shear localization in simulated quartz gouge: Effect of cumulative slip and gouge particle size, Pure and Applied Geophysics, v. 143, pp. 387-423.

Ikari, M. J., Marone, C., and Saffer, D. M., 2011, On the relation between fault strength and frictional stability, Geology, v. 39, pp. 83-86.

Logan, J. M., Dengo, C. A., Higgs, N. G., and Wang, Z. Z., 1992, Chapter 2 Fabrics of experimental fault zones: Their development and relationship to mechanical behavior, In: Evans, B., and Wong, T.-f. (Eds), International Geophysics Series, Volume 51, Fault Mechanics and Transport Properties of Rocks. A Festschrift in Honor of W. F. Brace, Academic Press, New York, pp. 33-67.

Logan, J. M., Friedman, M., Higgs, N., Dengo, C., and Shimamoto, T., 1979, Experimental studies of simulated gouge and their application to studies of natural fault zones, Proceedings of Conference VIII, Analysis of Actual Fault Zones in Bedrock, U. S. Geol. Surv., Open File Rep., 79-1239, pp. 305-343.

Marone, C., 1998, Laboratory-derived friction laws and their application to seismic faulting, Annual Review of Earth and Planetary Sciences, v. 26, pp. 643-696.

Marone, C., and Kilgore, B., 1993, Scaling of the critical slip distance for seismic faulting with shear strain in fault zones, Nature, v. 362, pp. 618-621.

Marone, C., Raleigh, C. B., and Scholz, C. H., 1990, Frictional behavior and constitutive modeling of simulated fault gouge, Journal of Geophysical Research, v. 95, pp. 7007-7025.

Marone, C., and Scholz, C. H., 1988, The depth of seismic faulting and the upper transition from stable to unstable slip regimes, Geophysical Research Letters, v. 15, pp. 621-624.

Moroto, N., 1991, Rowe's stress dilatancy theory and variational principle, Proceedings of the 26th Annual Conference of the Japan Society of Soil Mechanics and Foundation Engineering, The Japan Society of Soil Mechanics and Foundation Engineering, Tokyo, pp. 549-550 (in Japanese).

Niiseki, S., 2001, Formulation of Rowe's stress-dilatancy equation based on plane of maximum mobilization: Powders and Grains 2001, Proceedings of the Fourth International Conference on Micromechanics of Granular Media, Sendai, Japan, 21-25 May, 2001, edited by Kishino, Y., A.A. Balkema Publishers, pp. 213-216.

Onuma, K., Muto, J., Nagahama, H., and Otsuki, K., 2011, Electric potential changes associated with nucleation of stick-slip of simulated gouges, Tectonophysics, v. 502, pp. 308-314.

Reynolds, O., 1885, On the dilatancy of media composed of rigid particles in contact, Philosophical Magazine Series 5, v. 20, pp. 469-481.

Rowe, P. W., 1962, The stress-dilatancy relation for static equilibrium of an assembly of particles in contact, Proceedings of the Royal Society London A, v. 269, pp. 500-527.

Schofield, A., and Wroth, P., 1968, Critical State Soil Mechanics, McGraw-Hill, London, 310 pp.

Scholz, C. H., Wyss, M., and Smith, S. W., 1969, Seismic and aseismic slip on the San Andreas fault, Journal of Geophysical Research, v. 74, pp. 2049-2069.

Terada, T., and Miyabe, N., 1929, Experimental investigations of the deformation of sand mass by lateral pressure, Bulletin of the Earthquake Research Institute, University of Tokyo, v. 6, pp. 109-126.

Wong, T.-f., Baud, P., and Klein, E., 2001, Localized failure modes in a compactant porous rock, Geophysical Research Letters, v. 28, pp. 2521-2524.

by Kazuhei Kikuchi[1], Kazutoshi Abiko[2], Hiroyuki Nagahama[1] and Jun Muto[1]*

Self-affinities analysis of fault-related folding

1 Department of Earth Science, Tohoku University, 6-3, Aramaki Aza Aoba, Aoba, Sendai, Miyagi 980-8578, Japan.
E-mail: kazuhei.kikuchi.s6@dc.tohoku.ac.jp
2 Industrial and Economic Department, Murayama Area General Branch Administration Office, Yamagata Prefectural Government, 19-68, 2 Chome, Teppomachi, Yamagata, Yamagata, Japan.

The Mid-Niigata Prefecture Earthquake did not rupture the earth's surface and occurred along a fault hidden well under folded terrain. In order to evaluate the seismic activity of such hidden earthquakes beneath fault-related folds, a new method to analyze self-affinities is introduced. Based on this analysis, the geometry of a fold is shown to be self-affine and can be variously scaled in different directions. The size and temporal properties, b-value in Gutenberg - Richter's law and p-value in the modified Omori's law, express aftershock activity. Then, from the analyzed data of the folds, we estimate the b-value and p-value of the hidden earthquake under the fault-related folds. These estimated b-values and p-values are concordant with seismologically obtained ones in the aftershock sequence of the Mid-Niigata Prefecture Earthquake.

Introduction

The Mid-Niigata Prefecture Earthquake occurred in Niigata Prefecture, Japan, 2004 (M_w 6.6). The main shock was followed by a large number of aftershocks with four being over M_w 6 (Konagai et al., 2012). The Mid-Niigata Prefecture Earthquake took place in a fold-and-thrust belt that has been growing since the late Pliocene in a Miocene rift basin along the eastern margin of the Japan Sea (Okamura et al., 2007). The epicenter region of the Mid-Niigata Prefecture Earthquake is located near the Niigata-Kobe Tectonic Zone, recognized as a region of large strain rate along the Japan Sea coast and in the northern Chubu and Kinki districts of Japan (Sagiya et al., 2000). The focal mechanisms of these strong shocks, estimated by Hi-net and F-net (Honda et al., 2005) were reverse fault types oriented northwest that is concordant with the trend of pre-existing fold axes (Konagai et al., 2012). The epicenters of the aftershocks were distributed along the NNE and SSW direction within a length of about 30 km (Honda et al., 2005).

Okamura et al. (2007) earlier pointed out that the Mid-Niigata Prefecture Earthquake was associated with fault-related folding. Such earthquakes taken place in "blind" folded terrains are named "hidden earthquakes" (Stein and Yeats, 1989). The location and amount of slip for the hidden earthquakes cannot in fact be observed directly. The Northern Apennine Mountains in Italy have been built by earthquakes along faults hidden well under the surface. Such earthquakes unlike their more familiar counterparts do not rupture the earth's surface (Stein and Yeats, 1989).

The Mid-Niigata Prefecture Earthquake killed about 40 people and injured about 3000, largely as a result of building collapse. More than 100,000 residents were forced to evacuate their homes (Sidle et al., 2005). Moreover, despite the moderate size of the earthquake, thousands of landslides caused damages to roads, farmland, or residential areas. The economic loss due to these landslides was initially estimated at 8 billion US dollars, making this one of the costliest landslide events in history (Kieffer et al., 2006). An effective and quick stabilization of slopes in the Mid-Niigata mountainous terrain is thus considered to be a pressing need (Konagai et al., 2012).

In general, many folds are apparently curved or jagged on a wide range of scales, so that their geometries appear to be similar when viewed at different magnifications. Using the method of Matsushita and Ouchi (1989a, 1989b), we analyzed the self-affinities of folds in the North Honshu Arc, Japan (Kikuchi et al., 2013). Nagumo (1969a, b) pointed out that the *b*-value of Gutenberg–Richter's law is related to the sharpness of plastic bending deformation of a medium. Under this Nagumo's assumption, Kikuchi et al. (2013) proposed a new relation between the *b*-value of Gutenberg–Richter's law and the self-affinities of folds related to earthquakes. Moreover, Nanjo et al. (1998) derived a relation between the *p*-value of modified Omori's law and *b*-values. In this paper, we analyze the self-affinity for the folds existed near the epicenter of the Mid-Niigata Prefecture Earthquake. Then we estimate the *b*-value and *p*-value of the hidden earthquake under the fault-related folds.

Data of the transect profiles of folds

For folds in the inner belt of the Northeast Honshu Arc, Kikuchi et al. (2013) applied a method to examine the aftershock sequence along the transect profiles of folds shown by the lines 1 to 9 in Figure 2. In this study, we analyzed folds 8 and 9 included in the zone of the Niigata-Kobe Tectonic line.

Kikuchi et al. (2013) used the following method; first define the smallest fixed length scale as a unit length scale α, and measure the curve length $N\alpha$ by this scale between arbitrary points *A* and *B* on the curve. Then, calculate the *x*- and *y*-variances, X^2 and Y^2 of all measured points between the two points *A* and *B*:

$$X^2 = \frac{1}{N}\sum_{i=1}^{N}(x_i - x_c)^2 \text{ and } Y^2 = \frac{1}{N}\sum_{i=1}^{N}(y_i - y_c)^2, \quad (1a)$$

with

$$x_c = \frac{1}{N}\sum_{i=1}^{N} x_i \text{ and } y_c = \frac{1}{N}\sum_{i=1}^{N} y_i, \quad (1b)$$

where (x_i, y_i) is the coordinate of the i th measured point P_i on the

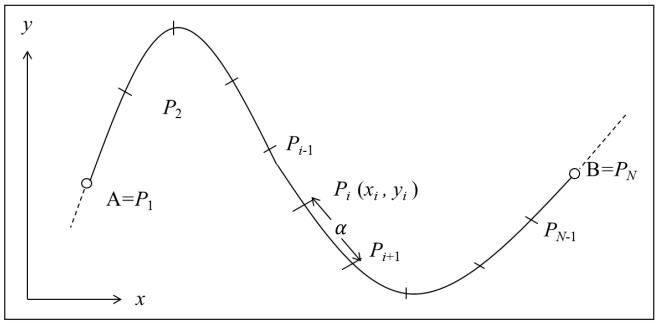

Figure 1. Measurement of a curve length N between a pair of points A and B on a given curve. x and y are coordinates, (x_i, y_i) is the coordinate of the i-th measured point, P_i (x_i, y_i) on the curve.

curve. The standard deviations of *X* and *Y* indicate the approximate widths of that part of the curve. Let us then repeat this measurement procedure for many pairs of points on the curve and determine the distribution using Log-Log plots of *X* and *Y* vs. *N* whether they scale as

$$X \propto N^{v_x} \ , \ Y \propto N^{v_y} \ , \qquad (2)$$

where v_x and v_y are different in general.

The profiles near the epicentral region of the Mid Niigata Prefecture Earthquake (folds of the transect lines 8 and 9) are shown in Fig. 3a and Fig. 4a. From these profiles, Log *X*-Log *N* and Log *Y*-Log *N* can be approximated by straight lines (dotted lines) with different slopes ($v_x \neq v_y$). This means that these profiles are differently scaled in a different direction indicating self-affine. The self-affine properties can be characterized by a Hurst exponent ($H = v_y/v_x$) (Feder, 1988; Peitgen and Saupe, 1988). From Fig. 3b, H = 0.84 and H = 0.88 from Fig. 4b. For a crossover from mid-Niigata area to Northeast Honshu Arc area, Log *Y*-Log *N* is approximated by two straight lines crossing at a point.

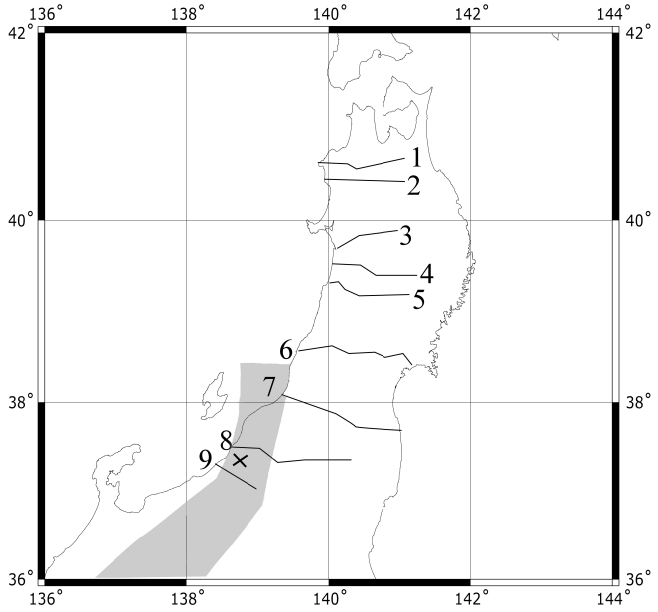

Figure 2. Map of the Northeast Honshu Arc. Numbered measurement lines are used for the analyses of self-affinity after Kitamura (1986). × represents epicenter of the Mid Niigata Prefecture Earthquake in 2004 (M_w 6.6, 37.3°N, 138.8°E). The Niigata-Kobe Tectonic Zone is denoted by a gray shaded area. Niigata-Kobe Tectonic Zone is recognized as a region of large strain rate along the Japan Sea coast and in the northern Chubu and Kinki districts, Japan (Sagiya et al., 2000).

Discussion

Generally, the Fourier spectral density $\tilde{S}(k)$ of a scale-invariant curve is related to wave number k by a power law equation. In this case the spectral exponent β and the Hurst exponent H are related as follows (Feder, 1988; Peitgen and Saupe, 1988) :

$$\beta = 2H + 1. \qquad (3)$$

The *b*-value in the Gutenberg-Richter's law is widely used as a measure of seismicity. Nagumo (1969a, b) proposed a relationship between the spectral exponent β and the *b*-value of Gutenberg–

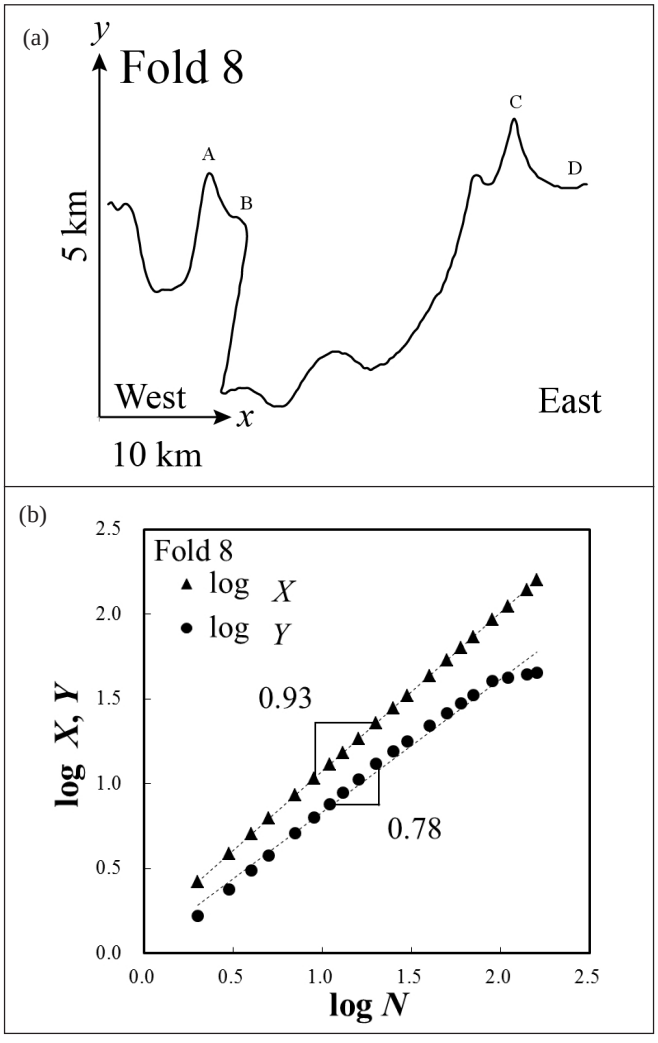

Figure 3. Analysis of the self-affinity of Fold 8. (a) Transect profile of Fold 8. Oginojo anticline (A), Yakushitoge pass (B), Higasiyama anticline (C) and the vicinity of Muikamachi fault (D). Muikamachi fault is the source fault of the Mid Niigata Prefecture Earthquake. (b) Log-Log plot of horizontal and vertical standard deviations (X and Y) and curve length N. Pairs (Log X, Log N) and (Log Y, Log N) are lineally approximated by the method of least square fitting. The slopes represent $v_x \approx 0.93$, $v_y \approx 0.78$ and $H = 0.84$.

Richter's law (Gutenberg and Richter, 1944; see Appendix I) given by

$$\beta = 6 - 4b, \tag{4}$$

under the following assumptions (see Appendix II).

Nagumo (1969a, b) pointed out that the *b*-value of Gutenberg–Richter's law is related to the sharpness of the plastic bending deformation of the medium. It was equated bending of the strata with fold. Under Nagumo's assumptions and Eqs. (3) and (4), Kikuchi et al. (2013) can derived a relation between the *b*-value of Gutenberg–Richter's law and the Hurst exponent *H* for the crustal deformation as

$$2H = 5 - 4b. \tag{5}$$

Based on Eq. (5) and the Hurst exponent *H* of the fault-related folds, we can estimate *b*-values for the epicenter region of the Mid Niigata Prefecture Earthquake hidden below the fault-related fold. From the analyzed data of $H = 0.84$ for Fold 8 and $H = 0.88$ for Fold 9, *b*-value can be estimated to be 0.83 and 0.81, respectively. These estimated *b*-values are concordant with seismologically obtained *b*-values of 0.80-0.87 in the aftershock sequence of the Mid Niigata Prefecture Earthquake (Enescu et al., 2007).

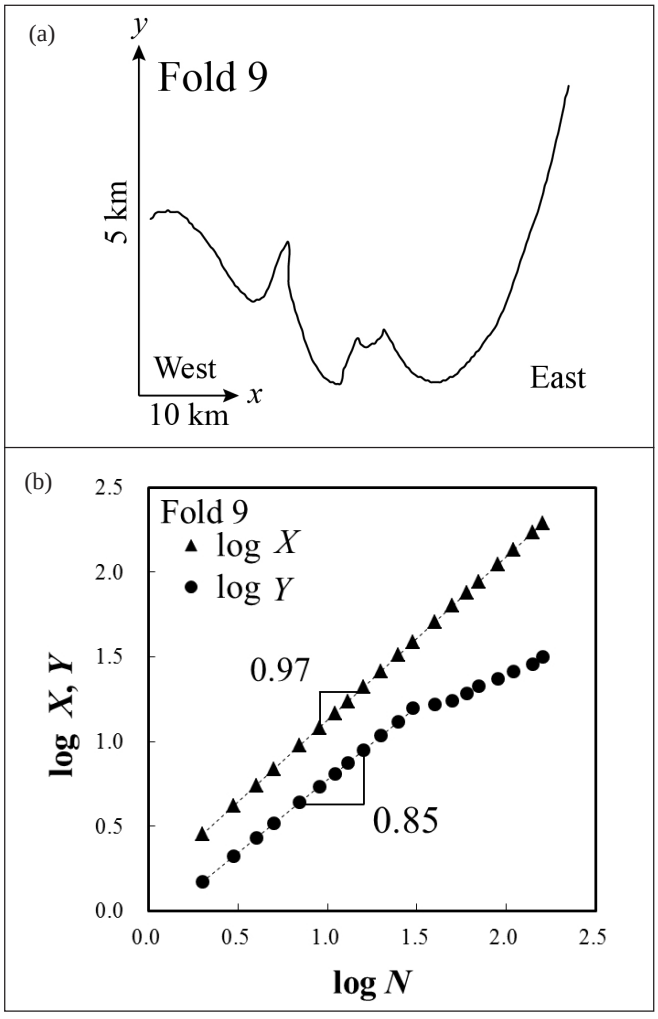

Figure 4. Analysis of the self-affinity of Fold 9. (a) Transect profile of Fold 9. (b) Log-Log plot of horizontal and vertical standard deviations (X and Y) and curve length N. Pairs (Log X, Log N) and (Log Y, Log N) are lineally approximated by the method of least square fitting. The slopes represent $v_x \approx 0.97$, $v_y \approx 0.85$ and $H = 0.88$.

Nanjo et al. (1998) derived a relation between the *p*-value of the modified Omori's law (see Appendix III) and *b*-value by,

$$b = (-2.10 \pm 0.35)p + (2.00 \pm 0.38) + \Delta, \tag{6}$$

where Δ is a constant around 1.0 ~ 1.5. In this paper, we use $\Delta = 1.15$. The *p*-value in the modified Omori's law is widely used as a measure of seismicity. Based on Eq. (6) and the *b*-value of the fault-related folds, we can estimate *p*-values for the epicenter region of the Mid Niigata Prefecture Earthquake hidden below the fault-related fold. From the analyzed data of $b = 0.83$ for Fold 8 and $b = 0.81$ for Fold 9, *p*-value can be estimated to be 1.10 and 1.11, respectively. These estimated *p*-values are concordant with seismologically obtained *p*-values of 1.10-1.13 in the aftershock sequence of the Mid Niigata Prefecture Earthquake (Enescu et al., 2007).

The size distribution of earthquakes expressed by the Gutenberg and Richter's law is equivalent to the fractal distribution of fault break areas by the relationship between the magnitude of the earthquake and its fault break area. The Hurst exponent for the crustal deformation can be related to the fractal dimension or the uniformity of the crustal fragmentation from mid-Niigata area to Northeast Honshu Arc area. Also, theoretical study suggested that *p*-value, which was a rate constant of aftershock decay, was related to the fractal dimension of a pre-existing fault system (Nanjo et al., 1998). Thus, we reinterpret the relationship between self-affinities of fold deformation and fault-related folding. Hence, for the mitigation of natural disasters, we can evaluate statistical properties of seismicity (*b*-value and *p*-value) of the hidden earthquakes by self-affinities of fault-related folds.

Conclusion

In order to evaluate the seismic activity of hidden earthquakes below the fault-related folds, a new method to analyze self-affinities is introduced. We applied it to large scale fold geometries of the Neogene and Paleogene around the epicenter region of the Mid Niigata Prefecture Earthquake. Based on this analysis, the geometry of the fold is shown to be self-affine and can be differently scaled in different directions. Based on the self-affinity of active folds, we can pre-estimate the *b*-values of the Gutenberg-Richter's law and *p*-value of the modified Omori's law for hidden earthquakes under the fault-related folds. Therefore, this analysis method is useful to evaluate the risk of hidden earthquakes associated with fault-related folding as was discussed by Stein and Yeats (1989) in the Northern Apennine Mountains, Italy. We need to evaluate the future risk of hidden earthquakes which cause geohazards as landslides. In this paper, we have shown the importance of the geometrical structures (self-affinities) of active folding is a crucial one. In order to predict activities or aftershocks (i.e. to pre-estimate the *b*-values of the Gutenberg-Richter's law and *p*-values of the modified Omori's law) for hidden earthquakes occurred along a fault hidden well under folded terrain, an examination of the relation of the geometrical structures of pre-existing active fold systems will be an open challenge in the Earth Sciences.

Acknowledgements

The authors would like to thank Masataka Ando, Chien-Hsin Chang, Sumito Morita, Yasutaka Omori, Yasuji Sawada and an

anonymous reviewer for valuable comments. K.K wishes to acknowledge Bhathiya Athurupana and Babu Ram Gyawali for help with the manuscript preparation. K.K. was supported by Tohoku University Institute for International Advanced Research and Education.

References

Enescu, B., J. Mori, and M. Miyazawa, 2007, Quantifying early aftershock activity of the 2004 mid-Niigata Prefecture earthquake (M_w6.6): Journal of Geophysical Research, v. 112, B04310, DOI: 10.1029/2006JB004629.

Feder, J., 1988, Fractals: Plenum Press, New York.

Gutenberg, B., and C.F. Richter, 1944, Frequency of earthquakes in California: Bulletin of the Seismological Society of America, v. 34, pp. 185-188.

Honda, R., S. Aoi, N. Morikawa, H. Sekiguchi, T. Kunugi, and H. Fujiwara, 2005, Ground motion and rupture process of the 2004 Mid Niigata Prefecture earthquake obtained from strong motion data of K-NET and KiK-net: Earth, Planets and Space, v. 57, pp. 527–532.

Kieffer, S. D., R. Jibson, E. M. Rathje, and K. Kelson, 2006, Landslides triggered by the 2004 Niigata Ken Chuetsu, Japan, Earthquake: Earthquake Spectra, v. 22, pp. 47-73, DOI: 10.1193/1.2173021.

Kikuchi, K., K. Abiko, H. Nagahama, H. Kitazato, and J. Muto, 2013, Self-affinities of landforms and folds in the Northeast Honshu Arc, Japan: Acta Geophysica, v. 61, pp. 1642-1658, DOI:10.2478/s11600-013-0151-z.

Kitamura, N. (ed.) 1986, Cenozoic Arc Terrane of Northeast Honshu, Japan: Hobundo, Sendai (in Japanese).

Konagai, K., Z. A. Kazmi, and Y. Zhao, 2012, Chapter 14 Extracting earthquake induced coherent soil mass movements: in S. D'Amico., ed, Earthquake Research and Analysis - New Frontiers in Seismology, In Tech, Shanghai, pp. 361-380, DOI: 10.5772/2458

Matsushita, M., and S. Ouchi, 1989a, On the self-affinity of various curves: Physica D, v. 38, pp. 246-251, DOI: 10.1016/0167-2789(89)90201-7.

Matsushita, M., and S. Ouchi, 1989b, On the self-affinity of various curves: Journal of the Physical Society of Japan, v. 58, pp. 1489-1492, DOI: 10.1143/JPSJ.58.1489.

Nagumo, S., 1969a, A derivation of Ishimoto-Iida's formula for the frequency distribution of earthquakes from a deformation~fracture relation: Zisin (Seismological Society of Japan), v. 22, pp. 136-143 (in Japanese with English abstract).

Nagumo, S., 1969b, Deformation~fracture relation in earthquake genesis and derivation of frequency distribution of earthquakes: Bulletin of the Earthquake Research Institute, The University of Tokyo, v.47, pp. 1015-1027.

Nanjo, K., H. Nagahama, and M. Satomura, 1998, Rates of aftershock decay and the fractal structure of active fault systems: Tectonophysics, v. 287, pp. 173-186.

Okamura, Y., T. Ishiyama, and Y. Yanagisawa, 2007, Fault-related folds above the source fault of the 2004 mid-Niigata Prefecture earthquake, in a fold-and-thrust belt caused by basin inversion along the eastern margin of the Japan Sea: Journal of Geophysical Research, v. 112, B03S08, DOI: 10.1029/2006JB004320.

Omori, F. 1895, On the After-shocks of earthquakes: The Journal of the College of Science, Imperial University, Japan, v. 7, pp. 111-200.

Peitgen, H. O., and D. Saupe (eds.) 1988, The Science of Fractal Images, Springer, Berlin.

Sagiya, T., S. Miyazaki, and T. Tada, 2000, Continuous GPS array and present-day crustal deformation of Japan: Pure and Applied Geophysics, v. 157, pp. 2303–2322. DOI: 10.1007/PL00022507.

Sidle, C. R., T. Kamai, and A. C. Trandafir, 2005, Evaluating landslide damage during the 2004 Chuetsu Earthquake, Niigata Japan: EOS, v. 86, pp. 133-136.

Stein, R. and R. S. Yeats, 1989, Hidden earthquakes: Scientific American, v. 260, pp. 48-57.

Utsu, T. 1961, A statistical study on the occurrence of aftershocks: Geophysical Magazine, v. 30, pp.521-605.

Appendix I: Gutenberg-Richter's low

Gutenberg-Richter's law (Gutenberg and Richter, 1944) is expressed by

$$\log N(M) = -bM - \phi, \tag{I-1}$$

where $N(M)$ is the number of earthquakes with a magnitude greater than M, and ϕ and b are constants.

Appendix II: Nagumo's assumptions

Nagumo's assumption 1.

The density of earthquake occurrence is assumed to be proportional to the curvature of the plastic bending deformation of the medium:

$$N(x) = \frac{c}{d} \cdot \left| \frac{d^2 w}{dx^2} \right|, \tag{II-1}$$

where $N(x)$ is number of earthquakes, c is a proportional constant, d is an unit of dislocation, and w is deflection.

Nagumo's assumption 2.

The frequency distribution of earthquakes with respect to their size is assumed to be proportional to the spectrum distribution of structural wave number of plastic deformation:

$$N(a)\, da = N(k)\, dk, \tag{II-2}$$

where a is an amplitude of seismic motion, and k is wave number.

Nagumo's assumption 3.

The frequency distribution of earthquakes in a certain area is assumed to be proportional to the area of focal region:

$$N(k) = S \cdot \int_{-\infty}^{\infty} N(x) e^{-ikx}\, dx, \tag{II-3}$$

where S is an area of earthquake focal region.

Appendix III: Modified Omori's law

The modified Omori's law (Utsu, 1961) is expressed by

$$n(t) = \frac{\tilde{k}}{(\tilde{c} + t)^p}, \tag{III-1}$$

where $n(t)$ is the frequency of aftershocks per unit time at time t after the main shock, and $\tilde{k}$, $\tilde{c}$, and p are constants.

In the case of $p = 1$, Equation (III-1) is given by

$$n(t) = \frac{\tilde{k}}{(\tilde{c} + t)}, \tag{III-2}$$

This relation is called Omori's law (1895).

by A.G. Rodnikov, N.A. Sergeyeva and L.P. Zabarinskaya

Crustal and mantle structure of the Sea of Okhotsk, Pacific Northwest: A review

Geophysical Center of the Russian Academy of Sciences, 119296 Moscow, Molodezhnaya, 3, Russia. *E-mail: rodnikov@wdcb.ru*

The deep structure of the Sea of Okhotsk under seismically dangerous regions is studied. The main feature of the deep structure in the region is the occurrence of an asthenospheric layer in the upper mantle. Asthenospheric diapirs can effectively rise through the crust, causing destruction of the lithosphere, formation of deep basins, faults and rifts accompanied by shallow-focus earthquakes, and eruptions of volcanoes. The vast majority of earthquakes are confined to the Kuril Island Arc, where the Pacific Plate is subducted under the continent. The seismicity in the region is a result of active tectonics in the subduction zone. This zone is traced to a depth of 700 km. In the west, the Okhotsk Sea Region is bounded by the deep faults extending along Sakhalin, where earthquakes are localized in the crust. The ancient subduction zone under Sakhalin is established. In the late Cretaceous to Paleogene the subduction of the Okhotsk Sea Plate under Sakhalin ceased. The reactivation of this ancient subduction zone may currently be in response to the strong earthquakes in Sakhalin.

Introduction

The main objective of the review is to give better insight into the role of the deep structure of the seismically dangerous regions relating to continental margins. In fact, approximately one-third of the human population lives within the continental margins, meaning they live in a risk zone. The Okhotsk Sea Region on continental margins is characterized with high seismicity, volcanic eruptions and other natural cataclysms. We constructed the geodynamic models for the Sea of Okhotsk to study a deep structure of the crust and upper mantle in such zones. The Okhotsk Sea Region is a large lithospheric plate of the transition zone from the Eurasian continent to the Pacific. The region is located in the contact zone of three lithospheric plates: Eurasian, North American and the Pacific (Fig.1).

Seismicity of the Okhotsk Sea Plate

The location of the Okhotsk Sea Plate in the contact zone of three lithospheric plates (Eurasian, North American and Pacific) is the cause of a high seismicity on its boundaries (Fig.2).

The highest seismic activity is observed along the Kuril Island Arc. Here the Pacific Plate is moving towards and being subducted under the continent, forming a seismic zone traced to a depth of 700 km. The seismicity is a result of the active subduction zone tectonics in the region. In the west, the Okhotsk Sea Plate is bounded by deep faults extending along Sakhalin. The deep faults correspond mostly to the system of right-lateral strike-slip faults and thrusts. There the earthquakes for the major part are localized in the crust (Zlobin, 2005). Shallow-focus earthquakes are connected with rift structures of a Kuril Basin and Tatar Strait Trough (Rodnikov et al., 2005).

Okhotsk Sea Geotraverse

The Okhotsk Sea Geotraverse crosses Sikhote Alin, Sakhalin, the Kuril Basin, Kuril Island Arc and Pacific (Fig. 3). The crust is constructed according to data from Galperin and Kosminskaya (1964), Zverev and Tulina (1971), Rodkin and Rodnikov (1996), and Piip and Rodnikov (2004), the upper mantle is constructed from Structure and Dynamics of the Lithosphere and Asthenosphere of the Okhotsk

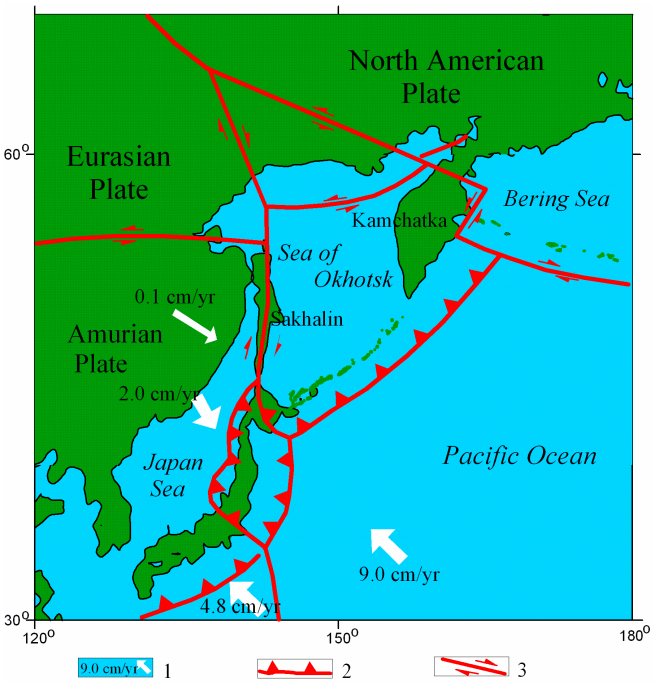

Figure 1. Tectonic map of the Okhotsk Sea Region.1—velocity of plate movement from GPS data; 2—subduction zones; 3—faults. Arrows show plate movement direction. Map is adopted from Kiratzi and Papazachos (1996), Maruyama et al. (1997), Cruise Reports (2000), and Rodnikov et al. (2001) .

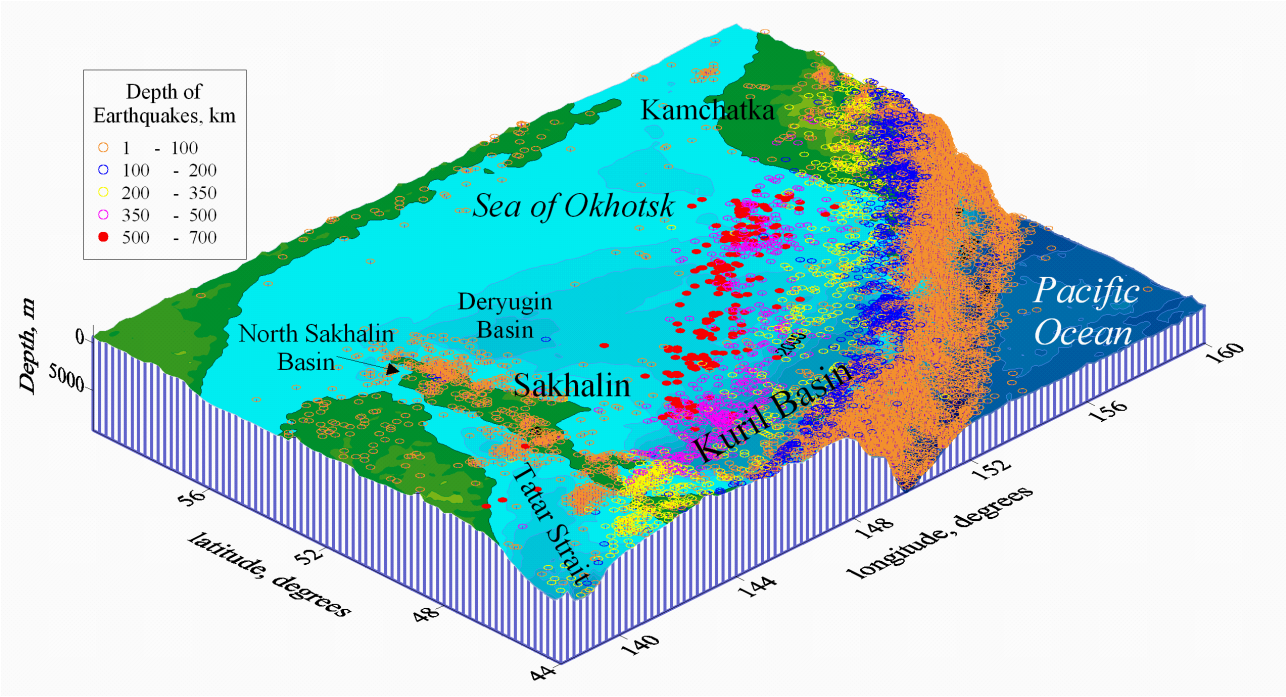

Figure 2. Spatial distribution of earthquakes in the Okhotsk Sea Region for1904-2012, according to Earthquake Catalogs at the USGS National Earthquake Information Center.

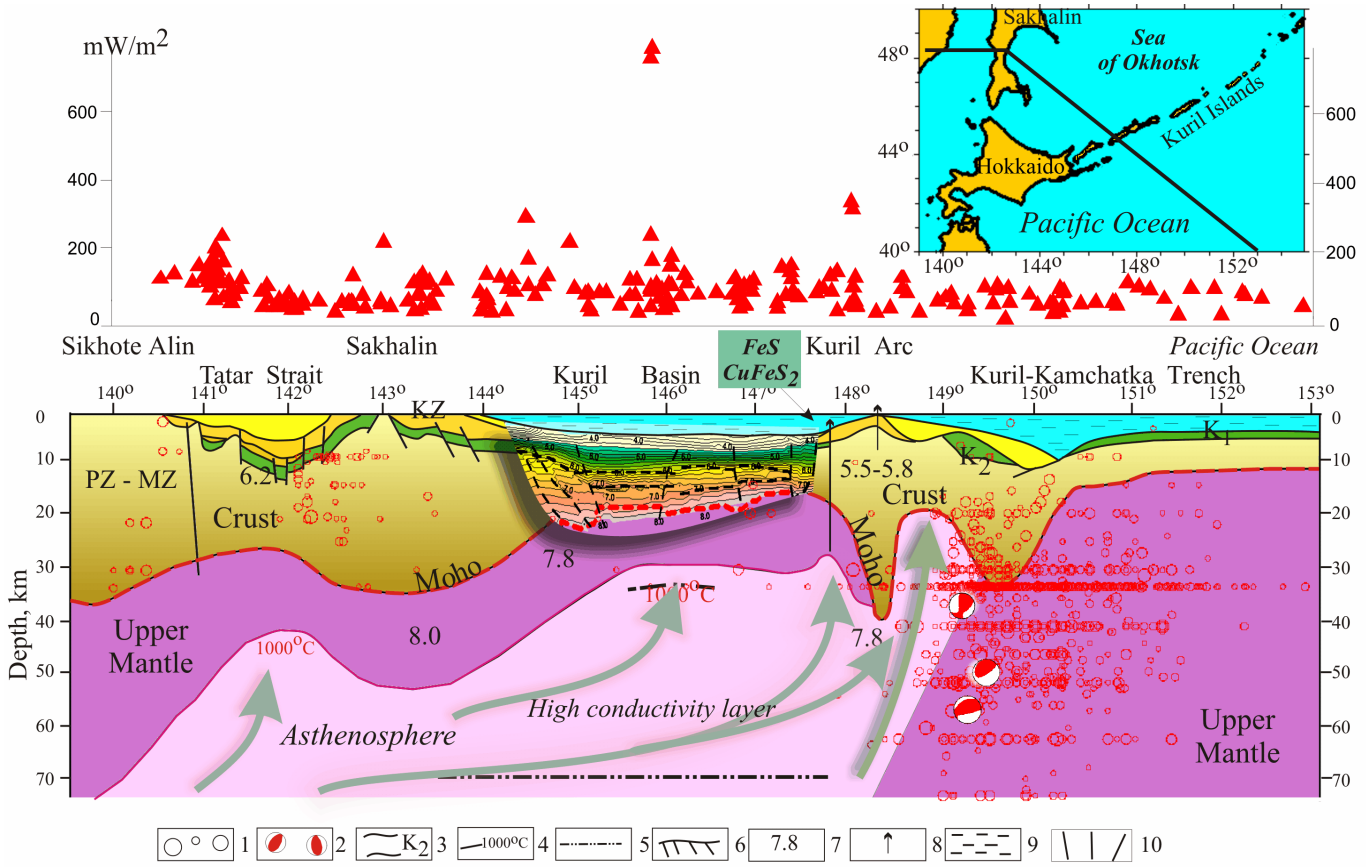

Figure 3. Geotraverse of the Okhotsk Sea Region. At the right top the geotraverse position is shown. Below the distribution of heat flow measurements is shown along the profile. 1 – location of earthquake hypocenters;2 - focal mechanism; 3 - geological layers; 4 – isotherm; 5 – boundaries of high conductivity layer; 6 – Moho discontinuity; 7 – seismic velocities, km/s; 8 – volcanoes; 9- water;10 – faults.

Sea Region (Structure, 1996), and Rodnikov et al. (2001), and a heat flow is constructed from Smirnov (1980), Pollack et al. (1991), and Structure (1996). The thickness of the crust along the geotraverse varies from 35-40 km under Sakhalin and the Kuril Islands to 8-10 km under the Kuril Basin (Structure, 1996; Rodnikov et al., 2005; Piip and Rodnikov, 2004). In the Cenozoic, the large part of the sedimentary basins was formed.

The asthenosphere in the upper mantle was essentially established according to the geothermal data (Smirnov, 1980; Smirnov and Sugrobov, 1980; Tuessov and Epanishnikov, 1996). The upper surface of the asthenosphere is on the 1000–1200 °C isotherms that indicate partial melting conditions (Smirnov and Sugrobov, 1980). The structure of the crust and upper mantle, coefficients of heat conductivity of rocks, and the analysis of thermal model of spreading were used to calculate the deep temperature values of heat flow. The depth, where there is a partial melting in the upper mantle, is taken as an asthenosphere surface. The asthenosphere surface in the Sea of Okhotsk is limited by the isotherm of 1000 to 1200°C (Rodnikov et al., 2008). Similar calculations of deep temperatures were carried out for other marginal seas of the western part of the Pacific Ocean (Smirnov et al., 1991). The asthenosphere in the Okhotsk Sea Region is confirmed by seismic, magnetotelluric and geological data. The asthenosphere is characterized by the lower values of seismic wave velocity (Galperin and Kosminskaya, 1964; Snegovskoi, 1974; Structure, 1996). Magnetotelluric sounding allocates conducting layers (Lyapishev et al. 1987), where partial melting takes place in the upper mantle. In an asthenosphere the magmatic centers are located. The crust over of the asthenospheric diapirs is usually thin, and rift structures are widespread. Magma eruptions, generally basalts (tholeiites), often occur along rifts (Filatova and Rodnikov, 2006).

The Sikhote Alin Region is the continental margin of the Asian continent. The results of magnetotelluric sounding in Sikhote Alin showed that the asthenosphere is located in the upper mantle at a depth of 120 km (Structure, 1996). Magmatic activity continued from the Cretaceous to the Early Quaternary. The Paleogene – Quaternary basalt eruptions consist of tholeiites, subalkaline basalts and olivine basalts. Tholeiites are close to basalts of MORB type and apparently related to magmatic sources in the asthenosphere (Structure, 1996).

The Tatar Strait is a large graben composed of a thick layer (up to 8 to10 km) of the Mesozoic to Cenozoic sedimentary formations. The basement of the strait is composed of the Triassic to Early Cretaceous terrigenous sandy-clayey and volcanogenic-siliceous sediments with P-wave seismic velocities up to 6.0 km/s. The Moho surface lies at a depth of about 25 to 30 km. Seismic velocities along the Moho are 7.7 to 7.8 km/s (Structure, 1996). Probably, the formation of the rift structure in the Tatar Strait is associated with the upwelling of the asthenosphere. There are three stages of magmatic activity in the Tatar Basin: The Eocene to Oligocene basalts, lower to middle Miocene tholeiites and middle Miocene to Pliocene basalts (Filatova and Rodnikov, 2006).

The Island of Sakhalin is separated from the Asian continent by the Cenozoic rift of Tatar Strait. This island is composed of Paleozoic, Mesozoic and Cenozoic rocks. The thickness of the crust provides about 30 to 35 km. Seismic wave velocities vary from 7.8 to 8.3 km/s in Moho (Structure, 1996). Major part of earthquakes is localized in the crust. In Eastern Sakhalin an ancient (Upper Cretaceous to Paleogene) subduction zone is distinguished (Grannik, 1999; Rodnikov et al., 2002; Rodnikov et al., 2013). On the surface it is manifested by an ophiolite complex, which separates the North Sakhalin Basin from Deryugin Basin of the Sea of Okhotsk. This complex is represented by harzburgite, dunite, wehrlite, rodingite, gabbro and amphibolite forming ophiolite suites (Rozhdestvenskiy, 1988). It is supposed that 100 million years ago, the oceanic lithosphere of the Sea of Okhotsk subducted under Sakhalin, the eastern part of which was an andesite island arc. In western Sakhalin, behind andesite island arc, there was a back-arc basin where sandy to clayey deposits accumulated in the Late Cretaceous to Paleogene, which subsequently formed the basement of the Cenozoic North Sakhalin oil and gas basin. Approximately 20 to 15 million years ago subduction of the lithosphere of the Sea of Okhotsk apparently ceased. It is established that the Deryugin Basin was formed at the place of an ancient deep trench, and the North Sakhalin Basin is located above the ancient (Late Cretaceous to Paleogene) subduction zone. The position of ancient subduction zone under Sakhalin is a cause of strong earthquakes here. Therefore, this region is one of the seismically active places in Russia (Rodnikov et al., 2013).

The Kuril Basin is a back-arc basin. The thickness of the sediments with the age from Oligocene to Pliocene-Quaternary is near 4000 m. The thickness of the crust attains 8 to10 km. The depth of Moho in Kuril Basin is at approximately 12 - 15 km. The seismic velocities on the Moho-boundary are 7.4 to 7.6 km/s (Piip and Rodnikov, 2004). In the central part of the Kuril Basin, a rift structure, probably of a spreading structure, is located. The basin is characterized by a high heat flow. The asthenosphere in the mantle appears beneath the Kuril Basin at a depth of 25 km (Structure, 1996). The electromagnetic research was conducted in the Kuril Basin, and in a depth of 30 km in the upper mantle a high conductivity layer was identified (Lyapishev et al., 1987). The nature of the layer is associated with partial melting. There are three stages of magmatic activity in the Kuril Basin; the early to middle Miocene, middle to late Miocene and Pliocene times (Filatova and Rodnikov, 2006).

Further, the geotraverse crosses the Kuril Island Arc consisting of two island arcs and a trough between them. The trough is 45 to 60 km wide and filled with Neogene and Quaternary tuffaceous and sedimentary deposits. The thickness of sediments in the axial zone reaches more than 3 km. The crustal thickness under the trough is as small as 20 km. The asthenosphere in the upper mantle is established at a depth of 20 km, causing the split of the lithosphere, rift structures formation, basalt magma eruptions, and hydrothermal activity (Structure, 1996).

Geodynamic model of the deep structure in the Okhotsk Sea region

The asthenosphere is located in the upper mantle of the Sea of Okhotsk at a depth of 50-70 km and beneath the Northwest Pacific Basin at a depth of approximately 100 km (Fig. 4). The formation of the asthenosphere within the Okhotsk Sea Plate is associated with a subduction zone over which it is located (Zhao et al., 2010). From the asthenosphere the diapirs go up to a depth of 25 to 30 km under the sedimentary trough of the Tatar Strait, Deryugin Basin and Kuril Basin, causing an active tectonics, which manifest themselves in volcanic, seismic and hydrothermal activities (Rodnikov et al., 2002). Beneath the North Sakhalin sedimentary basin, which contains almost all the Sakhalin oil and gas fields, the asthenosphere is located at a depth of approximately 70 km (Structure, 1996).

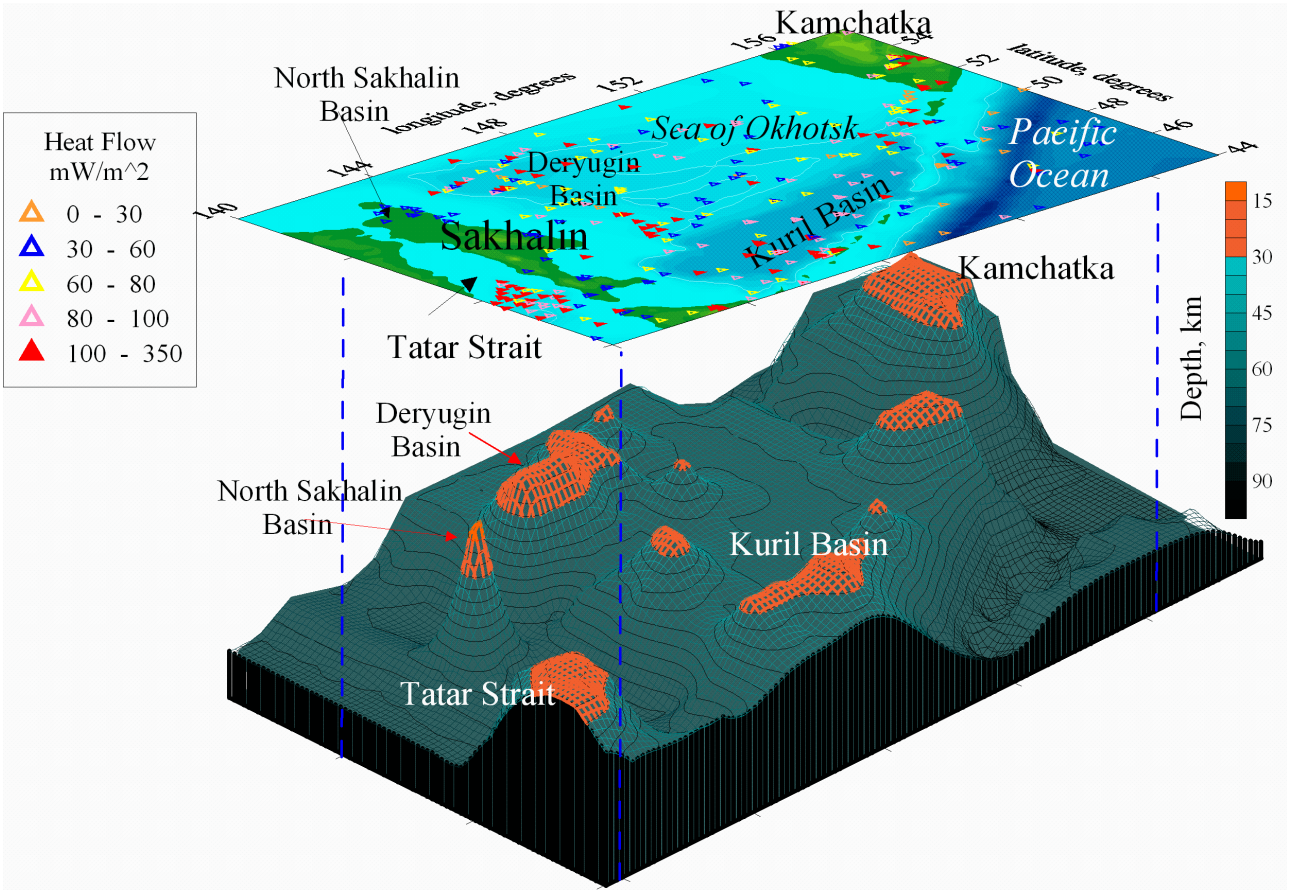

Figure 4. Geodynamic model of the deep structure of the Okhotsk Sea Region. Above - the heat flow measurements in mW/m^2 (Pollack et al., 1991) on the bathymetry chart. The asthenosphere at the upper mantle of the Sea of Okhotsk is located at a depth of 50 to70 km. The diapirs of partial melting go up to the asthenosphere, reaching a depth of 25 to30 km beneath the Tatar Strait Trough, Deryugin Basin and Kuril Basin and causing an active tectonic regime manifested in volcanic, seismic and hydrothermal activity. The area of the red color shows the magma formation.

Conclusions

A main feature of the deep structure of the Okhotsk Sea Region is related to the occurrence of asthenospheric layer in the upper mantle, processes in which define formation of structures of the crust. When the asthenosphere reaches the crust, fragmented lithosphere, formation of rift structures, eruption of basalts, accompanied by shallow-focus earthquakes, occur.

In the east of the Okhotsk Sea Region the seismicity is associated with the rapid subduction of the Pacific Plate beneath the Eurasian Plate along the offshore Kuril-Kamchatka Trench. In the west under Sakhalin the ancient subduction zone is established. It is probable that the Neftegorsk earthquake May 28, 1995 was a result of reactivation of this ancient subduction (Rodnikov et al., 2013).

The deep basins of the Sea of Okhotsk are located over the asthenospheric diapirs, containing hot mantle fluids. The asthenospheric layer under the Tatar Basin is at a depth of 50 km, under Kuril Basin is at 20 km. There are three stages of magmatic activity in Cenozoic, when basalt magmas erupted.

Acknowledgement

We would like to thank the Russian Foundation for Basic Research for financial support of our research work (RFBR Project No: 12-05-00029-a).

References

Cruise Reports: Komex V and VI. Kuril Okhotsk Sea Marine Experiment. 2000, Eds.: Biebow N., Ludmann T., Karp B., and Kulinich R, Kiel, pp. 295.

Filatova, N.I., and Rodnikov, A.G., 2006, The Sea of Okhotsk Geotraverse: Tectonomagmatic Evolutin of Cenozoic Extension Structure and Implication for Their Deep Structure: Doklady Earth Sciences, v. 9, pp. 1346-1350.

Galperin, E. I., and Kosminskaya, I. P. (Eds.), 1964, The Crustal Structure of the Transition Region between Asia and the Pacific Ocean, Nauka, Moscow, 308 p.

Grannik, V.M., 1999, Reconstruction of seismic focal zone of East Sakhalin volcanic paleoarc from rare-earth elements distribution: Dokl. Ros. Akad. Nauk, v. 1, pp. 79-83, (in Russian).

Kiratzi, A.A., and Papazachos C.B., 1996, Moment-tensor summation to derive the active crustal deformation in Japan: Bulletin of the Seismological Society of America, v. 86, no. 3, pp. 821-831.

Lyapishev, A. M., P. M. Sychev, and V. Yu. Semenov, 1987.The electric conductivity of the upper mantle in the Kuril Basin, Sea of Okhotsk, Pacific Geology, v. 4, pp. 45-55.

Maruyama S., Isozaki Y., Kimura, G., and Terabayashi M., 1997, Paleo-

geographic maps of the Japanese Islands: Plate Tectonic Synthesis from 750 Ma to the present: The Island Arc, v. 6, no. 1, pp. 91-120.

NEIC PDE catalog. National Earthquake Information Center, U.S. Geological Survey. http://earthquake.usgs.gov/regional/neic/index.php.

Piip V. B., and Rodnikov A.G., 2004. The Sea of Okhotsk crust from deep seismic sounding data. Russian Journal of Earth Sciences, v. 6, no. 1. pp. 1-14.

Pollack H.N., Hurter S.J., and Johnson J.R., 1991, The new global heat flow compilation: Department of Geological Sciences, University of Michigan, U.S.A.

Rodkin M.V., and Rodnikov A.G., 1996. Back-arc basin origin and structure. Physics of the Earth Planetary Interiors, v .15, no. 3/4, pp. 235-246.

Rodnikov A.G., Sergeyeva N. A., and Zabarinskaya L. P., 2001, Deep structure of the Eurasia-Pacific transition zone: Russian Journal of Earth Sciences, v. 3, no. 4, pp. 293-310.

Rodnikov A.G., Sergeyeva N.A., and Zabarinskaya L.P., 2013. Ancient subduction zone in the Sakhalin Island, Tectonophysics, v. 600, pp. 217-225.

Rodnikov A.G., Sergeyeva N.A., Zabarinskaya. L.P., Filatova N.I., Piip V.B., and Rashidov V.A., 2008, The deep structure of active continental margins of the Far East (Russia): Russian Journal of Earth Sciences, v. 10, no. 4, pp. 1-24.

Rodnikov, A.G., Sergeyeva, N.A., and Zabarinskaya, L. P., 2002, Deep structure of Deryugin basin (the Sea of Okhotsk): The Pacific Geology, v. 4, pp. 3-8.

Rodnikov, A.G., Zabarinskaya, L.P., Piip, V.B., Rashidov, V.A., Sergeyeva, N.A., and Filatova, N.I., 2005. The Okhotsk Sea Geotraverse: Bulletin of Kamchatka Regional Association "Educational-Scientific Center", Earth Sciences, v. 5, pp. 45-58, (in Russian).

Rozhdestvenskiy, V.S., 1988. The geological structure and tectonic development of Schmidt peninsula (Sakhalin Island). The Pacific Geology, v. 3, pp. 62-71 (in Russian).

Smirnov Ya.B., 1980, Termal field of the territory of the USSR. Geological Institute. Moscow, 150 p. (in Russian).

Smirnov, Ya.B., and Sugrobov, V.M., 1980, The Earth heat flow in Kuril – Kamchatka and Aleutian provinces: Volcanology and seismology, v. 2, pp. 3-17, (in Russian).

Smirnov Ya.B., Yamato M., Uyeda S., Galushkin Yu.I., Muraviev A.V., Sugrobov V.M., Zhang Ruhui, Wu Qianfan, Li Rucheng, and Zhang Wanxia, 1991, Heat Flow. In: The North China Plain – Philippine Sea – Mariana Trench Geotraverse (Eds.: A.G.Rodnikov, N.Isezaki, T.Shiki, S.Uyeda, Liu Guodong), Moscow, Nauka, pp. 97-119 (in Russian).

Snegovskoi, S. S., 1974. Seismic Reflection Survey and the Tectonics of the Southern Okhotsk Sea and the Pacific Margin, Nauka, Novosibirsk, 86 p.

Structure and Dynamics of the Lithosphere and Asthenosphere of the Okhotsk Sea Region, 1996. Rodnikov, A.G., Tuezov, I.K., Kharakhinov, V.V., (Eds.), National Geophysical Committee, Moscow, 337 p. (in Russian).

Tuessov I.K., and Epanishnikov V.D., 1996, Lithospheric and asthenospheric structure of the Sea of Okhotsk Region. In: Structure and dynamics of the Lithosphere and asthenosphere of the Okhotsk Sea Region (Eds.: A.G.Rodnikov, I.K.Tuessov, V.V. Charachinov). Moscow, National Geophysical Committee, pp. 112-202 (in Russian).

Zhao D., Pirajno F., and Liu L., 2010, Mantle structure and dynamics under East Russia and adjacent regions: Russian Geology and Geophysics, v. 51, no. 9, pp. 1188-1203.

Zlobin, T.K., 2005, Recurrence and regularities in the dynamics of strong earthquakes seismic processes in Sakhalin: Dokl. Ros. Akad. Nauk, v. 4, pp. 524-527, (in Russian).

Zverev, S. M., and Yu. V. Tulina (Eds.), 1971, The Deep Seismic Sounding of the Earth Crust in the Sakhalin-Hokkaido Sea Zone. Nauka, Moscow, 286 p.

by Jose Luis González[1], Jesús Martínez-Frías[2] and Niichi Nishiwaki[3]*

Geoethical elements in risk communication

1 National Security Department, Avda.Puerta de Hierro s/n, 28071, Madrid, Spain.*E-mail: jlgonzalez@dsn.presidencia.gob.es*
2 Instituto de Geociencias, IGEO (CSIC-UCM) and Associate Unit CSIC-UVA, Facultad de C.C. Geológicas, c/José Antonio Novais, 2, 28040, Madrid, Spain.*E-mail:j.m.frias@igeo.ucm-csic.es*
3 Professor Emeritus, Nara University, 1500 Misasagicho, Nara City 631-8502, Japan. **E-mail: niichi@osaka.zaq.jp*

Risk communication process contains not only scientific but also ethical elements, which have been discussed only in recent years. A systematic and detailed discussion about this subject is necessary to be generally accepted by human societies. Risk communication on natural hazards is a three-way process involving: 1) scientists, 2) scientists and public authorities, and 3) scientists and the public and the mass media. It is important to note that the perception of risk is not only a matter of scientific and technical evaluations but also feelings of fear and outrage (including emotional and cultural aspects). It is necessary to expand the range of assessment taking into account the High-impact Low-frequency events, as well as incorporating new ways of thinking as the black swan theory. Crisis analysis should include the study of unusual or unexpected events in order to improve risk communication planning, additionally considering geoethical elements.

Introduction

Geoethics was born at a junction of geology and ethics (Nemec, 1992), and has developed for last two decades by extending its application to many field of geosciences (s.l.) including planetary geology (Martínez-Frías et al. 2009; Martínez-Frías et al, 2011; González and Martínez-Frías, 2011). The AGID (Association of Geoscientists for International Development) Working Group for Geoethics issued the International Declaration on Geoethics (AGID WG for Geoethics, 2011), in which the following recommendations are included:

- To emphasize the significance of geoethics in the context of facing extraordinary natural hazards and disasters in the course of recent years.
- To incorporate a geoethical approach to needed new legal aspects (including insurance policy) and to an ethical way of thinking.
- To strengthen the links of geoethics with the new aspects of the geosciences education.
- To recommend the inclusion of geoethical subjects into deontological codes.
- To emphasize the liaison with the mining engineers activities.
- To remark a need of searching new priorities for 3rd Millennium fitting the Word Millennium Goals.
- To recommend links for incorporating geoethics into any activity related with the abiotic world.

This Declaration was recently updated (2013) and extended with a new one in the context of the AGID's International Conference of Geoethics. Geoethics is clearly defined as follows in the main website of the International Association of Geoethics (IAGETH) (http://icog.es.iageth).

> *"Geoethics is an interdisciplinary field between Geosciences and Ethics, dealing with the way of human thinking and acting in relation to the significance of the Earth as a system and as a model. It includes not only scientific but also educational, technological, methodological and social-cultural aspects, such as sustainability, development, geodiversity and geoheritage, prudent consumption of mineral resources, appropriate measures for predictability and mitigation of natural hazards, geosciences communication, museology, and others".*

The study of the geological record evidences that our planet has been constantly affected by extremely serious natural (terrestrial and cosmic) hazards. There is an increased interest about the causes and effects of these hazards to human societies. Crisis analysis should include the study of unusual or unexpected events in order to improve risk communication planning. Geoethical elements should be taken into the account in the framework of risk assessment and risk communication.

Geosciences information and duties relating natural hazards

A detailed search in the well-known Web of Science database crossing the terms: "geosciences", "information" and "risk" allows one to assess the "state of the art" about these issues. This search yields only 37 results in the Web research domains of "Science Technology" and "Social Sciences" confirming the need for incorporating social aspects in any geoscientific aspect of this issue. The research areas are: Geology, Engineering, Environmental Science, Ecology, Energy Fuels and Computer Sciences. The source journals are the following: Natural Hazards, Bulletin of Canadian Petroleum Geology, Comptes Rendus Geoscience, and Environmental Geology. The main Funding Agencies: the Australia Indonesia Facility for Disaster Reduction AIFDR, and Indonesian Agency for Disaster Management. All the documents appeared in the period 2000-2012. The results obtained are very similar if the term "risk" is substituted by "hazard" (32 results) although the source journals are different. In

this case they are: Episodes, Natural Hazards, Global and Planetary Change, and Journal of Geodynamics.

Geosciences information about matter related to natural hazards allows society to construct the safeguard system and to foresee and reduce the later damage. This information is also essential during the period in which a crisis is taking place. The crisis management of a natural hazard is an activity that is performed under time pressure, and requires decisions under uncertain conditions. In such a situation, any related geosciences information should be identified and used to develop options and the associated risks. These should be presented to politicians and other decision-makers. After a disaster has taken place, the missions are to rescue the people, and to recover and restore the damaged area. Crisis can arise from many natural hazards and can be sudden or slow in onset (Fig. 1). Effective communication on the risks associated with natural hazards during a crisis development is an essential and integral component of the crisis management process.

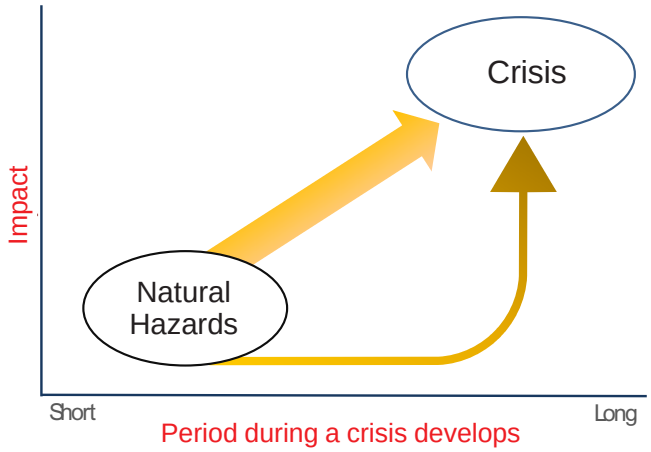

Figure 1. Crisis development from natural hazards.

The primary responsibility of geoscientists is to obtain detailed and advanced information through continuous scientific research on natural hazards. Geoscientists should act in an open way clearly transmitting the obtained information for the use by the society. Given that such information is very important and sensitive, its accuracy, reliability, speed, simplicity, acceptance and related characteristics should be examined in advance. Likewise, it is also necessary to prepare the guidelines on the dispatching the information at the site of the natural hazard, considering the content, level, method, timing and related issues (Nishiwaki, 2011). Geoscientists have not only scientific but also legal, social and ethical responsibility for their activities. Specifically in relation with natural hazards, the duties can be summarized as follow:

- To provide their knowledge and skills in risk mitigation to the society based on the current or previously published research.
- To cooperate with public authorities in crisis and disaster, by giving advice from scientific viewpoints.
- To assist in the transmission of information to society, by synthesizing and explaining the original information.

General principle of ethical element in risk communication

Geoscientists have both the rights and duties to keep independence and impartiality in risk communication. They should deal with interferences from outside in serious and humble manner, distinguish clearly own and outside interests, and reject improper pressures and demand if necessary. It is their social responsibility to make professional decisions in accordance with public interests on safety, health and environment of citizens and area in the crisis. Cooperation with others (scientists, governments, citizens, etc) is a principal factor in the framework of risk communication, and ethical dimension and legal obligation should be kept in the process. Other ethical principle in risk communication is the principle of beneficence that consists of two obligations: (1) the duty to help others further their legitimate interests, and (2) the commitment to help weigh and balance possible goods against possible harms. All ethical elements can inspire a *deontological code* (Martínez-Frías et al. 2011, González and Martínez-Frías, 2011; Nikitina, 2012; Vasconcelos, 2014) or good practices protocol applicable to Geosciences communicators working during natural hazards. The main function of the code is to regulate an ethical behavior in a communication process during a natural hazard event. It also should serve to inspire, give courage and support to ethical geoscientists, but should also provide a basis for action against untrustworthy people. In contrast to the legal codes, *ethical codes* should not only prohibit conducts, but should have a positive emphasis and focus on desirable models of professional behavior.

Relations among scientists, authorities, mass media and the general public

As previously defined, risk communication on natural hazards is a three-way process, which takes place among scientists, between scientists and public authorities, and between scientists and the public and the mass media. The communicators on natural hazards, whenever possible, seek feedback from the recipients to assess whether and how messages are understood and accepted. It is also essential to obtain the scientific consensus in public communication, by learning to work with other professionals. The mutual agreement should be made in advance for the cooperation to put into practice scientific procedures in crisis. Open and tolerant attitude to external scientific vision is helpful for the constructive cooperation with other professionals. Effective dialogue (even from a geoeducational perspective) should be realized with public authorities. Team work is required for the communication. It is also important to transfer the concept of probability to public authorities, which is involved in the risk assessment of natural hazard, being aware of the differences of standpoints.

Geoscientists are requested to make scientific decisions in a limited time in crisis of natural hazard. Thus, they should learn and be trained to work under time pressure (although geoscientists are scientists, not the crisis managers). Regarding the contacts of geoscientists with the media on the natural hazards and its risk assessment, especially in the crisis, it is essential to use accurate language in the explanation, avoid distorted facts and facts out of the context, and prevent contradictory statements with other professionals. Appropriate geosciences information is vital for the accurate understanding of natural hazards. Publication of opinions based on geosciences information will enable people to form an informed opinion. It is also necessary to have a certain empathy with the local culture; this will facilitate the acceptance of the opinion/proposals from the outsiders.

Risk perception

Risk communication became more prominent in the late seventies. It resulted from industry effort to counter public concern about the use of technologies involving a perception of high risk, such as nuclear power and chemical pollution, for example. It was thought that clear and understandable information was enough for society to understand that the risks were less than what people feared. Nowadays, many experts believe that this approach is failing and is inadequate. The perception of risk is not only a matter of technical evaluation but feelings of fear and outrage (Sandman, 1993). The spectrum of risk perception can also be attributed to people's differing attitude and beliefs as well as wider social or cultural values, and the disposition that people adopt towards natural hazards (Haynes et al., 2008). Therefore, a risk communication that ignores the emotional and cultural aspects may be incomplete. Based on these criteria, we can distinguish four types of risk communication scenarios or crisis communication:

- *Scenario 1*. It coincides with a high risk situation and low hazard perception, to which citizens are apathetic. Communication should focus on promoting the reaction so that danger be well understood and the recommended actions can be carried out. In this situation one can find a government that wants to evacuate the population before an imminent natural hazard that is not socially perceived.
- *Scenario 2*. It occurs in a low risk situation and high hazard perception. The public is more concerned and angry than the danger required. In these cases, the messages should focus on reducing the alarm and explain the problem in a realistic way.
- *Scenario 3*. It matches a dangerous situation and balanced hazard perception, where the audience is not too apathetic or excessively active. The communication is based on interpersonal dialogue, supplemented by the transmission of messages through specialized media.
- *Scenario 4*. It occurs in crisis situations, when the audience is concerned about a natural disaster that is about to happen or has already happened. In this case, the communicators must articulate a message that explains exactly what is happening and how to act.

New threats and challenges in risk communication

In the information age, people can easily access massive and diverse information(although the users themselves need to evaluate/verify such information). It is important to stress that in this scenario there are new types of threats. Increasing of information manipulation is a serious problem, as it can lead citizens to confusion or indecisiveness during a crisis. In a hyper connected world, the digital wildfire (or flaming) is easily invoked, regardless whether intentionally or accidently. Such fire is extremely dangerous from a social perspective as can lead to a panic and riot. For instance, in 1938, thousands of Americans mistook the radio broadcast of the adaptation of the novel by H.G. Wells "The War of the Worlds" with a real event and everyone panicked believing that the world had been invaded by Martians. In 2012, an anonymous twitter user spread the false rumor that the New York Stock Exchange trading floor was flooded with water during Hurricane Sandy. This significantly increased the perception of risk in the population. Today, the rules of digital content are still being produced. Collaborative efforts among geoscientists are required in the social media to avoid dangerous consequences. Internet remains an uncharted domain in geoethical action. Controlling the spread of false information online on natural hazards and rapidly

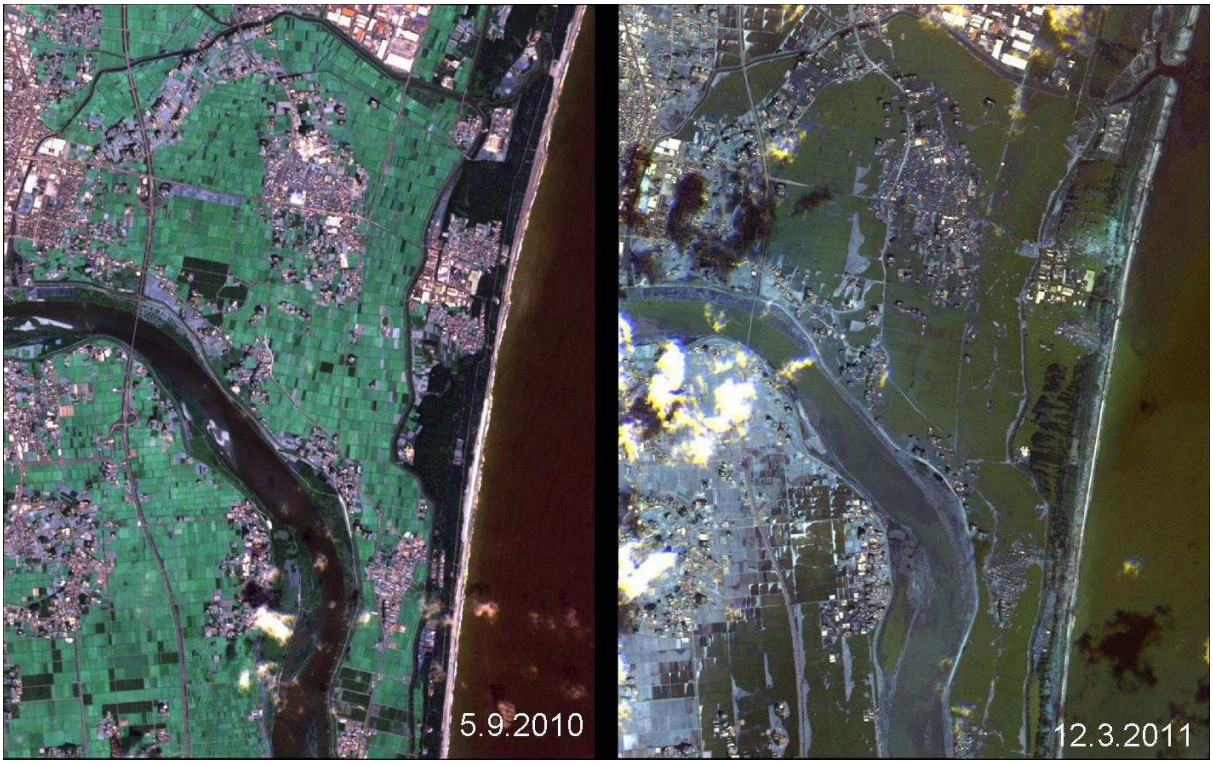

Figure 2. Japan's coastline before and after the Tsunami. Courtesy: NASA

publishing accurate information should be a goal of Geoethics.

In the recent years the theory and techniques of risk assessment have been developed, and it becomes possible to assess more types and range of natural hazards. It is, however, necessary to introduce new perspectives. It is indispensable to enlarge the range of assessment, and include the High-impact Low-frequency (HILF) events (High-Impact Low-Frequency Event Steering Committee, 2010). Though the HILF are complex and uncertain, they should be studied and assessed because of their potential for tremendous damage. However, uncertainty is one of the main obstacles in risk communication. To make effective decisions a risk assessment is required, but often there are large gaps in our knowledge. Until the complete evaluation is available, it is necessary to learn to say "*we don't know*".

Recognizing the uncertainty of the HILF events, risk communication should contain messages that include statements such as "*our understanding of these risks is always improving*", or "*we do not yet have all the facts*". Honesty is a fundamental value in risk communication. Under uncertainty, communicators should never say "*don't worry, there is no risk*", or "*any concern is irrational*". It is necessary to talk to people about possible unexpected crisis as a consequence of a natural hazard. Paradoxically, talking freely about worst case scenarios from crisis is likelier to calm people than to frighten them (Sandman, 2004).

It is necessary to supplement our common sense with new ways of thinking, such as the black swan theory (Taleb, 2007). An event with catastrophic effects (Fig. 2), which had been believed a rare and unforeseen event, may be identified as a common event when new evidence has been found and a new model developed outside of current theories. Many security challenges associated with rapid changes occur in a society which is increasingly interconnected. These changes and resulting crisis can be unpredictable. However, risks are expected to be connected with the fragility of the economic system and, consequently, monitoring threats is not enough. We should strengthen the analysis of the vulnerabilities and inter-dependencies among the different kinds of risks, as well as identify the crisis scenarios (González, 2013). Crisis analysis should include the study of unusual or surprising events in order to improve risk communication planning. These scenarios are plausible futures that violate one of the assumptions that underlie a crisis response plan. The specific purpose is to help planners develop signposts for keeping a flexible preparedness framework (Deward, 2002).

Final consideration

It is a fundamental role in geosciences to try to clarify and predict natural hazards. Risk assessment should be discussed from scientific and technological view point on information processing, hazard modeling and forecasting, disaster alarming and mitigation, and related issues. The resulting information should be published and communicated in a timely manner so that it can be utilized for disaster mitigation. The communication should contain not only scientific but also ethical elements. The latter elements have been addressed only in recent years, and a more systematic and detailed analysis is crucial for their general acceptance by human societies.

Acknowledgements

We want to thank Prof. Yildirim Dilek, Miami University (USA), for his excellent review and extremely useful remarks, which have greatly improved the quality of our original manuscript. Thanks also to Dr. Yujiro Ogawa for his editorial work and our special thanks to Dr. Anthony Reedman (AGID) and Prof. Vera Kolb of University of Wisconsin-Parkside for their useful remarks and detailed revision of the English version.

References

AGID WG for Geoethics, 2011, International Declaration on Geoethics. (Pribram, Czech Republic, October 2011) :http://tierra.rediris.es/Geoethics_Planetary_Protection/AGID_Geoethics_International_Declaration.htm

Deward, J.A., 2002, Assumption-based planning: A tool for reducing avoidable surprises: Cambridge University Press, 268 p.

González, J. L., and Martínez-Frías, J., 2011,Geoética: un reto para la deontología profesional: Tierra y Tecnología, no. 40, pp. 10-14.

González, J.L., 2013, Aspectos civiles de la gestión de crisis. En "Situación de crisis en la UE, conducción de crisis y reforma del sector de la seguridad": Documento de Seguridad y Defensa, no. 57, CESEDEN, abril 2013, pp. 47-73.

Haynes, K., Barclay, J., and Pidgeon, N., 2008, The issue of trust and its influence on risk communication during a volcano crisis. Bulletin of Volcanology, v. 70, no. 5, pp. 605-621.

High-Impact Low-Frequency Event Steering Committee, 2010, High-Impact, Low-Frequency Event Risk to the North American Bulk Power System: A Jointly-Commissioned Summary Report of the North American Electric Reliability Corporation and the U.S. Department of Energy's November 2009 Workshop. NERC, 118 p.

Martinez-Frias, J., Nemec, V., Nemcova, L., De la Torre, R., and Horneck, G., 2009,Geoethics and Geodiversity in Space Exploration: Implications in Planetary Geology and Astrobiology: 9th European Workshop on Astrobiology, EANA 09, 12-14 October 2009, Brussels, Belgium.

Martínez-Frías, J., González, J. L., and Pérez, F. R., 2011, Geoethics and Deontology: From fundamentals to applications in Planetary Protection: Episodes, v. 34, no. 4, pp. 257-262.

Nemec, V., 1992, Ethical Geology in the Education Process: 29th International Geological Congress, Kyoto, Japan, 24 August-3 September 1992.Section II-24-1 «New ideas and techniques in geological education», v. 3, no. 3, Abstract/Paper 06.

Nikitina, N., 2012, Geoethics: theory, principles, problems. Monograph. M: LLC Geoinformmark, 2012. ISBN 978-5-98877-049-7, 155 p.

Nishiwaki, N., 2011, Geoethical importance of information management before/after natural hazards: Abst. Mining Pribram Symp., pp. G5.1-4.

Sandman, Peter M., 1993, Responding to community outrage: strategies for effective risk communication: Falls Church, American Industrial Hygiene Association, 141 p., http://www.petersandman.com/media/RespondingtoCommunityOutrage.pdf.

Sandman, Peter M., 2004, Worst Case Scenarios. The Peter Sandman Risk Communication Website, http://www.psandman.com/col/birdflu.htm

Taleb, N. N., 2007, The Black Swan: The Impact of the Highly Improbable: London, Penguin Books, 366 p.

Vasconcelos, L. (2014) The deontological and ethical code of Mozambique. AGMM, http://www.icog.es/iageth/wp-content/uploads/2014/06/Dentological-EthicalCode_Mozambique2.pdf

*by Shinji Takarada, Joel C. Bandibas, Yuzo Ishikawa and *G-EVER Promotion Team*

Global earthquake and volcanic eruption risk management activities, volcanic hazard assessment support system and Asia-Pacific region hazard mapping project in G-EVER

Geological Survey of Japan, AIST, Site7, 1-1-1, Higashi, Tsukuba 305-8567, Japan. *E-mail: s-takarada@aist.go.jp*

The Asia-Pacific Region Global Earthquake and Volcanic Eruption Risk Management (G-EVER) Consortium among the Asia-Pacific geohazard research institutes was established in 2012 with the main objective of reducing the risk caused by earthquakes, tsunamis and volcanic eruptions worldwide. The first G-EVER workshop was held in Tsukuba, Japan in February 2012. The G-EVER1 accord was approved by the workshop participants which made 10 recommendations that focused on the enhancement of collaboration, sharing of resources and making information about the risks of earthquakes and volcanic eruptions freely available and understandable. The G-EVER Promotion Team in Geological Survey of Japan was organized in Nov. 2012 to coordinate the G-EVER related activities. The G-EVER Hub website was setup to promote the exchange of information and knowledge about volcanic and seismic hazards among the Asia-Pacific countries. Establishing or endorsing data interchange and analytical methods standards for geohazard institutes of the world are important to promote data sharing and comparative analyses. Several G-EVER Working Groups and projects were proposed such as the Next-generation volcanic hazard assessment WG and the Asia-Pacific region earthquake and volcanic hazard mapping project. The volcanic assessment support system is developed based on eruption history, volcanic eruption database and numerical simulations. The G-EVER hazard assessment support system is implemented with user-friendly interface, making the risk assessment system easy to use and accessible online. The Asia-Pacific region earthquake and volcanic hazard mapping project aims to make a sophisticated online hazard information system that provides past and recent earthquake and volcanic hazards information, risk assessment tools for earthquake and volcanic eruption hazards and links to global earthquake and volcanic eruption databases. The hazard mapping project plans to create the system with the cooperation of Asia-Pacific countries.

Figure 1. The first workshop of Asia-Pacific Region Global Earthquake and Volcanic Eruption Risk Management (G-EVER1) at AIST, Tsukuba, Japan, February 22-24, 2012.

Introduction

The Asia-Pacific Region Global Earthquake and Volcanic Eruption Risk Management (G-EVER) Consortium among the geohazard research institutes in the Asia-Pacific region was established in 2012. G-EVER aims to formulate strategies to reduce the risks caused by earthquakes, tsunamis and volcanic eruptions worldwide (Takarada, 2013a).

G-EVER activities

The First Workshop on Asia-Pacific Region Global Earthquake and Volcanic Eruption Risk Management (G-EVER1) was held in Tsukuba, Japan from February 22 to 24, 2012 to discuss measures in order to reduce the risks of disasters caused by natural geohazard events like earthquakes, tsunamis, and volcanoes worldwide (Fig. 1). There were 152 participants from 12 nations and regions and, 56 from national and international institutes. Participants were deeply saddened by recent disasters that occurred in Sumatra, Christchurch and Tohoku, but were also encouraged by successful cases of mitigation and progress on a various of local and global risk reduction efforts. We believe that increased international collaboration between geohazard institutes and organizations in the Asia-Pacific can advance the science of natural hazards thereby, contributing to the reduction of disaster risks from earthquakes, tsunamis, and volcanic eruptions. The participants approved the G-EVER1 accord during the workshop and the following recommendations were made:

1. Establish a consortium of Asia-Pacific geohazard research institutes, with the goal of enhancing collaboration, sharing resources, and making information about risk from earthquakes

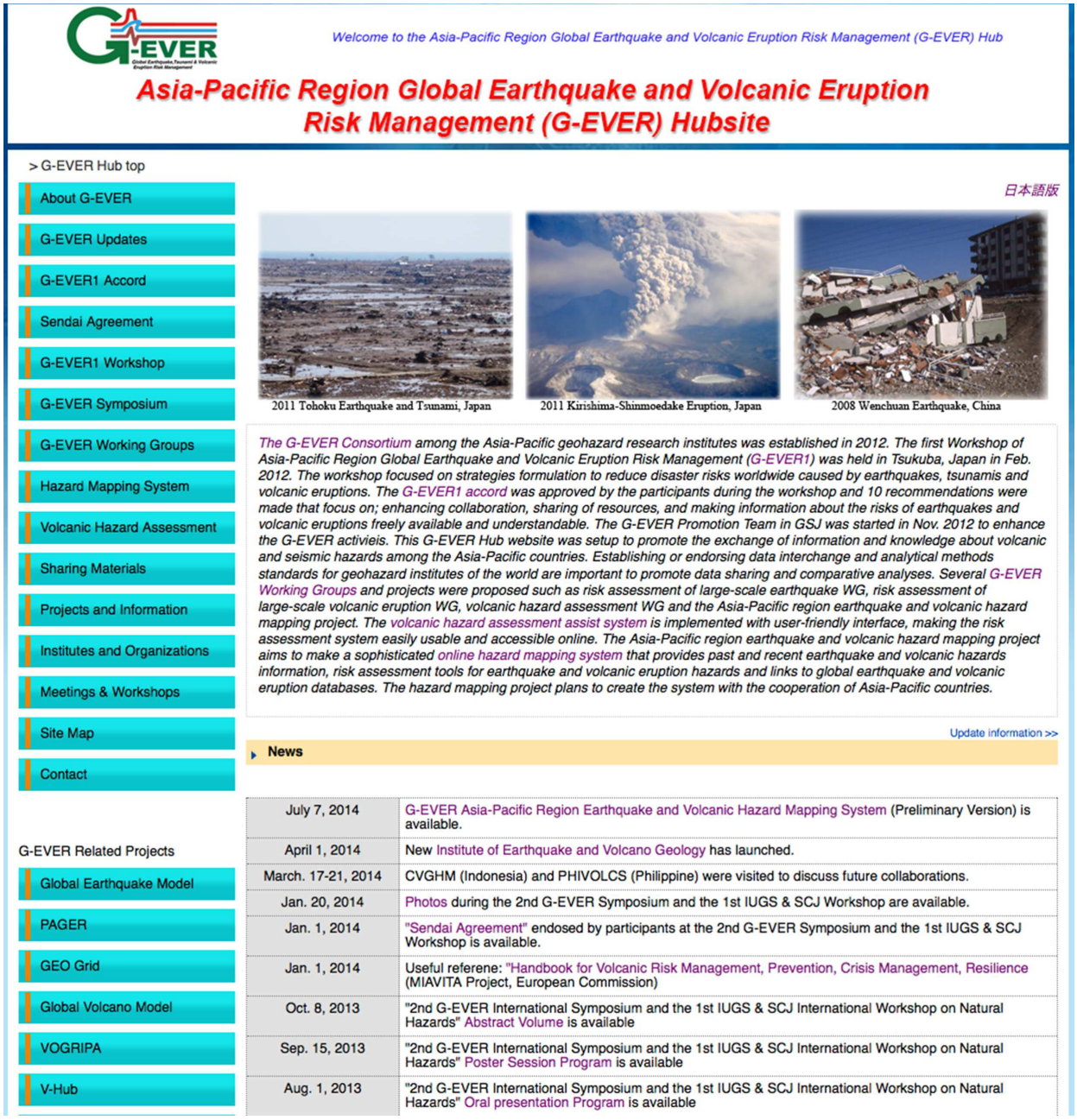

Figure 2. G-EVER Hub site (http://g-ever.org). All G-EVER related information is available on this website.

and volcanic eruptions freely available and understandable.

2. Promote the use of hazard information in decision-making by citizens, governments, and businesses, so our science supports mitigation actions.
3. Develop a website hub for the consortium in English and major Asian languages, which would link to websites of allied global efforts, such as VHub, GEM Nexus, and the International Seismological Centre (ISC).
4. Establish or endorse data interchange standards and standardized analytical methods for geohazard institutes of the world to promote data sharing and comparative analyses.
5. Actively participate in related global risk reduction efforts, such as the Integrated Research on Disaster Risk (IRDR) Program, Global Earthquake Model (GEM), Global Volcanic Model (GVM) and their component databases like World Organization of Volcano Observatories Database (WOVOdat) and GEM Faulted Earth.
6. Promote "the borderless world of science" with trans-border hazard maps built using common data sets, more uniform and advanced methods and software than has been possible in the past.
7. Promote exchange visits among researchers of the consortium, and encourage opportunities for graduate study in geohazards.
8. Encourage the formation of working groups for broad, multi-disciplinary, and unifying themes.
9. Promote best practice training on interaction with the media, outreach to citizens and school children on hazard preparedness, and interaction between volcanologists and Volcanic Ash Advisory Centres in the region.
10. Convene a G-EVER workshop every 2 years in Asia-Pacific countries in conjunction with major regional events (such as AOGS, WPGM and AGU meetings).

The G-EVER Promotion Team of Geological Survey of Japan was formed in November 2012. The G-EVER Hub website (Fig. 2; http://g-ever.org) was setup to promote the exchange of information and knowledge about volcanic and seismic hazards among the Asia-Pacific countries. Establishing or endorsing standards on data sharing and analytical methods is important to promote the sharing of data and analyses results. The major activities of G-EVER include participation in global risk reduction efforts such as the Integrated Research on Disaster Risk (IRDR) Program, Global Earthquake Model (GEM) and Global Volcanic Model (GVM).

The 1st G-EVER International Symposium was held in Tsukuba, Japan on March 11, 2013 which coincided with the second anniversary of Tohoku Earthquake (Takarada, 2013b). The 2nd G-EVER Symposium and IUGS&SCJ International Workshop was held in Sendai, Tohoku Japan on October 19-20, 2013. The workshop was attended by 94 individuals from 12 nations and regions and 30 national and international institutes. The participants crafted the Sendai Agreement and unanimously endorsed it (See Tsukuda and G-EVER Promotion team (2014), this volume).

Several G-EVER Working Groups and projects were proposed such as: (1) Risk mitigation of large-scale earthquakes WG, (2) Risk mitigation of large-scale volcanic eruptions WG, (3) Next-generation volcanic hazard assessment WG, and (4) Asia-Pacific region earthquake and volcanic hazard mapping project.

G-EVER volcanic hazard assessment support system

The next-generation volcano hazard assessment WG is developing a useful system for volcanic eruption prediction, risk assessment, and evacuation strategy at various eruption stages. The G-EVER Volcanic Hazard Assessment Support System is based on volcanic eruption history datasets, volcanic eruption database and numerical simulations (Fig. 3, Takarada, 2013c). Volcanic eruption histories including precursor phenomena leading to major eruptions are important to predict future volcanic eruptions. Likewise, a high quality volcanic

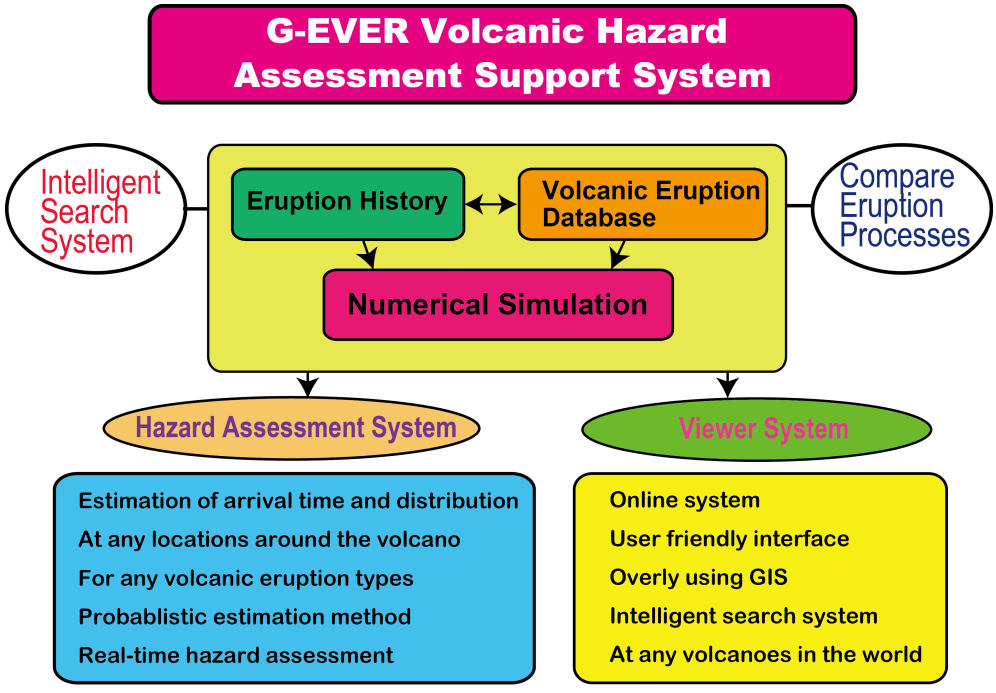

Figure 3. Concept diagram of the G-EVER volcanic hazard assessment support system. The system is based on eruption history, volcanic eruption database and numerical simulation.

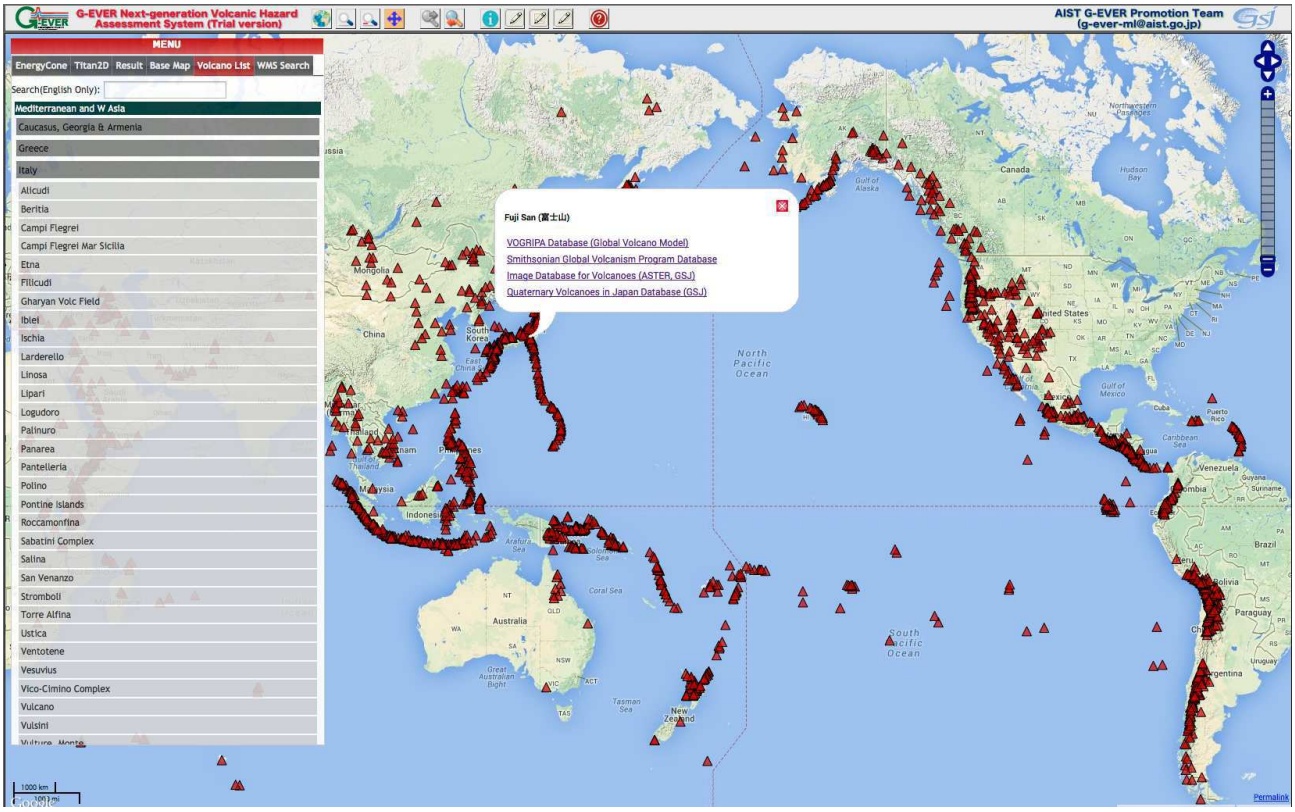

Figure 4. G-EVER volcanic hazard assessment support system (Trial version). Any volcano can be searched from the Quaternary volcano list in the world. Links to major volcano databases such as Smithsonian Global Volcanism Database, VOGRIPA Database (Global Volcano Model), ASTER satellite image database (GSJ) and Quaternary Volcanoes in Japan (GSJ).
http://volcano.g-ever1.org/vhazard/HazardAssessment/

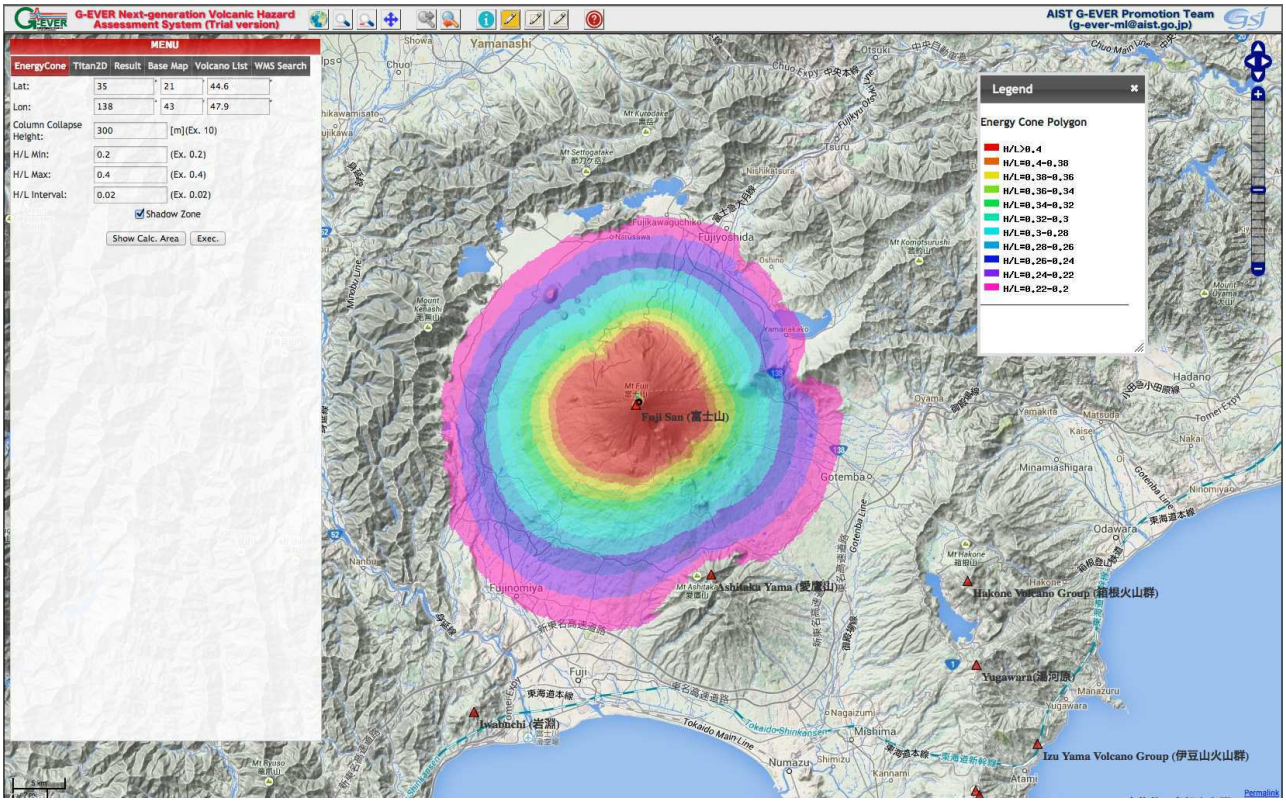

Figure 5. An energy-cone simulation result at Fuji Volcano, Japan, using G-EVER volcanic hazard assessment support system. Almost all volcanoes in the world can be evaluated with this system because of the wide coverage of ASTER Global DEM.

eruption database, which contains compilations of eruption dates, volumes, and styles, is important for the volcano hazard assessment system. Formulating international standards on how to estimate the volume of volcanic materials is necessary to make a high quality volcanic eruption database. GIS based spatial distribution database of volcanic materials (e.g. Tephra and pyroclastic flow distributions) is required for accurate area and volume estimation and risk assessments.

The volcanic eruption database is developed based on past eruption results, which only represent a subset of possible future scenarios. Therefore, numerical simulations with controlled parameters are needed for more precise volcanic eruption predictions. The "best-fit" parameters of the past worldwide major eruptions have to be estimated and the simulation results database should be made.

The use of the system should enable the visualization of past volcanic eruptions datasets such as distributions, eruption volumes and eruption rates, on maps and diagrams using timeline and GIS software. Similar volcanic eruption types should be easily searchable

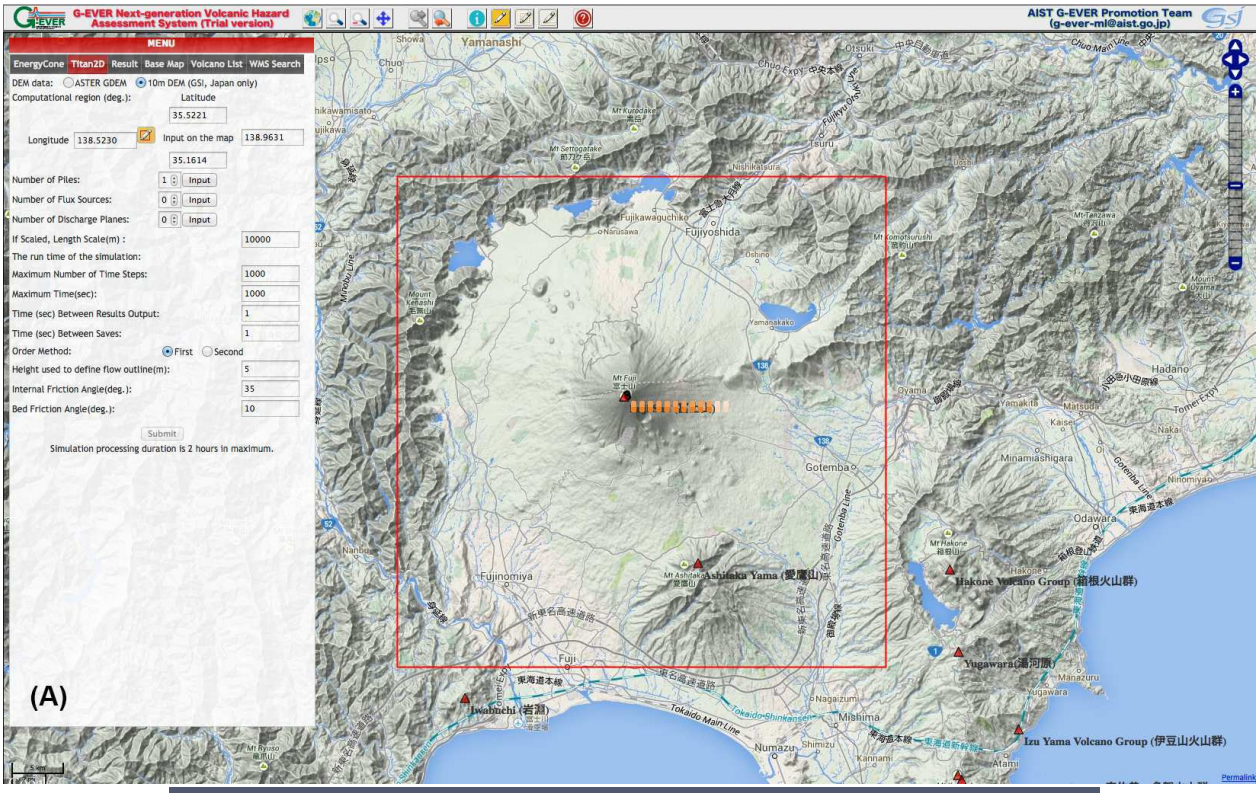

Figure 6. A Titan2D simulation result at Fuji Volcano, Japan, using G-EVER volcanic hazard assessment support system. (A) Online simulation view on the Titan2D menu. (B) the result can be visualized using a free 3D software (eg. Paraview). A pyroclastic density current, derived from a summit eruption with 2.7x10^{7}m^3 in volume, descending down along a western valley. A 10-degree basal friction was used for the simulation.

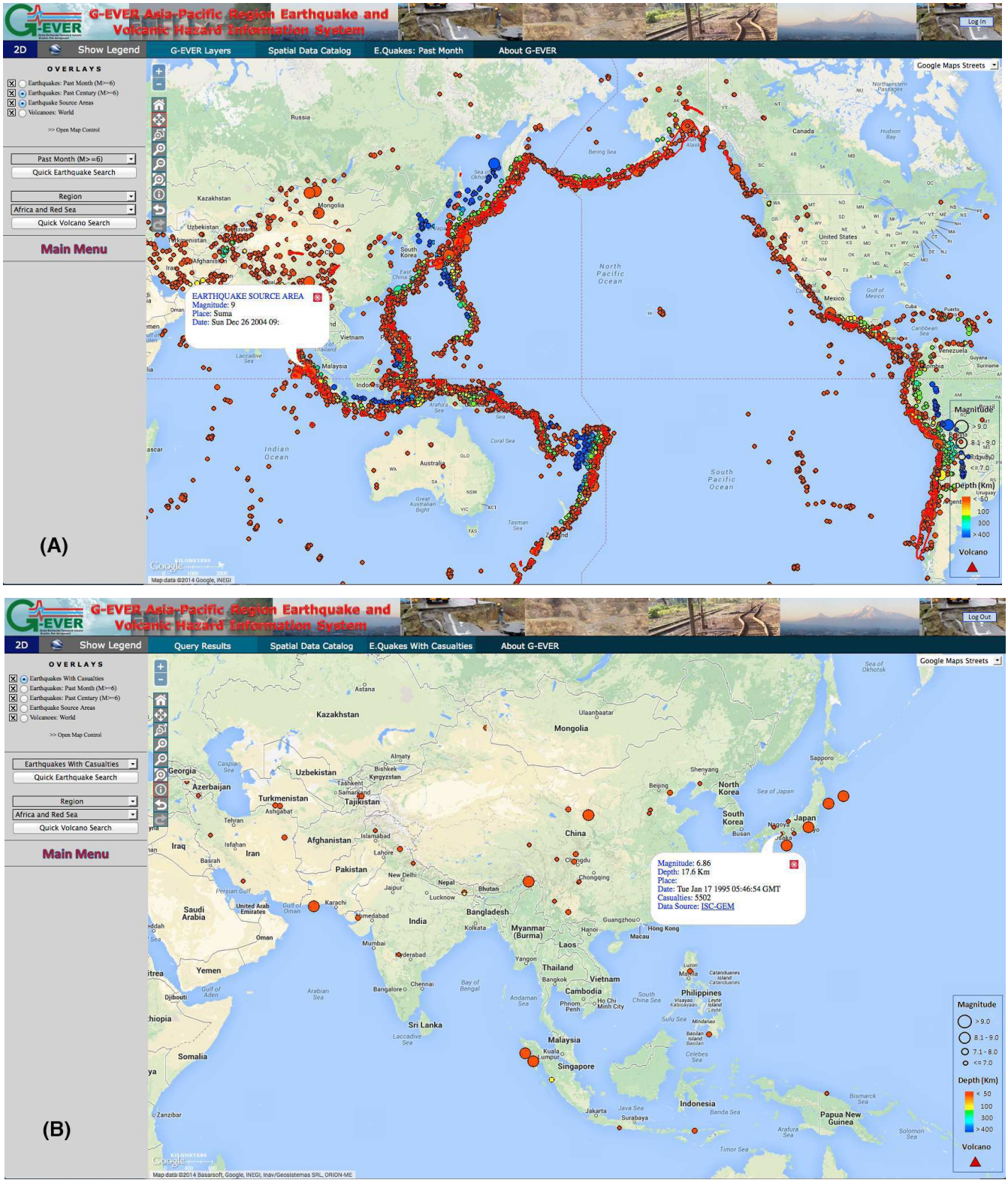

Figure 7. Preliminary version of G-EVER Asia-Pacific Region Earthquake and Volcanic Hazard Information System (http://ccop-geoinfo.org/G-EVER). (A) Distribution of epicenter of large-scale earthquakes (M>6) since 1971 (USGS and ISC-GEM) are shown. Red-line areas indicate large-scale earthquake source regions. Detailed information is available by clicking on earthquake epicenters. (B) Epicenter of large-scale earthquakes with more than 1,000 casualties.

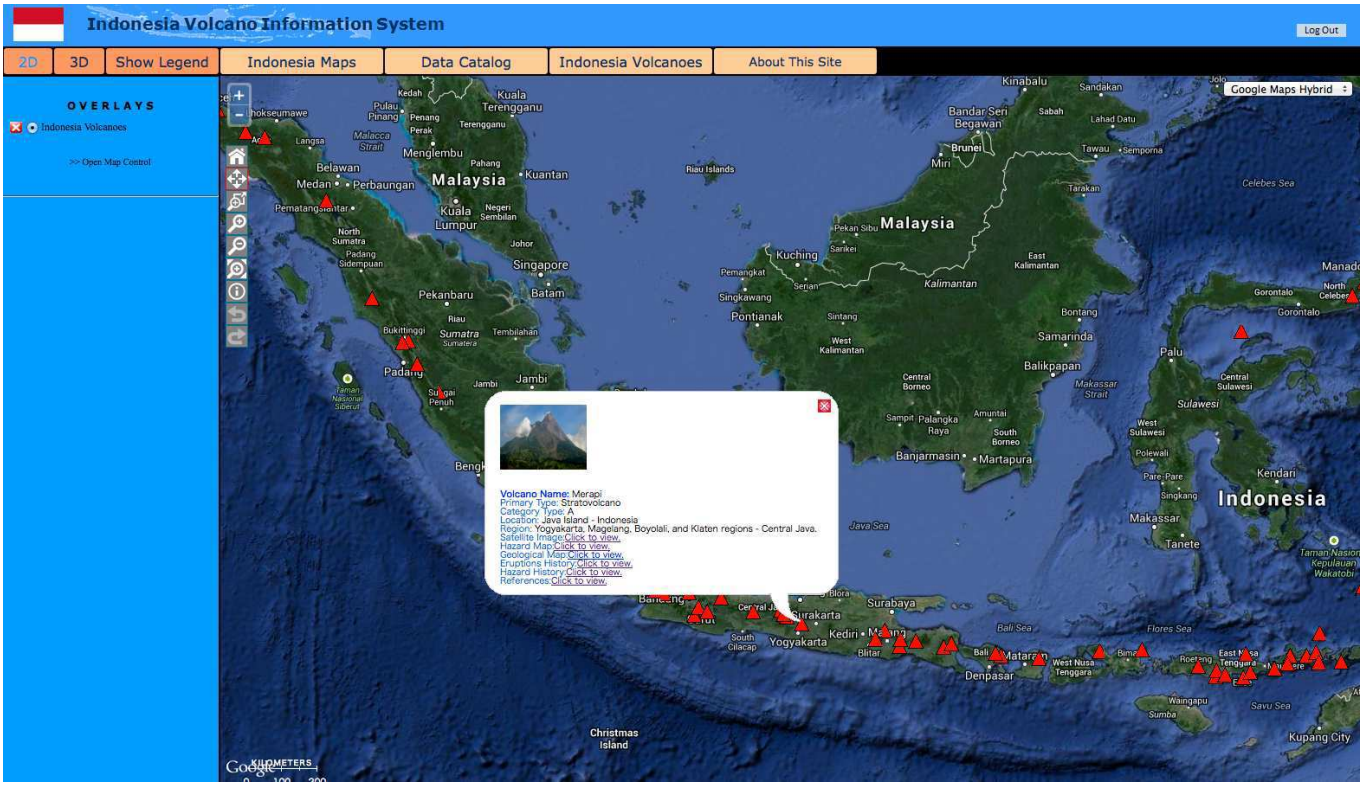

Figure 8. Preliminary version of Indonesia Volcano Information System. Type A volcanoes, which erupted after 1600AD, are shown on the map. Volcano type, category, satellite image, hazard map, geological map, eruption history, hazard history and references of each volcano can be seen on this system.

from the eruption database. Using the volcano hazard assessment system, the time and area that would be affected by volcanic eruptions at any locations near the volcano can be predicted using numerical simulations. The system should estimate volcanic hazard risks by overlaying the distributions of volcanic deposits on major roads, houses and evacuation areas using GIS enabled systems. The G-EVER hazard assessment support system is implemented with a user-friendly interface, making the risk assessment system readily usable and accessible online.

A preliminary version of the G-EVER volcanic hazard assessment support system (Fig. 4) that can run energy cone (Fig. 5; Marlin and Sheridan, 1982) and Titan2D (Fig. 6; Pitman et al., 2003; Sheridan et al., 2004) simulations at any volcano in the world is available since 2013. The system using ASTER Global DEM (30m resolution) and 10m DEM dataset is used in Japan region. Links to major volcanic databases, such as Smithsonian GVP (Global Volcanism Program, http://www.volcano.si.edu/), VOGRIPA (Volcano Global Risk Identification & Analysis Project; http://www.bgs.ac.uk/vogripa/), ASTER Satellite image (https://gbank.gsj.jp/vsidb/image/), and Volcanoes of Japan (https://gbank.gsj.jp/volcano/), are available from each volcano on the map. Almost all volcanoes in the world can be evaluated using this volcanic hazard assessment support system. Currently, the system covers more than 3200 Quaternary volcanoes worldwide. Links to major volcanic databases in the world are useful to examine eruption history in detail. Using Google and Bing maps as base maps provides more information for hazard evaluations. Combining simulation results and distributions of roads, hospitals, evacuation sites and airports are useful for hazard and risk assessments.

Asia-Pacific region earthquake and volcanic hazard mapping project

The Asia-Pacific region earthquake and volcanic hazard mapping project aims to develop an advanced online information system that provides past and recent earthquake and volcanic eruption information (e.g. age, location, scale, affected areas and fatalities) and risk assessment tools for earthquake and volcanic eruption hazards. A printed map version will also be published as the new version of the Eastern Asia Geological Hazard Map (Kato and Eastern Asia Natural Hazards Mapping Project, 2002) of the Commission for the Geological Map of the World (CGMW). The online hazard information system provides useful information about earthquake and volcanic hazards in an interactive and user-friendly interface (Fig. 7). Past and recent large-scale earthquakes and volcanic eruptions, tsunami inundation areas, active faults distributions, and major landslides are going to be shown on the map. Links to major earthquakes and volcanic eruptions databases are available in the system. The earthquake and volcanic eruption hazard mapping project will be implemented with the cooperation of major research institutes and organizations in the Asia-Pacific region such as PHIVOLCS (Philippine), CVGHM (Indonesia), GNS Science (New Zealand), EOS (Singapore), USGS (USA) and CCOP (Coordinating Committee for Geoscience Programmes in East and Southeast Asia). A preliminary hazard information website collaborating with CVGHM is under construction (Fig. 8). Volcano type, category, satellite image, hazard map, geological map, eruption history, hazard history and reference of active volcanoes can be displayed on this system.

Conclusion

The G-EVER consortium among the Asia-Pacific geohazard research institutes was started in 2012 to reduce the risks caused by earthquakes, tsunamis and volcanic eruptions worldwide. The G-EVER1 accord with 10 recommendations was approved by G-EVER1 workshop participants. The next-generation volcanic hazard assessment Working Group released the G-EVER hazard assessment support system making the hazard and risk assessment easily usable and accessible online. The Asia-Pacific region earthquake and volcanic hazard mapping project made a preliminary hazard mapping system that provides earthquake and volcanic hazard information, risk assessment tools and links to major databases in the world. The project plans to create the system with the cooperation of Asia-Pacific countries.

Acknowledgements

We greatly appreciate the discussion and generous supports from the president, Dr. Eikichi Tsukuda (AIST), vice president, Dr. John Eichelberger (Univ. of Alaska) and the Management Board and Steering Committee Members of G-EVER Consortium.

References

Kato, H. and Eastern Asia Natural Hazards Mapping Project, 2002, Eastern Asia Geological Hazards Map, 1:7,700,000. Geological Survey of Japan, AIST, 2 sheet maps and explanatory note, 49 p.

Marlin, M.C. and Sheridan, M.F., 1982, Computer-assisted mapping of pyroclastic surges. Science, v. 13, pp. 637-640.

Pitman, E.B., Patra, A., Bauer, A., Sheridan, M., Bursik, M., 2003, Computing debris flows and landslides. Phys. Fluids, v. 15, pp. 3638-3646.

Sheridan, M.F., Stinton, A.J., Patra, A., Pitman, E.B., Bauer, A. and Nichita, C.C. (2004) Evaluating Titan2D mass-flow model using the 1963 Little Tahoma Peak avalanches, Mount Rainier, Washington, Jour. Volcanol. Geotherm. Res., v. 139, pp. 89-102.

Takarada, S., 2013a, Asia-Pacific Region Global Earthquake and Volcanic Eruption Risk Management (G-EVER) Consortium: the new hazard mitigation activities, *IAVCEI 2013 abstract*, Kagoshima, 4A1_4H-O4.

Takarada, S., 2013b, G-EVER Consortium activities and the next-generation volcanic hazard assessment system. Proceeding of the 1st Asia-Pacific Region Global Earthquake and Volcanic Eruption Risk Management (G-EVER) International Symposium. Open-file report of Geological Survey of Japan, no. 583, pp. 12-22.

Takarada, S., 2013c, The next-generation real-time volcanic hazard assessment system in G-EVER, *IAVCEI 2013 abstract,* Kagoshima, 4P1_4D-O21.

**G-EVER Promotion Team Members: Shinji Takarada, Yasuto Kuwahara, Yuzo Ishikawa, Naoji Koizumi, Toshihiro Uchida, Akira Takada, Norio Shigematsu, Ryuta Furukawa, Tadashi Maruyama, Ryosuke Ando, Junko Hara and Joel Bandibas in Geological Survey of Japan, AIST.*

by Eikichi Tsukuda and [*]*G-EVER Promotion Team*

Report of the 2nd G-EVER International Symposium and the 1st IUGS and SCJ International Workshop on Natural Hazards and the "Sendai Agreement"

Geological Survey of Japan, AIST, Site7, 1-1-1, Higashi, Tsukuba 305-8567, Japan. *E-mail: e-tsukuda@aist.go.jp*

The Asia-Pacific Region is an area with a high risk of catastrophic natural disasters such as earthquakes, tsunamis and volcanic eruptions. In today's highly globalized economy, when a major disaster occurs, it can create unpredictable turmoil not just in the affected area but also the rest of the world. Countermeasures against these natural disasters are crucial for the sustainable development. We believe that continuous efforts to develop an effective international framework to reduce the risk of natural disasters are very important. It is expected that geological institutions will collaborate and create a system to gather and process information to formulate disaster mitigation measures in the Asia-Pacific Region. This system must be easy to use and freely accessible to the public to meet societal needs. The Sumatra earthquake of December 26, 2004 and Tohoku earthquake of March 11, 2011 clearly show the urgency of developing an information and knowledge system for infrequent natural hazards. We also have to recognize that smaller events could have adverse effect to society. For example, the magnitude of the February 2011 Christchurch earthquake was just 6.3 (M_L), but caused major damage to the second largest city of New Zealand and 185 casualties. Volcanic ash ejected from the Eyjafjallajökull eruptions in Iceland on April 2000 caused more than 20,000 airline flight cancellations a day in Europe, resulting to the largest air-traffic shut-down since World War II. The IATA estimated that airline companies lost US$200 million a day during the shut-down. After the 2011 Tohoku earthquake, more efforts for the prevention and reduction of the risks of natural disasters have been made all over the world. The G-EVER Consortium promotes natural disaster risk reduction activities through the collaboration different research institutes worldwide. The consortium's major activities are the following:

1. Establish a framework for cooperation of research institutes and organizations working on volcanic disaster prevention in the Asia-Pacific region.
2. Enhance the exchange and sharing of information on seismic and volcanic disaster prevention.
3. Formulate international standards for the database, data exchange and disaster risk assessment.

The 2nd G-EVER International Symposium and the 1st IUGS & SCJ International Workshop on Natural Hazards aimed to encourage extensive discussions on the present situation of natural disaster mitigation of earthquake, tsunami, volcanic eruption and landslide in the Asia and Pacific regions. The discussions included (1) prioritization of important researches to make society strong and resilient, (2) development of suitable hazard maps which are essential to society and Asia-Pacific scale hazard assessment activities, and (3) the importance of contributions to solid earth science. There were also discussions on the mitigation processes needed in the next-decade to reduce the risks of natural hazards.

The 2nd G-EVER International Symposium and the 1st IUGS & SCJ International Workshop on Natural Hazards was held in Sendai, Tohoku, Japan on Oct. 19-20, 2013 (Fig. 1). The symposium was organized by the G-EVER Consortium, Geological Survey of Japan, AIST, the International Union of Geological Sciences (IUGS) and Science Council of Japan (SCJ). It was co-organized by the Geological Society of Japan and the Coordinating Committee for Geoscience Programmes in East and Southeast Asia (CCOP). Tohoku University, Disaster Prevention Research Institutes (DPRI) of Kyoto University, National Research Institute for Earth Science and Disaster Prevention (NIED), GNS Science, Philippine Institute of Volcanology & Seismology (PHIVOLCS), the Seismological Society of Japan, the Volcanological Society of Japan, Japan Association for Quaternary Research, Japanese Society for Active Fault Studies, Japan Society of Engineering Geology, and Tokyo Geographical Society supported the symposium (Fig. 2).

Figure 1. Participants of the 2nd G-EVER International Symposium and the 1st IUGS & SCJ International Workshop on Natural Hazards which was held in Sendai, Tohoku, Japan, on October 19-20, 2013.

Figure 2. Organizers, Co-organizers, institutes and societies supporting the 2nd G-EVER International Symposium and the 1st IUGS & SCJ International Workshop on Natural Hazards.

There were 94 participants representing 12 nations and regions and 13 institutes attended the symposium. Invited speakers were Ian Lambert and Roland Oberhaensli (both from IUGS), Akira Ishiwatari (Tohoku Univ.), Kuniyoshi Takeuchi (ICHARM), John Eichelberger (Alaska Univ.), Chris Newhall (EOS), Shinji Takarada (GSJ), Setsuya Nakada (ERI), Peter Bobrowsky (Simon Fraser Univ.), Kiichiro Kawamura (Yamaguchi Univ.), Masahiro Chigira (Kyoto Univ.), Cheng-Horng Lin (Academia Sinica), Dong Shuwen (CAGS), Ruizhi Wen (CEA), Yuzo Ishikawa (GSJ), Nguyen Hong Phuong (VAST), Pilar Villamor (GNS Science), Ken Xiansheng Hao (NIED), Toru Matsuzawa (Tohoku Univ.), Yuichiro Tanioka (Hokkaido Univ.), Mark Cloos (Univ. Texas), Takuya Nishimura (Kyoto Univ.), Yasutaka Ikeda (Univ. Tokyo), Kazuhisa Goto (Tohoku Univ.), Daisuke Sugawara (Tohoku Univ.), James Goff (Univ. NSW), Masataka Ando (Shizuoka Univ.), Phil Cummins (ANU), Ronald Harris (Brigham Young Univ.) and Yildrim Dilek (Miami Univ.).

There were intensive discussions on how to reduce the risks of natural disasters such as earthquakes, tsunamis, landslides and volcanic eruptions. The program and abstract volume are available at the G-EVER Hubsite http://g-ever.org/en/symposium/symposium2.html.

Schedule:

Oct. 19 (Sat) 9:30-18:10

Session 1: Scientific challenges for risk reduction of natural disasters: Overview

Session 2: Volcanic eruption, landslides and seismic hazards

Oct. 20 (Sun) 9:00-18:30

Session 3: Hazard assessment, 2011 Tohoku-oki earthquake and subduction tectonics

Session 4: 2011 Tohoku-oki earthquake and tsunamis

General Discussion

Oct. 21 (Mon)

Field trip to the area on the Pacific coast of Tohoku that was affected by the March 11, 2011 Tsunami. One conspicuous outcrop was observed at the inundation area, approximately 1 km inland from the seashore in Iwanuma City, Miyagi Prefecture, Sendai Bay (Fig. 3). Here some layers of past tsunami deposits were identified by the Board of Education of Iwanuma City.

During the symposium, the participants drafted the "Sendai Agreement" and unanimously endorsed it. A broad consensus for future natural hazard mitigation strategies was developed.

THE SENDAI AGREEMENT

- Study the processes leading to natural disasters through the support of international, broad-based, and inter-disciplinary scientific studies relevant to the entire System Earth.
- Improve the methods and content of hazard maps, for society and hazard assessment activities in Asia-Pacific region.
- Create or help build comprehensive international databases, including on past disasters and hazards, and also on geological and geophysical features of subduction zones of the world.
- Promote scientific research on topics such as geodetic measurements, submarine landslides and predicting the maximum aftershocks from major earthquakes, including the 2011 Tohoku-oki earthquake.
- Enhance systematic mapping/dating of paleo-tsunami deposits in all regions especially those with significant populations and infrastructure.
- Promote innovative practical applications of monitoring data.
- Strive for better hazard assessments by seeking convergence of a variety of methods and disciplines, and also try to understand any discrepancies.
- Improve the quantity and quality of data on past events (paleo), recent events (modern analogues), including that from monitoring, and other precursors of future events, including better

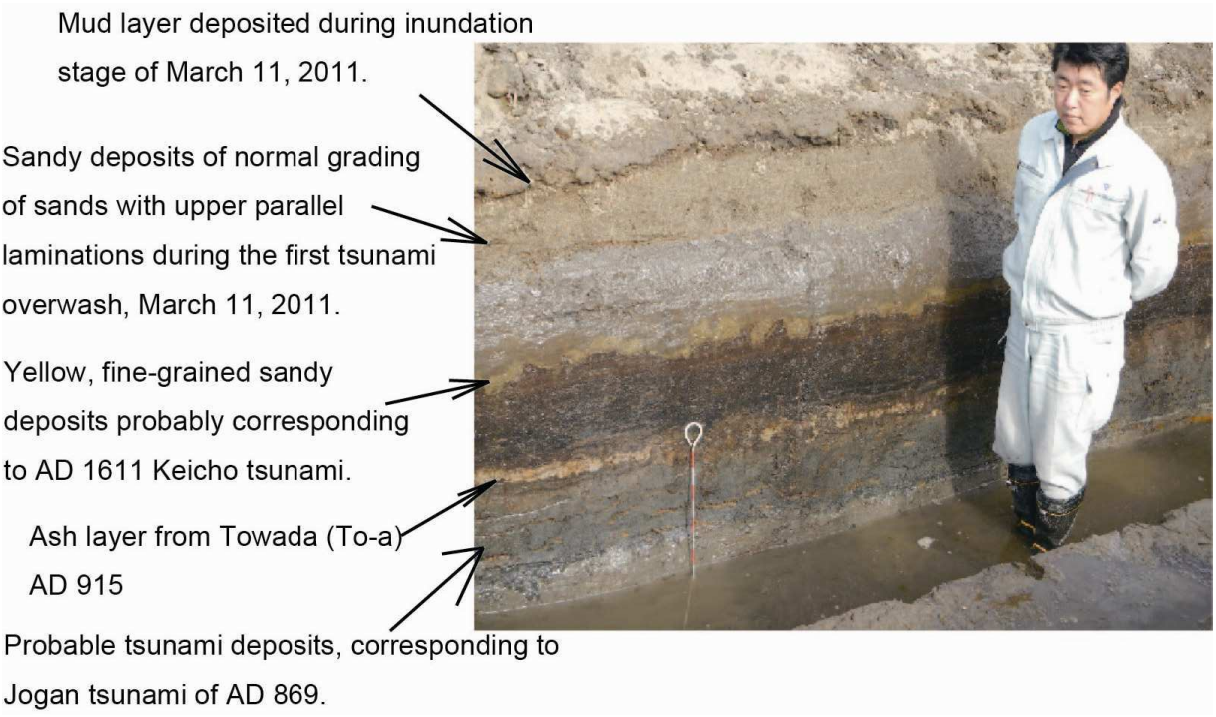

Figure 3. Vertical trench surface of Iwanuma City, 1 km inland from the present shoreline. Three tsunami deposits were identified, from the top, at the time of 2011 Tohou-oki earthquake and tsunami, probable 1611 Keicho earthquake and tsunami, and probable 869 Jogan earthquake and tsunami, respectively. Between the latter two, 915 Towada volcanic ash (To-a) is intercalated. Some paddy field soils and swamp deposits are also dated to confirm the ages of the tsunami deposits. Red and white band scale 5 cm each. Refer to the home page of the Board of Education of Iwanuma City, http://www.city.iwanuma.miyagi.jp/kakuka/050300/050302/kikakuten.html.

understanding and modeling of what controls occurrence and magnitude of events.

- Promote better translations from hazard to risk – including damage curves, values at risk, etc.
- Improve outreach mechanisms, including visualizations, to enhance communication with end users from early stages of research to outreach stages. Develop multidisciplinary teams and communicate uncertainty to end-users.
- Improve methods for communicating authoritative information to underpin decision-making. Offer training to public officials and local people to reduce geo-risks.
- Promote the optimum use of geoscientific information by public officials and other decision makers. Lessons-learned and best practices are the most useful types of warning information. Gather feedback from public officials and engage in dialogue about what decisions they need to make and what information they need to make those decisions.
- Develop creative new options for mitigating impacts, based on scientific, technical and socio-economic expertise, and develop effective means to have advice used in policies/decisions. Engineers, social scientists and economists should be involved.
- Play international leadership, coordination, and best practices through ICSU.
- Participate in related global risk reduction efforts, such as Integrated Research on Disaster Risk (IRDR) Program, Future Earth, Global Earthquake Model (GEM), and Global Volcanic Model (GVM).

We hope that our activities will help to build a better future for Earth. The 3rd United Nations (UN) World Conference on Disaster Risk Reduction will be held in Sendai Japan on March 14-18, 2015. I hope our efforts will be an important model for the future disaster risk reduction activities in the world.

We greatly appreciate the generous contributions and support from IUGS, Science Council of Japan, Tohoku University, IRIDeS of Tohoku University, and Board of Education of Iwanuma City.

G-EVER Promotion Team Members: Shinji Takarada, Yasuto Kuwahara, Yuzo Ishikawa, Naoji Koizumi, Toshihiro Uchida, Akira Takada, Norio Shigematsu, Ryuta Furukawa, Tadashi Maruyama, Ryosuke Ando, Junko Hara and Joel Bandibas in Geological Survey of Japan, AIST.

Pursuing the evolution of the Asian Tethyan realm – Third International Symposium of IGCP-589

21- 22 October 2014, Tehran, Iran

The Third International Symposium of IGCP-589 "Development of the Asian Tethyan Realm: Genesis, Process and Outcomes" was held between 21st and 22nd October, 2014 in the Amirkabir Technical University, Tehran, Iran. The symposium was preceded by a two-day pre-symposium field-excursion (October 19-20) and followed by a four-day post-symposium field excursion (October 23-26). With the total involvement of the Geological Survey of Iran, the organizer of this event, the hospitality of Amirkabir Technical University, and the active support of IUGS and UNESCO, this event has been successfully conducted.

More than 30 delegates from China, Germany, India, Iran, Italy, Japan, Malaysia, Poland, Thailand, and Turkey participated in this event and exchanged their latest findings and achievements on evolution of the Tethys. Twenty one oral presentations and 10 poster presentations with good participation among women and students dealt with the key problems of Asian Tethyan realm. Papers covered different disciplines of geological sciences in resolving the Tethyan issues and highlighted the importance of multidisciplinary approaches of the projects presented. Deliberations on various problems of common concern, such as stratigraphical correlation, paleogeogrphic evolution, petrological assemblages, tectonic configuration, identification of similarities and differences between the different parts of the Tethyan Realm and a common minimum programme to address the irresolvable issues were the highlights of the symposium.

Choosing Iran as the place to convene this event owes to not only its significant geographic location with excellent geological records of the development of the western Tethys, but also the good geological research capacity of the country and the involvement of international teams.

Pre-symposium and post-symposium excursions were designed to provide the participants an opportunity to (i) visit the places, where the closing of the Paleo-Tethys and subsequent evolution are well demonstrated, and (ii) see the places, that recorded the drift of the Cimmerian blocks and evolution of the Neotethys. As a result the Alborz Mountains became the target area of the Pre-symposium excursion, and the central Iran blocks and the Sanandaj-Sirjan zone became the objective of the post-symposium excursion. In addition to studying the critical geological sections, participants also enjoyed during the pre-symposium excursion the nice green landscapes and loft mountains in the Alborz, and during the post-symposium excursion wild landscape in central Iran and lively historical cities of Yazd and Isfahan.

Symposium participants gather under a large poster of the symposium in front of the venue.

The IGCP project 589 is led by Xiaochi Jin (China), Katsumi Ueno (Japan), Graciano Yumul Jr. (Philippines), and Pol Chaodumrong (Thailand). The project started in 2012 and held its inaugural international symposium in Xi'an, China and second in 2013 in Boracay Island, Philippines. Field excursions were successfully conducted in the Qinling Orogen in central China and Panay Island of Philippines respectively. It was decided, amongst other matters, at the business meeting on the second day of the symposium that the fourth international symposium of IGCP-589 will be held next year in Thailand. Field excursions are planned to be conducted in northern Thailand, a geologically very complicated region that accommodates the complexes of eastern Paleo-Tethyan suture(s). Prof. Jin Xiaochi thanked the Iranian colleagues for excellent hospitality and for the successful organization of the symposium and field excursions. He also invited the delegates to participate in yet another exhilarating experience next year at Thailand.

Xiaochi Jin,
Institute of Geology,
Chinese Academy of Geological Sciences,
26 Baiwanzhuang Road,
Beijing 100037, China;
E: jinxchi@cags.ac.cn;
jinxchi@sina.com,

Mohammad Ghassemi
Research Institute for Earth Sciences,
Geological Survey of Iran, Meraj Ave.,
Azadi Sq., Tehran, Iran

David R. Oldroyd (1936-2014)

Many members of the IUGS community know David Oldroyd and will be sad to learn of his recent passing, age 78 years. Our President has written to Jane Oldroyd, and their sons, to express our sincere condolences.

David was born in Luton UK. He went up to Emmanuel College at Cambridge University. He was awarded a BA in Natural Science in 1958. Initially, he veered towards chemistry but was attracted to geology because he enjoyed the fieldwork. After leaving Cambridge, he worked as a school teacher in north London but emigrated to New Zealand in 1964, again to teach at schools, but, while there, registered for a MSc at University College, London, which he was awarded on the basis of a dissertation on "Geology in New Zealand prior to 1900" in 1967.

The history of geology thus became his passion. David soon relocated to the School of History and Philosophy of Science at University of New South Wales in Sydney, Australia where, as it turned out, he spent the rest of his career. There, he received his PhD for a thesis on "From Paracelsus to Haüy: the development of mineralogy in relation to chemistry" in 1974.Subsequently rising to Head of School and Professor, he was awarded a D.Litt in 1993, before retiring in 1996 as an Honorary Visiting Professor .

David was a Fellow of the Geological Society, London, and Australian Academy of the Humanities. He was also a Corresponding Member of the International Academy of History of Science as well as a Councillor of the History of Earth Sciences Society and a Councillor, and later, President of the Australasian Association for the History, Philosophy, and Social Studies of Science. But the IUGS community would have best known him as Secretary General of its Commission on the History of Geological Sciences (INHIGEO) from 1996–2004 and as Vice-President of that Commission for Australasia and Oceania from 2004-2012. He was also an INHIGEO Honorary Senior Member.

David was a prodigiously active author, editor and reviewer which amounted to some 62 refereed journal articles, 21 refereed essay reviews and book chapters, 37 encyclopedia articles, and 113 book reviews. He also

authored 6 books (which were widely translated) and edited 4 more. His editorial work involved journals, encyclopedias and dictionaries. He was the Editor of the journal "Earth Sciences History" from 2008-2013.

David's prizes and awards included the most outstanding paper from The Annals of Science (1990–1992), the Sue Tyler Friedman Medal of the Geological Society, London, for "distinguished contributions to the recording of the history of geology" (1994), the History of Geology Award of the Geological Society of America for "contributions of fundamental importance to our understanding of the history of the geological sciences" (1999) and the Tom Vallance Medal of the Geological Society of Australia (2014). This was capped by National Recognition by the Australian Commonwealth Government which deservedly awarded him a Centenary Medal, "for services to Australian society and the humanities in the study of the history of science" (2003).

David's books on the history of geology were diverse ranging from general reviews such as "The Highlands Controversy: Constructing Geological Knowledge through Fieldwork in Nineteenth-Century Britain" and "Thinking About the Earth: A History of Ideas in Geology" to more specific works such as "The Iconography of the Lisbon Earthquake". An internet search immediately confirms his contribution to our science as an author or editor. Those who knew David will mourn his passing but those who did not know him should go to the internet site: http://aahpasss.org/2014/11/09/vale-david-oldroyd.

There they will find an interview, in David's own words, typically modest and humorous, about his career and ideas, not least that those who engage in the history of geology should also do fieldwork to support their investigations. In the interview, he revealed that he entered the geosciences more by accident and design. It is very fortunate for our profession and for IUGS that he did and he will be sadly missed by many.

Following David Oldroyd's death, the INHIGEO Secretary General has received an exceptional number of written memories of him. Selected extracts from these reminisces follow. They tell much about David's kind character, intellectual acumen and generous contribution to the geosciences.

"The remembrance of David, his kindness, help and professional advice will always be in my heart"

"With whatever I have done for INHIGEO, he has been the spirit behind it. I will miss him a lot"

"He was a giant in the history of geology"

"David will be missed as a dear friend and an accomplished scholar"

"I was using his book 'Thinking about the Earth' when I received the INHIGEO email"

"He gave a lot to INHIGEO and I think it is difficult to imagine future INHIGEO meetings without him"

"a man with sweet humour and kind heart"

"It was always exciting to speak and correspond with him"

"David was not only a wonderful scholar but also a lovely, very generous man"

"It is difficult to think of INHIGEO without him"

"The scientific and organisational activity of this charismatic person is widely known."